

International Energy Agency

IEA District Heating

Programme of Research, Development and
Demonstration on District Heating and Cooling

ADVANCED ENERGY TRANSMISSION FLUIDS FOR DISTRICT HEATING AND COOLING

Published by

Netherlands agency for energy and the environment

Novem



acting as operating agent for
the IEA District Heating and Cooling project

1993: P 7

Dear reader:

The Executive Committee of the IEA Implementing Agreement on District Heating and Cooling is interested in improving the impact of the R&D activities and the effectiveness of the programme.

For this reason the Operating Agent needs your support. May I ask you to be so kind as to complete the following questionnaire and return it to:

Novem BV
Attn. Mr. J.C. Resing
P.O. Box 17
NL-6130 AA SITTARD
The Netherlands

What is your name and address?

Name:

Address:

What is your professional relation to the item of the report?

How did you receive your copy of the report?

Do you appreciate the activities, described in the report?

Do you have suggestions for further dissemination of the results presented in the report?

Do you have any suggestions for further tasks, or comments to the activities of the Implementing Agreement?

International Energy Agency
Programme of Research, Development and Demonstration
District Heating and Cooling
Annex III

ADVANCED ENERGY TRANSMISSION FLUIDS

Final Report of Research

March 1993

■

Submitted to:

NOVEM, BV
Sittard, The Netherlands

by:

Earth Resources, Ltd.
Silver Spring, Maryland, USA

Table of Contents

	<u>Page</u>
1. Summary	1-1
2. Introduction	2-1
3. Performance of Plate Heat Exchangers Operating With Friction-Reducing Additives	3-1
4. Environmental Effects of Surfactant Friction Reduction Additives	4-1
5. Ice Slurry Based District Cooling Systems	5-1
6. The Influence of Friction Reduction Additives on Corrosion Rates of District Heating System Materials	6-1

1. SUMMARY

This report describes the results of research and testing undertaken by the International Energy Agency (IEA). Under Annex III of the IEA's program, the Experts Group on Advanced Transmission Fluids for District Heating and Cooling Applications undertook four research projects that addressed: performance of plate heat exchangers operating with friction reduction additives; environmental effects of surfactant friction reduction additives; use of ice slurries in district cooling systems; and corrosion effects of friction reduction additives.

1.1 PERFORMANCE OF PLATE HEAT EXCHANGERS OPERATING WITH FRICTION-REDUCING ADDITIVES

Bruun & Sorensen Energiteknik AS of Risskov, Denmark, undertook an investigation of the effects of friction-reducing additives on the performance of plate heat exchangers. An experimental plate heat exchanger (.7MW) was installed in the district heating center in Lind, Denmark, in parallel with the existing main (10 MW) heat exchanger at the center. Over a ten month period, tests were conducted using the friction reduction additive "tenside" at concentrations of 100, 215, and 400 parts per million (ppm). Supply and return temperatures and flow rates were measured, as was the pressure loss across the primary (additive) side of the experimental heat exchanger. The heat transfer coefficient (α) and heat transmission coefficient (k) of the heat exchanger were then calculated.

The results of testing showed that the calculated heat transfer coefficient for the plate heat exchanger operating with tenside can approximate that of pure water, if flow velocity across the exchanger plates is increased. The higher the concentration of tenside, the greater the velocity must be increased, however. This same characteristic is also apparent for the exchanger heat transmission coefficient, with the K-value being improved at the same overall flow rate by reducing the total gap area of the heat exchanger plates.

In order to compensate for the reduction in heat transfer associated with the use of friction-reducing additives, higher flow velocities through the exchanger must be employed while maintaining the required effective exchanger surface area. Three design alternatives can be considered:

1. Utilize longer plates. Elongated plates will compensate for the reduced heat transfer coefficient without significantly changing other exchanger parameters. By allowing the exchanger to remain as a single-pass system, this alternative minimizes total pressure losses across the heat exchanger and maintains all piping connections on the same side of the plate heat exchanger for ease of installation and servicing. In a new plant installation where sufficient space can be made available for the longer plates, this alternative would appear to be the most practical.

2. Increase the number of plates. If an existing plant is being modified to utilize friction-reducing additives, it may be possible to add additional plates to the heat exchanger to compensate for the reduced heat transfer coefficient. However, preliminary calculations indicate that the number of plates required to maintain return temperatures in the primary district heat system may be substantial (up to 100% more).
3. Convert to a two-pass system. In an existing plant where space and cost constraints may be apparent, converting the plate heat exchanger into a two-pass configuration may be possible. The associated velocity and turbulence increases will improve heat transfer coefficient and lower primary side return temperature. The negative aspects of this alternative include a significant increase in system pressure loss, and problems associated with more complex piping connections.

1.2 ENVIRONMENTAL EFFECTS OF SURFACTANT FRICTION REDUCTION ADDITIVES

The use of friction-reducing additives in district heating and cooling systems must take into consideration their impact on the environment, and the health and well being of all living organisms that may come into contact with the additives during their use and disposal. The University of Dortmund therefore undertook an investigation of one popular class of friction reducing additives, cationic surfactants, to assess their hazard potential when used in district heating and cooling applications. This effort included a comprehensive review of the available literature pertaining to cationic surfactants, combined with testing of the adsorption characteristics of surfactant solutions in selected soil types.

The structure of the cationic surfactants under consideration for use in district heating systems is very similar to that of other cationic surfactants in wide use today. As such, their toxicological and ecological properties are similar:

- primary biodegradability > 80%
- ultimate biodegradability > 60%
- fish toxicity > 1 mg/l
- bacteria toxicity > 1 mg/l

Two important characteristics of cationic surfactants serve to reduce the exposure risk associated with their accidental release into the environment:

- they form neutral salts when in contact with anionic surfactants that are present in all waste waters and surface water.
- they adsorb on all solid surfaces.

To assess the potential for damage due to leakage in a district heating or cooling system employing cationic surfactants, adsorption testing was conducted using several common soil types. The results of these tests indicated that surfactants are irreversibly adsorbed, with the rate of adsorption influenced by the amount of clay present in the soil.

1.3 ICE SLURRY BASED DISTRICT COOLING SYSTEMS

With the evolution of residential and commercial buildings into tighter, more energy-efficient structures, and the greatly increased use of electrical equipment and appliances within them, the need for space cooling has increased significantly. District cooling systems provide an attractive means of cooling buildings, especially in higher density commercial areas. Accordingly, research is being conducted to improve the energy and operating performance of large chilled water systems. One particular technology, the use of ice-water slurries, provides an opportunity to greatly increase the cooling energy capacity of a given volume of cooling water, leading to reductions in capital costs for system construction, as well as reductions in pumping costs associated with system operation.

Under this IEA annex, Energy, Mines and Resources Canada developed a design manual for ice slurry based district cooling systems. The manual summarizes several system design alternatives, which are each organized in accordance with the major elements comprising a typical district cooling system: ice slurry generation; distribution; storage; and utilization. These design alternatives illustrate the diversity that currently exists among the technologies that can be employed for ice slurry based district cooling.

The design manual also identifies a number of areas where research, development, or testing is required to support the various system design alternatives.

1.4 THE INFLUENCE OF FRICTION REDUCTION ADDITIVES ON CORROSION RATES OF DISTRICT HEATING SYSTEM MATERIALS

The use of friction-reducing additives in district heating and cooling systems provides an opportunity to reduce system costs and improve operating performance. However, the potential exists for these additives to have deleterious effects on metal piping and other distribution system components. The IEA therefore conducted a preliminary study, in 1990, of the corrosion effect of cationic surfactants in solutions of tap water, deionized water, and tap water containing corrosion inhibitor. Subsequently, a more detailed study of the corrosion effects of friction reduction additives was determined to be required, and was undertaken by the Ohio State University under this IEA annex.

Pitting corrosion rate susceptibility and corrosion rate tests were carried out on AISI type 304 stainless steel, SAE 1112 (API Grade B) carbon steel, copper, 90/10 copper/nickel, and 60/40 copper/zinc samples. Corrosion environments included tap water, deionized water, deoxygenated water, deionized/deoxygenated water, and a 50% tap water- 50% deionized water mixture. Tests were carried out at

temperatures between 60°C and 110°C, and also at 25°C to approach district cooling system temperatures, with pH values varied between 7 and 10. The effects of several friction reduction additives on pitting susceptibility and corrosion rates were assessed. Additional tests were conducted using corrosion inhibitors in combination with friction reduction additives.

The results of testing showed that, with the exception of pitting susceptibility in tap water, the addition of Habon-G or Ethoquad T/13-50 (plus NaSal) friction reduction additives either improves or has no negative effect on pitting susceptibility or corrosion rates of the iron-based or copper-based metals typically found in district heating and cooling systems at temperatures of 60°C and 110°C, and in some cases gave improved results. However, adverse corrosion effects were found when friction reduction additives containing chlorides were tested.

2. INTRODUCTION

Under Annex III of the International Energy Agency's Implementing Agreement on District Heating and Cooling, the Experts Group on Advanced Transmission Fluids continued its program of research, development, and testing that was originally initiated in 1987. Member country representatives from Canada, Denmark, Finland, Germany, the Netherlands, Sweden, and the United States developed a research program that addressed major concerns relating to the use of friction reduction additives (FRAs), and looked further into the problems associated with advanced district cooling technologies. Based on a review of proposals submitted by several research groups, the member country representatives selected four projects to be carried out under this annex, and activities were initiated in early 1991.

The performance of heat exchangers in systems utilizing friction-reducing additives was identified as an area of concern, since earlier testing had shown that FRAs caused a degradation in heat transfer performance proportional to improvements in friction reduction. Bruun & Sorensen was therefore asked to undertake a project to test heat exchanger performance in a system using these additives, and to develop alternatives to overcome any losses in heat exchanger performance.

A second concern of the Experts Group centered on the potential environmental and health effects associated with surfactant friction-reducing additives, the leading candidate chemical under consideration for use in district heating systems. The University of Dortmund performed a comprehensive literature review and assessment of the environmental effects of surfactants, and performed tests to determine their adsorption properties in various soil types as a means of assessing the potential impacts of district heating system leakage and spills on the local environment.

In Annex II, the Experts Group performed a preliminary evaluation of the potential for increased corrosion of district heating and cooling system metals due to their exposure to friction-reducing additives. Under Annex III, the Ohio State University expanded this evaluation to test several candidate additives in a variety of water compositions and in combination with corrosion inhibitors. Testing was also carried out at two temperature ranges common to district heating system operation.

Also under Annex II, research and testing of ice slurry mixtures as a means of improving the energy transport capability of district cooling systems was carried out. In an effort to move this exciting technology out of the research stage toward practical consideration as a viable concept for building cooling, Annex III supported Energy, Mines and Resources Canada in the development of a manual which provides design guidelines and alternatives for the use of ice slurries in district cooling systems.

Each of these four research projects has now been completed, and the results of the efforts are presented in the following chapters of this report. In addition, a fourth annex addressing advanced transmission fluids has been approved, and several new research and testing projects will be initiated in the technology area in the near future.

3. PERFORMANCE OF PLATE HEAT EXCHANGERS OPERATING WITH FRICTION-REDUCING ADDITIVES

Flemming Hammer and Michael Sørensen
Bruun & Sørensen Energiteknik AS
Ravnsøvej 6, DK-8240 Risskov

3.1 PURPOSE

The purpose of this project is to examine the heat transmission in plate heat exchangers where drag-reducing additives are used in one of its circuits. On the basis of the measuring results achieved, another aim is to prepare a solution model to avoid possible negative impact on the heat transmission in the heat exchanger.

3.2 BACKGROUND

3.2.1 Introduction

For several years Bruun & Sørensen Energiteknik A/S (B&S) have worked in co-operation with Herning Municipal Works and Hoechst AG with "smooth" water (i.e. tenside-enriched water) on various demonstration projects in Lind/Herning.

In 1989, demonstration project 1 was carried out in co-operation between Hoechst AG, who developed the additive, Herning Municipal Works, who made the system available, and B&S who was in charge of executing the project.

Currently, demonstration project 2, including the demonstration of a new type additive produced by Hoechst, is being carried out. Project 2 will be terminated in autumn 1992.

Moreover, in 1991 B&S carried out a theoretic project concerning water hammer in transmission systems with smooth water. The project was carried out by means of the computer program "LICFLOW". The result was that tenside addition to ordinary district heating water did not necessarily entail serious water hammer problems in the case of normal operation, i.e. operation at velocities not causing water hammer problems in a transmission system with ordinary district heating water.

Furthermore, a project concerning water treatment is being carried out. The purpose of the project is to uncover the impact of using "smooth" water in that type of part flow filters present in most of the superior district heating transmission systems. Fælleskemikerne (ELSAM) participate in this project.

The results of the two demonstration projects have proved to be very good, as a reduction of the pressure loss by up to 70-80% has been achieved, and electricity for pumping has been reduced by a corresponding figure. But it should be borne in mind that the heat transmission from the "smooth" water to the plate wall has been reduced because of the additive's turbulence-reducing effect. It is obvious that the number and shape of the plates as well as flow and temperatures are essential parameters. Only to a certain extent can these parameters be changed in the existing plant whose primary purpose is to supply the required heat to Lind.

At Herning, previous tests concerning the use of "smooth" water - based on the additive Habon, developed by Hoechst AG - have proved a reduction of heat transfer coefficient on the smooth water side of up to 30%. The advantage is a considerable reduction in the pressure loss in pipes and consequently considerable saving in electricity consumption. The reduced heat transmission causes reduced output which is why the flow must be increased. The result is inferior cooling. Therefore, it is very vital to find the right heat exchanger configuration in order to achieve the best possible cooling. As regards operation by tenside, this exchanger configuration must be found experimentally.

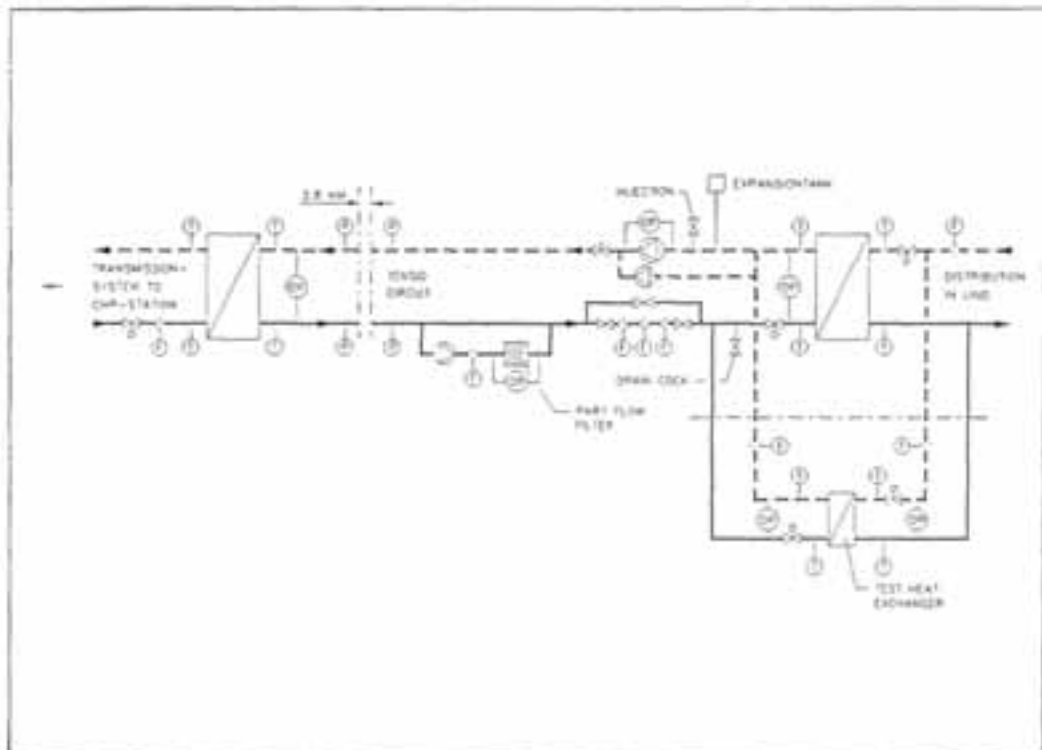


Fig. 3.1 Transmission system Lind - position of experiment plate heat exchanger

For reasons of supply security, it is not possible to deliberately make changes in the existing plate heat exchanger at the heat central in Lind. Therefore, a smaller experiment plate heat exchanger has been installed instead, in parallel to the existing plate heat exchanger. The position of the experiment exchanger is shown in fig. 3.1. The nominal effect of the existing plate heat exchanger is approx. 10 MW, while the nominal effect of the new one is approx. 0.7 MW i.e. featuring a size not affecting the heat supply in Lind. The experiment-plate heat exchanger was made available by APV Baker A/S who also followed the experiment during the whole period.

The test plate heat exchanger is provided with measuring equipment on both sides for flow and temperature and is designed in such a way that it is possible to change plate set combination and dimensions.

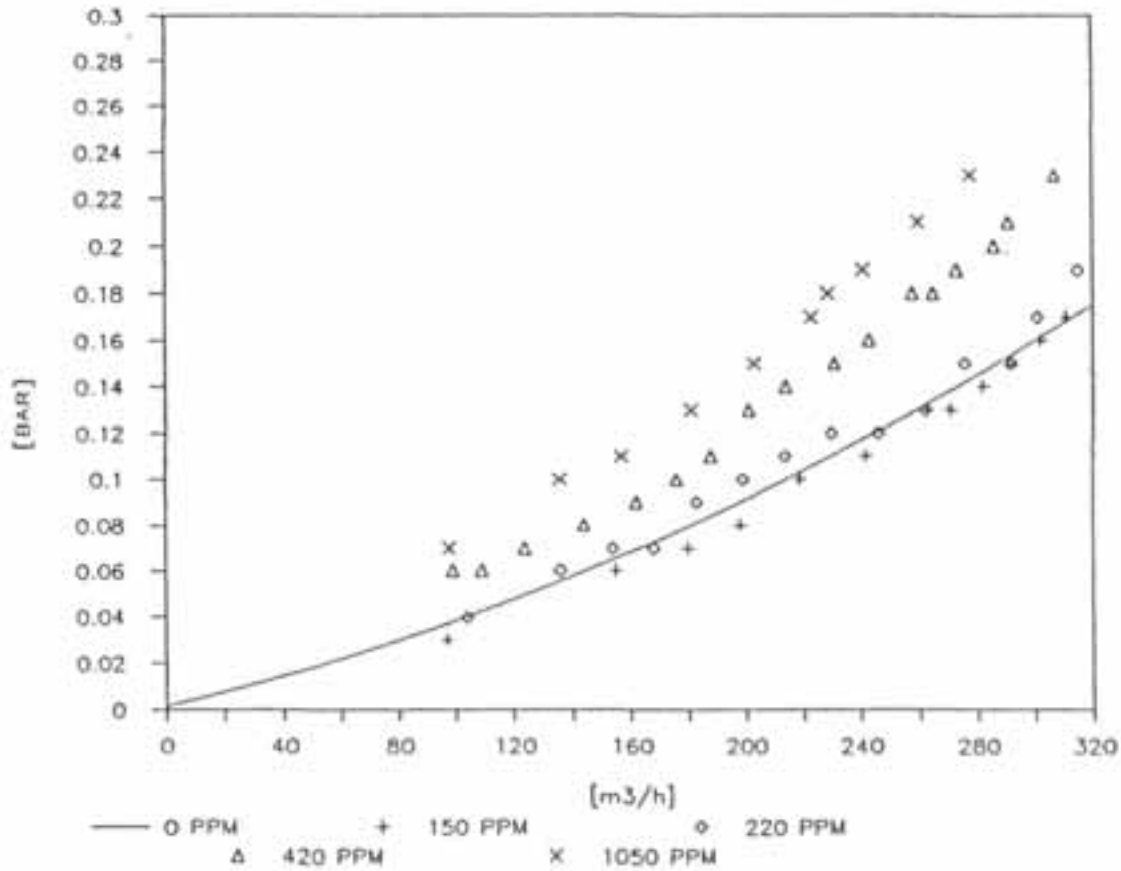


Fig. 3.4 Pressure loss in plate heat exchanger BV16 1989

As regards the pressure loss over the plate heat exchanger (see fig. 3.4) it has been observed that the pressure loss at tenside concentrations larger than approx. 250 ppm was larger than at corresponding ordinary district heating water. On the other hand, it has been observed that the pressure loss at concentrations below approx. 200 ppm is less than that for corresponding district heating water. In connection with this experiment, it has been estimated that the optimum tenside concentration as regards pressure loss for the entire system is approx. 220 ppm.

3.3 WORKING METHOD

3.3.1 Variable Parameters

As mentioned above, the purpose of the experiment was to observe the effect of adding tenside to district heating water as regards heat transmission in the exchanger, and afterwards to examine the possibilities of compensating for effects by re-building the plate heat exchanger. In order to carry out the experiment, different parameters were changed.

3.3.1.1 Variable Parameters within the Heat Exchanger:

- Plate angle which in this case varies from 30° (thermally short plates) to 60° (thermally long plates). These terms are explained under paragraph 3.5.2.
- The number of plates which in this case vary between a plate stack consisting of 23 plates and a plate stack consisting of 43 plates.

3.3.1.2 External Variable Parameters:

- The plate flow rate i.e. water velocity through the heat exchanger which in this case vary from 0 m/s to 1.5 m/s.
- Tenside concentration, which in this case varies from 0 ppm (i.e. ordinary district heating water) to 400 ppm.

The changes and the following measurements have been carried out according to the the experiment progress described in paragraph 3.3.4.

3.3.2 Data Collection

The measuring data consists of forward and return temperatures on both the primary side (tenside side) and the secondary side (Lind side) as well as the current flow on both sides of the exchanger. Moreover, the differential pressure is measured between the forward and return pipe on the primary side.

Measuring data are collected in a mobile data logger. Afterwards data are transferred to a PC and further processed.

3.3.3 Data Processing

The data logger collects data each five seconds and each metering series stretches over five minutes. Thus simple average values are calculated for the individual metering series. On the basis of these metering series it is possible to calculate the heat transfer coefficients (α) and the heat transmission coefficients (k) as a function of the water velocity in each individual case.

3.3.4 Execution of the Experiment

The measurements on the experiment exchanger, placed at the heating central in Lind, were carried out in the course of 1991 and the first few months of 1992.

The first experiment was carried out in May 1991, when tenside was not yet added to the district heating water. This experiment was to form the basis for comparison with tenside-enriched water. From the beginning, the heat exchanger plates were of the type "thermally long plates".

The results were presented to APV Baker A/S who found them in accordance with expectations, and consequently they constituted a good basis for later comparison.

In the initial experiments, the purpose was to obtain a "balanced flow" in the plate heat exchanger, i.e. the same flow on both sides of the exchanger. Experiments with the flow were carried out with volumes of approx. 2.5 m³/h to approx. 22.5 m³/h.

Parallel to the smooth water project experiments were carried out at 100 ppm and 400 ppm with the same exchanger configuration. Later, when the tenside concentration in the system was diluted to the estimated optimum concentration as regards pressure loss, experiments were carried out at 215 ppm.

As the differential pressure meter was defective during these three metering series, no metering data for differential pressure from these three experiments are available. Almost at the same time as when the long-term experiment was started (i.e. operation at the optimum tenside concentration at 215 ppm over a longer period), the plate stack was reduced by approx. 50%, corresponding to approx. 50% reduction in the heating area surface. Measurements were carried out for this plate heat exchanger configuration as well, and the differential meter was repaired at that time. In February 1992 the heat exchanger plates were replaced by "thermally short plates". The terms "thermally long plates" and "thermally short plates" are explained in paragraph 3.5.2. This experiment will be terminated when the main smooth water demonstration project ends, as it will then be possible to carry out reference measurements with ordi-

nary district heating water on both sides of the heat exchanger. Preliminary results indicate - not surprisingly - that the application of those plates will lead to considerably poorer heat transmission in the plate heat exchanger, however, a relatively modest pressure drop compensates for this.

3.4 MEASURING RESULTS

3.4.1 Data for Experiment Plate Heat Exchanger

The experiment plate heat exchanger used consisted in its first configuration of 43 pcs. thermally long plates and had a nominal heat output of approx. 0.7 MW.

Upon calculating the heat transfer coefficients (α) and the heat transmission coefficients (k) the following values were applied:

Plate wall thickness $S = 0.0006 \text{ m}$

Heat conductivity $\lambda = 14.9 \text{ W / m} \cdot ^\circ\text{C}$

The effective heat surface area having 43 plates in the plate stack is described as A.1 having 6.97 m^2 .

The effective heat surface area having 23 plates in the plate stack is described as A.2 having 3.57 m^2 .

3.4.2 Pressure Loss

Fig. 3.4.2 shows pressure loss as a function of the velocity in the heat exchanger with thermally long plates. As regards ordinary district heating water (0 ppm) a pressure loss over the exchanger was registered which is slightly higher than the theoretical values stated by APV Baker A/S. This might be caused by inaccuracy of the metering devices. The pressure loss at concentration of 215 ppm is below the values for 0 ppm. This confirms experience from earlier experiments (see fig. 3.4). As mentioned in paragraph 3.3.4, the differential pressure meter was defective during the experiments at 100 ppm, 400 ppm and 215 ppm with full-scale plate stack (43 plates) on the heat exchanger. Therefore there are no measuring results available for these concentrations.

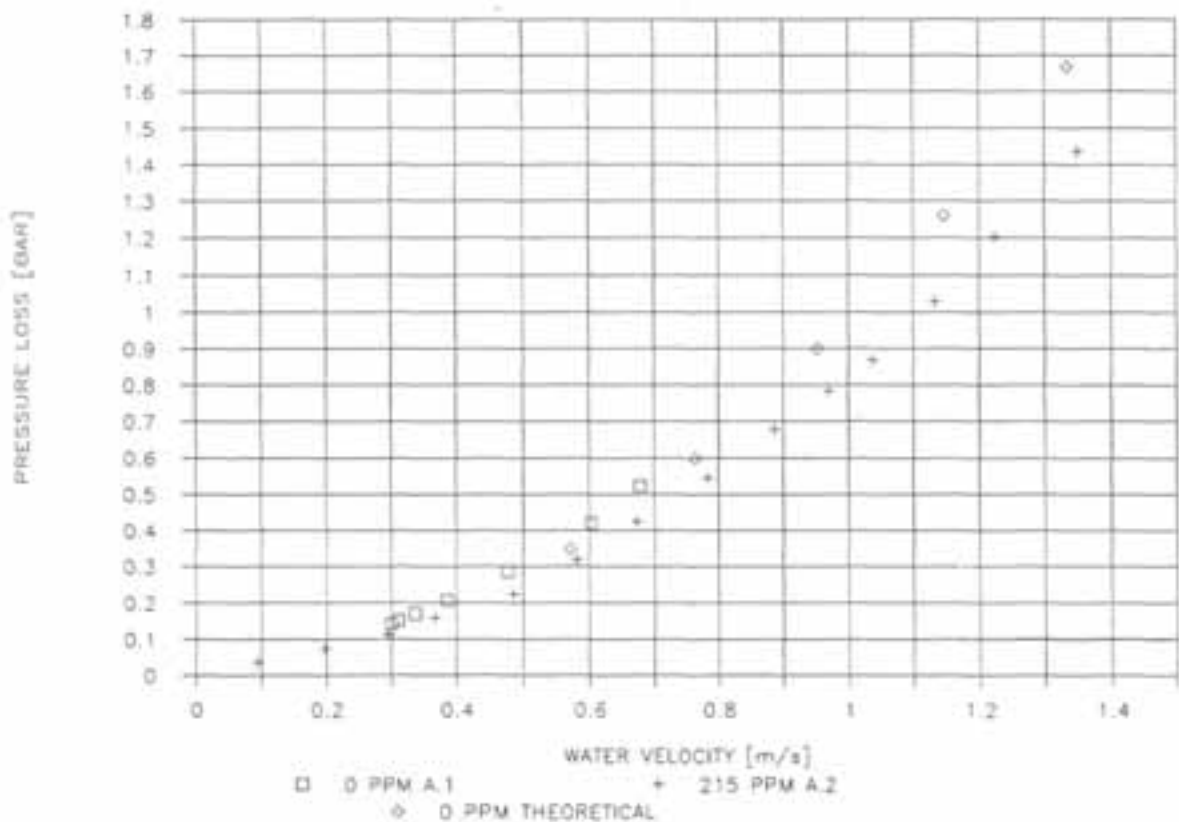


Fig. 3.5 Pressure loss in the experiment plate heat exchanger as a function of the water velocity in the exchanger. Thermally long plates.

3.4.3 Heat Transfer Coefficients (α)

According to theory the heat transfer in a heat exchanger is given by the following formula (formula 1):

$$Q = k \cdot A \cdot T_m$$

where

Q = transferred heat output [W]

k = heat transmission coefficient [W/m²·°C]

A = effective heat transfer area [m²]

T_m = the logarithmic mean temperature difference [°C]

Based on this formula the heat transmission coefficient k is calculated as Q, A and T_m are known factors.

Heat transmission coefficient k for a heat exchanger is also calculated by using the following formula (formula 2):

$$\frac{1}{k} = \frac{1}{\alpha_1} + \frac{S}{\lambda} + \frac{1}{\alpha_2}$$

α_1 and α_2 are heat transfer coefficients in the border area between medium and partition wall in the heat exchanger concerned. λ represents the heat conductivity in the partition wall and S is the thickness of the wall.

In the reference measurements with ordinary district heating water (0 ppm) on both sides of the exchanger and balanced flow, it is possible to determine the heat transfer coefficient, as it will be the same coefficient on both sides of the heat exchanger. The value is calculated according to the following re-writing of formula 2 combined with formula 1:

$$\alpha_1 = \alpha_2 = \frac{2}{\frac{1}{k} - \frac{S}{\lambda}} = \frac{2}{\frac{A \cdot T_m}{Q} - \frac{S}{\lambda}}$$

The full curve on fig. 3.6 shows the heat transfer coefficient for ordinary district heating water as a function of the water velocity in the heat exchanger (the curve is adjusted to the calculated values). When tenside is added on the primary side, the heat transfer coefficient on this side of the exchanger (α_1) will be the only unknown factor in formula 2, as α_2 will be given for each water velocity on the secondary side and the heat transmission coefficient can be calculated. α_1 is calculated by using the following rewriting of formula 2:

$$\alpha_1 = \frac{1}{\frac{1}{k} - \frac{S}{\lambda} - \frac{1}{\alpha_2}}$$

Thus fig. 3.6 shows the heat transfer coefficient on the primary side for different tenside concentrations as a function of the velocity in the heat exchanger. In the earlier experiment it was only possible to increase the water velocity in the heat exchanger to a limited extent - from 0 - 0.3 m/s. Thus it has not been possible to examine how the heat transfer conditions will turn out to be in the case of relatively high velocities. In this experiment it has been possible to carry out measurements at velocity intervals ranging from 0 - 1.5 m/s. These high velocities are obtained by halving the number of plates on the heat exchanger. This happened when the tenside concentration in the system was 215 ppm. We assume 215 ppm is the optimum concentration regarding the pressure loss in the entire system. Fig. 3.6 indicates that the heat transfer coefficients for tenside solution are considerably lower than those for ordinary district heating water in lower velocity regions.

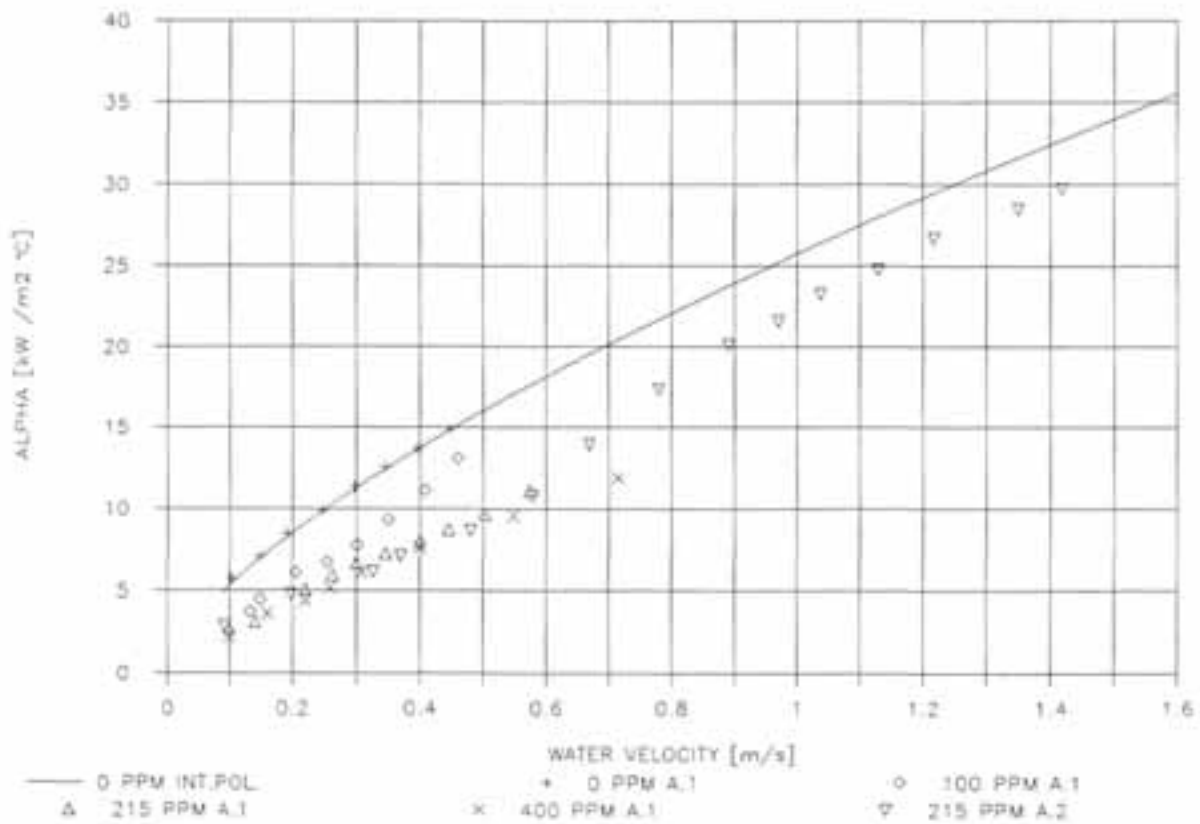


Fig. 3.6 Heat transfer coefficient (α). Thermally long plates.

Moreover, it can be stated that the heat transfer coefficient decreases in the case of increasing tenside concentrations. But on the other hand, it can clearly be stated that the heat transfer coefficient, at a given velocity depending on the present tenside concentration, approaches and adopts a value which is only app. 10% below the value for ordinary district heating water. E.g. it can be seen that this happens at approx. 1.0 m/s at 215 ppm.

3.4.4 Heat Transmission Coefficient (k)

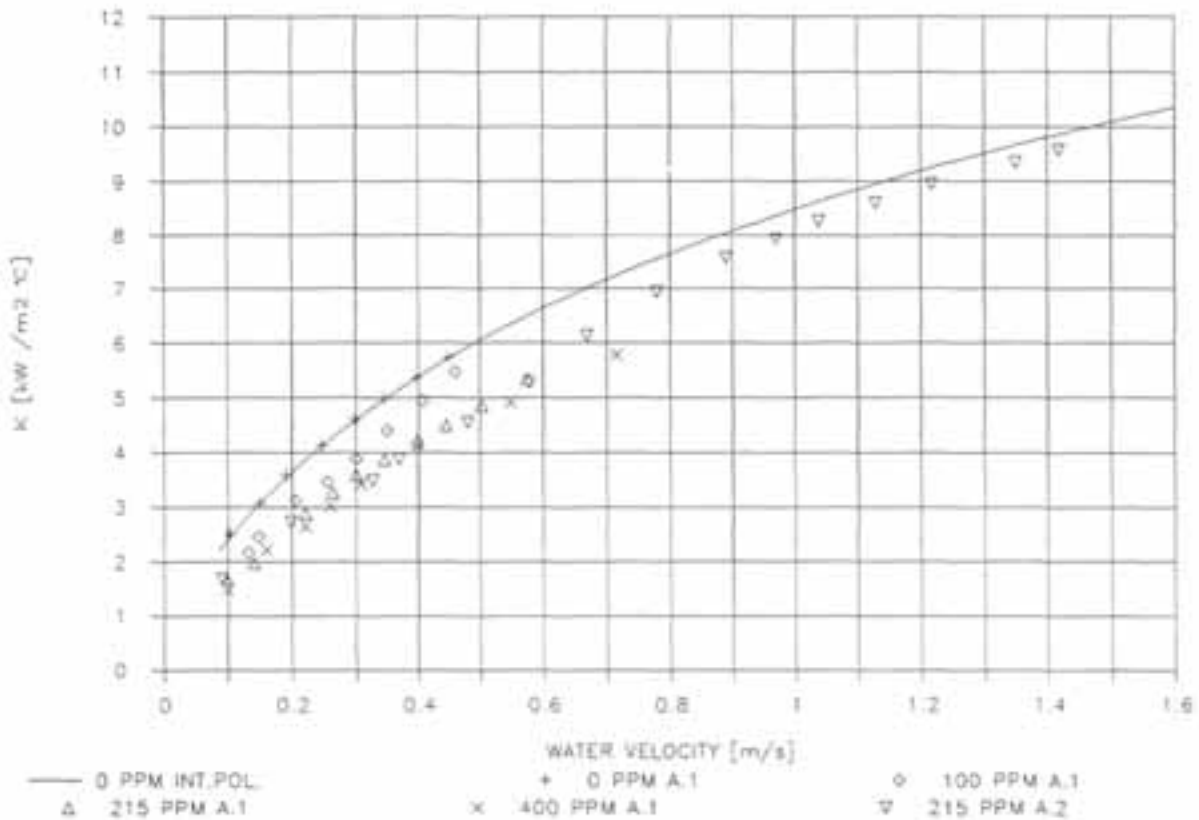


Fig 3.7 Heat transmission coefficient (k) as a function of the water velocity in the heat exchanger. Thermally long plates.

The graph in fig. 3.7 shows the calculated heat transmission coefficients as a function of velocity in the heat exchanger at balanced flow. The tendency observed in the *a* graph, i.e. the fact that the heat transfer coefficient at relatively high velocities in the heat exchanger reaches a level which is only a little below the corresponding level for ordinary district heating water, is clearly underlined. Once again, it can be seen that the higher the tenside solution the higher is the water velocity required before the heat transmission coefficient for ordinary district heating water is approached. In this case the discrepancy is only app. 5%. The reason why the *k*-value curve for 215 ppm is closer to the reference curve than what could be observed for the heat transfer values at the same tenside solution is that by calculating the heat transmission coefficients (*k*-values) the units $1/a^2$ and s/λ are included. a^2 values are values for ordinary district heating water (0 ppm).

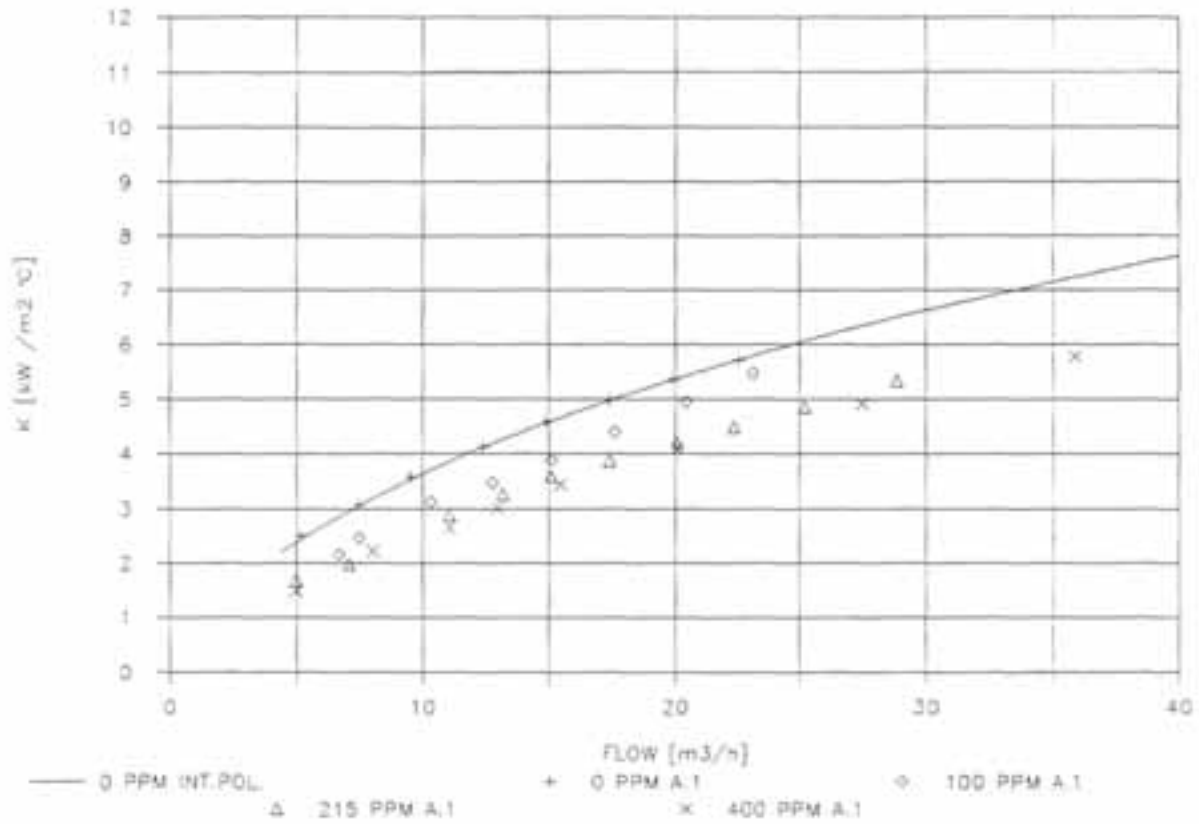


Fig. 3.8 Heat transmission coefficient (k) as a function of the total water flow in the heat exchanger (A.1). Thermally long plates.

The graph in fig. 3.8 shows the calculated heat transmission coefficient as a function of the total water flow in the heat exchanger at full-scale plate stack (43 plates).

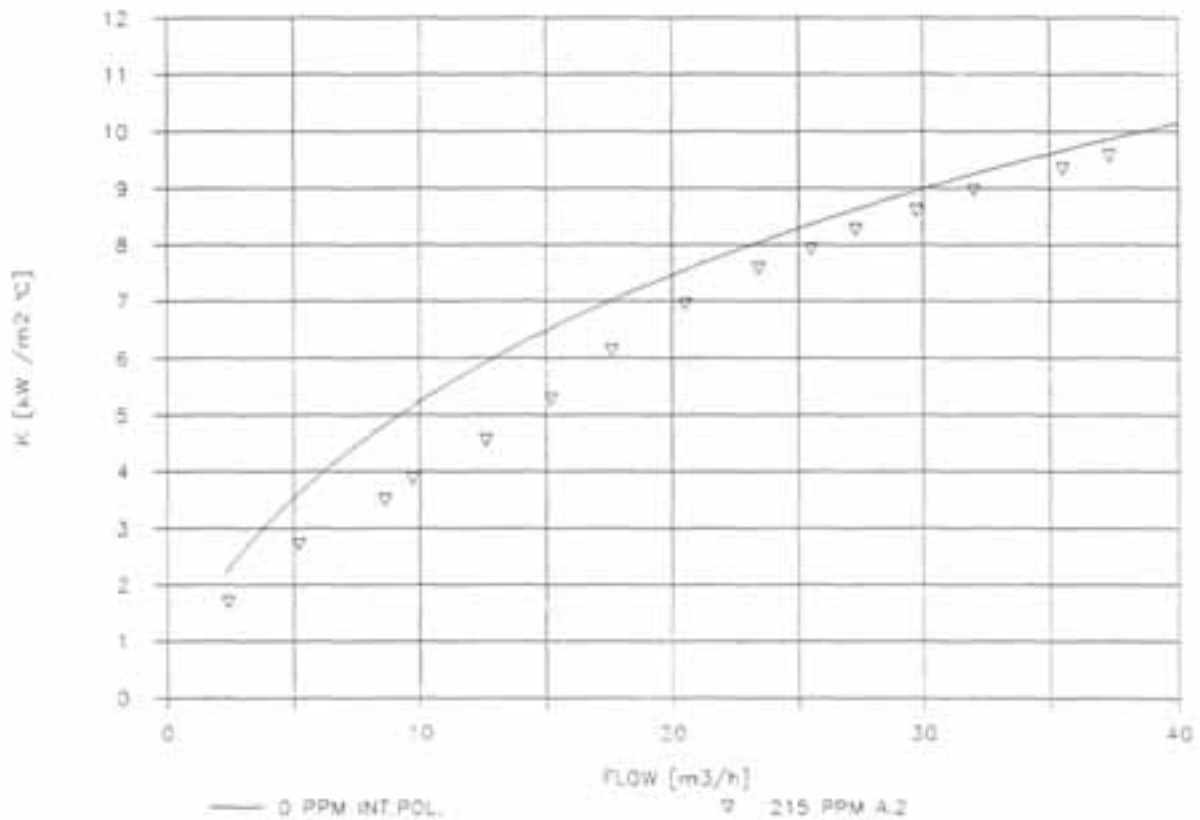


Fig. 3.9 Heat transmission coefficient (k) as a function of the total water flow in the heat exchanger (A.2). Thermally long plates.

The graph in fig. 3.9 shows the calculated heat transmission coefficients as a function of the total waterflow for 50% of the plate stack (23 plates). The reduction of the heat surface area involves a reduction of the total plate gap area, i.e. a better heat transmission coefficient can be achieved at the same flow because of the increased water velocity in the heat exchanger. On the other hand, due to the reduced effective heating surface area it will not be possible to maintain the necessary heat output at the same flow.

3.5 EVALUATION AND COMPARISON OF DIFFERENT PLATE HEAT EXCHANGER CONFIGURATIONS

There are various methods of compensating for heat transfer reduction in various ways when friction-reducing additives are used for district heating systems.

The use of a friction-reducing additive will result in reduced heating transfer capacity from the primary to the secondary side in the heat exchanger equipment. The reduction dimension depends on the tenside concentrations. It also depends on the velocity, just as is the case for district heating water.

In this section, the various possibilities of compensating for this reduction for a plate heat exchanger is described in a draft.

The optimum method of compensating for reduced heat transfer coefficient will depend on the operation parameters of the actual installation and, of course, the financial resources available.

3.5.1 Increase in the Number of Plates

The heat transfer area in the plate heat exchanger can be increased by simply increasing the number of plates in the plate stack.

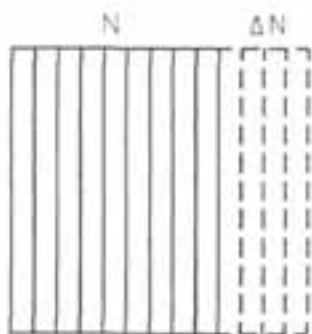


Fig. 3.10 Increase in number of plates

In case the number of plates, and thereby the total effective heating surface are extended, the total plate gap area will be extended too. Given that the total water flow through the heat exchanger remains at the same level, a reduction in the water

velocity in the heat exchanger will be caused. The heat transmission coefficient will therefore be lowered, independent of a possible tenside addition.

3.5.2 Change of Plate Angle

By making the the angle of the wavy section on the plate larger relative to the vertical line, increased heat transmission coefficient for the heat exchanger is achieved, provided the heat transfer area remains the same.

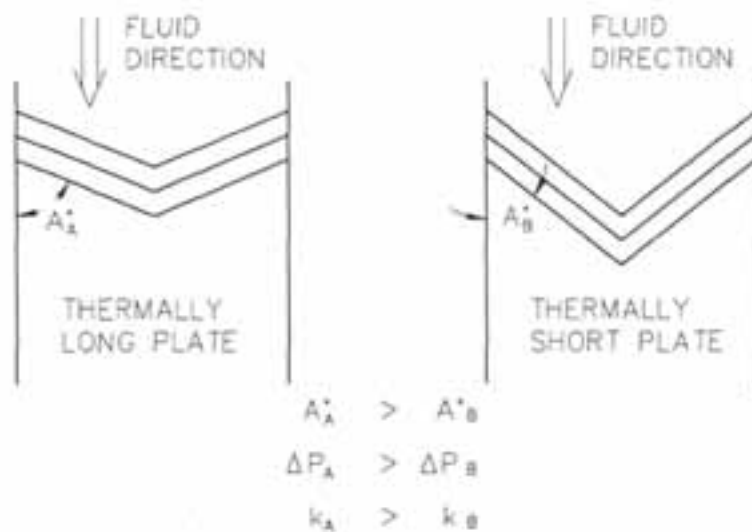


Fig. 3.11 Change of plate angle

A large angle corresponds to the "thermally long plates" which are characterized by good heat transmission properties combined with large pressure loss over the plates. A small angle corresponds to the "thermally short plates" which are characterized by a relatively poorer heat transmission combined with a relatively small pressure loss over the plates.

3.5.3 Multipass Plate Heat Exchanger

Increasing the thermal length of the plate heat exchanger by changing it to a so-called multipass machine will increase the length at which the fluid must pass. Thereby it is ensured that the desired outlet temperatures are achieved despite the heat transmission coefficient reduction.

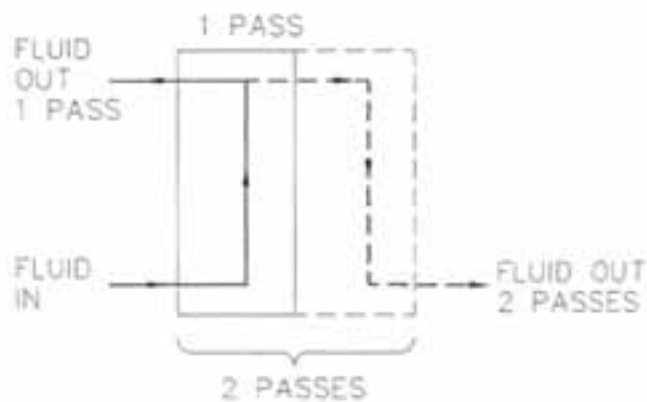


Fig. 3.12 Multipass plate heat exchanger

An increase in pressure drop will be the result.

3.5.4 Longer Plates

The plate heat exchanger plates are manufactured in various lengths but with the same geometry.



Fig. 3.13 Longer plates

Therefore, an elongated plate could compensate for reduced heat transmission coefficient without changing other parameters except for the pressure drop which would, of course be, correspondingly higher.

3.5.5 Other Plate Dimensions

As a last possibility, other plate types might be used. Either larger plates or a thermally harder plate (smaller plate gap).



Fig. 3.14 Other plate dimensions

3.5.6 Calculation Examples for Different Heat Exchanger Combinations, Smooth Water Applications and Ordinary District Heating Water Applications

As described in the previous sections, the design of a heat exchanger will greatly influence the output of a given heat exchanger, and the cooling of the district heating water in it.

To illustrate this, a number of calculation examples have been made. The point of departure is a heat exchanger in which the heat-carrying medium is ordinary district heating water (fig. 3.15). In the other examples, the heat-carrying medium is smooth water. The secondary side conditions are the same as regards forward and return temperatures. Flow is the same in all examples. On the primary side, the forward temperature is the same whereas return temperature and flow which are stated in parentheses, will vary from the reference example in the other examples.

There is no direct connection between the calculation examples and the experiment heat exchanger as the experiment heat exchanger is different as regards configuration and output. Thus the results have not been reached by measurements, but by calculations on the basis of fixed parameters. Experience from the experiments of determining the k-values have been applied in the examples for which smooth water on the the heat exchangers primary side was used. The purpose of the calculation method was to satisfy both of the following equations:

$$Q = k \cdot A \cdot T_m \quad \text{and}$$

$$Q = c_p \cdot \Delta t \cdot q$$

where

Q = transferred heat output [W]

k = heat transmission coefficient [W/m²·°C]

A = effective heat transfer area [m²]

T_m = the logarithmic mean temperature difference [°C]

c_p = 4190 J/kg·°C

Δt = temperature difference [°C]

q = flow, primary side [kg/s]

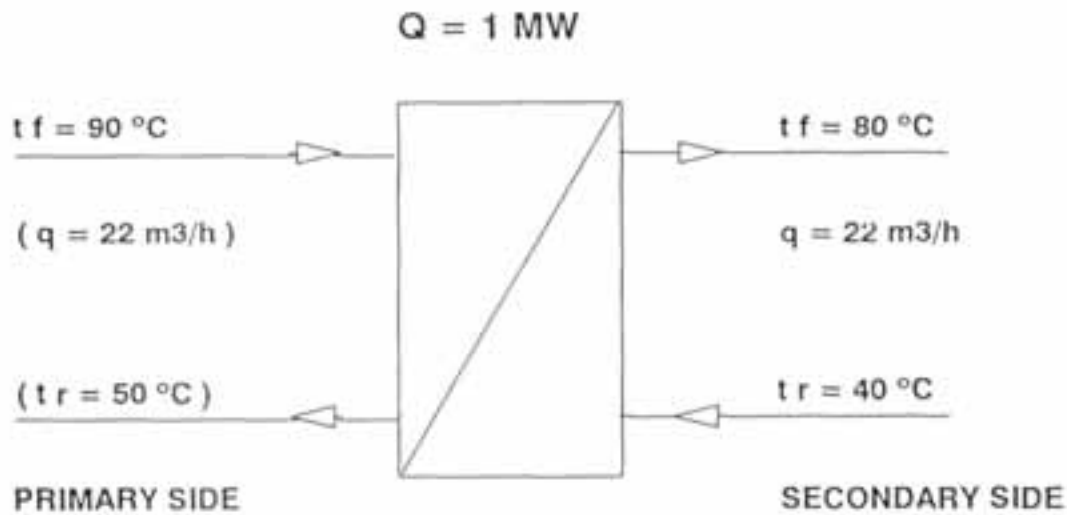


Fig. 3.15 Reference conditions

In all examples, heat exchanger output is 1.0 MW and the various heat exchanger configurations are stated in the table in fig. 3.16

	TENSIDE-SOLUTION	HEAT TRANSFER AREA [m ²]	NO. OF PASSES	TYPE OF PLATE	
1	0 ppm	20.65	1	T. L.*	
2	215 ppm	20.65	1	T. L.	
2A	215 ppm	22.05	1	T. L.	+10%
2B	215 ppm	30.45	1	T. L.	+50%
2C	215 ppm	40.95	1	T. L.	+100%
3	215 ppm	20.65	2	T. L.	
4	215 ppm	21.50	1	T. L.	ELONGATED
5	215 ppm	30.98	3	T. S.**	

*THERMALLY LONG **THERMALLY SHORT

Fig. 3.16 Heat exchanger configurations

All heat exchanger configurations in ex. 2A-C are variants of configuration 2. In these three examples, the heat transfer area has been increased by 10%, 50%, and 100% respectively. This means that the total plate gap area is increased by these percentages. This measure is described in section 3.5.1.

In the heat exchanger configuration in ex. 3, a double-pass system has been used which is described in section 3.5.3.

The configuration of ex. 4 with elongated plates is described in section 3.5.4.

The configuration in ex. 5 is a combination of a multipass system and the application of thermally short plates which is described in sections 3.5.3. and 3.5.2 respectively.

Under the given conditions, operating conditions for the various exchanger configurations are as stated in the table in fig. 3.17.

	FLOW [m ³ /h]	VELOCITY [m/s]	PRESSURE LOSS [BAR]	HTC# [W/m ² *°C]	t _r [°C]
1	22.0	0.24	0.13	4825	50.0
2	25.9	0.28	0.16	3900	55.5
2A	25.5	0.26	0.14	3700	55.0
2B	23.5	0.17	0.09	3000	52.0
2C	22.5	0.12	0.07	2400	50.5
3	20.8	0.45	0.54	5600	47.5
4	22.5	0.33	0.24	4500	50.5
5	21.0	0.45	0.25	3600	48.0

#HEAT TRANSMISSION COEFFICIENT

Fig. 3.17 Operating conditions

As appears from ex. 2C, operating conditions can be achieved that are very close to those for the reference system by increasing the heat transfer area by 100%. When the heat transfer area is increased, velocity, and thereby transmission coefficient, are reduced. A further advantage of this configuration is a considerable reduction in pressure loss in the heat exchanger.

From ex. 3 it appears that a high level of cooling of district heating water can be achieved by applying a double-pass system. However, pressure loss in the exchanger will be relatively high when this exchanger configuration is applied.

Fig. 3.18 is a rough drawing of the pressure loss in the exchanger in relation to the pressure loss in the rest of the system for the Herning/Lind demonstration circuit. It can be concluded that when applying tenside it is appropriate to increase the water velocity in the heat exchanger thereby increasing the pressure loss.

Curve 1 shows the pressure loss as a function of the flow for the total system when single-pass exchangers at both ends of the transmission pipe, and ordinary district heating water are used.

Curve 2 shows the pressure loss as a function of the flow for the total system when double-pass exchangers at both ends of the transmission pipe, and a tenside solution of 215 ppm are used.

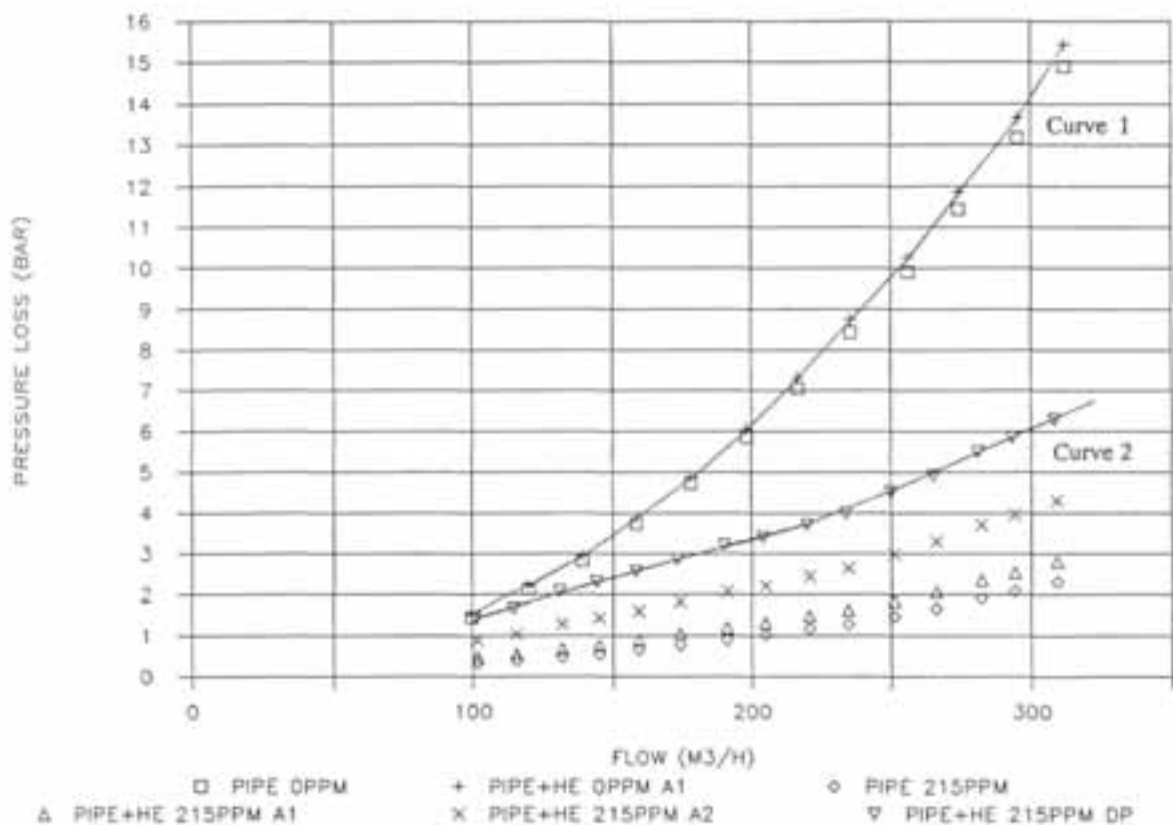


Fig. 3.18 Transmission system, Lind - Pressure loss in pipes and plate heat exchangers

It shows that the benefit of reducing the pipe loss has not been wasted, as the total pressure loss is app. 40% of the loss that applies to ordinary district heating water with "single-pass" at both ends of the transmission pipes.

In ex. 4 the configuration with elongated plates offers operating conditions that are very similar to those of the reference system. However, pressure loss in the exchanger is somewhat higher because of the reduced plate gap area and the elongated plates.

Ex. 5 with a combination of a multipass system and thermally short plates offers very favourable operating conditions. The results of these calculations should however not be seen as final as the measurements for the thermally short plates are not yet terminated.

3.6 Conclusion

From a heat transmission point of view, it will, as regards operation with tenside, be an advantage to increase the velocity in the heat exchanger to such an extent that the heat transmission coefficient approaches the reference heat transmission coefficient at 0 ppm as closely as possible (refer to fig. 3.7). By how much the velocity can be increased depends on how large the acceptable pressure loss over the heat exchanger is. A possibility of increasing the velocity will be operation with a "multipass machine" described under paragraph 3.5.3. This operation mode has a disadvantage with respect to installation, as it will be impossible to keep the pipe connections collected in the one end of the heat exchanger. Firstly, it will entail space problems, but it will also make it difficult to replace the plates. Moreover, it must be expected that there will be a relatively large pressure loss over the heat exchanger.

Taking as a starting point the problems involved in this experiment, it was stated that a higher velocity in the heat exchanger could be reached by reducing the plate stack and thus the total plate gap area. By reducing the heating surface area, i.e. the heat transfer area. However, this will also be reduced causing the nominal effect to be lowered. The solution to this problem will be to take steps as described under paragraph 3.5.4, i.e. to make the plates longer. Thus the desired higher velocity in the exchanger can be achieved while the heating surface area is maintained. It has not been possible to carry out experiments with this kind of plates under the given circumstances, as this would require an other shape of the plate heat exchanger rack.

As appears from the calculation examples in paragraph 3.5.6, the problem can probably be solved by increasing the heat transfer area by app. 100% which the measuring results also do indicate. However, this measure will take up much space, and will in most cases entail the replacement of the existing rack.

Thus there will be various methods of solving the problems that arise when of smooth water is used in the plate heat exchangers. The appropriate solution must be chosen on the basis of the given conditions in each case. The present report is thus to be considered as a tool for dimensioning heat exchangers in connection with operation with smooth water.

4. ENVIRONMENTAL EFFECTS OF SURFACTANT FRICTION REDUCTION ADDITIVES

J. Helmig, A. Steiff, P.-M. Weinspach
University of Dortmund
Germany

4.1 INTRODUCTION

In the last years district heating systems have become more important for the supply of heat for households and industry. To reduce the costs for district heating systems cationic surfactants have been investigated for their suitability as drag reducing additives. By adding of cationic surfactants to the network water it is possible to reduce the pressure loss in the pipe system considerably. Thus the costs for the pumping of the water can be decreased [1, 2].

A further aspect of adding surfactants is the decrease of heat loss in the pipe system because when there is a reduction of the pressure loss there is a corresponding reduction of heat loss.

Two main advantages may result from the use of surfactants:

- It is possible to save costs for the operation of a district heating network or
- the capacity of existing plants can be extended.

With respect to the special requirements that drag reducing additives must meet, quaternary ammonium salts showed the most promising results. They are effective up to temperatures of about 140°C and they are stable over a long period of time. The maximum concentration of these additives would be 1,500 wppm.

First demonstration projects (in Völklingen, Germany) showed promising results for the application of drag reducing additives in transport systems with straight pipes. In distribution systems, which have a branched structure, the drag reducing effect will not be so significant. This means that for the present surfactants will only be added to transport systems.

For the application of surfactants as drag reducing additives in district heating networks their influence on the operation behaviour must be known. This means the normal operation and also in the case of an accident. Although the networks are designed as closed systems the possibility that the surfactant solution gets out of the system should be investigated. In this case the special behaviour of the surfactant solution has to be known.

To prevent any risks, measures against leakages and penetration into the boiler feed water will be demonstrated. For a possible extended application of additives in a complete district heating system measures against a penetration into the water circuits at customers installations are also regarded.

In this study the hazard potential of the surfactants will be assessed. In a first step literature data are collected and compared with the special data for the drag reducing additives.

The mobility of surfactants when they enter the environment will be investigated in adsorption experiments.

After examining the literature and reviewing the results of all tests it should be possible to give a final statement for the application of surfactants. This includes possible modifications for the operation of the network system.

4.2 SURFACTANTS

4.2.1 General Properties of Surfactants

Surfactants are substances with great interfacial activities. They will accumulate at all interfaces like gas/liquid, solid/liquid and solid/gas. This behaviour is caused by the asymmetric structure of the surfactant molecules. The molecules are composed of a hydrophilic (water soluble) and a hydrophobic (non water soluble) part.

The hydrophobic molecule part is mostly an n-alkyl chain; the hydrophilic head group a polar or an ionic group.

Surfactants are divided into four groups:

- non-ionic surfactants,
- anionic surfactants,
- cationic surfactants and
- amphoteric surfactants.

In the case of ionic (anionic or cationic) surfactants counterions with the opposite charge to the surfactant will also be present.

Because cationic surfactants are especially suitable as drag reducing additives in district heating networks these kinds of surfactants are considered in the following.

Surfactants show a special solution behaviour in water. In a lower temperature range they are almost insoluble in water but when the temperature exceeds the so-called *Krafft-temperature* the solubility increases considerably. This increase in solubility is caused by the formation of micelles which are agglomerates of about several hundred molecules (Figure 4.1).

The concentration above which micelles are formed is called the *critical micelle concentration I* (cmc_1). The form of the micelles is first spherical, with a diameter of about two times the length of a single molecule.

At higher concentrations the spherical micelles transform to rodlike micelles. The concentration is called *critical micelle concentration II* (cmc_{II}) or *transition concentration* (c_t).

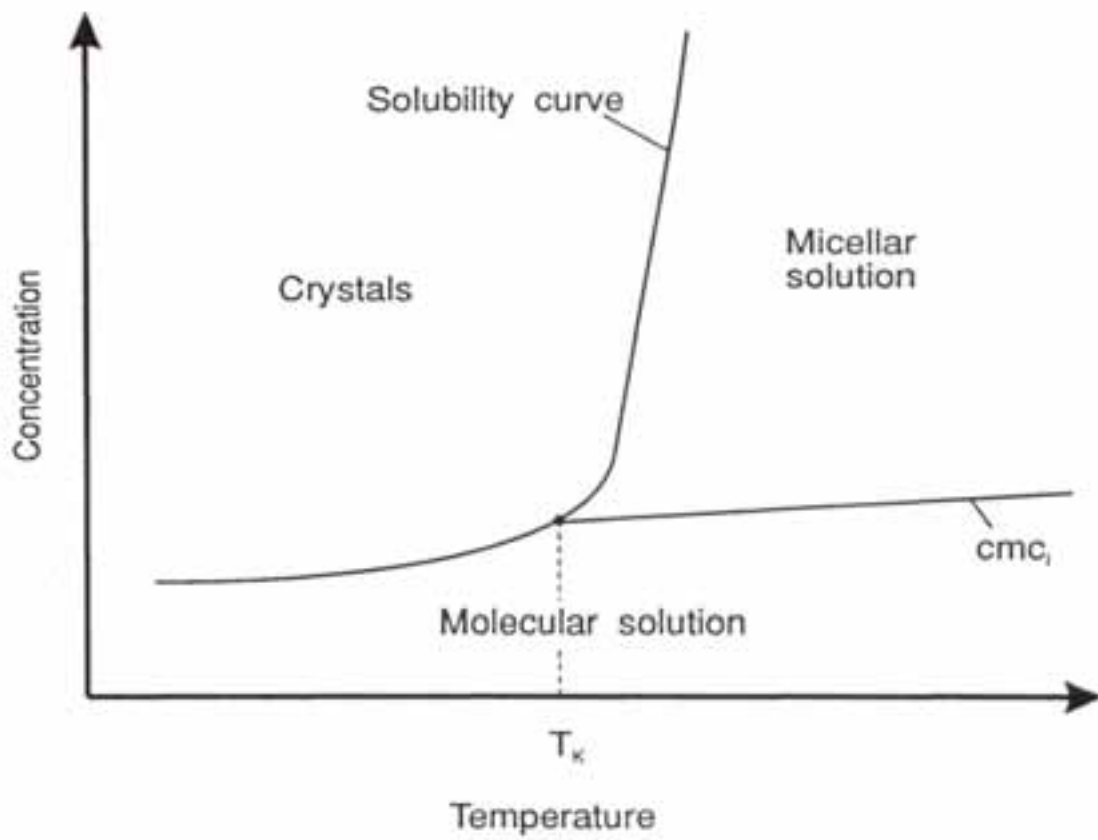
The rodlike micelles grow in length with increasing concentration.

Another characteristic feature of surfactants is their adsorption tendency to all surfaces. There are two possibilities for the surfactant molecules to interact with the surface: by the hydrophobic tail or by the hydrophilic headgroup. The mechanism depends on the characteristics of the surface.

The adsorption equilibrium can be described by the adsorption isotherm, which shows the amount of adsorbed surfactant in relation to the equilibrium concentration of the surfactant in the solution. The adsorption isotherm for cationic surfactants normally can be divided into four segments (Figure 4.2) [3].

Figure 4.1:

Solution Behaviour of Cationic Surfactants in Water



1. The molecules adsorb in single form at the surface. There is no interaction between the molecules.
2. A monolayer has been formed; the surface is saturated. The isotherm reaches the first plateau.
3. By hydrophobic effects the surfactant molecules form *hemimicelles*. The adsorption increases again.
4. When the equilibrium concentration in the solution exceeds the cmc_1 a second plateau is reached. No further increase in the amount of adsorbed surfactant is possible.

For a homologous series of surfactants the concentration at which the saturation point is reached depends on the length of the alkyl chain. When the length of the alkyl chain is increased, the saturation concentration is reduced. The amount of adsorbed surfactant in the plateau region, however, is unaffected by the chain length [4].

When a reduced equilibrium concentration c/cmc_1 is used, one single curve results for the adsorption isotherms of a homologous series of cations.

4.2.2 Structure of the Surfactants Used as Drag Reducing Additives

Due to the formation of rodlike micelles cationic surfactants are suitable to reduce the pressure drop in turbulent pipe flow.

The best results can be obtained with *quaternary ammonium salts* with organic counterions. To adapt the effective temperature range of the drag reducing additives to different requirements of district heating systems (temperature of the return pipe = lower temperature limit, temperature of the supply pipe = upper temperature limit) the surfactants vary according to the length of the n-alkyl chain. The n-alkyl chain length of the surfactants are in the range of $n=16$ to $n=22$ (Figure 4.3).

The *n-alkyldimethylpolyoxethylammonium* - compounds have similar properties as the *n-alkyltrimethylammonium* - compounds. Today the *n-alkyldimethylpolyoxethylammonium* - compounds are preferred because they are easier to produce.

The counterion of the surfactants is always *3-hydroxy-2-naphthoate*; *salicylate* is only an additional counterion which is used to enlarge the temperature range of the drag reducing effect.

All these surfactants are manufactured by the *Hoechst AG*, Frankfurt (Germany).

The main data relating to the solution behaviour of these surfactants in water are summarized in Table 4.1.

When the length of the n-alkyl chain increases, the cmc_1 is lowered and the *Krafft-temperature* increases.

One important conclusion from these data is that the surfactants will precipitate when the temperature of the solution is less than the *Krafft-temperature* for each surfactant. But the crystals are very easily redissolved when the temperature is increased again.

Figure 4.2:

General Shape of the Adsorption Isotherm of
Cationic Surfactants on Soils
(Reproduced from [3])

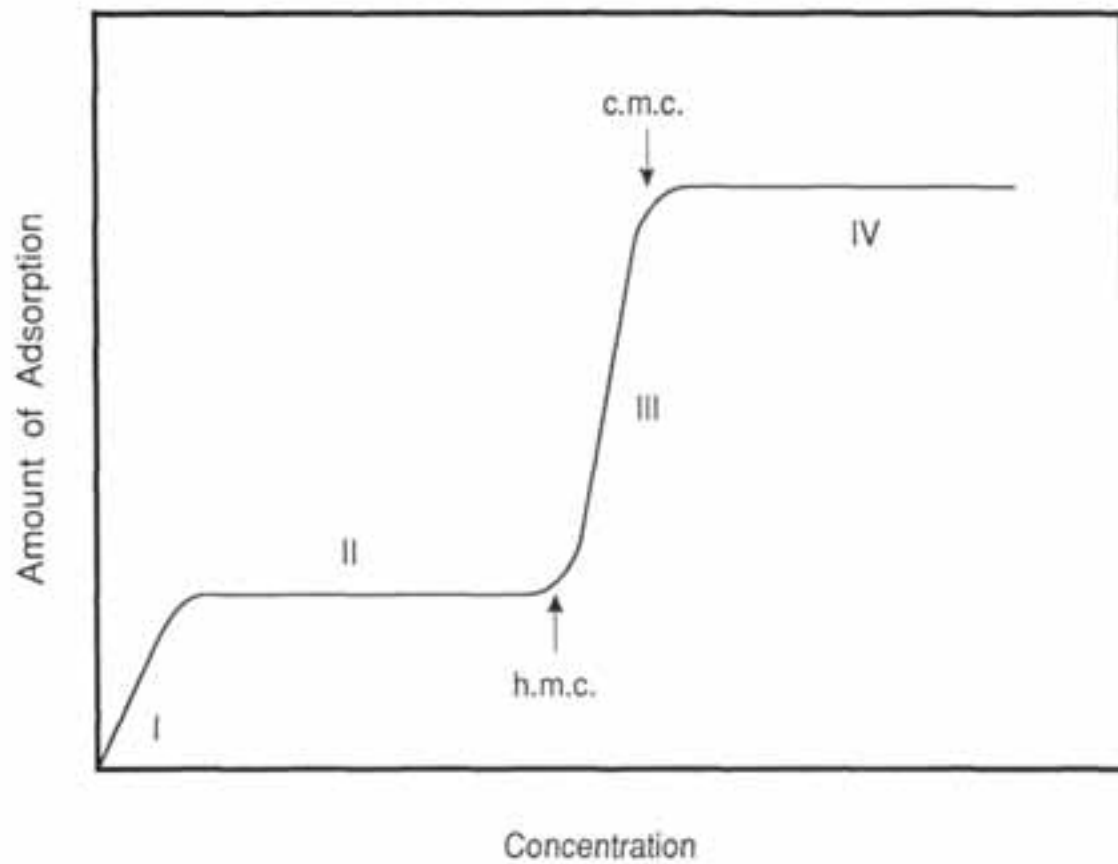


Figure 4.3:

Chemical Structure of the Cationic Surfactants which are Suitable as Drag Reducing Additives

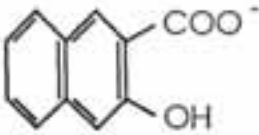
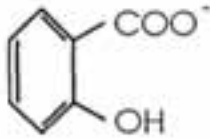
Trade-name	Quaternary ammonium-cation	Counterion
HABON	$\left(C_n H_{2n+1} - \overset{\text{CH}_3}{\underset{\text{CH}_3}{\text{N}}} - \text{CH}_3 \right)^+$ n=16 n-Alkyltrimethylammonium	 3-hydroxy-2-naphthoate
HABON-G	$\left(C_n H_{2n+1} - \overset{\text{CH}_3}{\underset{(C_2H_4O)_x H}{\text{N}}} - \text{CH}_3 \right)^+$ n=16 n-Alkyldimethylpolyoxethylammonium	 Salicylate (additional)
OBON	$\left(C_n H_{2n+1} - \overset{\text{CH}_3}{\underset{\text{CH}_3}{\text{N}}} - \text{CH}_3 \right)^+$ n=18	
DOBON	$\left(C_n H_{2n+1} - \overset{\text{CH}_3}{\underset{\text{CH}_3}{\text{N}}} - \text{CH}_3 \right)^+$ n=22	

Table 4.1:

Solubility Data for the Drag Reducing Additives
n-alkyltrimethylammonium-3-hydroxy-2-naphthoate

Surfactant	Krafft-temperature	Critical micelle concentration I	
	[°C]	[wppm]	[mmol/l]
HABON	25	30	0.063
OBON	35	10	0.020
DOBON	45	6	0.011

4.3 DESIGN AND OPERATION OF DISTRICT HEATING NETWORKS

4.3.1 Normal Operation

District heating networks are closed systems which transport heat from a power plant to the consumers. The transport medium is water.

The networks can be divided into two types:

1. Primary networks have a direct pipe system from the producer to the household stations.
2. Secondary networks are subdivided by heat exchangers into a transport system and one or more supply systems.

In the housesubstations two kinds of installations are typical (see also 4.7):

1. Direct housestations:
The district heating water goes directly through the radiators and the heat exchangers for the hot water production.
2. Indirect housestations:
The district heating system is separated by a heat exchanger from the consumer system.

In some cases, an intermediate circuit has to be installed for the heating of drinking water, especially if foreign substances (corrosion inhibitors) are added to the network water.

The quality of the network water is normally very pure. To prevent corrosion in the network system the network water must meet some requirements (Table 4.2).

To guarantee these properties the water is purified in a bypass purification stage. The water is cleaned by ion exchangers and a degassing stage to remove salts and oxygen.

Another possibility to guarantee these properties is to purify the additional water which is continuously added to the network system.

Chemicals which are normally added to the network water are *sodium hydrozide (NaOH)* to regulate the pH, oxygene binding agents or special corrosion inhibitors.

4.3.2 Operation with Drag Reducing Additives

The maximum concentration of the drag reducing additives in a district heating system can be 1,500 wppm (1.5 g/l). In this concentration range the surfactants raise the electrical conductivity considerably and lower the surface tension of the network water. This may have consequences for the corrosion behaviour and the foaming of the water.

A further point is the question whether these substances have toxic properties, because, in the case of an accident, it is possible that the surfactant solution gets into the environment or into subsystems of the network.

Table 4.2:

Quality of the Network Water of District Heating Systems (from [5])

Electrical conductivity	$\mu\text{S}/\text{cm}$	None saline		Saline
		10 - 30	> 30 - 100	> 100 - 1,500
General requirements	-	clear, no sediment		
pH	-	9 - 10	9 - 10.5	9 - 10.5
Oxygen (O_2)	mg/l	< 0.1	< 0.05	< 0.02
Alkaline earths	mmol/l	< 0.02	< 0.02	< 0.02
Phosphate	mg/l	< 5	< 10	< 15
With use of oxygen binding agents:				
Diamide N_2H_4^*	mg/l	0.3 - 3	0.3 - 3	0.3 - 3
Sodium sulphite Na_2SO_3	mg/l	-	-	< 10

*Only for systems without direct heating of drinking water

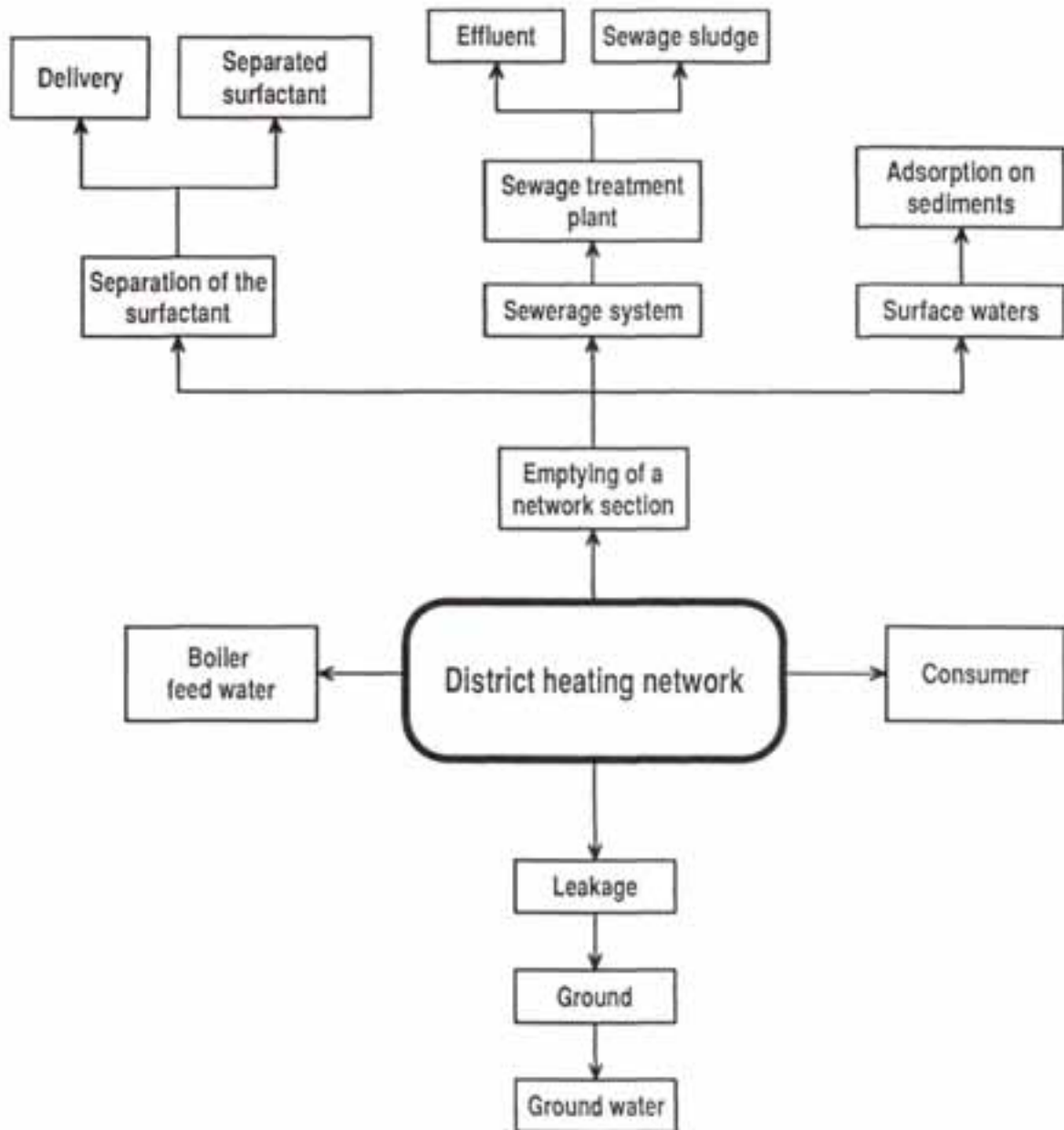
The following pathways have to be investigated (Figure 4.4):

1. The possibility of a leakage in the district heating system and the penetration into the ground or into surface waters. (This problem is mainly relevant to distribution systems).
2. When a section of the network must be drained off because of repair work, a procedure for the handling of the surfactant solution is required.
3. The surfactants will influence the purification steps. The latter must be modified.
4. In the case of an leakage in the heat exchanger at the power plant the surfactant solution can penetrate into the boiler feed water.
5. The surfactant solution can penetrate into the water for domestic use (only relevant if surfactants are added to direct systems; this is not planned yet)

For all these situations it is necessary to assess the hazards associated with the surfactants and to know their special behaviour.

Figure 4.4:

Possible Pathways for the Surfactants in the Environment



4.4 ENVIRONMENTAL HAZARDS ASSOCIATED WITH SURFACTANTS

To assess the environmental hazards of a chemical it is important to examine a lot of properties:

- Sources and quantity of the emitted substance
- Mobility
 - solubility in water
 - vapour pressure
 - boiling point and melting point
 - *Ostwald*-solubility
 - *Henry*-coefficient
 - adsorption power (to soil)
 - density
 - surface tension
 - viscosity
- Persistence
 - transformation processes
 - UV-adsorption
 - electron affinity
 - chemical oxygen demand (COD)
 - biochemical oxygen demand (BOD)
 - biodegradability
 - half-life period in the environment
- Accumulation behaviour
 - distribution in equilibrium
 - distribution coefficient n-octanol/water
 - solubility in fats
 - factor of bio-accumulation
- Direct nocuousness
 - mutagenicity
 - carcinogenicity
 - embryotoxicity
 - acute toxicity

- threshold limit value
- Indirect nocuousness
 - dissociation
 - formation of complexes
 - surface activity
 - corrosiveness
 - redox potential
 - formation of transformation and degradation products

The OECD uses two concentrations to assess the environmental hazards of a chemical:

- *Predicted environmental concentration (PEC)*:
This concentration is a calculated value from all quantities of emission on the one side and all elimination processes on the other side.
- *No observed effect concentration (NOEC)*:
This concentration means the maximal concentration at which no nocuous effect can be observed over a long period of time (chronic toxicity).

If the PEC is much less than the NOEC the substance can be regarded as harmless (in the calculated concentration range).

All the above-listed properties are hardly available for all substances. So experts have chosen four main criteria to assess the environmental hazards associated with chemicals [6]:

- acute oral toxicity LD_{50}
- acute fish toxicity LC_{50}
- acute bacteria toxicity EC_{50}
- biodegradability.

4.4.1 Toxicological and Ecological Data for Surfactants in General

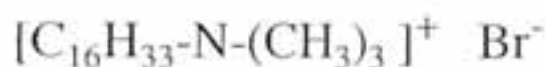
Surfactants are a group of chemicals used widely in the whole world. The most important surfactants are the anionic surfactants in detergents. Cationic surfactants are used for *detergents, disinfectants, corrosion inhibitors, tar emulsifiers* etc. The chemical structure of these cationic surfactants is almost identical to the drag reducing additives. The only differences are the n-alkyl chain length and the counterions (Figure 4.5).

The production quantities for the most important surfactants in Germany and worldwide are given in Table 4.3.

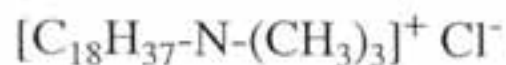
Figure 4.5:

Chemical Structure of Cationic Surfactants which are already Used Mainly in Detergents and Cosmetics Compared to the Drag Reducing Additives

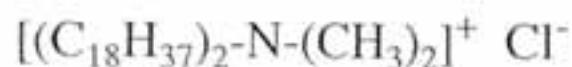
- Cetyltrimethylammoniumbromide (CTAB)



- Stearyltrimethylammoniumchloride (STAC)



- Distearyldimethylammoniumchloride (DSDMAC)



- HABON:



Table 4.3:

Quantity of Production for Some Important Surfactants (from [6, 7, 8]).

Class of surfactant	Name of surfactant	Production	
		in Germany [t/a]	Worldwide [t/a]
Anionic surfactants		132,000	5,000,000 ^a
	Linear alkylbenzene sulfonate	87,000	
	Secondary alkane sulfonate	16,000	
	Alcohol ether sulphate	20,000	
Nonionic surfactants		93,000	2,300,000
	Alcoholethoxylate	50,000	
	Nonylphenoethoxylate	10,000	
Cationic surfactants		23,000	560,000
	Distearyldimethylammoniumchloride	15,000	
	Hexadecyltrimethylammoniumbromide	< 1,000	
Amphoteric surfactants		5,500	90,000
	Total production	253,500	7,950,000

^aSoaps are not included

A large part of these substances get into the environment after they are used in households and industry. The surfactants get normally into sewerage systems or into surface waters.

The main problem related to the surfactants in the environment is their fish toxicity. This is caused by the interfacial activity which damage the epithelium of the skin and the gills of the fish. This effect begins when the surface tension is lowered to 50 mN/m (surface tension of water \approx 72 mN/m). After a period of time the gills are swollen and do not function any longer and the fish dies [9].

To prevent an accumulation of surfactants in the environment several countries enacted detergent laws which demand a biological degradability $>$ 80% (Germany, Italy, France, EEC). This requirement of biodegradability includes only the primary biodegradability, which means, in the case of surfactants, the loss of the interfacial activities. Although this is a very important fact, because the interfacial activities mainly cause the fish toxicity, this does not mean that the surfactants are really degraded. But when the surfactants are primarily biodegraded the fish toxicity is reduced to about two orders of magnitudes.

The detergent law demands special properties only for anionic and non-ionic surfactants; cationic surfactants are not mentioned. Nevertheless, the cationic surfactants should also fulfill these demands.

Some further requirements which have not been enacted in laws but which surfactants should fulfill are [7]:

- primary biodegradability \geq 80%
- ultimate biodegradability \geq 60%
- acute ecological toxicity
 - $LC_{50} \geq 1$ mg/l
 - $EC_{50} \geq 1$ mg/l
- quantity of production

Data for the anionic surfactant *Linear alkylbenzene sulfonate*, the non-ionic surfactant *Alcohol-etoxylate* and the two cationic surfactants *Distearyldimethylammoniumchloride (DSDMAC)* and *Cetyltrimethylammoniumbromide* are given in Table 4.4.

The anionic and the non-ionic surfactants fulfill all these requirements; the cationic surfactants do not fulfill the requirement for the fish toxicity.

Cationic surfactants, however, show a special behaviour when they get into the environment. The fish toxicity and the mobility in the environment are lowered considerably by two effects [9, 12, 13]:

- they adsorb to each solid because of their great adsorption power,
- they form neutral salts with anionic surfactants which are present in all waste waters.

Table 4.4:

Toxicological and Ecological Data for Important Surfactants
(Data from [6, 10, 11])

Surfactant	LD ₅₀ [mg/kg]	LC ₅₀ [mg/l]	EC ₅₀ [mg/l]	Primary biodegradability [%]
LAS	650 - 2,480	3 - 10	8.9 - 14	93 - 97
Alcoholethoxylate		3 - 30	5 - 200	96
DSDMAC	> 2,000	1 - 10	10 - 100	> 90
CTAB	410 - 430	0.25 - 0.4	0.4 - 90	98

The adsorption power to solids can be expressed by the adsorption constant

$$K_{ad} = \frac{m_{solid}}{m_{solution}} \quad (4.1)$$

This adsorption constant describes the relation between the adsorbed surfactant m_{solid} and the rest concentration of surfactant in the solution $m_{solution}$ in the state of equilibrium.

The adsorption constants are very high for cationic surfactants (Table 4.5).

Because of adsorption effects the concentration of cationic surfactants in surface waters is much less than one could expect from the quantity of consumption. The surfactants are immobilized by adsorption and eliminated from the water.

Investigations on the fish toxicity have demonstrated that the toxicity is lowered when the cationic surfactants are mixed with anionic surfactants. In this case, both kinds of surfactants form neutral salts and lose their surface activity by this process. The results from toxicity tests for a mixture of an anionic and a cationic surfactant are shown in Figure 4.6.

Although the toxicity of cationic surfactants is reduced by adsorption and the formation of neutral salts it is very important that cationic surfactants are ultimately biodegradable. Total degradability means the degradation (or mineralisation) to CO_2 , H_2O , NH_4^+ , SO_4^{2-} or PO_4^{3-} . This process of degradation prevents the surfactants from accumulating in the environment.

The test methods used to determine the ultimate biodegradability are the OECD-Screening test, the inherent test and the simulation test. The degradation will be indicated by measuring the sum parameters, like dissolved organic carbon (DOC), oxygen (O_2) or carbon dioxide (CO_2).

The main tests are compared in Table 4.6.

In literature many data can be found for the ultimate degradation of cationic surfactants, especially quaternary ammonium compounds. An overview for the surfactant *CTAB* is given in Table 4.7.

These results show a great dependence on the test method. The most reliable test may be the *Coupled units test*, which simulates aerobic conditions comparable to sewage treatment plants. Under these test conditions *quaternary ammonium compounds* are ultimately degradable (see Table 4.8).

These data confirm the ultimate biodegradation of cationic surfactants under aerobic conditions. However, degradation under anaerobic conditions has not been measured yet [13].

Besides these laboratory tests investigations have been done using actual river water to simulate natural conditions comparable to surface waters.

The substances used in the test were *CTAB*, *STAC* and *DSDMAC*. Under the special conditions of the screening test only *CTAB* is significantly degradable. This behaviour is quite different for river water. In this medium all three surfactants are highly degradable. These results show that laboratory tests underestimate the biodegradation of cationic surfactants [14].

Also, the presence of sediments does not change the degradation behaviour. This means that surfactants which are adsorbed on soils can also be biodegraded.

Another significant value from these measurements is the half-life period for mineralization.

Table 4.5:

Adsorption Constants for some Cationic Surfactants (from [14])

Surfactant	Adsorption constant
Stearyltrimethylammoniumchloride (STAC)	225,677
Distearyldimethylammoniumchloride (DSDMAC)	71,051
Cetyltrimethylammoniumbromide (CTAB)	12,489

Figure 4.6:

Decrease of the Aquatic Toxicity of the Cationic Surfactant C_nTACl by
Formation of Neutral Salts with an Anionic Surfactant
(Reproduced from [15])

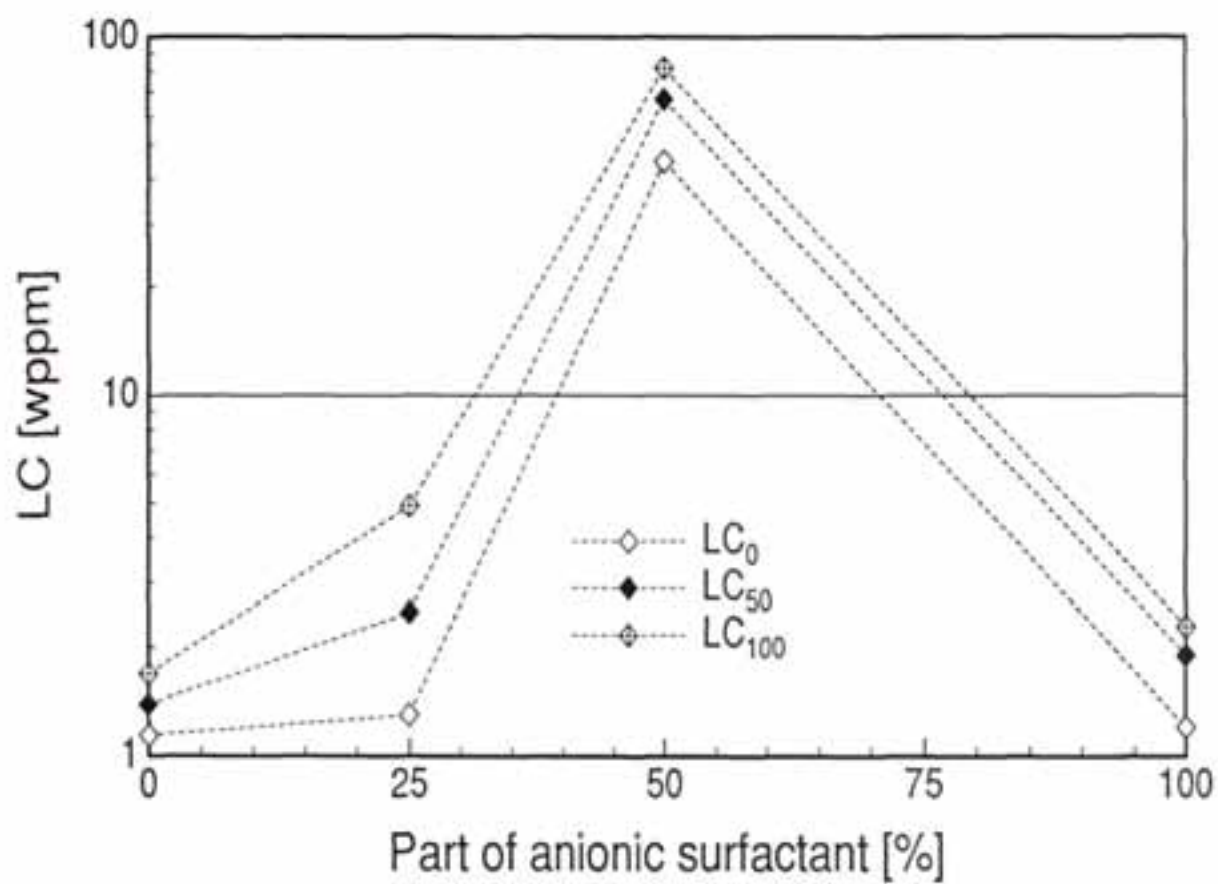


Table 4.6:

Test Methods for the Ultimate Biodegradation of Surfactants (from [10])

Test method	Characteristic feature of the test	Parameter	Duration of test [d]	limit of degradation which classifies the surfactant to be well degradable
Modified OECD-Screening test	static test (small amount of organism)	DOC (total degradation)	28	> 70%
Closed bottle test	static test (small amount of organism)	O ₂ (total degradation)	28	> 60%
Sturm test	static test (small amount of organism)	CO ₂ (total degradation)	28	60%
Zahn-Wellens test	static test (small amount of organism)	DOC (total degradation)	28	> 70%
Coupled units-test	continuously test (simulation of a sewage plant)	DOC (total degradation)	not defined	> 70%

Table 4.7:

Comparison of the Results of Different Tests for the Ultimate Biodegradation of CTAB (Data from [6])

Test method	Analytical criterion	Initial concentration	Degradation
		[mg/l]	[%]
Closed Bottle Test	% BOD	2	0
		5	0
		10	0
		3.2	75
Modified OECD Screening Test	% DOC	8	63
		16	74
		41	63
Sturm Test	% CO ₂	8	100
		16	20
		32	13
Coupled Units Test	% DOC	5 - 15	73 - 99
		10	98
		15	100

Table 4.8:

**Ultimate Biodegradation of Cationic Surfactants in the
Coupled Units Test**

Surfactant	Initial concentration		Retention time [h]	Degradation [%]	Literature
	[mg/l]	[mg C/l]			
CTAB	15	9.4	3	107 ± 19	[16]
	15	9.4	6	104 ± 6	[16]
	5 - 15			73 - 99	[6]
	10			98	[6]
STAC	0.1 - 1			60 - 90	[17]
DSDMAC	20	15.6	3	108 ± 9	[16]
+ LAS	20	28	3	83 ± 3	[16]
	20	15.6		98	
DBDMAC				87 ± 7	[11]

For a system consisting of river water and sediment the half-life period is about 3-6 days, independent of the surfactant concentration (0.01 g/l up to 0.1 g/l) [14].

The degradation of *STAC* in soils was measured for 5 different soil types. The half-life period is between 3.2 and 8.7 days for a cationic surfactant with a alkyl chain length of $n=18$ [18].

The adsorption and biodegradation mechanisms lead to concentrations in the environment which are much less than one would expect from the rates of consumption. With a per capita consumption of 0.33 kg of ionic surfactants per year and a supposed quantity of waste water of about 200 l per person and day, the resulting concentration would be about 4.5-5 mg/l, but the measured values are only in the range of 0.005-0.030 mg/l [13]. This concentration is much less than the LC_{50} of *DSDMAC* (0.6-6 mg/l) or *CTAB* (0.25-0.4 mg/l).

For the cationic surfactant *DSDMAC* the *no observed effect concentration* (NOEC) was also determined [19]:

$$NOEC = 0.05 - 0.5 \text{ mg/l}$$

The NOEC for *DSDMAC* is also much less than the measured concentration in the environment. This means that this substance can be regarded as harmless.

In sewage treatment plants cationic surfactants are also known to cause no problems in the biological stages. Up to concentrations of about 20 mg/l investigations have shown that they do not affect the purification performance.

4.4.2 Toxicological and Ecological Data for Friction Reduction Additives

The cationic surfactants which are suitable as drag reducing additives in district heating networks are not a new group of chemicals. They have a similar structure to those cationic surfactants which are already used as detergents, disinfectants etc. .

So the environmental behaviour of the drag reducing additives can be assessed by the known behaviour for these substances.

But there are also some additional data relating especially to drag reducing additives, which are given from the *Hoechst AG*, the manufacturer of the additives (Table 4.9).

For the additive *DOBON-G* the main toxicological and ecological data LD_{50} , LC_{50} , EC_{50} and the primary biodegradability are in the same range as the data for those cationic surfactants which are used in many products (Table 4.4).

The use of *Sodium salicylate* will only be necessary for special operation conditions in district heating systems when the temperature range for the drag reducing effect has to be enlarged.

The additional additive *Sodium salicylate* has a much less hazard potential with respect to fish toxicity. The LC_{50} is > 100 mg/l.

According to these data the additives may be classified as *non-toxic* for man and they have not to be labeled. Thus the requirements set by the *detergent law* (primary biodegradability $> 80\%$) are met. But they must be regarded as toxic to fish. The *IMCO/FAO/UNESCO/WHO* classify surfactants with a lethal concentration of

Table 4.9:

Toxicological and Ecological Data for DOBON-G (Data from [20])

Criterion		DOBON-G
Lethal dosis LD ₅₀	[mg/kg]	> 2,000
Fish toxicity LC ₅₀	[mg/l]	7.1
Bacteria toxicity EC ₅₀	[mg/kg]	> 1,000
Primary biodegradability	[%]	> 93
Sensitization		no indication
Mutagenicity		no indication
Embryotoxicity		no indication
Carcinogenicity		no indication
Skin compatibility (Rabbit skin)		irritative
Mucous membrane compatibility		not irritative

- 1-100 mg/l as *toxic*,
- < 1 mg/l as *very toxic*.

Although toxicological and ecological data are only given for the additives with an alkyl-chain length of 22 (*DOBON-G*), the additives with an alkyl-chain length of 16 and 18 will have a similar behaviour. For the most important property, fish toxicity, investigations on the surfactant C_n TACI show that the chain length n has only little influence in the range from $n = 16$ to $n = 22$ (Figure 4.7).

From the data in Table 4.9 the following conclusions can be drawn:

The drag reducing additives show similar properties to other surfactants which are widely used in household products. Compared to the surfactant *linear alkylbenzene sulfonate* which is one of the most frequently used detergents in households the toxicological and ecological data for the drag reducing additives are almost identical.

For a final assessment of the hazard potential it is necessary to predict the possible concentrations which can occur in the environment. In district heating systems the maximum concentration would be 1.5 g/l. This concentration would be much too high for the aquatic environment. But at that moment when the network water gets into the environment the concentration is lowered because of dilution. Here it will lose the primary property, the surface activity, by adsorption effects and by the formation of neutral salts. So one can expect that the surfactants are no longer toxic to fish.

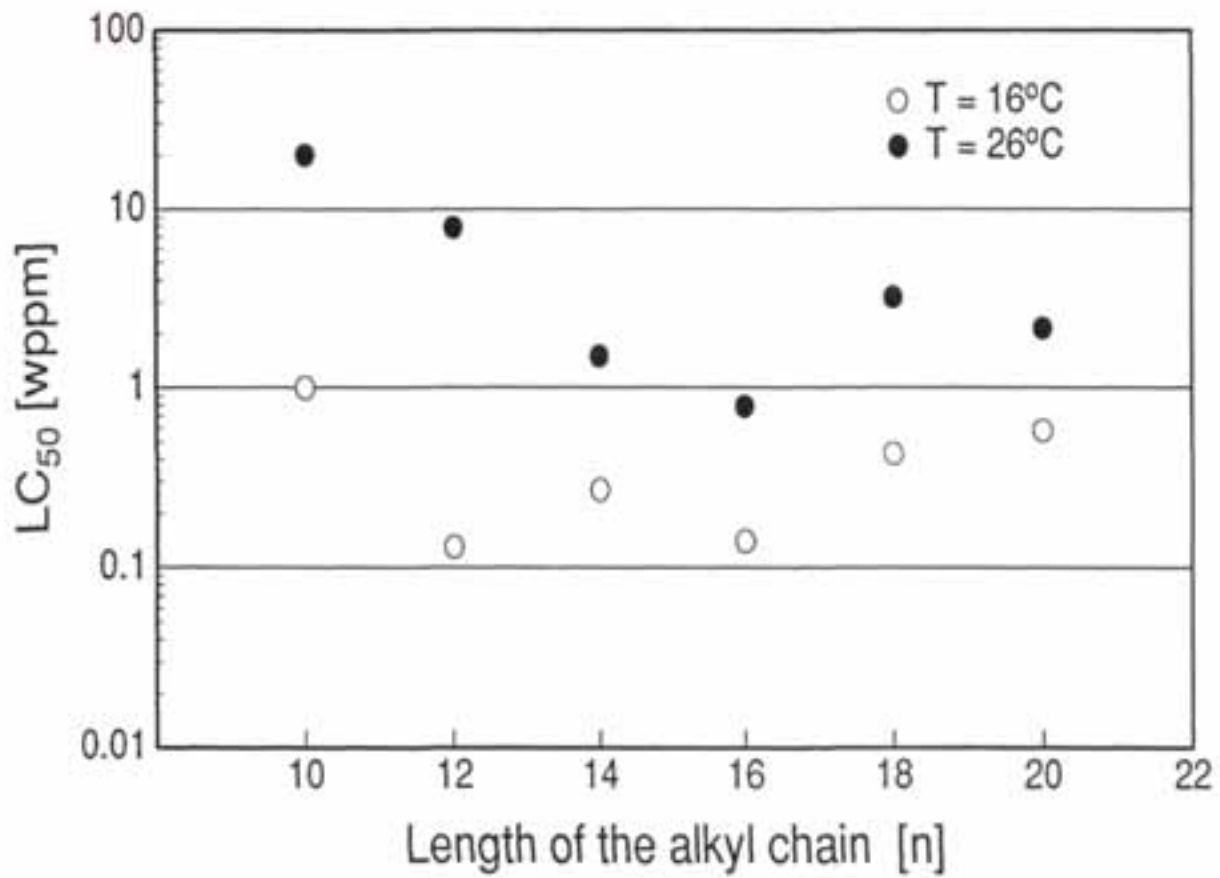
To avoid concentrations, which are harmful for the environment, it should be one aim to keep the concentration in the district heating system as small as possible. Furthermore, leakages have to be identified immediately and countermeasures to be carried out.

The main features which can be deduced from literature on surfactants with similar structures and which have been partially confirmed by data on the drag reducing additives are summarized here again:

- The rate of consumption for cationic surfactants would increase only a little when drag reducing additives are used.
- The additives fulfil the requirements of detergent laws concerning primary biodegradability (> 80%).
- Cationic surfactants have been shown to be ultimately biodegradable.
- The drag reducing additives are classified as *non-toxic for man*.
- They are *toxic for fish*.
- The hazardous potential (especially fish toxicity) is lowered considerably by adsorption on soils and formation of neutral salts.

Figure 4.7:

Dependance of the Fish Toxicity on the Length of the Alkyl Chain for a Homologous Series of C_n TACl
(Reproduced from [21])



4.5 ADSORPTION BEHAVIOUR ON SOILS

The adsorption behaviour on soils is a very important fact to know about the cationic surfactants. In the case of a leakage the penetration behaviour can be assessed and the danger for the surfactants to get into the ground water is calculable.

To investigate this behaviour two guidelines are available for the testing of chemicals:

- OECD-guideline for the testing of chemicals:
Adsorption/Desorption [22]
- Instruction sheet from the German Institute for Forestry and Agriculture, Speyer
"Prüfung des Versickerungsverhaltens von Pflanzenschutzmitteln" [23]

The tests are carried out with standard soils to get results which may be comparable to other tests. However, it is not possible to prescribe exactly the soils to be used.

The soils which are selected for the tests are different in the following parameters:

- cation exchange capacity
- clay content
- organic matter content
- pH

4.5.1 Characteristics of Soils

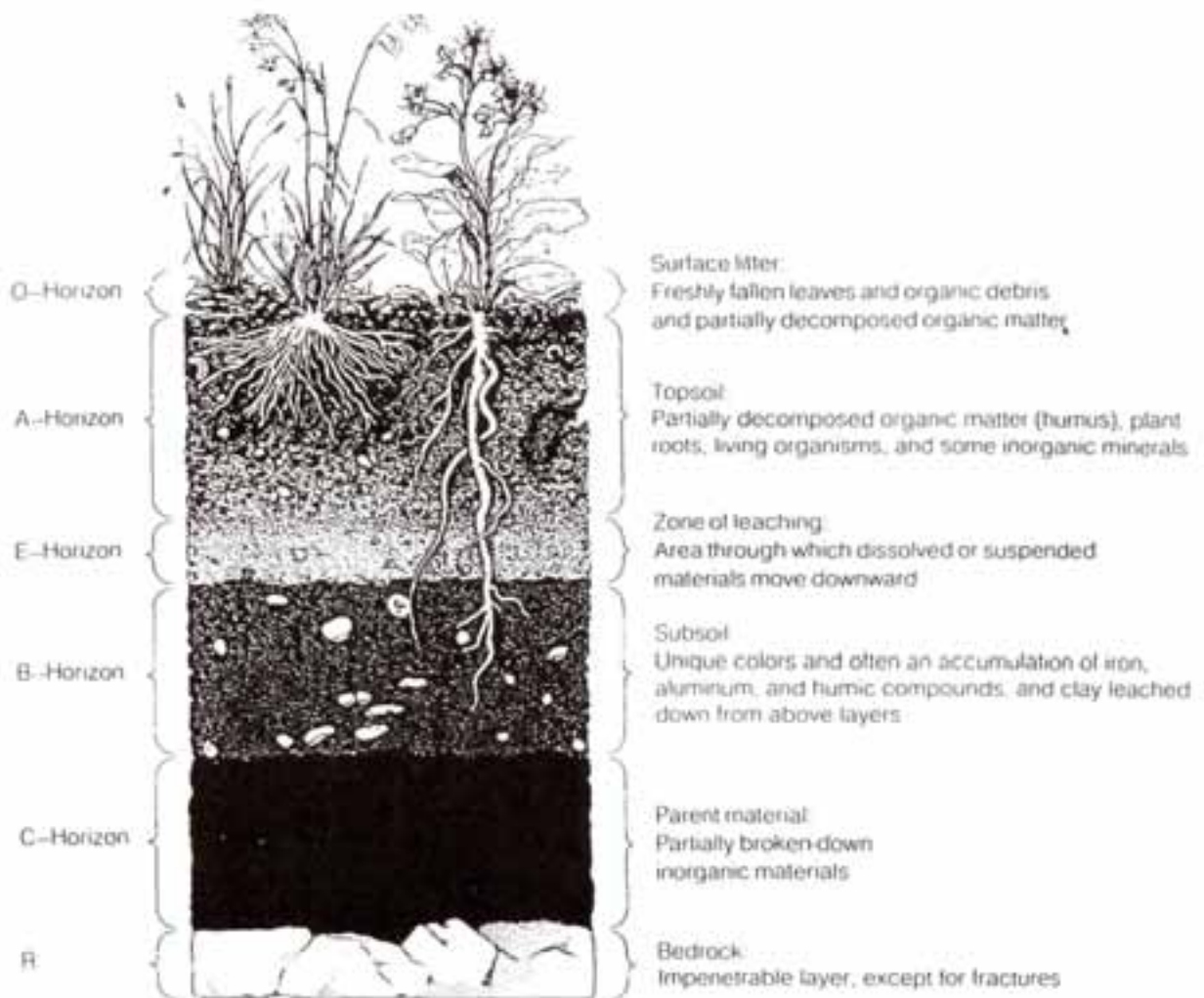
A soil is the upper part of the earth's crust. It consists of minerals and organic materials (humus).

Soils vary according to the stages of development, which are determined by

- climate
- initial stone material
- gravitation
- relief
- flora and fauna
- ground water

The development begins at the surface and goes towards deeper layers. A layer with a specific state of development is called *horizon*. Figure 4.8 shows a cross-sectional view of the horizons in the soil.

Figure 4.8:
Profile of a Soil (from [24])



The sequence of horizons determines the *type of soil*. The types of soil are usually classified according to the color of the soil.

Another criterion used in classifying soils is form and size of the soil particles. They are divided into two main fractions:

- *fine soil*: diameter of the particles < 2 mm
- *gravel*: diameter of particles > 2 mm

Fine soil is subdivided into

- *clay*: diameter of particles < 2 μm
- *silt*: diameter of particles 2 μm –63 μm
- *sand*: diameter of particles 63–2,000 μm

A mixture of different fractions determines the *soil texture*. The porosity of a soil is dependent on the composition of clay, silt and sand.

The most important *types of soils* (from the German classification system) are described in the following:

- *Gley-Braunerde* (international: *Cambisol*):
The name *Gley-Braunerde* refers to its significant brown color. The color is caused by the ironoxide-hydrates. The clay is distributed uniformly over the whole depth.
- *Parabraunerde* (international: *Luvisol*):
The *Parabraunerde* forms in the same climate zone as *Gley-Braunerde*, but it is a further state in the development process. The clay fraction has moved to deeper layers and iron and the organic matter have been washed out. The upper layers are clay reduced (0 – 60 cm), the deeper layers are enriched with clay.
- *Podsol* (international: *Podzol*):
The *Podsol* has a highly reduced content of iron and clay. Heavy rainfalls cause a high penetration of water which continuously transports substances to deeper layers. Because of the loss of iron the color is grey.

Braunerde and *Parabraunerde* can be considered as former stages of development of *Podsol*.

The adsorption behaviour of soils is determined by the content of clay, organic matter and oxides. The capacity for ion exchange is called *anion exchange capacity (AEC)* and *cation exchange capacity (CEC)*, respectively.

The clays and the humus matter are the most important cation exchanger, the oxides and hydroxides exchange primarily anions.

Clays are formed by weathering processes from stones. The main components are *alumosilicates* with OH-groups.

The crystals are formed by layers of O- and OH-ions (ligands) with small cations like Si, Al, Fe and Mg in the interspaces. The layers are bound by hydrogen bond or by the implantation of cations or hydroxides. So different forms of clays exist:

- *kaolinites*,
- *illites*,
- *smectites* and
- *chlorites*.

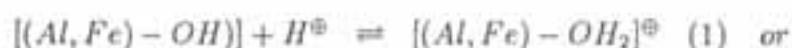
These clays have different capacities for exchanging cations. The cation exchange capacity (CEC) varies from 0.03–0.15 mval/g for *kaolinite* up to 0.7–1.3 mval/g for *smectite* [25].

Cationic surfactants are known to be well adsorbed on clays [26]. They are bound by ion exchange and hydrophobic interactions between the alkyl chains.

Because of the second adsorption mechanism the adsorption capacity of clays for cationic surfactants exceeds the *cation exchange capacity*. For *bentonite* (clay type *smectite*) the amount of adsorption is very high, which can be seen from the adsorption isotherm (see Figure 4.9). The normal CEC for *bentonite* is 60–120 mval/100 g [27], but 1.2 g Surfactant (OBON) corresponds to 240 mval/100 g. This is 2–2.5 fold the CEC for *bentonite*, a result which has also been reported in literature [26].

Thus the adsorption capacity for cationic surfactants on clays is not limited by the CEC. Further adsorption occurs by *van der Waals* linking of the hydrocarbon chains (hydrophobic effect).

Oxides and *hydroxides* are also weathering components of soils. They are present as Al-, Fe-, Mn-, Si- and Ti-oxides and hydroxides. When they transfer a proton they can carry a positive or negative charge:



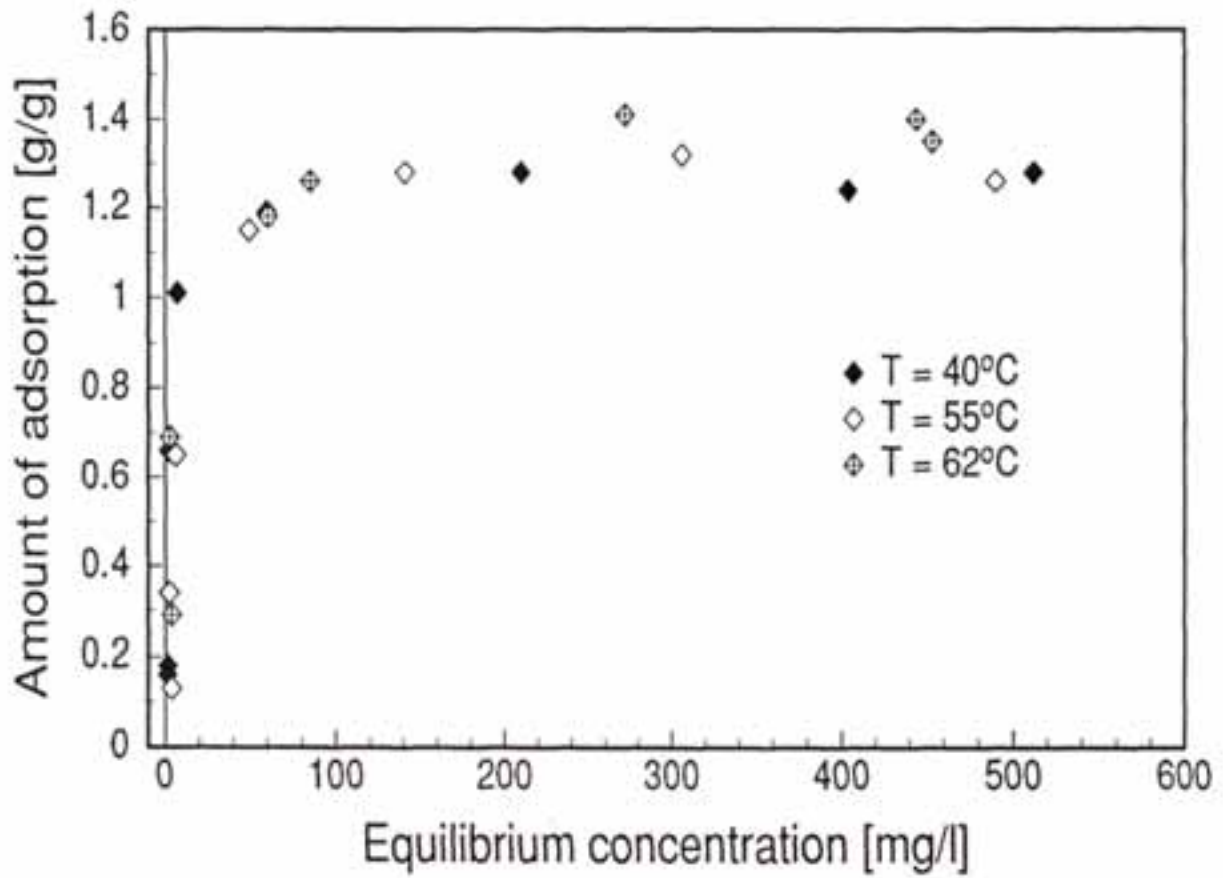
In this form the hydroxides can participate in anion exchange (1) or in cation exchange (2).

The kind of charge depends on the pH of the medium. For a pH which is typical of soils the hydroxides are anion exchangers.

The *organic matter* consists of dead plants and animals. They are high molecular organic substances with many functional groups like -OH (hydroxides), -COOH (carboxyle), or >C=O (carbonyle). These groups can dissociate or associate protons; they are also able to exchange ions.

Figure 4.9:

Adsorption Isotherm for the System OBON/Bentonite



4.5.2 Test Program

Test Materials

It is very difficult to define the characteristics of a soil and to get general results. By choosing three standard soils which are available from the German *Institute for Forestry and Agriculture* it was possible to vary the main parameters over a wide range. In addition to the standard soils two natural soils which are common in Germany were tested, *Parabraunerde* and *Podsol*. From the *Parabraunerde* three samples at different depths were taken. The parameters of the soils are compared in Table 4.10.

The maximum amount of adsorption which may be expected for a soil is given by

$$\left(\frac{x}{m}\right)_{\max} = \frac{cec \cdot M}{val} \quad (4.2)$$

M : molecular weight of the adsorbed substance

val : valence of the adsorbed ion
(= 1 for the cationic surfactants)

The tests were carried out with all surfactants listed in Figure 4.3.

Description of the Tests

The testing program followed the OECD-guideline for the testing of chemicals and the instruction sheet on testing of the percolation behaviour of plant protective agents, from the German *Institute for Forestry and Agriculture*.

Adsorption isotherm The adsorption behaviour of any substance to a soil can be expressed by the adsorption isotherm, which shows the dependence of the amount of adsorbed surfactant on the equilibrium concentration for a constant temperature.

For all tests a surfactant solution with a certain concentration was prepared. To this solution different amounts of soils were added, then they were stirred sufficiently so that equilibrium was reached. At the end of the adsorption process the concentration of the surfactant in the equilibrium solution was measured. The amount of adsorbed surfactant (only the cationic part) was calculated in this way:

$$\frac{x}{m} = \frac{c_{\text{init}} - c_{\text{equi}}}{m} V_{\text{solution}} \quad (4.3)$$

x : amount of adsorbed surfactant (cation)

m : mass of solid

c_{init} : initial concentration of the surfactant cation

c_{equi} : concentration of the surfactant cation in equilibrium

The parameters for the tests were:

Table 4.10:

Comparison of the Main Properties of the Investigated Soils

Soil	Cation exchange capacity [mval/kg]	Organic carbon content [%]	Clay content [%]
Standard soil 1	49	0.70	3.5
Standard soil 2	97	2.25	5.1
Standard soil 3	95	0.97	8.3
Parabraunerde	140 ^a	unknown	unknown
Podsol	30 ^a	unknown	unknown

^afrom [25]

- type of soil,
- surfactant.

Desorption To investigate the desorption behaviour the saturated soil from the adsorption experiments was dispersed in pure water. After 3 h the concentration of surfactant in the solution was determined. From this concentration the degree of desorption was calculated.

Percolation behaviour The percolation behaviour of surfactant solutions was investigated in glass columns. The column was filled with soil and the solution was added to the surface of the soil using a pipette (Figure 4.10).

The surfactant concentration in the outlet was monitored. At the beginning it was 0, but when a certain volume of surfactant solution had percolated through the soil the concentration increased. At this point the soil was saturated with surfactant. The capacity was calculated as follows:

$$\frac{x}{m} = \frac{V_{surf} \cdot c_{surf}}{m} \quad (4.4)$$

- $\frac{x}{m}$: adsorption capacity of the soil
 V_{surf} : Volume of percolated surfactant solution until the soil is saturated
 c_{surf} : concentration of the surfactant solution

Analysis of the Cationic Surfactants

The cationic surfactants consist of two parts, the *n-alkyltrimethylammonium-* or the *n-alkyl-dimethylpolyoxethylammonium-cation* respectively and the *3-hydroxy-2-naphthoate*. Both parts had to be analyzed separately.

Two-phase-titration In this method titration takes place in the two-phase system, water/chloroform. The cationic part of the surfactants can be analyzed as *disulfine-blue-active* substance. The sample is mixed with an indicator and *chloroform* and is titrated with the anionic surfactant *sodiumlaurylsulfate*.

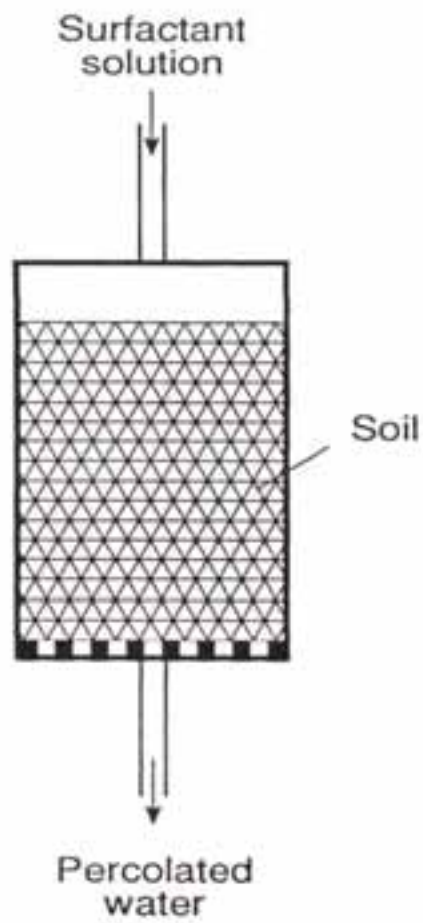
The endpoint of the titration is indicated by a change in color. From the amount of *sodiumlaurylsulfate* the content of cationic surfactant can be calculated.

Photometer The organic counterion (*naphthoate*) has an aromatic system of electrons which can be analyzed with a photometer. *Naphthoate* has a maximum absorption at a wavelength of 350 nm. For this wavelength the relation between the amount of absorption and the surfactant concentration is determined. This correlation is linear in a concentration range up to 200 wppm.

For both analytical methods the samples must not contain any pollutants. To guarantee this requirement all soil particles are separated by a centrifuge before starting the analysis.

Figure 4.10:

Column for the Testing of the Percolation Behaviour of Surfactant Solutions



4.5.3 Results

Preinvestigations

The temperature for the adsorption measurements was set at 50°C. This guarantees that the temperature is always above the Krafft-temperature for all surfactants.

The first step to determine the adsorption isotherms for the cationic surfactants to soil was to investigate the dependence of adsorption on time. The soils used for this test have been the *standard soil 1* and *Parabraunerde*.

The results show an increase of the amount of adsorbed surfactant in a time range up to 2.5 h. After this time the adsorption reached the equilibrium state and no further increase could be noticed (Figure 4.11).

Based on this test the time for all further adsorption experiments was set at 3 h.

Adsorption Isotherms

At first the adsorption behaviour was determined for three different concentrations of the surfactant *DOBON* to *Parabraunerde*. The results are shown in Figure 4.12.

The adsorption isotherm increases very steeply in the lower concentration range. The plateau where the soil is saturated is already reached at an equilibrium concentration of 0.02–0.08 mol/l or 11–44 wppm, respectively.

This concentration corresponds almost exactly with the critical micelle concentration for *DOBON*. Thus the adsorbent (soil) is in equilibrium only with the monomolecular phase of the surfactant solution. When the formation of micelles begins the soil is saturated. At low *critical micelle concentrations* for the drag reducing additives, the saturation concentration can be expected to be very low in general.

To calculate the dependence of the adsorption behaviour on different types of soils the isotherms for all soils were investigated. The results are shown in Figure 4.13 for the three standard soils and in Figure 4.14 for the natural soils *Parabraunerde* and *Podsol*.

The main difference between all isotherms is the amount of adsorbed surfactant in the plateau region. In Table 4.11 the maximum amount of adsorbed surfactant is compared to the clay content and the cation exchange capacity for each soil.

It is obvious that the characteristic factor primarily determining the adsorption behaviour of a soil is the clay content. For the three *standard soils* the maximum amount of adsorption increases with the clay content. For *Parabraunerde*, where the clay content is not quantitatively known, this tendency can also be seen for samples taken at different depths. As described earlier the clay content normally sinks to deeper layers over long time periods. The adsorption capacity in the plateau region is the same for the *Parabraunerde* samples taken from depths of 0–20 cm and 40–60 cm. It is comparable to the *standard soil 1*. But for the layer 80–100 cm the adsorption capacity increased about 85% from 27.8 to 51.3 mg surfactant per g soil. This is due to clay enrichment at layers deeper than 80 cm.

Figure 4.11:

Time Dependence of the Adsorption of the Cationic Surfactant DOBON on the Standard Soil 3 and Parabraunerde

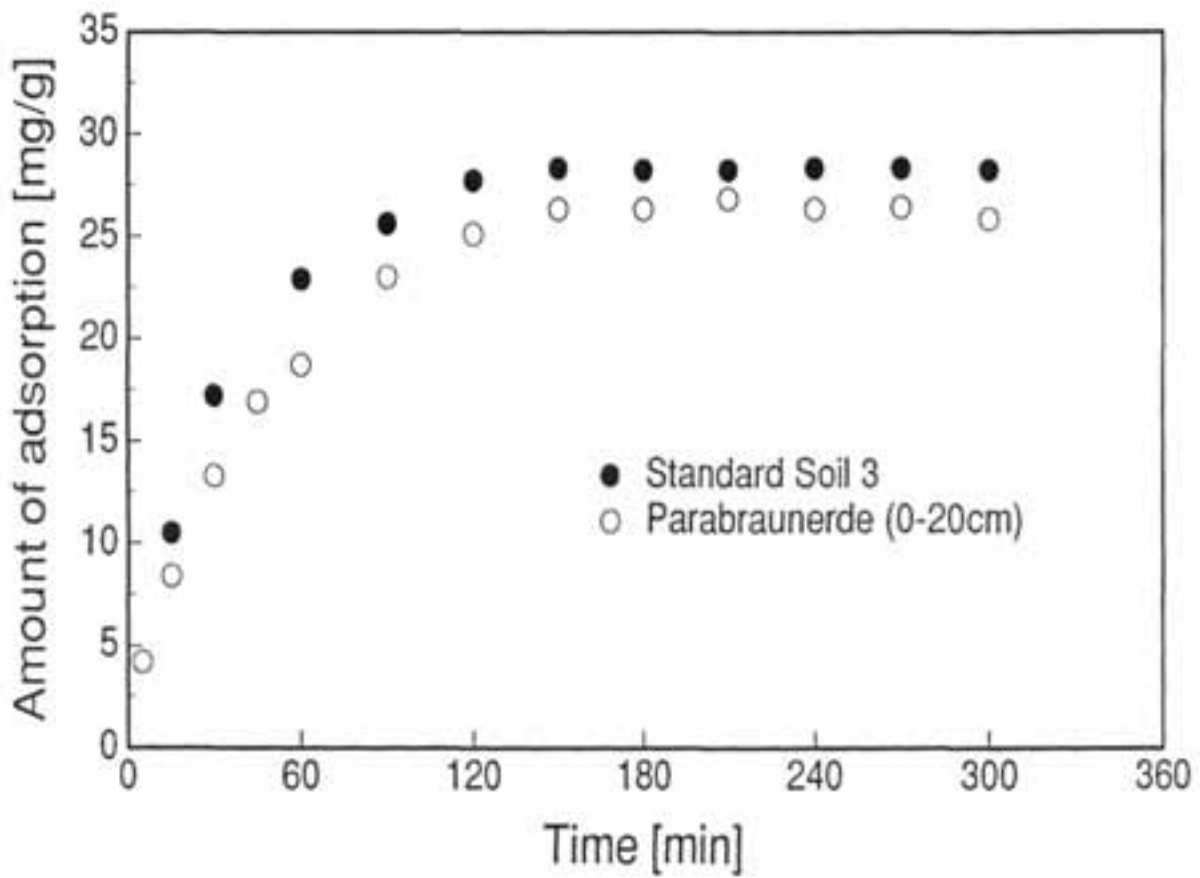


Figure 4.12:

Adsorption Behaviour of the Cationic Surfactant DOBON on Parabraunerde for Different Initial Concentrations

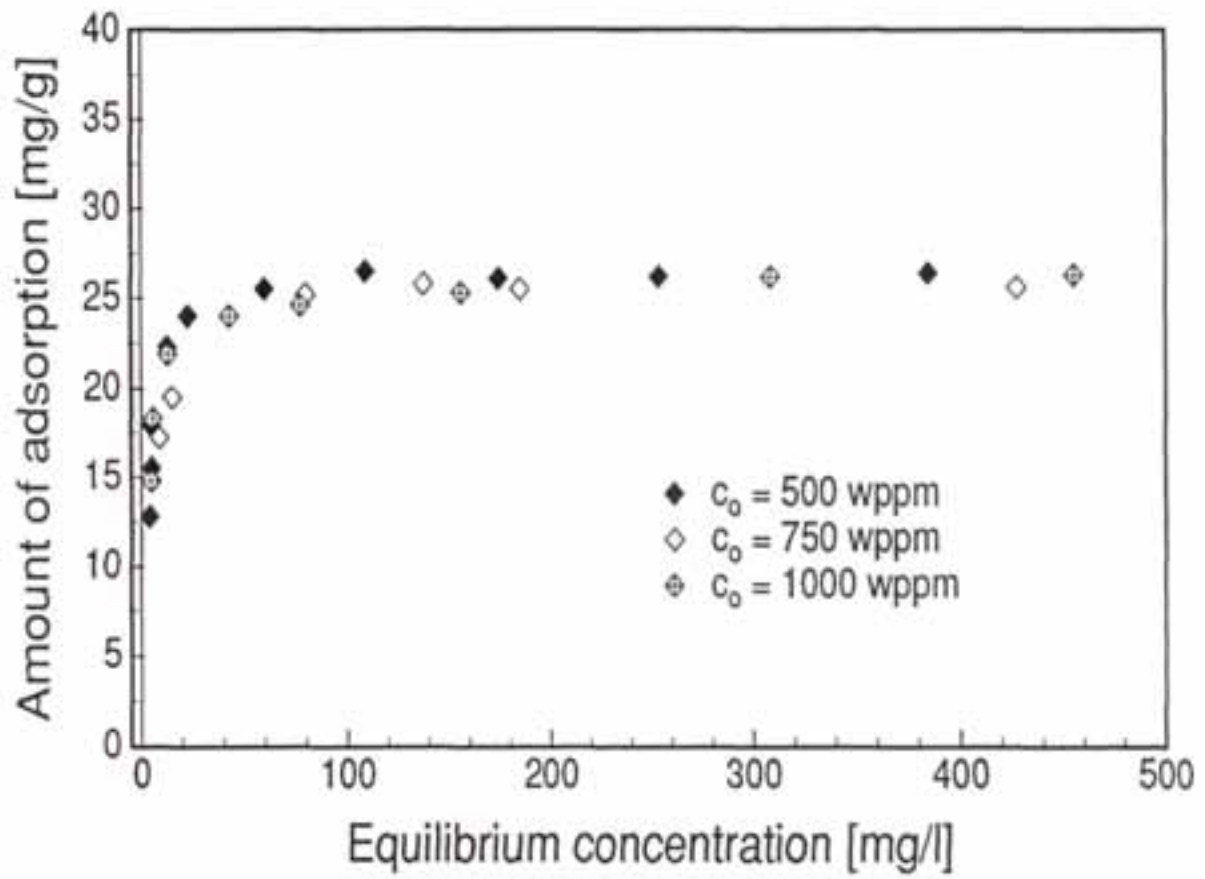


Figure 4.13:

Adsorption Behaviour of the Cationic Surfactant DOBON
on the three Standard Soils

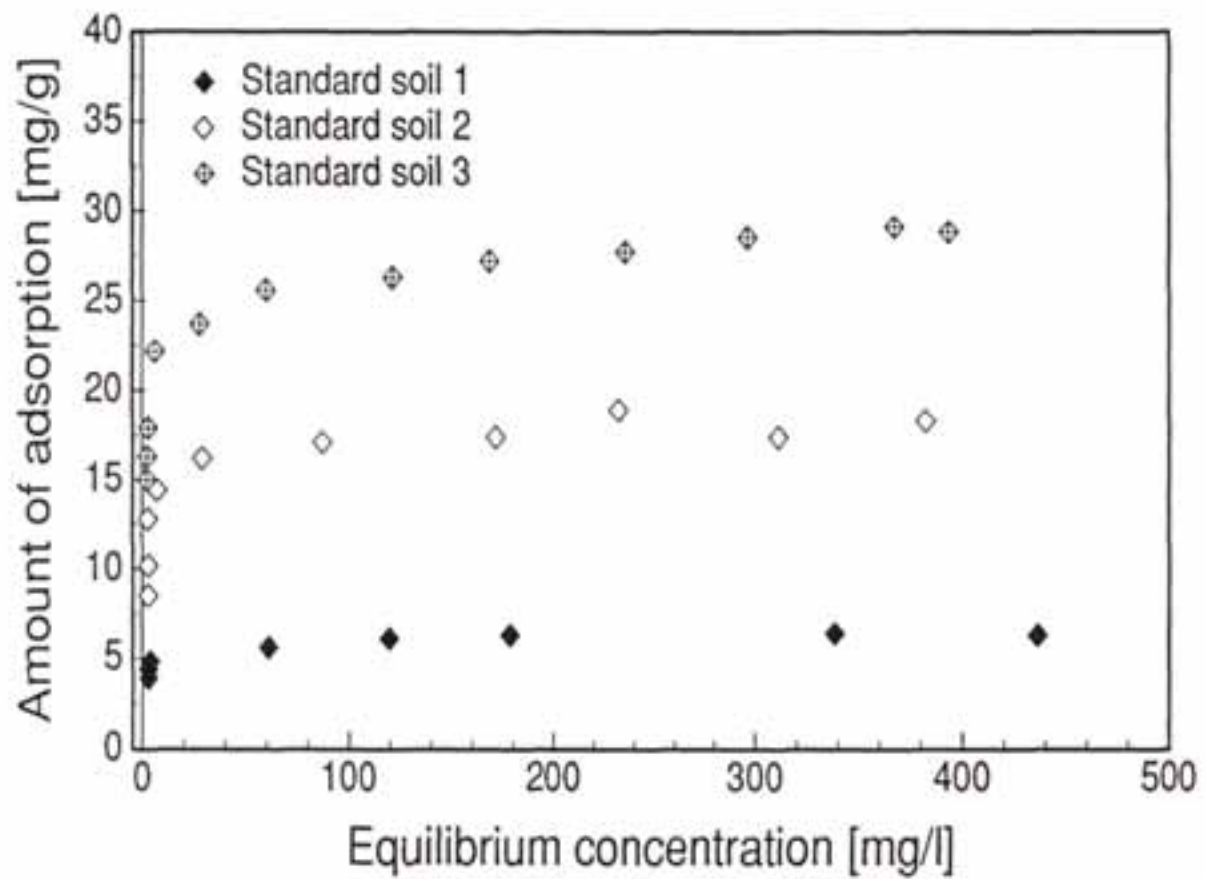


Figure 4.14:

Adsorption Behaviour of the Cationic Surfactant DOBON on Parabraunerde (3 Samples of Different Depths) and Podsol

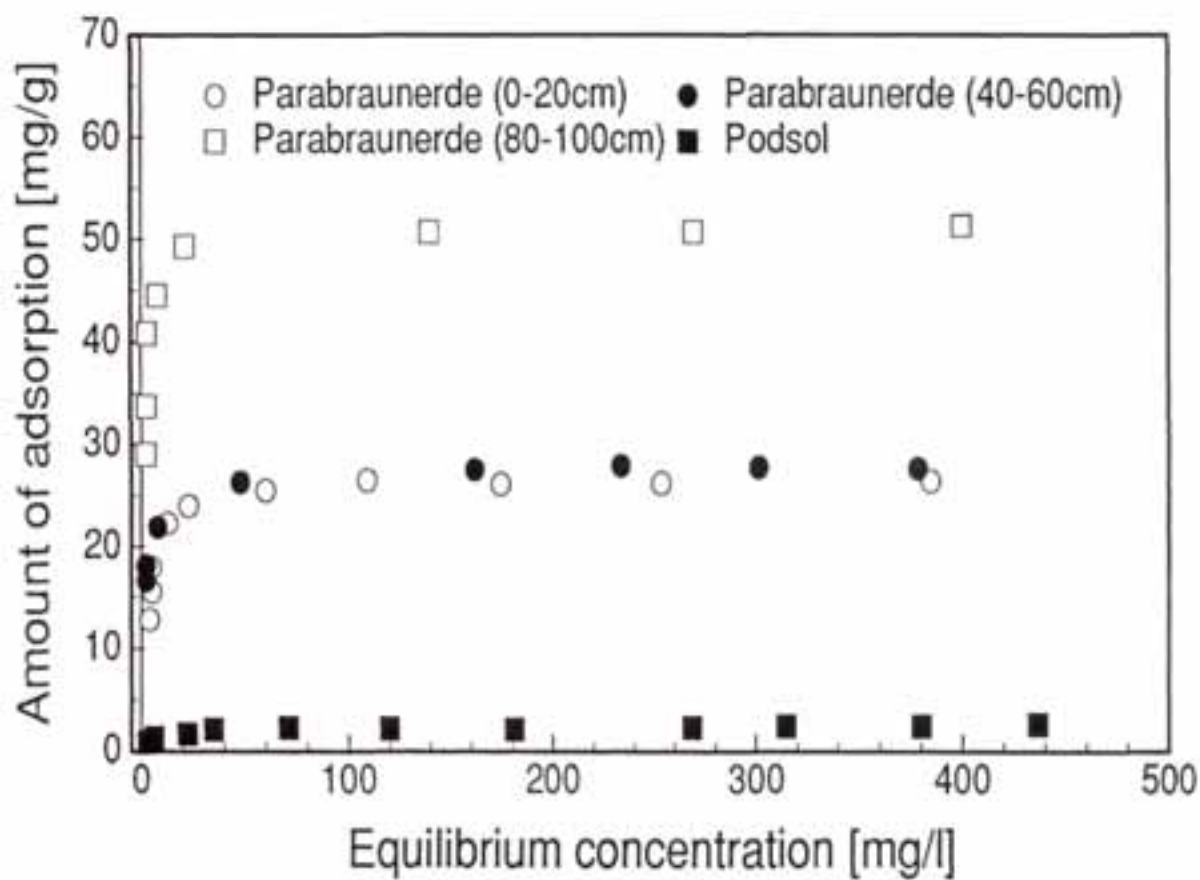


Table 4.11:

Comparison of the Maximum Amount of Adsorption in the Plateau Region
for the Surfactant DOBON for all Investigated Soils

Soil	CEC	Clay content	$(x/m)_{max}$		
	[mval/100 g]	%	[mg/g]	[mmol/kg]	[mval/100 g]
Standard soil 1	4.9	3.5	6.4	17.4	1.74
Standard soil 2	9.7	5.1	18.2	49.4	4.94
Standard soil 3	9.5	8.3	29.0	78.7	7.87
Parabraunerde 1	14	not known	26.6	72.1	7.21
Parabraunerde 2	14	not known	27.8	75.4	7.54
Parabraunerde 3	14	not known	51.3	139.1	13.9
Podsol	not known	not known	2.5	6.81	0.681

The tests with the soil *Podsol* also confirm this dependency on the clay content. *Podsol* is the soil which has reached the latest state of development that is where the clay is mostly washed out. The adsorption capacity is only very small, even much less than for the *standard soil 1*.

Another conclusion from these measurements is that the cation exchange capacity is not the property of soils which allows to predict directly the adsorption capacity of the cationic surfactants. The *standard soils 1* and *2* have almost the same cation exchange capacity but a different adsorption behaviour. So it is also important to know which component of the soil is responsible for the cation exchange. It is advantageous if the organic clay is the main cation exchanger.

Also, not all the cations will be replaced by the surfactant cations. One reason may be the competition between surfactant molecules and other cations which are present in the solution (CaCl_2 is always given to the test solutions). Another explanation may be that not all places with exchangeable cations can be reached by the larger surfactant molecules.

The influence of competitive cations was investigated using CaCl_2 at different concentrations (0–0.1 mol/l). The maximum amount of adsorption decreases with increasing Ca^{2+} -concentration in the solution. The concentration of Ca^{2+} , however, is very high and very much exceeds the initial surfactant concentration (0.0009 mol/l). Under real conditions one can expect that the adsorption capacity for cationic surfactants is not lowered considerably by competitive ions.

In Table 4.12 the adsorption data for the *standard soils* are related to the organic content, cation exchange capacity and clay content.

The related adsorption capacities underline the fact that no single parameter can describe the adsorption behaviour, but a soil with a high cation exchange capacity and a high clay content can be expected to have a high adsorption capacity for the cationic surfactants.

Besides the influence of different soils on the adsorption behaviour, the influence of different lengths of the alkyl chain and the influence of the head group of the surfactants was assessed. For the *standard soil 3* the adsorption isotherm for the three *n*-alkyltrimethylammonium-products are given in Figure 4.15.

For all three *standard soils* the adsorption capacity decreases with increasing chain length (see Table 4.13).

Normally, the amount of adsorbed surfactant in the plateau region is independent from the alkyl chain length. Only the increase in adsorption before the saturation point is steeper with longer chains. Steric hindrance may be the reason for the decrease in adsorption capacity in the series

$$\left(\frac{x}{m}\right)_{\max} (\text{Habon}) > \left(\frac{x}{m}\right)_{\max} (\text{Obon}) > \left(\frac{x}{m}\right)_{\max} (\text{Dobon})$$

The *n*-alkyldimethylpolyozethylammonium-products also show different results when compared to the *n*-alkyltrimethylammonium-products. The adsorption capacity is higher when the structure of the head group is changed (see Figure 4.16 and Table 4.13).

This increase will be due to the possible delocalisation of the positive charge of the headgroup by the inserted *polyozethyl*-group. Thus the repulsion between two molecules is lowered. Multilayer adsorption is easier because of this effect.

Table 4.12:

Amount of Adsorbed Surfactant in Relation to Characteristic Properties of the Standard soils

Soil	$\frac{(x/m)_{max}}{\% OC}$	$\frac{(x/m)_{max}}{CEC}$	$\frac{(x/m)_{max}}{\text{Clay content}}$
Standard soil 1	914	1.30	182
Standard soil 2	808	1.88	357
Standard soil 3	2,990	3.05	349

Figure 4.15:

Adsorption Behaviour of the *n*-Alkyltrimethylammonium-
Products on the Standard Soil 3

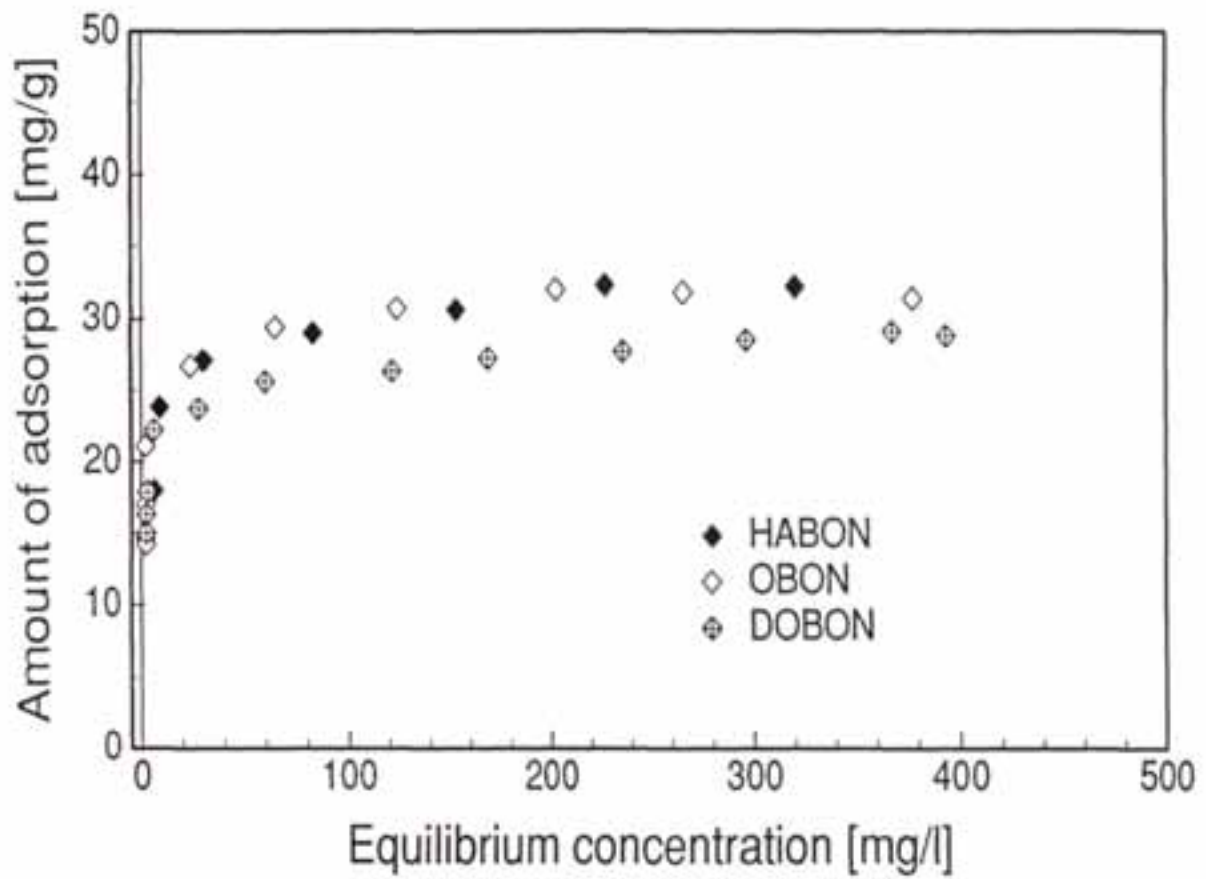


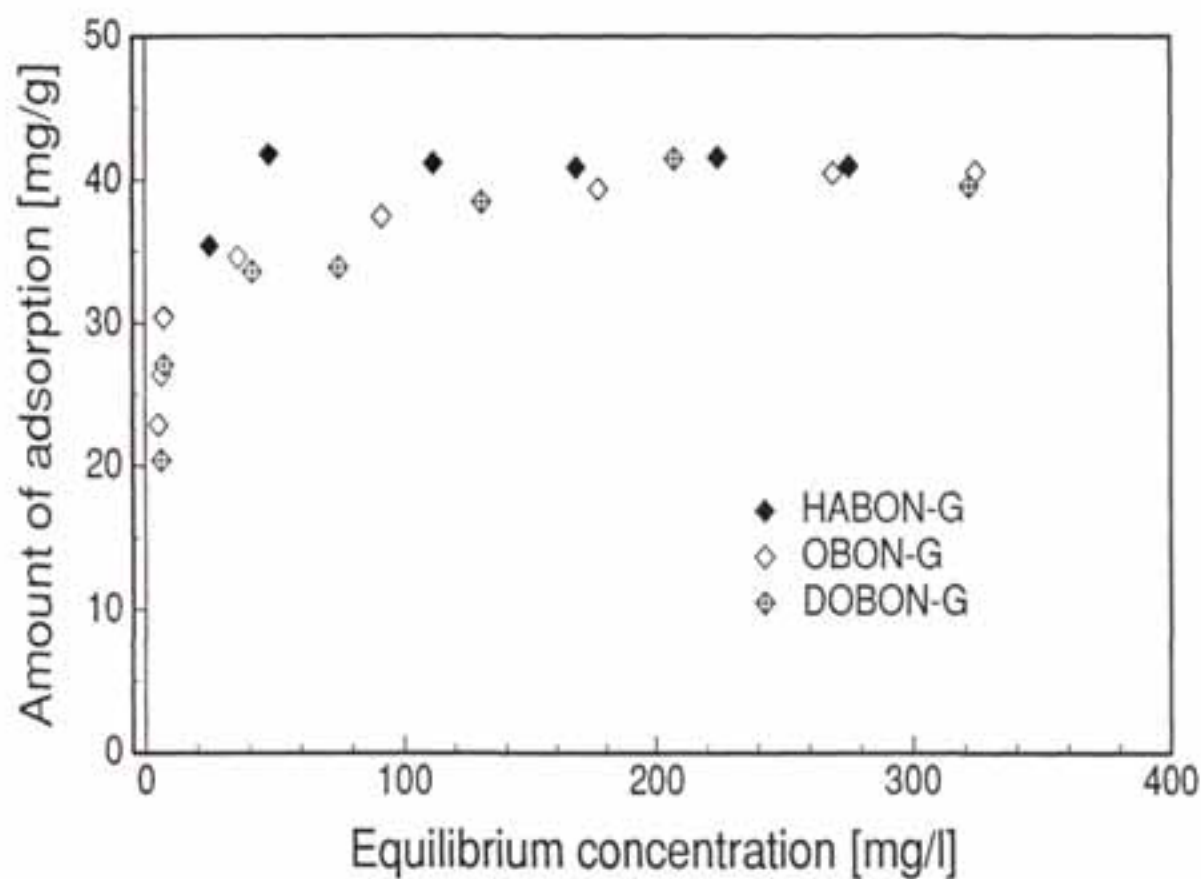
Table 4.13:

Adsorption Capacities for the Standard Soils for Surfactants with Different Length of the Alkyl Chain and Different Head Groups

Soil	Surfactant	$(x/m)_{max}$	
		[mg/g]	[mmol/kg]
Standard soil 1	Habon	8.1	28.5
	Obon	8.3	26.6
	Dobon	6.4	17.4
Standard soil 2	Habon	21.3	74.9
	Obon	19.8	63.4
	Dobon	18.2	49.4
Standard soil 3	Habon	32.6	114.6
	Obon	31.9	102.0
	Dobon	29.0	78.8
Standard soil 3	Habon-G	41.7	123.9
	Obon-G	41.1	112.7
	Dobon-G	41.0	97.4

Figure 4.16:

Adsorption Behaviour of the n-Alkyldimethylpolyoxethylammonium-Products on Standard Soil 3



The adsorption data for the system cationic surfactant/soil are evaluated by two relations:

- *Freundlich*-isotherm:

$$\frac{x}{m} = k c^{1/n} \quad \text{or} \quad (4.5)$$

$$\log \frac{x}{m} = \log k + \frac{1}{n} \log c \quad (4.6)$$

- *Langmuir*-isotherm:

$$\frac{x}{m} = \frac{kbc}{1 + kc} \quad \text{or} \quad (4.7)$$

$$\frac{c}{x/m} = \frac{c}{b} + \frac{1}{kb} \quad (4.8)$$

The relation from *Freundlich* presumes that no saturation occurs. Only data with equilibrium concentrations smaller than the saturation concentration should be evaluated.

Figure 4.17 and 4.18 show the adsorption isotherm for the system *Parabraunerde/Dobon* for both equations in linear form.

It is significant that the description of the adsorption isotherm by *Langmuir* fits all points well, although the whole concentration range is evaluated including the data in the saturation region. The maximum amounts of adsorption in the plateau region are given in Table 4.13.

The data are also evaluated by the *Freundlich* isotherm as proposed in the *OECD*-guideline. In Table 4.14 all results, especially the adsorption constants, are summarized. As mentioned before only the data with concentrations smaller than the saturation concentration are considered.

The adsorption constants are also related to the content of organic matter of each soil:

$$k_{oc} = \frac{k}{\% OC} \quad (4.9)$$

The k_{oc} -values are in the same order of magnitude than the known literature data for other cationic surfactants with similar structures (Table 4.5).

It must be mentioned that by evaluation of the adsorption data with the *Freundlich* equation the adsorption power will be underestimated because here only the low equilibrium concentrations are considered. But the lower limit for the concentration analysis of the cationic surfactants is 2-3 wppm or 2-3 mg/l respectively. The deviation for the lower concentration in Figure 4.17 confirms this inaccuracy.

In contrast to this for the *Langmuir* isotherm all data are evaluated und the calculation will be more accurate (see Figure 4.18).

The results presented up to here concerned only the cationic part of the surfactants, the *n*-alkyltrimethylammonium or *n*-alkyldimethylpolyoxethylammonium-compounds respectively.

Figure 4.17:

Evaluation of the Adsorption Data for the System DOBON/Parabraunerde by the Freundlich-Equation (4.6)

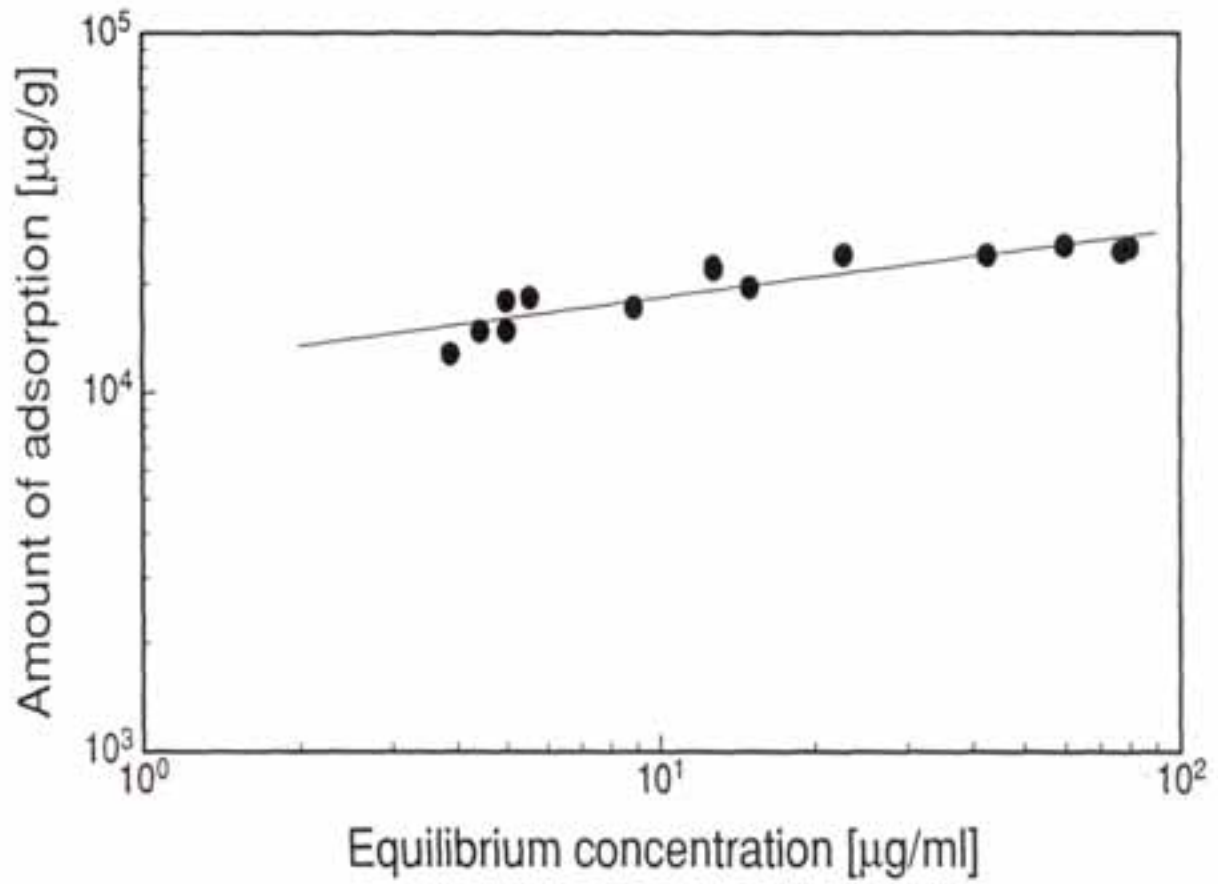


Figure 4.18:

Evaluation of the Adsorption Data for the System DOBON/Parabraunerde by the Langmuir-Equation (4.8)

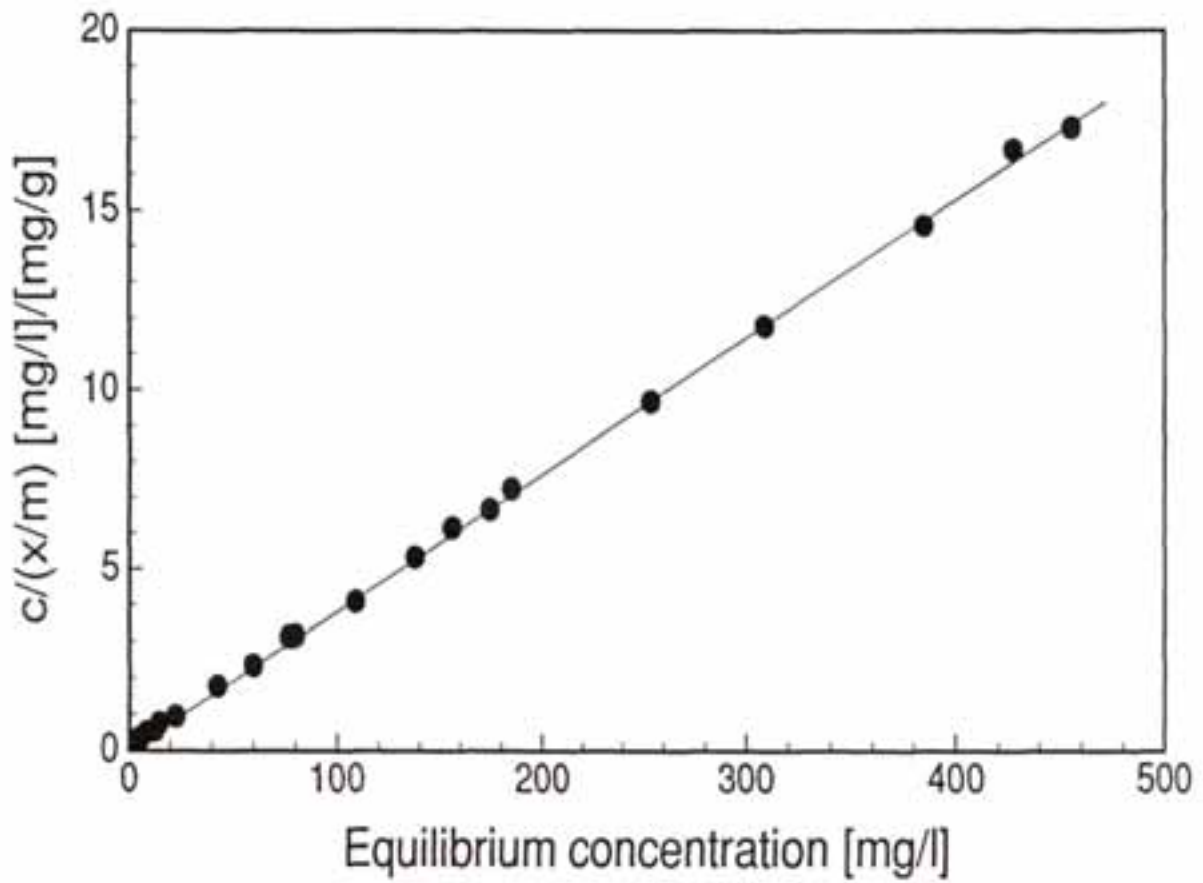


Table 4.14:

Adsorption Constants of the Evaluation by the Freundlich Isotherm

Soil	Surfactant	n	k	k _{oc}
			$\left[\frac{\mu\text{g/g}}{\mu\text{g/ml}} \right]$	$\left[\frac{\mu\text{g/g}}{\mu\text{g/ml}} \right] \cdot \frac{1}{\% \text{ OC}}$
Standard soil 1	Habon	7.25	3,871	553,000
	Obon	9.09	4,157	594,000
	Dobon	11.68	4,015	574,000
Standard soil 2	Habon	8.2	11,240	500,000
	Obon	9.9	13,508	600,000
	Dobon	11.94	11,982	533,000
Standard soil 3	Habon	5.35	13,677	1,410,000
	Obon	15.15	13,508	1,393,000
	Dobon	16.29	19,705	2,031,000

But also the counterion, the *3-hydroxy-2-naphthoate*, must be investigated for its adsorption behaviour. In all test runs the concentration of the counterion was analysed, too.

The photometric analysis, however, is influenced by substances which are extracted by the surfactant solution from the soil. This is due to the content of humus in the soil, which contains components with an aromatic structure. The presence of these substances can be proved by reference tests with water and soil. In these tests an UV-absorption at a wavelength of 354 nm can be measured which depends linearly on the amount of soil in the water. To take care of this influence by foreign substances for all adsorption test runs one sample was filled with water instead of surfactant solution to assess the absorption which is caused by humus (and not by the surfactant counterion).

The general behaviour for the counterion adsorption is shown in Figure 4.19. The dominant component for the adsorption is also the clay content. Investigations of the adsorption of *3-hydroxy-2-naphthoate* on *bentonite* showed that the counterion can not directly be adsorbed to clays. The mechanism of the adsorption of the counterions is based on the cation adsorption. The negatively charged counterions will be attracted by the positive charged headgroups of those cations which are adsorbed by hydrophobic interaction in the second layer on the clay surface. Because of the difficult estimation of the concentration of *naphthoate*, which can be seen from the deviations of the results, the anion adsorption is only described qualitatively.

The fact that the anion adsorption depends also mainly on the clay content of the soil is underlined by measurements with *Parabraunerde* and *Podsol*. The results are comparable to those from the cation adsorption.

Percolation Behaviour

The percolation tests were very difficult to carry out. The first experiments which have been done exactly as described in the instruction sheet from the german *Institute of Forestry and Agriculture* showed the following effects:

First the surfactant solution percolated well through the soil in the column and the concentration was almost zero in the outlet.

But the percolation rate of the surfactant solution decreased from 25 ml per hour to 10 ml per day. At the end no further surfactant solution could penetrate into the soil. At the surface of the soil a layer of surfactant had formed which stopped any further percolation of the surfactant solution. Up to a volume of surfactant solution of 3.17 l no cation could be analysed in the outlet. From the results of the adsorption isotherms a volume of 7.53 l would have been expected to saturate the soil.

New test runs were carried out with smaller amounts of soil in the percolation column. The results of 15 g *standard soil 2* are shown in Figure 4.20 for both the cation and the anion. If a maximum amount of adsorption of 18.2 mg surfactant per g soil is assumed the saturation point could be expected for a volume of surfactant solution of \approx 860 ml.

The increase of the concentration in the outlet corresponds well with this value. But it is surprising that the concentration decreases again after 1,800 ml. A reason for this behaviour may be the precipitation of the surfactants in the column which was observed by the appearance of a pink color at the top of the soil column.

Figure 4.19:

Adsorption Behaviour of the Counterion (3-hydroxy-2-naphthoate)
on the Standard Soils

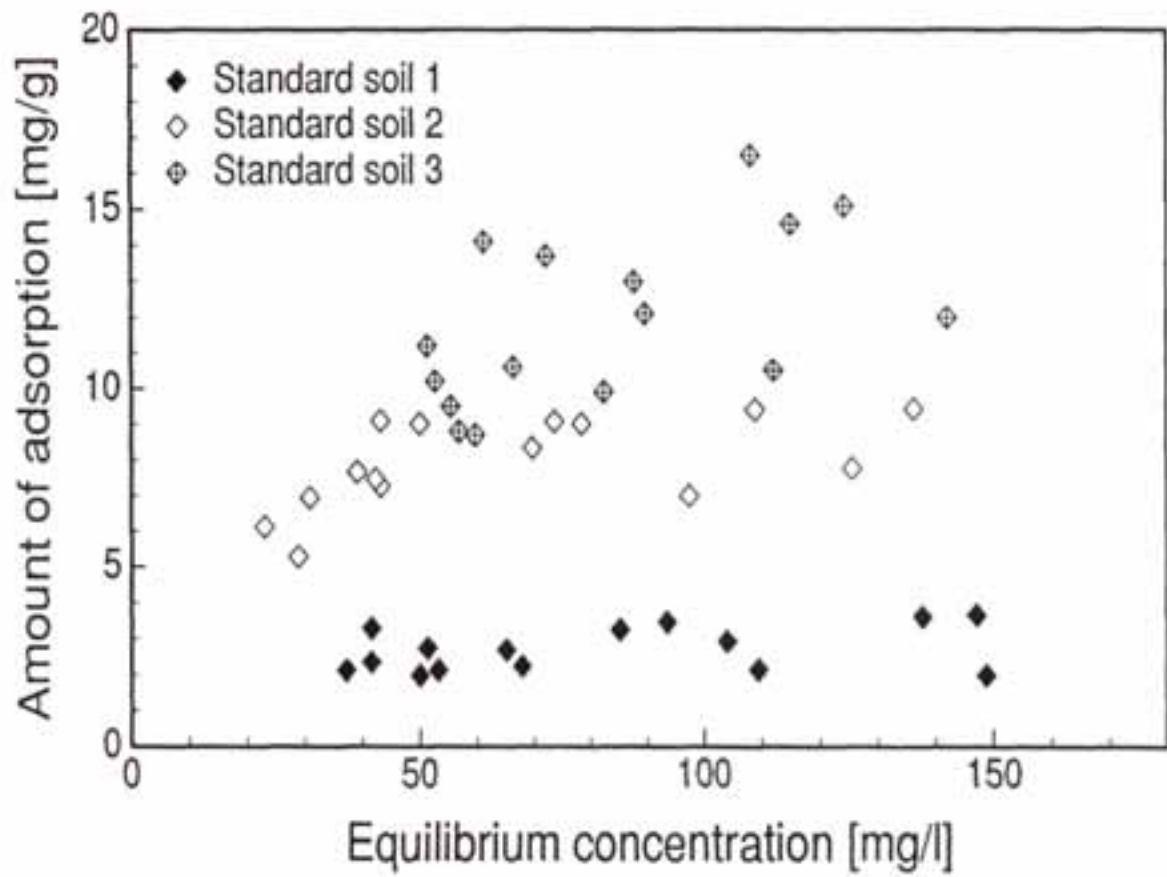
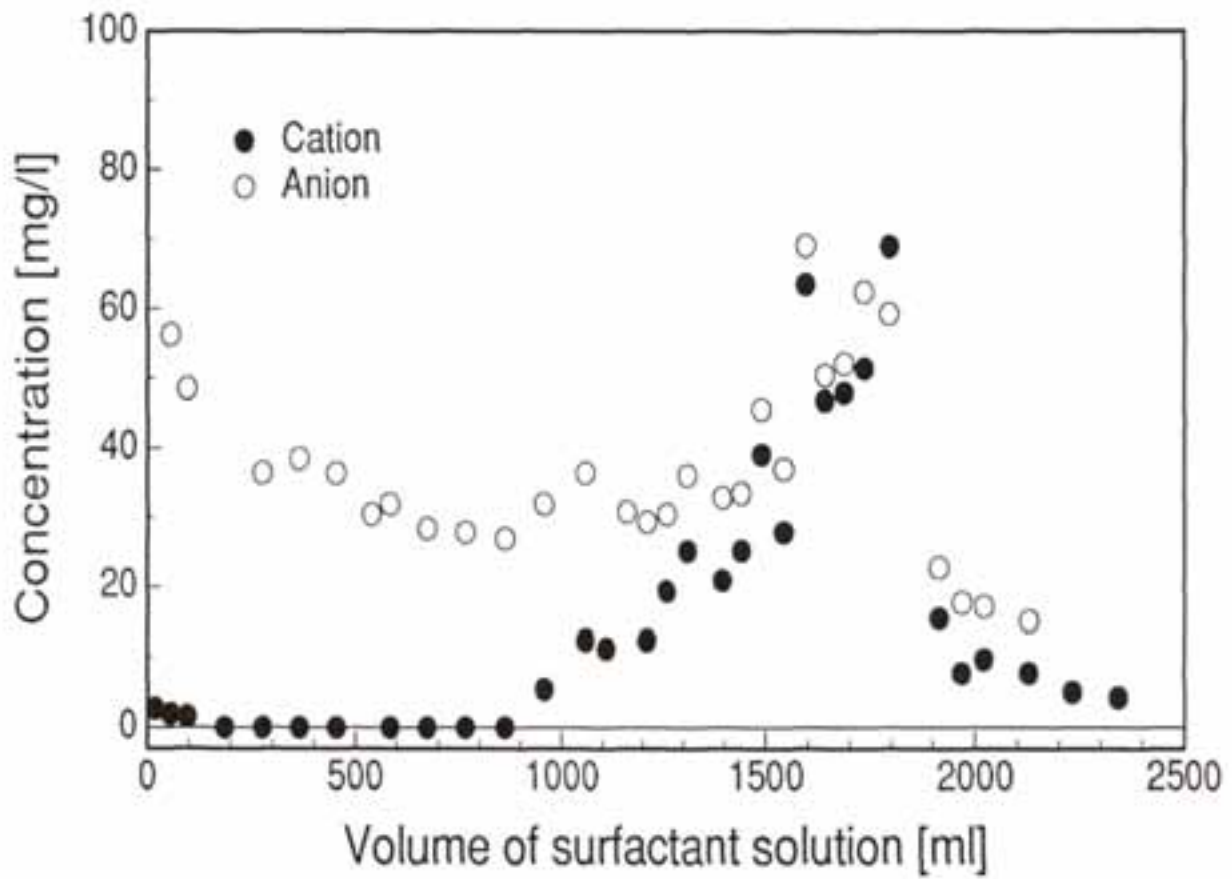


Figure 4.20:

Percolation Behaviour of a Solution of
DOBON ($c=480$ wppm) in a Column with Soil



The concentration of *naphthoate* goes parallel to the cation concentration. This is a further prove for the combined adsorption mechanism for both components. At the beginning the *naphthoate* concentration decreases from a high initial value. This is due to the outwashing of substances which are absorbing at the same wavelength as *naphthoate*.

Desorption Behaviour

The desorption behaviour is very important for the assesement of the endangering of ground water. The desorption medium was water with CaCl_2 at pH 3 and 7 and *methanol*.

In the case of water no desorption was observed, neither for the cation nor for the anion. Only with *methanol* a part of the adsorbed surfactant was desorbed.

These results correspond to data from literature [28, 29]. Due to the adsorption mechanism by ion exchange between the surfactant cations and the clay the adsorption can be regarded as irreversible.

4.5.4 Conclusions from the Adsorption Tests

The adsorption tests confirm the strong adsorption power for cationic surfactants on soils. Already soils with small clay content have an adsorption capacity which may be sufficient to adsorb or to immobilize respectively the surfactants when a surfactant solution penetrates into the ground.

Simulation tests with a surfactant solution with a concentration of 480 wppm demonstrate that all surfactants are removed by an amount of soil which is ≈ 35 -fold the amount of surfactant in the solution. With a soil density of 2.65 g/cm^3 this is equivalent to a volume of soil which is ≈ 6.6 -fold the volume of the surfactant solution.

In the case of a leakage this means that all surfactants will be immobilized by a small volume of soil around the leakage. A subsequent desorption by percolating water would not occur.

But for all these results from the adsorption tests one has to take into consideration that a natural soil can have a different structure compared to the test soils. If the contact between soil and surfactant solution is not very intensive, for example by a high porosity or the formation of channels, the effect of immobilization will be much smaller.

Surfactants can increase the draining in the ground because they lower the surface tension. An influence on the growth of plants was not observed yet. Waste waters with a content of cationic surfactants of 50 mg/l indicated no impairment to plants [30].

4.6 PENETRATION OF THE SURFACTANT SOLUTION INTO THE BOILER FEED WATER

The requirements for the quality of boiler feed water are normally much higher than for district heating water (see Table 4.2).

The electrical conductivity should be less than $0.2 \mu\text{S}/\text{cm}$, this means that the water is completely desalted.

If the boiler feed water would not be prepared in this way the dissolved salts would deposit on the turbine blades. This is due to the steam solubility of the salts. The efficiency of the turbine would be decreased.

In the case of *combined heat and power* (CHP)-plants the boiler feed water circuit and the district heating network are connected by heat exchangers (Figure 4.21). At this point it is possible that district heating water gets into the boiler feed water by a leakage and increases the content of salts with consequences which are described above.

Normally there is only a hazard potential for the district heating water to penetrate into the boiler feed water if the pressure on the steam side is less than the pressure on the district heating side. The pressure on the steam side depends on the condensation point of the steam.

To prevent this industrial accident the heat exchangers must be bypassed immediately if a leakage occurs. The quality of the water can be monitored by measuring the electrical conductivity. An increase of the conductivity would indicate the penetration of district heating water into the boiler feed water.

A further control unit is often installed to monitor organic substances in the boiler feed water. Organics can be analysed by a photometer.

If surfactants are added to the water of the district heating network two aspects are important:

1. The electrical conductivity is increased by the ionic surfactants.
2. The surface tension of the water is lowered.

Both aspects would cause a lot of problems in the boiler feed water circuit. If the surface tension is lowered the formation of foam is possible. The steam would carry droplets to the turbine and the containing salts would deposit on the turbine blades. Thus the effect of salt deposition would be increased. In this case the water supply must be stopped immediately.

However, the presence of surfactants would also be indicated by an increase in electrical conductivity. This measurement system is already installed and can be used to monitor the penetration of surfactants into the boiler feed water, too.

A special analysing of the surfactants can be carried out by measuring the UV-absorption with a photometer. The absorption spectrum for the surfactant *DOBON* is given in Figure 4.22. The organic counterion (*naphthoate*) of the surfactants causes an absorption in the range 285–305 nm and 315–390 nm respectively. A photometer allows a direct control of the surfactants.

The part of the circuit which can be contaminated with surfactants has to be kept very small.

Figure 4.21:

Structure of a CHP plant
(1 = Boiler; 2 = Turbine; 3 = Generator; 4 = Condenser;
5 = Heat Exchanger; 6 = Consumer)

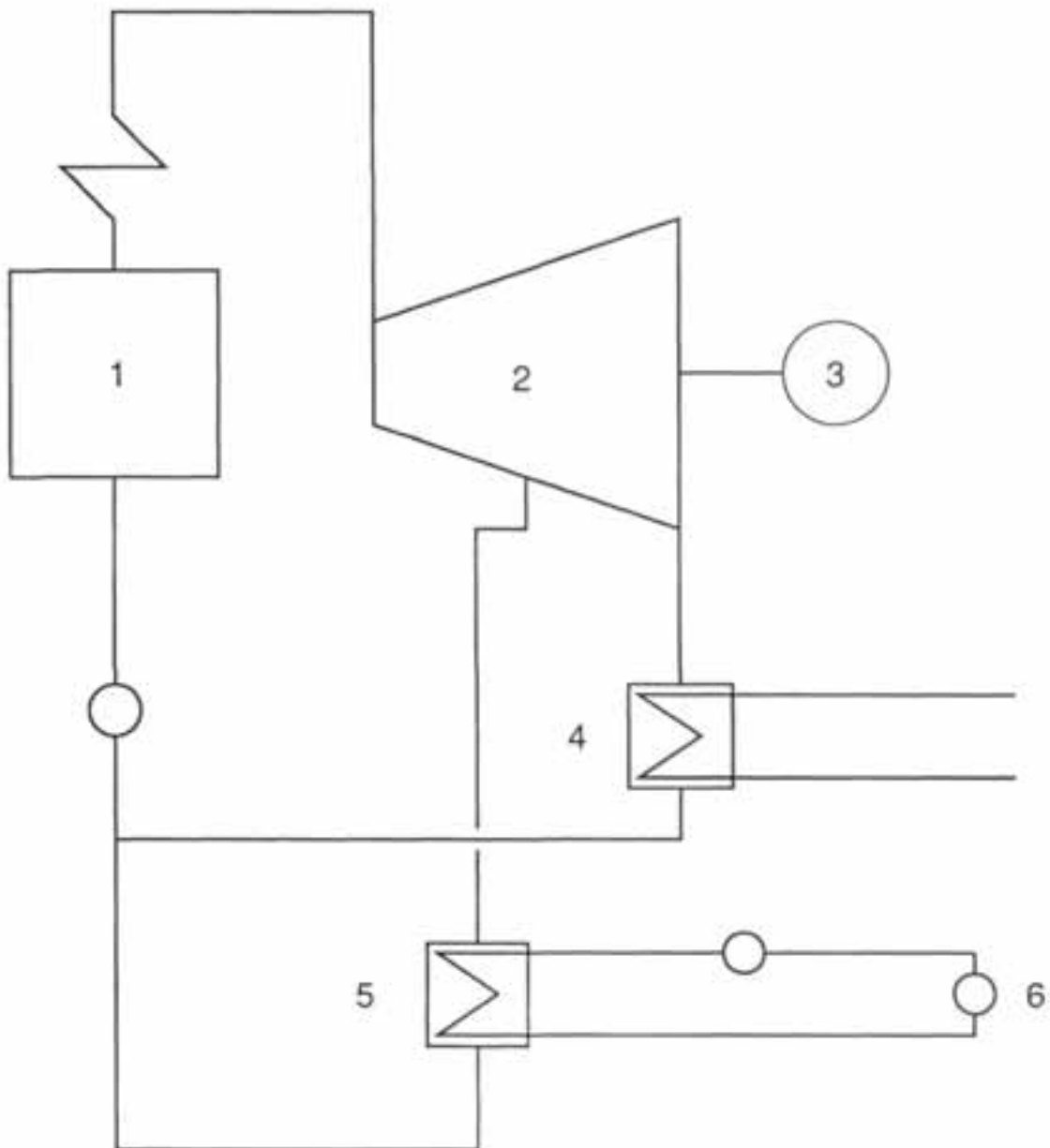
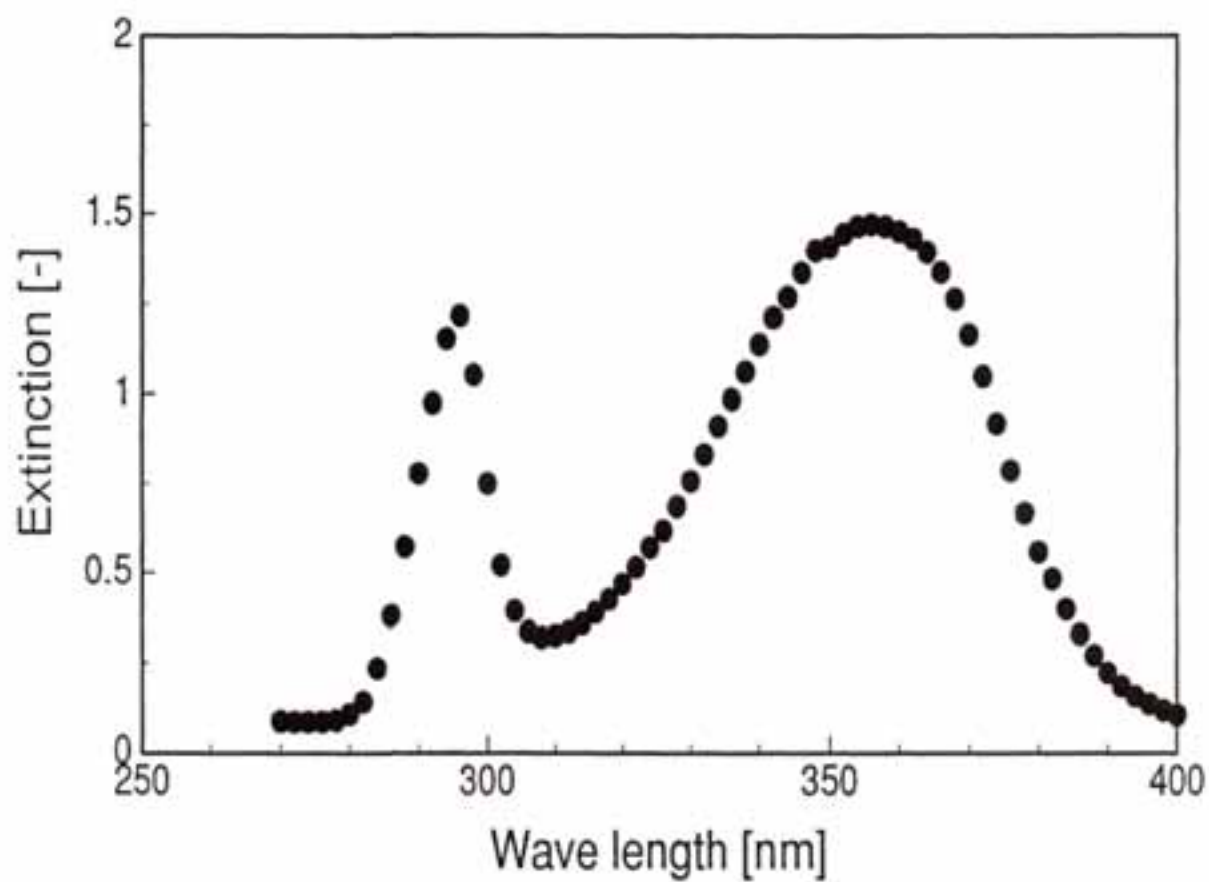


Figure 4.22:

UV-Absorption Spectrum for the Cationic Surfactant DOBON
(Concentration ≈ 200 wppm)



Due to the adsorption behaviour of cationic surfactants it is very difficult to clean the system again.

An additional security mechanism to prevent the surfactants to penetrate into the boiler feed water circuit is the installation of an adsorber resin column to hold back the surfactants when they are entering the boiler feed water circuit. Organic resins are able to adsorb cationic surfactants (see also 4.8).

4.7 PENETRATION OF THE SURFACTANT SOLUTION INTO THE HOT SERVICE WATER OF THE HOUSE SUBSTATIONS

In the house substations the hot service water is heated by a heat exchanger (hot water heating plant). The house substations are divided into

- direct and
- indirect systems (see Figure 4.23).

In direct systems the network water can penetrate into the drinking water in the case of a leakage.

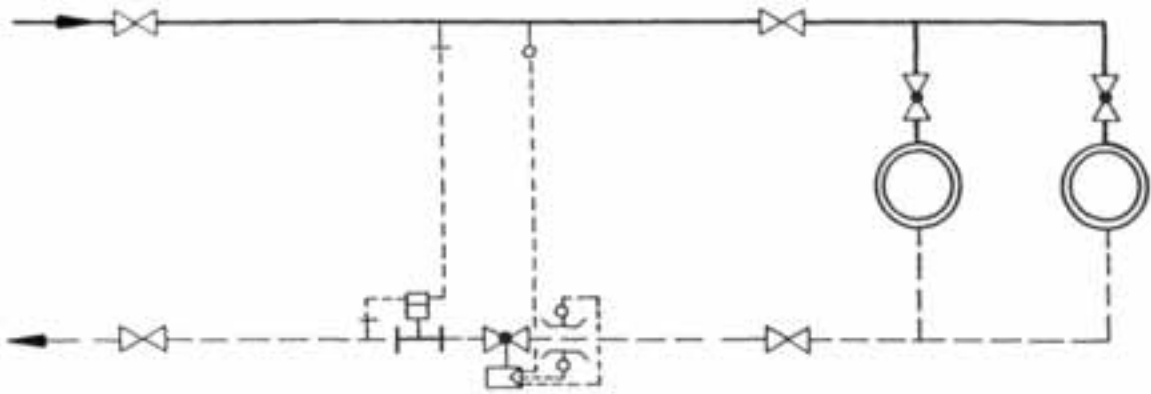
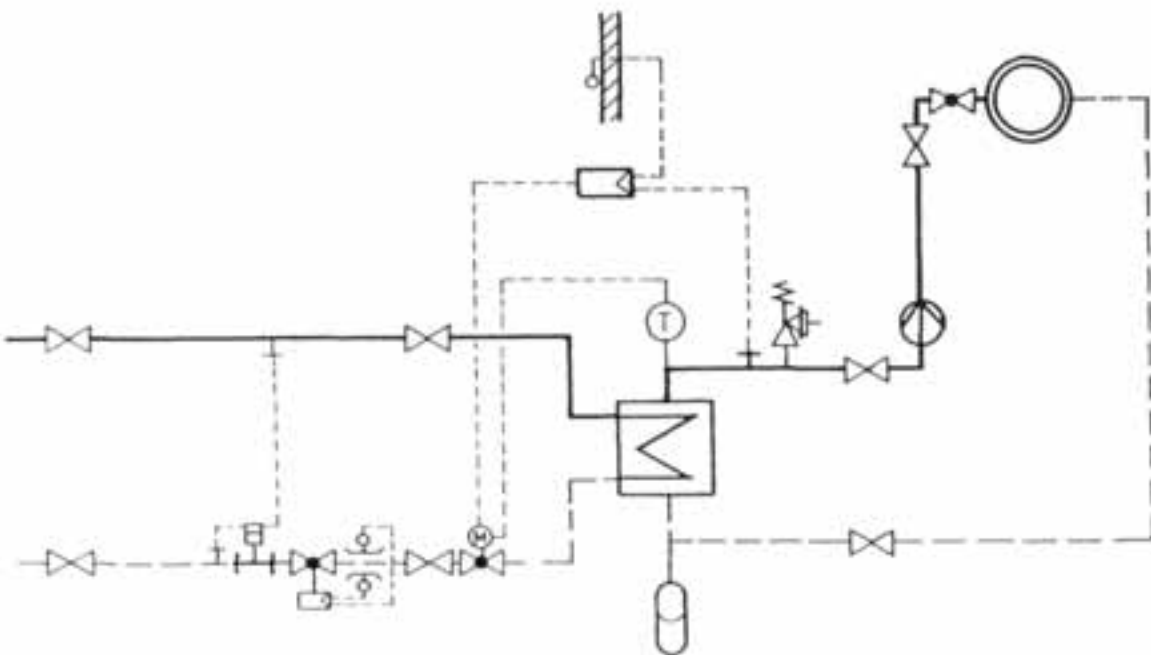
Because of this hazard in Germany the use of foreign substances is regulated by special demands in the *German Industrial Standards* DIN 1988 [31]. The additives are divided into five groups which cause different consequences for the heating of drinking water:

1. Class 1:
without endangering of health and without impairment of taste, odour and color, that means the condition of the drinking water is not changed.
(example: heated drinking water, cloudiness by air bubbles)
2. Class 2:
without endangering of health, impairment of taste, odour and color.
(Example: coffee, iron bacteria)
3. Class 3:
with endangering of health by poisoning and by substances which are little toxic. These are substances which are toxic, not very toxic and not carcinogenic.
(example ethylene glycol, copper sulphate)
4. Class 4:
with endangering of health by poisoning with substances which are toxic and very toxic, carcinogenic or radioactive.
These are substances with an acute toxicity LD_{50} smaller than 200 mg per kg bodyweight (tested for rats).
(example: lindane, parathion, hydrazine)
5. Class 5:
with endangering of health by pathogenic agents.
(example: hepatitis virus, salmonella)

According to the lethal dosis the surfactants which are used in the investigations for district heating systems can be classified to class 3:

LD_{50} for DOBON-G > 2,000 mg/kg bodyweight

Figure 4.23:

**Direct and Indirect House Substations
(Reproduced from [5])****Direct House Substation:****Indirect House Substation:**

For additives which are classified to class 4 or 5 an intermediate heat circuit has to be installed to produce hot service water. Based on the lethal dosis alone this is not necessary for the use of surfactants in district heating systems.

If the drag reducing additives are only used for transport systems, no problems can occur. The distribution network which supplies the house substations is separated by a heat exchanger. A penetration of the surfactants into the hot water circuit can be excluded.

4.8 WATER HANDLING IN THE CASE OF A LEAKAGE

In the normal operation of a district heating system the water quality is very pure. Thus it will be no problem to drain off parts of the network and to let the water into the environment (after cooling down).

If surfactants are added to the network water, these have to be separated before the network water enters the environment.

Three separation processes are suitable for surfactant solutions:

- ultrafiltration
- adsorption on *bentonite*
- adsorption on *lewatite*

4.8.1 Ultrafiltration

The *ultrafiltration* is a pressure driven membrane process which is able to separate macromolecules from smaller molecules in a solution.

In the case of a surfactant solution this means that the micelles are kept back and the single molecules permeate through the membrane. So the surfactant concentration in the permeate will be as high as the *critical micelle concentration*.

Investigations with drag reducing additives show that the maximum *molecular weight cut off* (MWCO) for a membrane to separate micelles is 100,000 dalton. A MWCO of 100,000 dalton means that molecules with a molecular weight greater than 100,000 dalton are rejected by the membrane.

Typical flux characteristics for ultrafiltration investigations are shown in Figure 4.24. The dependence of the permeate flux on the transmembrane pressure ($p_{trans} = (p_{in} + p_{out})/2$) can be divided into two regions:

1. Membrane controlled region:
The flux increases linearly with increasing transmembrane pressure.
2. Gel-layer controlled region:
The flux is independent from pressure. A gel-layer has formed.

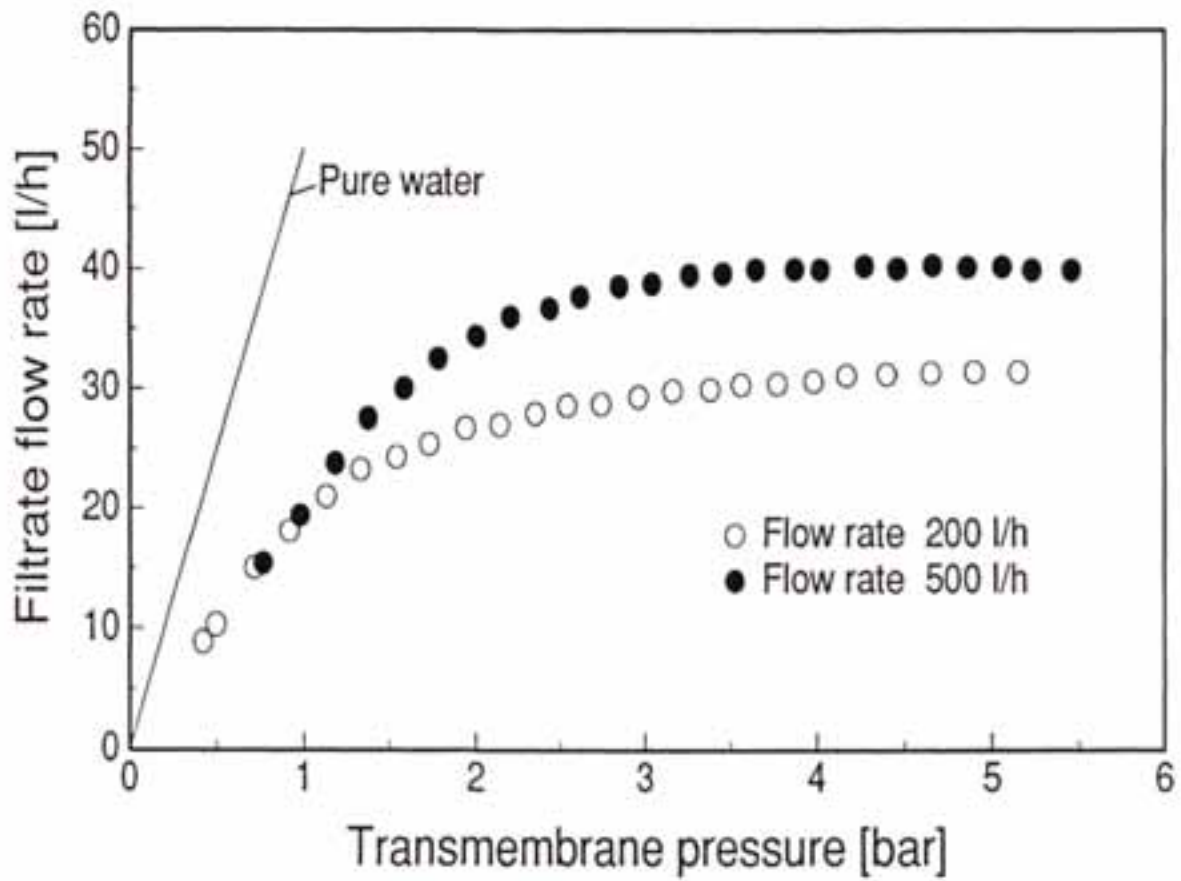
The ultrafiltration is a favorable process with respect to the following points:

- No additional substances are necessary.
- The surfactant is separated in concentrated form, it is directly reusable.

But there are also some disadvantages:

Figure 4.24:

Flux Characteristic of an Ultrafiltration Membrane
for the Cationic Surfactant OBON



- The flux decreases with increasing concentration. This means that the concentration rate for this process is not very high.
- The smallest permeate concentration one can expect is the *critical micelle concentration*. To separate the surfactant quantitatively an additional process is necessary.

By these features the *ultrafiltration* is a suitable process to produce a stream with a reduced surfactant concentration (almost zero), but it is not well applicable to concentrate a large volume of surfactant solution.

For a bypass purification it would be possible to separate the surfactants from the network water before the water enters the purification stage. Then the permeate will be purified as normal and the concentrate is added again to the purified water behind the purification stage.

4.8.2 Adsorption on Bentonite

Bentonite is a clay mineral with a high adsorption capacity for cationic surfactants. The minimum amount of bentonite to adsorb all surfactants from solution is 1.5-fold the amount of surfactant in the solution:

$$m_{\text{ben}} \geq 1.5 \cdot m_{\text{surf}} \quad (4.10)$$

m_{ben} : mass of bentonite which is necessary

m_{surf} : mass of surfactant in the solution

But even if the cationic part of the surfactant is removed up to 100% the counterion (*naphthoate*) is only separated to 50%. This rate can not be improved by adding more *bentonite* because the counterion is adsorbed by the cation on the clay.

The adsorption is irreversible, the adsorbed surfactant is lost and must be replaced.

For the separation of the surfactants it is possible to add the *bentonite* continuously to the solution. The *bentonite* must be presoluted in water. A static mixer will guarantee a good phase contact between *bentonite* and surfactant. To reach the adsorption equilibrium it is necessary to install a pipe reactor to have a sufficient residence time to reach the adsorption equilibrium. At last the bentonite-surfactant complex is separated from the water. The separation equipment can be a decanter, a filter press or a microfilter (see Figure 4.25).

In the following example the amount of *bentonite* is calculated for an assumed surfactant solution of 100 m³:

100 m³ surfactant solution

concentration: 1,000 wppm = 1.0 mg/l

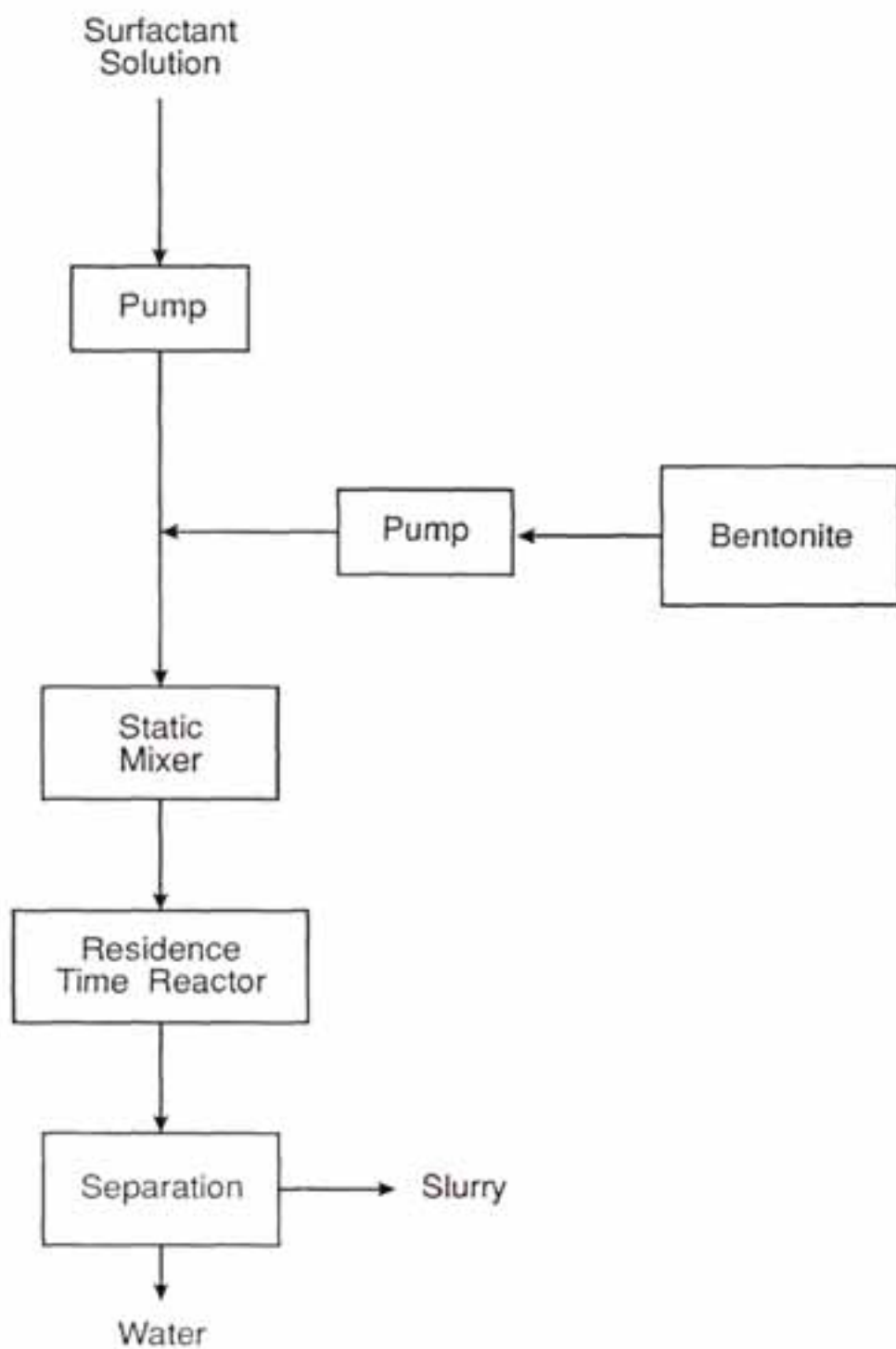
100 kg surfactant

⇒ amount of *bentonite*: 200 kg

⇒ volume of the *bentonite* suspension (2.5%): 8 m³

Figure 4.25:

Continuous Adsorption Process with Bentonite



The adsorption on *bentonite* was already tested in a large scale test in discontinuous mode in the demonstration project at Völklingen, Germany. The surfactant solution was drained off from the network into a basin. Here the clay was added in solid form to the solution. The amount of *bentonite* was 3-fold the amount of surfactant.

For the initial surfactant solution, the mixture of surfactant solution with *bentonite* and the filtrate after separating the *bentonite* with a micro filter the *dilution factor* ϕ was estimated. (The dilution factor means the factor by which the solution must be diluted to be no longer fish toxic).

For the pure surfactant solution the dilution factor was $\phi=400$. Already the addition of *bentonite* lowered the dilution factor to $\phi=6$. This decrease from 400 to 6 proves the fact that alone the loss of the surface activity by adsorption reduces the fish toxicity considerably. When the bentonite-surfactant complex was separated by filtration the dilution factor became only $\phi=2$. The surfactant concentration was almost zero.

The remaining little toxicity of the filtrate is caused by the *naphthoate* which is only adsorbed to $\approx 50\%$.

4.8.3 Adsorption on Lewatite

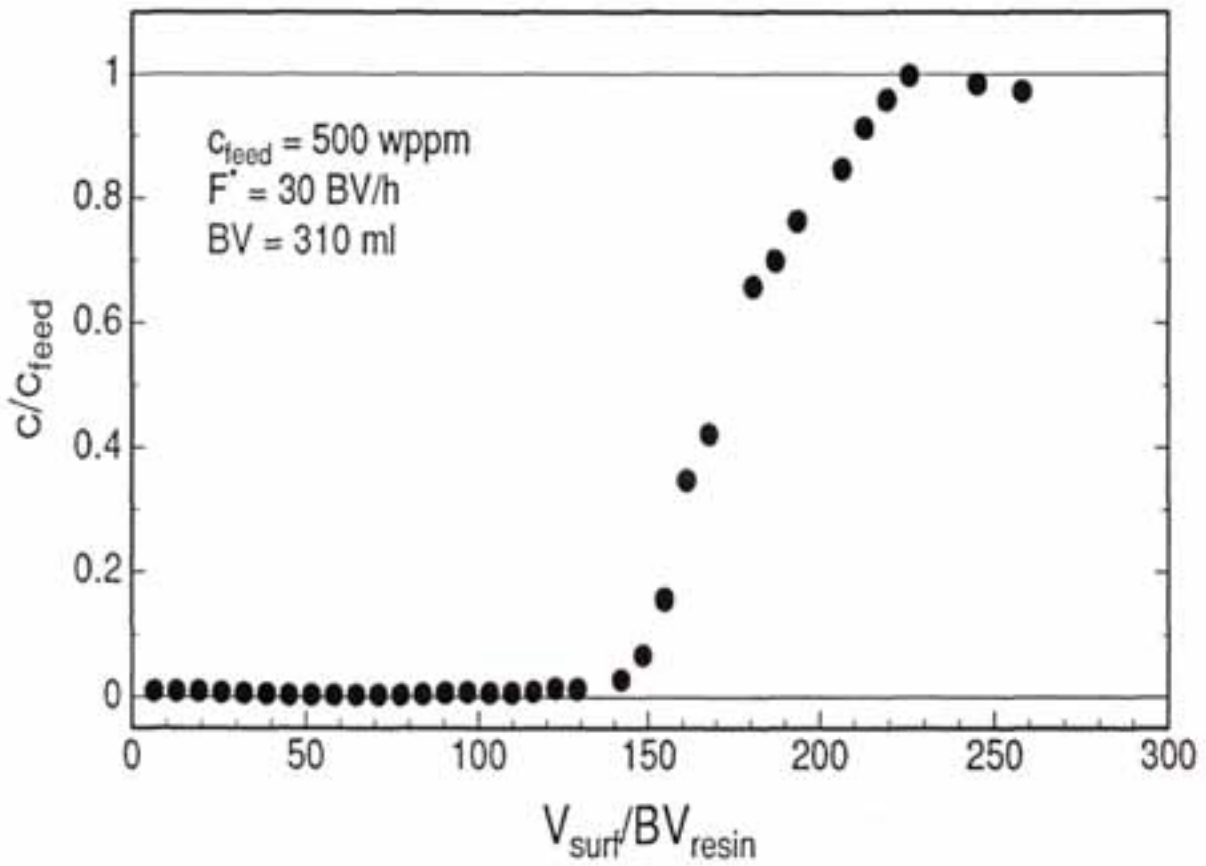
Lewatite is an organic resin consisting of a polystyrene matrix. The adsorption capacity is 70 g surfactant per dm^3 resin (see Figure 4.26). The resin may be desorbed by organics as *methanol* or *propanol* and the surfactant is reusable.

The before mentioned example for *bentonite* may also be calculated for *lewatite*:

- 100 m^3 surfactant solution
- concentration: 1,000 wppm = 1.0 mg/l
- \Rightarrow 100 kg surfactant
- \Rightarrow volume of *lewatite*: 2.9 m^3
- \Rightarrow flow rate 10-30 bed volumina per hour or
30-90 m^3 per hour

Figure 4.26:

Adsorption Behaviour of the Cationic Surfactants OBON on Lewatite
(BV=Bed Volume, V_{surf} =Volume of the Surfactant Solution)



4.9 CONCLUSIONS

In this study the potential hazard for the environment by drag reducing additives in district heating systems is assessed by literature data and investigations on the adsorption behaviour on soils.

A comparison of the chemical structure of the additives to other cationic surfactants which are used for other applications show that they are very similar in structure and therefore in their toxicological and ecological properties.

Cationic surfactants are often tested for their environmental behaviour. The main consequences from these tests are:

- primary biodegradability > 80%
- ultimate biodegradability > 60%
- fish toxicity > 1 mg/l
- bacteria toxicity > 1 mg/l

The primary degradability fulfils the demands from the german detergent law.

Two important mechanisms lower the fish toxicity and the effective concentration in the environment considerably:

1. Cationic surfactants form neutral salts with anionic surfactants which are present in all waste waters and surface waters.
2. They adsorb on all solid surfaces.

Furthermore the application of cationic surfactants in district heating systems would increase the total quantity of production only a little. The general ecological situation for cationic surfactants would not change.

The endangering by leakages has been assessed by adsorption tests. The results show that in the case of a leakage the surfactants are adsorbed irreversible on soils which prevents them from penetrating into the ground water. The dominant factor for the adsorption of cationic surfactants on soils is the clay content of the soil.

Besides the toxicological and ecological behaviour two technical aspects have been considered:

A penetration of the surfactant solution into the boiler feed water of the power plant has to be totally excluded. This demand is due to the great difference in the water quality for the district heating water and the boiler feed water. In the boiler feed water circuit the electrical conductivity is demanded to be < 0.2 $\mu\text{S}/\text{cm}$. The boiler feed water is always monitored with respect to this quality, so the penetration of the surfactant solution would also be indicated immediately. The following security procedure would be the same as for normal district heating water: the polluted water is stopped and drained off or purified again. For this point the application of surfactants would not cause any new problems.

If surfactants are used only in transport pipes, a penetration into the drinking water can be excluded. For an extended application in distribution systems it is advisable to install an intermediate circuit between the district heating system and the drinking water circuit.

In the case of repairing work, when a part of the network is drained off, a procedure for the handling of the water is necessary. Three processes are available to separate the surfactants from solution:

- ultrafiltration
- adsorption to bentonite
- adsorption to lewatite

All processes show different results with respect to the rest concentration, the use of additives and the form of the separated surfactant (reusable or not).

Another procedure for the water handling may be the storage of the water in the network. If buffer systems are present (heat storage) it is possible to pump the water from one segment which must be drained off into the remaining part of the network.

The main conclusion from this study is that the cationic surfactants used as drag reducing additives show the same properties than other cationic surfactants already used. But the concentration of the surfactant solution in the network is normally higher than the concentration of cationic surfactants in waste and river waters. This concentration will cause a steep local increase in concentration in the environment when a surfactant solution will get into surface waters or into the ground.

At the present the application of drag reducing additives is only planned for transport systems because here the drag reducing effect is particularly significant. Furthermore in this part of a network leakages are very rare and can be better controlled. In this case problems in housestations can be totally excluded.

Nomenclature

Symbols:

b	1	Constant
c	mg/l	Concentration
F*	BV/h	Flow rate
K_{ad}	1	Adsorption constant
k	1	Adsorption constant
M	g/mol	Molecular weight
m	g	Mass
n	1	Exponent
p	bar	pressure
T_K	°C	Krafttemperature
x	g	mass
V	dm ³	Volume
ϕ	1	Dilution factor

Subscripts:

ben	Bentonite
equi	Equilibrium
init	initial
in	Inlet
max	maximum
out	Outlet
surf	Surfactant
trans	transmembrane

Abbreviations:

AEC	Anion exchange capacity
BOD	Biological oxygen demand
BV	Bed volume
CEC	Cation exchange capacity
cmc	Critical micelle concentration
C_n TACl	n-Alkyltrimethylammoniumchloride
COD	Chemical oxygen demand

CTAB	Cetyltrimethylammoniumbromide
DBDMAC	Dibenzenedimethylammoniumchloride
DOC	Dissolved organic carbon
DSDMAC	Distearyldimethylammoniumchloride
EC	Effective concentration
hmc	Hemi micelle concentration
LAS	Linear alkylbenzene sulphonate
LC	Lethal concentration
LD	Lethal dosis
MWOC	Molecular weight cut off
NOEC	No observed effect concentration
OC	Organic carbon
PEC	Predicted environmental concentration
STAC	Stearyltrimethylammoniumchloride
wppm	Weight parts per million

Bibliography

- [1] M. Fankhänel.
Druckverlust und Wärmeübergang in Fernwärmesystemen bei Einsatz von mizellaren Widerstandsvermindernern.
Dissertation Universität Dortmund, 1989.
- [2] W.W. Althaus.
Anwendung widerstandsvermindernder Additive in Fernwärmesystemen.
Dissertation Universität Dortmund, 1991.
- [3] Y. Gao, J. Du, and T. Gu.
Hemimicelle Formation of Cationic Surfactants at the Silica Gel-Water Interface.
J. Chem. Soc., Faraday Trans I, 83 (1987) 8, pp. 2671-2679.
- [4] E. Jungermann.
Cationic Surfactants, Surfactant Science Series, Vol. 4.
Marcel Dekker, Inc. 1970.
- [5] Arbeitsgemeinschaft Fernwärme e.V.
Richtlinien für das Kreislaufwasser in Heizwasser- und Warmwasseranlagen (Industrie- und Fernwärmenetze).
- [6] G. Rippen.
Handbuch Umweltchemikalien.
Ecomed Verlagsgesellschaft mbH, Landsberg 1987.
- [7] P. Schöberl, K.J. Bock, and L. Huber.
Ökologisch relevante Daten von Tensiden in Wasch- und Reinigungsmitteln.
Tenside Surfactants Detergents 25 (1988) 2, S. 86-98.
- [8] Data from Hoechst Marketing Research.
- [9] B. Wachs.
Zur aquatischen Toxizität von Inhaltsstoffen der Wasch- und Reinigungsmittel.
Umweltverträglichkeit von Wasch- und Reinigungsmitteln, Bayrische Landesanstalt für Wasserforschung, Oldenburg Verlag, 1990.
- [10] H. Stache and K. Kosswig.
Tensidaschenbuch.
Carl Hanser Verlag, München 1990.
- [11] J. Falbe.
Surfactants in Consumer Products.
Springer-Verlag, Heidelberg, 1987.
- [12] P. Berth, P. Gerike, P. Gode, and J. Steber.
Zur ökologischen Bewertung technisch wichtiger Tenside.
Tenside Surfactants Detergents 25 (1988) 2, S. 108-115.
- [13] L.H. Huber.
Ecological behaviour of cationic surfactants from fabric softeners in the aquatic environment.
JAACS 61 (1984) pp. 377-382.

- [14] R.J. Larson and R.D. Vashon.
Adsorption and Biodegradation of Cationic Surfactants in Laboratory and Environmental Systems.
Developments in Industrial Microbiology, 24 (1983), S. 425-434.
- [15] L. Huber.
Forderungen an Tenside aus der Sicht der Wassergütewirtschaft.
Tenside Detergents, 17 (1980) 5, S.267 ff.
- [16] P. Gerike, W.K. Fischer, and W. Jasiak.
Surfactant Quaternary Ammonium Salts in Aerobic Sewage Digestion.
Water Research, 12 (1978), pp. 1117-1122.
- [17] R.S. Boethling.
Environmental Fate and Toxicity in Wastewater Treatment of Quaternary Ammonium Surfactants.
Water Research 18 (1984) 9, S. 1061-1076.
- [18] R.J. Larson and W.E. Bishop.
New Approaches for Assessing Surfactant Biodegradation in the Environment.
Soap Cosmet. Chem. Spec. (1988) pp. 58-64 and 118-122.
- [19] T.U. Kappeler.
Die aquatische Toxizität von Distearyl dimethylammoniumchlorid (DSDMAC) und ihre ökologische Bedeutung.
Tenside Detergents 19 (1982) 3, S. 169-176.
- [20] Hoechst AG.
Physikalische und chemische Eigenschaften von DOBON-G in 35%-iger Einstellung.
Datenblatt der Fa. Hoechst.
- [21] W. Knauf.
Bestimmung der Toxizität von Tensiden bei Wasserorganismen.
Tenside Detergents, 10 (1983) 5, S. 251-255.
- [22] OECD Guideline for Testing of Chemicals (Adsorption and Desorption).
- [23] Biologische Bundesanstalt.
Prüfung des Versickerungsverhaltens von Pflanzenschutzmitteln.
Biologische Bundesanstalt für Land und Forstwirtschaft, Merkblatt 37, 1. Auflage 1973.
- [24] G. Tyler Miller.
Living in the Environment.
Wadsworth Publishing Company, 1990.
- [25] P. Schachtschabel, H.-P. Blume, and G. Brümmer.
Lehrbuch der Bodenkunde.
Ferdinand Enke Verlag, Stuttgart 1989.
- [26] H. van Olphen.
An introduction to clay colloid chemistry.
John Wiley, 1977.
- [27] G. Lagaly.
Ton und Tonminerale.
Ullmann, Bd. 23, S.311 ff.

- [28] G. Wirzing.
Über den Verbleib kationenaktiver Tenside im Abwasser: Reaktion von kationaktiven Tensiden mit Bentonit.
Fresenius Z. Anal. Chem., 319 (1984), S.255-266.
- [29] H. Hellmann.
Remobilisierung und Bestimmung von k-Tensiden in Tonmineralien.
Fresenius Z Anal Chem 319 (1984), S. 267-271.
- [30] H.-P. Blume.
Handbuch des Bodenschutzes.
Ecomed Verlagsgesellschaft, 1990.
- [31] DIN 1988 (Germany).
Technische Regeln für Trinkwasserinstallationen
(Technical Directives for Drinking Water Installations.

5. ICE SLURRY BASED DISTRICT COOLING SYSTEMS

Bryan D. Knodel* and Chris W. Snoek

Energy, Mines & Resources Canada
Energy Research Laboratory
Energy Systems Technology Implementation
555 Booth Street
Ottawa, Canada, K1A 0G1
(* under contract)

5.1 INTRODUCTION

5.1.1 Project Overview

The International Energy Agency (IEA) has commissioned the Department of Energy, Mines and Resources (EMR) of Canada to develop a general design manual for a new generation of ice slurry based district cooling systems.

5.1.2 Purpose

The emergence of ice slurries for use in district cooling systems may be the most significant technical development since the birth of the industry. The large energy capacity of ice slurries can reduce the distribution flow rate up to 80% compared with conventional chilled water systems meeting the same load. Lower flow rates result in pipe diameter reductions of up to 60% or more and proportionally smaller pumps. These factors combine to lower both the capital cost and operating costs for the district cooling network. At the present time, the capital cost of ice slurry chillers is still fairly substantial, but work is in progress to bring the cost down. Existing District Cooling systems can be expanded using ice slurry without having to increase the pipeline capacity (Reference 1).

The emerging ice slurry district cooling technology has been pioneered by a relatively small and diverse group of researchers with limited interaction or information exchange. As a result, there is a great deal of variety between even fundamental component designs.

The preparation of a design manual is the first step in an important process of evaluation and re-definition for this emerging technology. The design manual will provide an important "Total System Perspective" which is essential for the development of a technically balanced solution to real problems. However, the design manual is in the same state of evolution as the technology it seeks to document. A comprehensive, technically proven design manual for ice slurry district cooling systems is only possible when such systems have been successfully demonstrated.

The use of ice slurry in a district cooling system will be most attractive when advantage can be taken of reduced demand charges and off-peak power rates. Also, in applications where the pipe diameter has a large effect on installed cost, ice slurry has the potential to improve the economics of the system.

5.1.3 Technical Approach

This design manual has been prepared using the most recent information from leading ice slurry district cooling researchers. The manual has been limited to ice slurry research without the use of friction reducing additives (FRA). The design manual begins with a summary of the specific design alternatives which are being developed. The design alternatives are organized according to the major elements of a district cooling system: ice slurry generation, distribution, storage, and utilization. The last section is a compilation of recommendations for further research. This material is also arranged according to the functional elements of a system.

5.2 ICE SLURRY DISTRICT COOLING - DESIGN ALTERNATIVES

5.2.1 System Overview

An Ice Slurry District Cooling system can be divided into several components; the Ice Slurry Generation system, Ice Slurry Distribution system, Ice Slurry Storage system, and Ice Slurry Utilization system. A successful district cooling application will require careful design of each of these elements.

5.2.1.1 Ice Slurry Generation

The Ice Slurry Generator is used to provide a continuous supply of ice slurry for the distribution network. Typically, the ice generator forms the evaporator section of a conventional vapour compression refrigeration cycle. The remainder of the cycle is commonly purchased as a packaged condensing unit including the compressor, condenser and auxiliary equipment and controls required for continuous reliable operation.

The compressor is usually driven by electric motors. However, alternative drives include steam turbines and internal combustion engines. These optional drives may be more attractive for district cooling applications from a total energy perspective where steam or low cost fossil fuels are available. Several types of ice generation systems are currently available for use in district cooling systems and still others are under development. The major ice generation technologies will be discussed in detail later in Section 5.2.2.

5.2.1.2 Ice Slurry Distribution

Ice Slurry Distribution systems include all of the equipment required to handle ice slurry produced by the Ice Slurry Generation system and deliver it to the end users. The basic elements of the ice slurry distribution system are the ice slurry vessel, the

distribution pumps, and the distribution network including piping and valves. A simple schematic of such a system is shown in Figure 5.1.

The ice slurry vessel provides the interface between the ice slurry generation system and the ice slurry distribution network. The ice slurry vessel is used to keep the ice slurry in a fluid state as it is produced and concentrated to operating levels. Three primary design concepts have been used thus far: mechanical mixing, free surface vortex flow, and a flooded vortex flow. The details of these approaches will be presented in Section 5.2.3.1.

The ice slurry distribution pump can be a simple water type centrifugal pump or a positive displacement design depending upon the design requirements.

The distribution network typically consists of a buried insulated piping system to supply ice slurry to buildings located around the network and return warm water to the central refrigeration plant. The distribution system can be constructed from a variety of piping and insulation materials.

5.2.1.3 Ice Slurry Storage

Depending on the system load curve, implementing ice storage into an ice slurry district cooling system has the potential to improve the overall economics of a system. The high energy absorption characteristics of ice which make it an ideal media for increasing the cooling capacity in the distribution network can also be used to provide Thermal Energy Storage for the entire district cooling system or for specific end users.

Cooling loads experienced by many buildings have been shown to vary significantly depending upon the time of day. In most cases the peak cooling load only exists for a few hours. Thermal Energy Storage is an increasingly popular technique which allows the refrigeration equipment of a single building, or an entire district cooling system, to be sized for the average rather than the peak cooling loads.

In the case of a district cooling system, Thermal Energy Storage is used to "level" the cooling loads of some or all of the buildings serviced by the network. The average cooling load for the network is satisfied by operating the Ice Slurry Generation system continuously at its full downsized capacity. During periods of low or no cooling load, the ice slurry is distributed to one or more ice storage tanks located around the distribution loop. Later, during peak cooling loads, the required capacity is supplied using a combination of installed refrigeration and stored cooling from the storage tanks.

Since ice slurry has a much higher energy storage density than chilled water, Thermal Energy Storage using ice slurry can be significantly more cost effective. For many installations the addition of Thermal Energy Storage can reduce the capacity of the central refrigeration plant by up to 50%. The actual reduction is based upon the specific cooling load curves for a given system. Figure 5.2 illustrates the basic concept of Thermal Energy Storage.

Figure 5.1

Ice Slurry District Cooling System

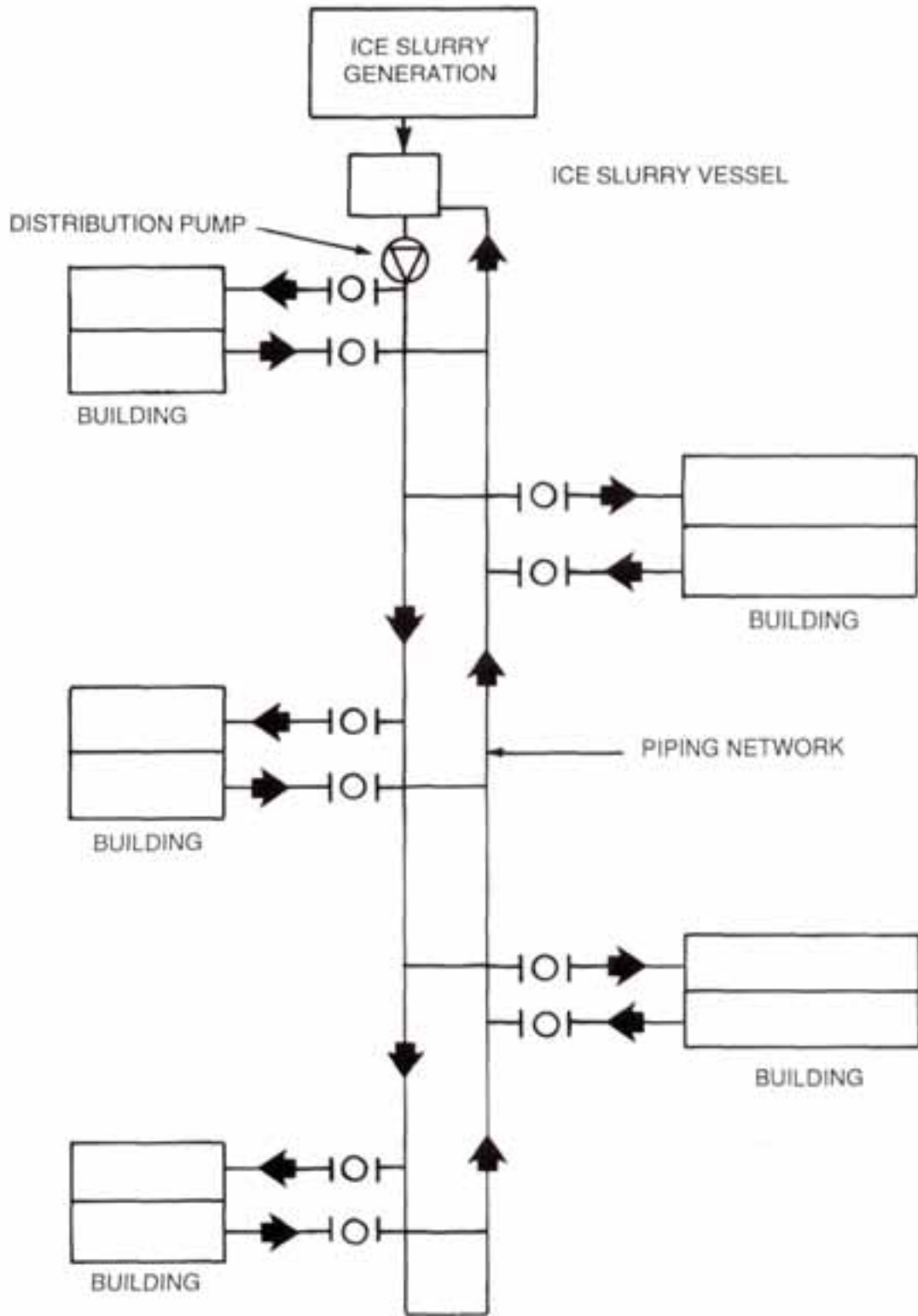
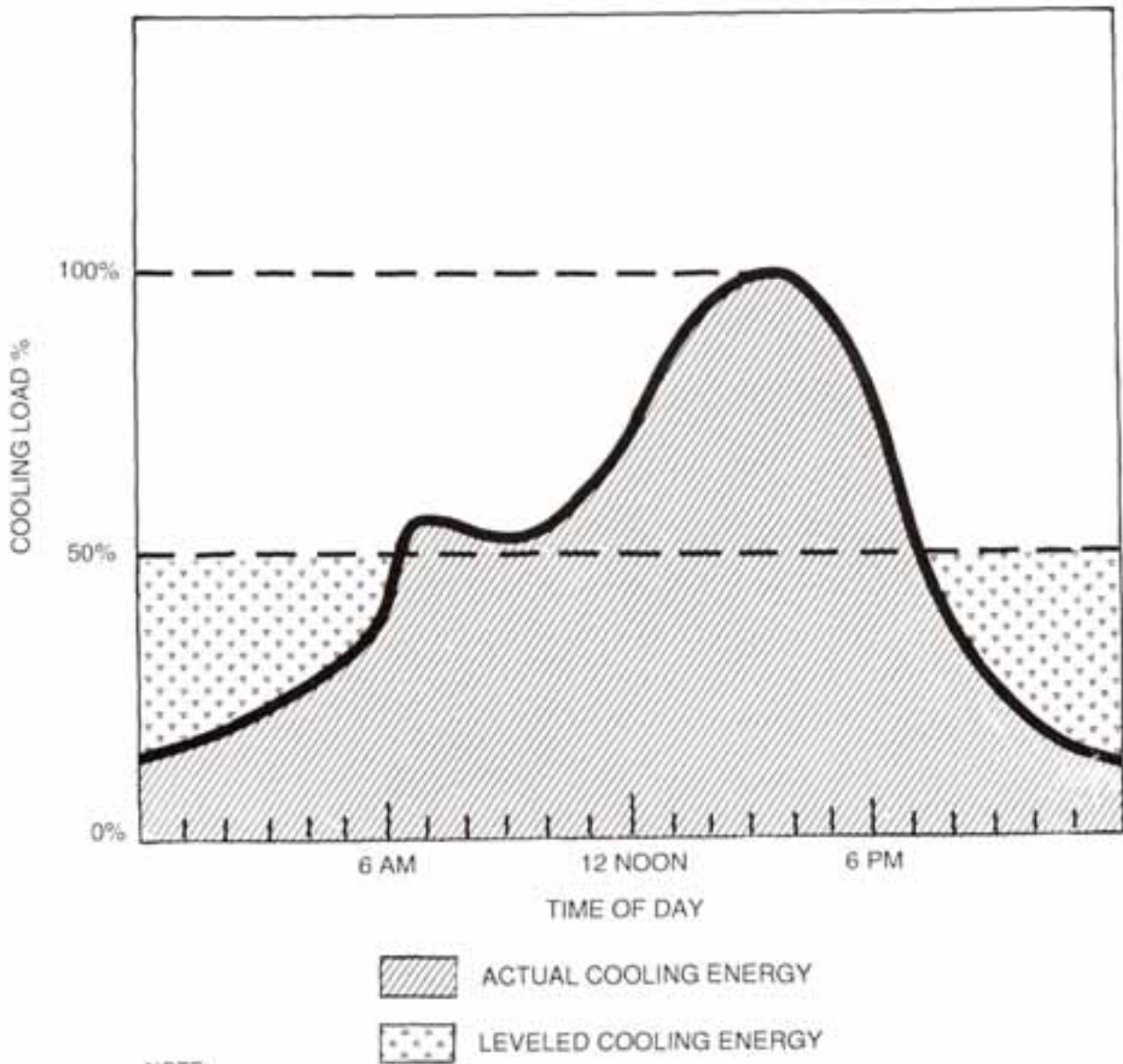


Figure 5.2

Cooling Load "Levelling"



NOTE:

The areas under the curves of the actual and leveled load are equal.

The benefits of load levelling can also be applied to the distribution system. This allows the system to be sized for the average rather than the peak cooling loads. This is accomplished by adopting a strategy known as Distributed Storage. The details of this method will be presented in Sections 5.2.4.2 and 5.2.5.2.

In addition to reducing the installed refrigeration capacity, Thermal Energy Storage also allows the district cooling system to take advantage of lower energy costs provided by many utilities in the form of time-of-day electricity rates. These rates represent an incentive, provided by the utility, to encourage consumers to purchase electricity during low demand hours at night.

The combination of reduced refrigeration capacity and lower electricity costs are important advantages available to district cooling systems which include Thermal Energy Storage.

5.2.1.4 Ice Slurry Utilization

The Ice Slurry Utilization system includes the equipment and controls required to satisfy, automatically, the end-user cooling load. In this portion of the system, the advantages of ice slurry in the distribution side of the district cooling system are transformed to satisfy conventional building cooling demands.

5.2.2 Ice Slurry Generation

5.2.2.1 Binary Solution Ice Slurry Generator

Methodology

The Binary Solution Ice Slurry Generator uses a refrigerated surface to supercool a binary solution without crystal nucleation on the surface. The refrigerated surface is typically a tube with refrigerant on the outside and binary solution on the inside. The surface is refrigerated using conventional refrigeration technology appropriate for the low temperature application. The ice is formed in the bulk fluid away from the refrigerated surface. This ice slurry technology can only operate with a binary solution which depresses the freezing point of the water.

Several freezing point depressants have been used successfully including ethylene glycol, propylene glycol, and salt solutions. Regardless of which additive is selected, the concentration increases as ice is generated. The increased concentration depresses the freezing point further and lowers the overall thermodynamic efficiency of the process as ice is produced.

Laboratory investigations are presently ongoing to develop systems in which the freezing point depressant is contained in the ice slurry generator and is excluded from the distribution lines.

Equipment Design

Two basic designs are currently commercially available to achieve crystal growth in the bulk fluid; the internal wiper and the falling film. The internal wiper system is constructed of one or more relatively large diameter (20 cm) horizontal tubes which are chilled on the outside. The binary solution flows through the inside of the tube. Mechanically driven wipers rotate inside the tube(s) to continuously disturb the boundary layer at the tube wall. The chilled solution is moved away from the wall prior to crystal growth. The Sunwell Engineering Co Ltd. of Woodbridge, Ontario, has perfected a design and its ice slurry generators are now used worldwide. The Sunwell ice slurry makers can operate with an ice slurry fraction of up to 25% per pass. They can also accommodate a small ice slurry fraction at the inlet. Figure 5.3 shows a sketch of the process.

The falling film ice slurry generator design is essentially a vertical shell and tube evaporator with the tubes extending above the upper tube sheet. The tube diameter is approximately 2 cm. The binary solution is distributed uniformly over the upper tube sheet where it overflows the rim of the extended tubes creating a falling film along the inner surface of the tubes. The falling film flow pattern, a special tube finish, and a controlled maximum heat flux, combine to eliminate ice growth on the tube surfaces.

The slurry exiting the ice generator is typically sent to a intermediate vessel where the ice is deposited and from which ice free water is supplied for continued ice production. The concentration of the accumulating ice is raised to the desired level prior to entering the distribution network. Additional information relative to this intermediate ice slurry concentration vessel will be given in Section 5.2.3.1.

Ice Slurry Characteristics

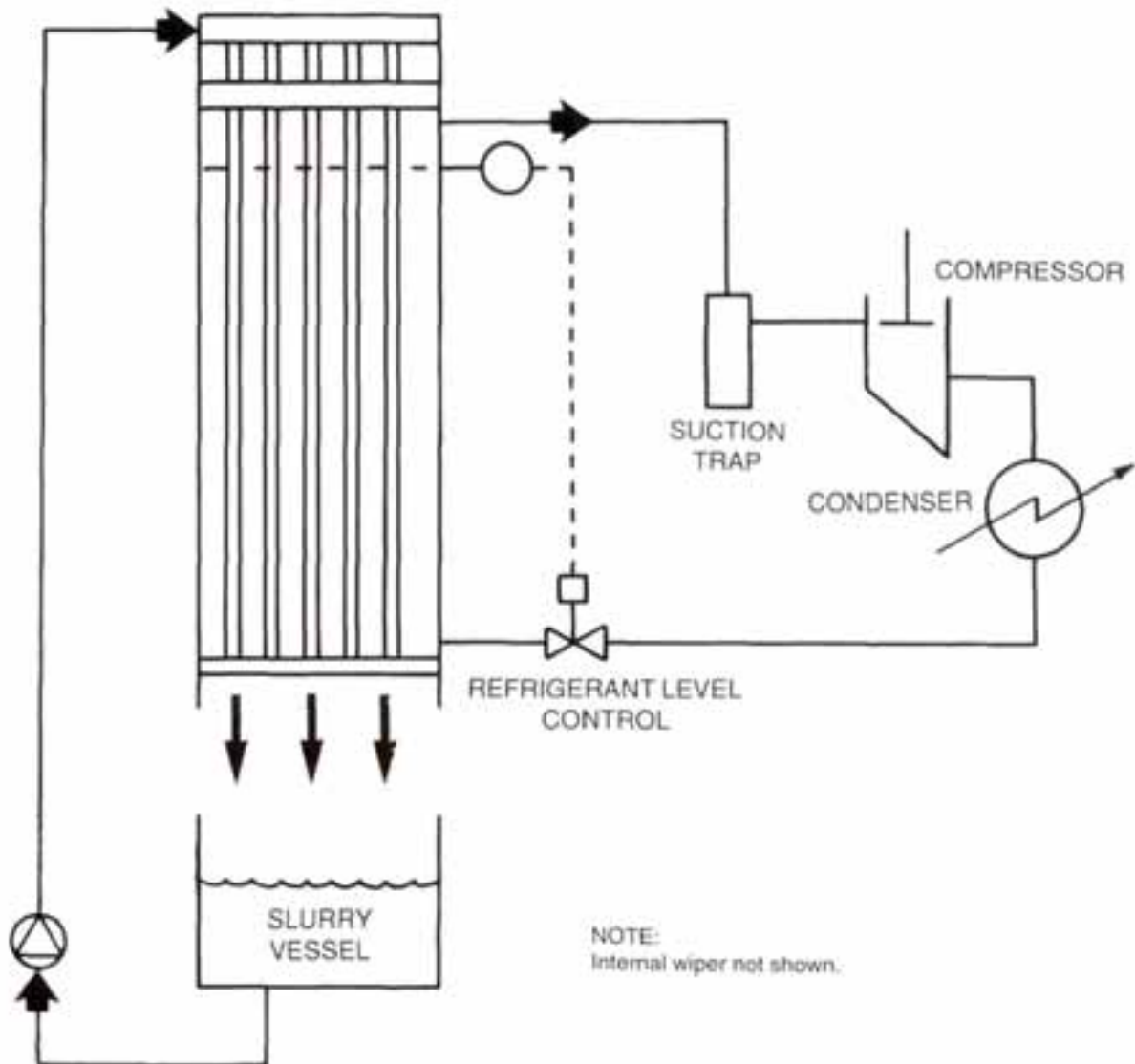
Regardless of which design is chosen, the Binary Solution Ice Slurry Generator produces a fine ice slurry with roughly spherical ice grains ranging from 0.1 mm to 0.25 mm in diameter in a binary carrier fluid, usually water/glycol.

The fine crystal size associated with these systems is the result of concentration gradients within the binary solution generated during the crystallization process. When a binary fluid is chilled below its freezing point, spontaneous nucleation initiates the growth of an ice crystal. The crystal being formed is composed of pure water extracted from the binary solution during the phase change process. As a result, the liquid in the immediate vicinity of the growing crystal experiences an increase in concentration as it loses pure water. The freezing point of this fluid drops proportionally with the increasing concentration.

Eventually, the freezing point is depressed to the point where continued crystal growth is not thermodynamically possible. The time scale for this process is quite rapid resulting in the termination of crystal growth while the crystals are relatively small.

Figure 5.3

Binary Solution Ice Slurry Generator with Internal Wiper



The flow characteristics of the fine binary ice slurry have been generally classified as homogeneous and Newtonian. The flow characteristics at moderate ice concentrations (less than 30%) for this slurry are similar to those of the binary solution alone. Flow analysis data for this slurry will be presented in greater detail in Section 5.2.3.2.

Status

The Binary Solution Ice Generator is commercially available in a relatively wide range of sizes from several suppliers. Small scale Binary Solution Ice Generators have been used in laboratory ice slurry district cooling research. This technology has also been used extensively for bulk ice slurry generation applications related to the food processing industry and for Thermal Energy Storage air-conditioning load levelling systems for individual buildings. Ice slurry based cooling systems are also currently being installed to cool the lower levels of deep mines. These applications require ice slurry pumping and in the case of the mine also ice harvesting as part of the system design.

5.2.2.2 Scraped Surface Ice Generator

Methodology

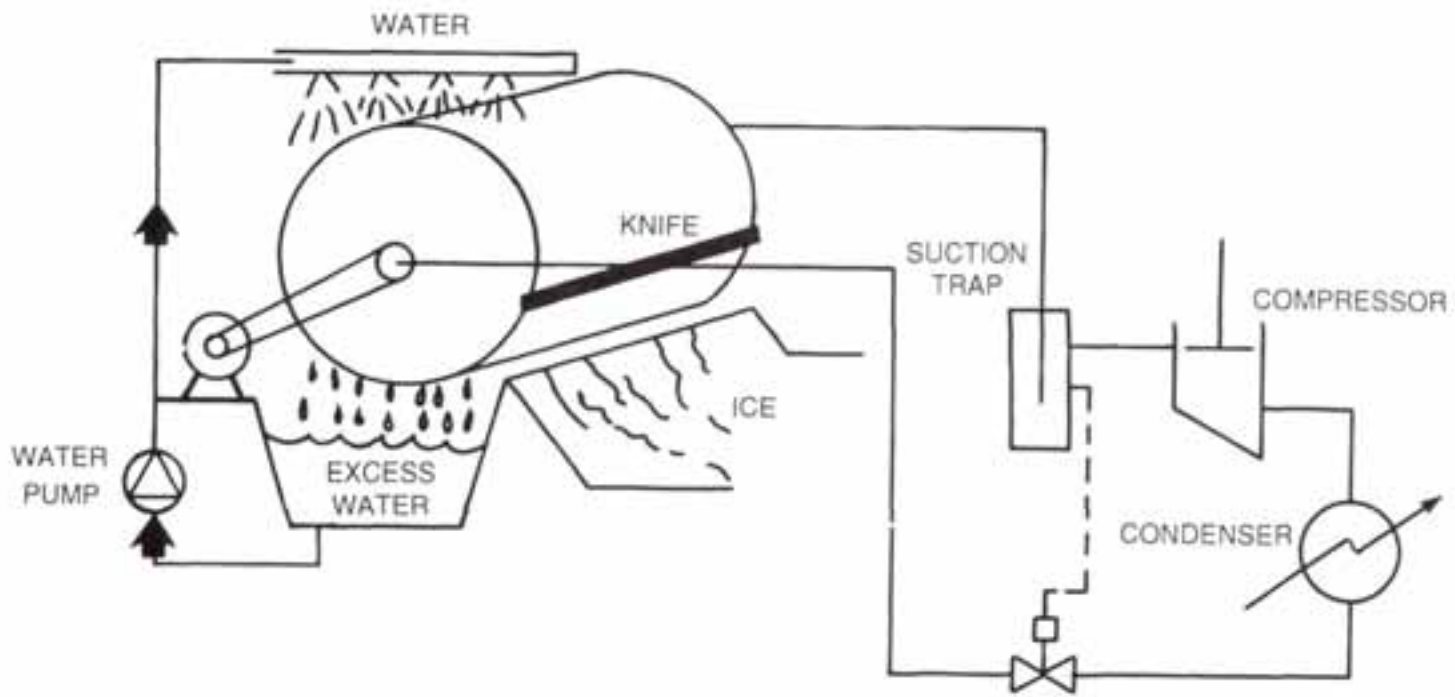
The Scraped Surface Ice Generator uses a refrigerated surface, in the shape of a drum, to build a layer of ice. The surface is refrigerated using conventional technology appropriate for the low temperature application. The ice is formed from water which flows over the chilled surface. The insulating property of ice reduces the efficiency of ice generation as the ice layer continues to build. To minimize this effect, the ice layer is continuously scraped from the surface of the drum by a knife.

Equipment Design

The refrigerated drum is specifically designed to insure uniform refrigerant circulation over the cold surface. Uniform refrigerant distribution is an important design consideration to insure consistent ice thickness. Uniform water distribution over the refrigerated drum is also important for consistent ice layer growth.

The water flow is generally much larger than the amount required for ice production. This excess water makes the design more forgiving during operation and helps move the ice shavings off the knife. The unit is designed to provide enough time for ice growth before the surface is scraped clean.

A sharp metal bar along the length of the drum provides the edge for ice removal. The energy required to scrape off the ice is provided by a drive which rotates the drum. Excess water and ice shavings fall from the knife and are collected in a basin below the unit. The process is shown in Figure 5.4.



5-10

Figure 5.4

Scraped Surface Ice Generator

Ice Slurry Characteristics

The Scraped Surface Ice Generator produces a combination of ice shavings and excess water which could be handled as a slurry. Further processing of the ice shavings may be required to achieve the desired ice crystal size for optimal flow behaviour. Actual attempts to generate an ice slurry from this technology have not been reported. Therefore, a thorough description of the resulting ice slurry characteristics is not possible at this time.

Status

The Scraped Surface Ice Generator is commercially available in relatively small capacities from several suppliers. Applications of the Scraped Surface Ice Generator have been limited to bulk ice generation systems related to the food processing industry. No attempts have been made to convert the ice into a pumpable slurry suitable for use in district cooling systems.

5.2.2.3 Defrost Cycle Ice Generator

Methodology

The Defrost Cycle Ice Generator uses a refrigerated surface to build a layer of ice. The refrigerated surface can be made in a variety of shapes. The most common is a tube or plate geometry. The surface is refrigerated using conventional refrigeration technology appropriate for the low temperature application.

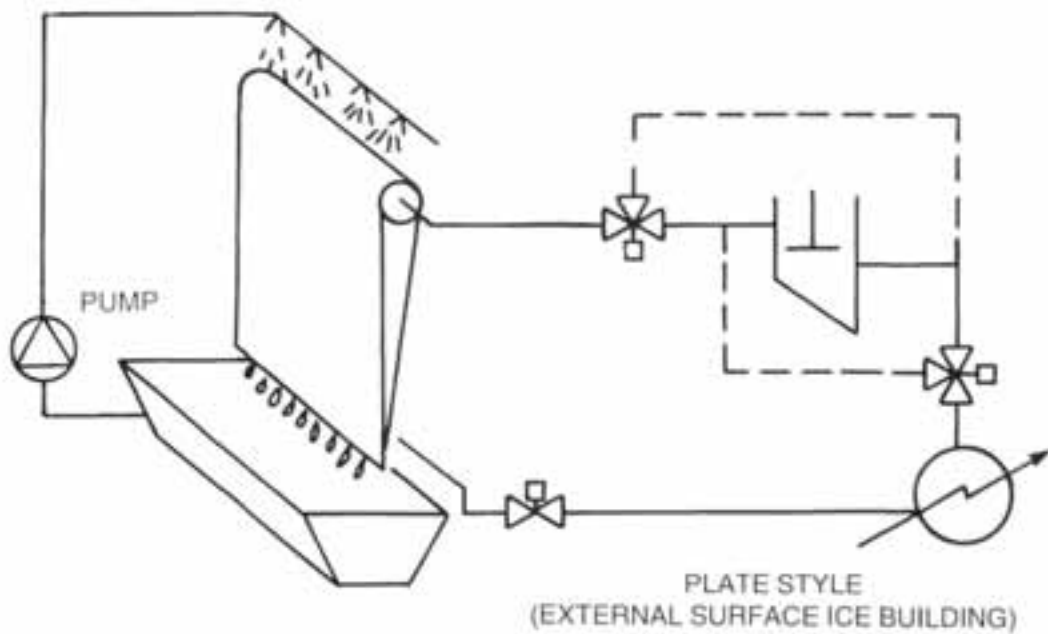
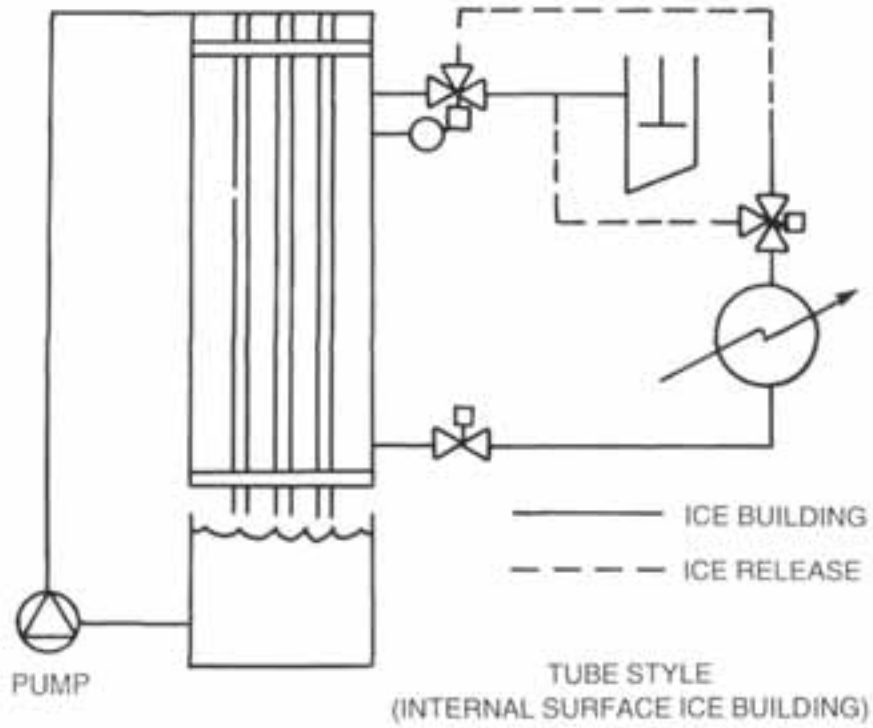
The ice is formed from water which flows down over the surface. The insulating property of ice reduces the efficiency of the ice generation as the ice layer continues to build. Therefore, the ice thickness is limited to a predetermined thickness of approximately 1 cm. Once this limit has been achieved, the refrigeration cycle is reversed sending hot refrigerant over the refrigerated surface. The surface is warmed causing the ice layer to fall off.

Equipment Design

The refrigerated plates or tubes are specifically arranged to insure uniform refrigerant circulation over the cold surface. Uniform distribution is an important design consideration for uniform ice thickness and even defrost operation. Uniform water distribution over the refrigerated surface is also important for consistent ice layer growth. The refrigerated surfaces are suspended over an ice reservoir which catches the ice as it falls from the plates. The refrigeration cycle is reversed in the same manner as a heat pump reverses from summer cooling to winter heating. The evaporator surface is transformed to the condensing surface with the actuation of solenoid valves. The operation of the tube and plate style equipment is shown in Figure 5.5.

Figure 5.5

Defrost Cycle Ice Generator



Ice Slurry Characteristics

The Defrost Cycle Ice Generator produces sheets or annuli of ice which fall from the chilled surface in a batch process. Additional processing of the ice would be required to achieve a continuous supply of ice slurry with the desired ice crystal size distribution and water content. Actual attempts to generate a continuous supply of ice slurry from this technology have not been reported.

Status

The Defrost Cycle Ice Generator is commercially available from several equipment suppliers in small to moderate sizes. Commercial applications of the Defrost Cycle Ice Generator have historically been limited to bulk ice generation in the food processing industry. More recently, this technology has been used for Thermal Energy Storage installations in buildings. As previously mentioned, no attempts have been made to convert the ice into a pumpable slurry suitable for use in district cooling systems.

5.2.2.4 Supercooled "Superpac" Ice Slurry Generator

Methodology

The Supercooled "Superpac" Ice Slurry Generator will typically use a modified conventional shell and tube evaporator to supercool fresh water without crystal nucleation on the heat transfer surface or in the bulk fluid. Crystallization is initiated after the supercooled water exits the evaporator.

Equipment Design

The supercooler design is usually similar to a conventional shell and tube evaporator with refrigerant on the shell side and water inside the tubes. Conventional refrigeration technology appropriate for the low temperature application is used in conjunction with a novel evaporator. The success of this technology rests on the ability to supercool water without initiating crystal growth within the evaporator.

After the supercooled liquid exits the evaporator, the crystallization process can be initiated immediately, or delayed until desired. The crystallization process can be initiated by directing the supercooled water over a flow obstruction. The unit operates with an ice free water source at the inlet to the evaporator and can, depending on the degree of supercooling, generate approximately 2 to 3% ice per pass.

Ice Slurry Characteristics

The ice crystals are formed after the water exits the evaporator. The size and shape of the crystals can be controlled by varying the operating conditions of the evaporator and by carefully selecting the method used to initiate nucleation. The ability to control the size and shape of the crystals produced is a significant advancement to achieve the optimum hydraulic behaviour for the distribution and storage of the ice crystals.

Status

The Supercooled "Superpac" Ice Slurry Generator was developed by Dr. M. Paradis of Laval University. Fundamental research on the supercooled process is ongoing at Laval University. For further details refer to References 2 and 3. A 2 ton demonstration unit has proven the technical feasibility of the concept. Other units are now in commercial operation. Experiments focused upon implementing this technology for district cooling are being pursued by the Centre de Recherche Industrielle du Quebec (CRIQ). In addition, the National Research Council of Canada (NRC) has conducted flow characterization studies. A 300 Ton prototype plant is currently planned to be used as a heat pump using 6°C mine water as the heat source.

5.2.2.5 Direct Freeze Ice Slurry Generator

Methodology

The Direct Freeze Ice Slurry Generator is based on a unique direct contact evaporator/freezer. Fresh water and liquid refrigerant are combined in the evaporator/freezer where the refrigerant is vaporized by direct contact heat transfer with the water and a portion of the water is frozen to form a slurry. The refrigerant vapour is recycled using a modified vapour compression cycle. The Direct Freeze Ice Slurry Generator provides continuous, efficient ice slurry generation. The process is shown in Figure 5.6.

Equipment Design

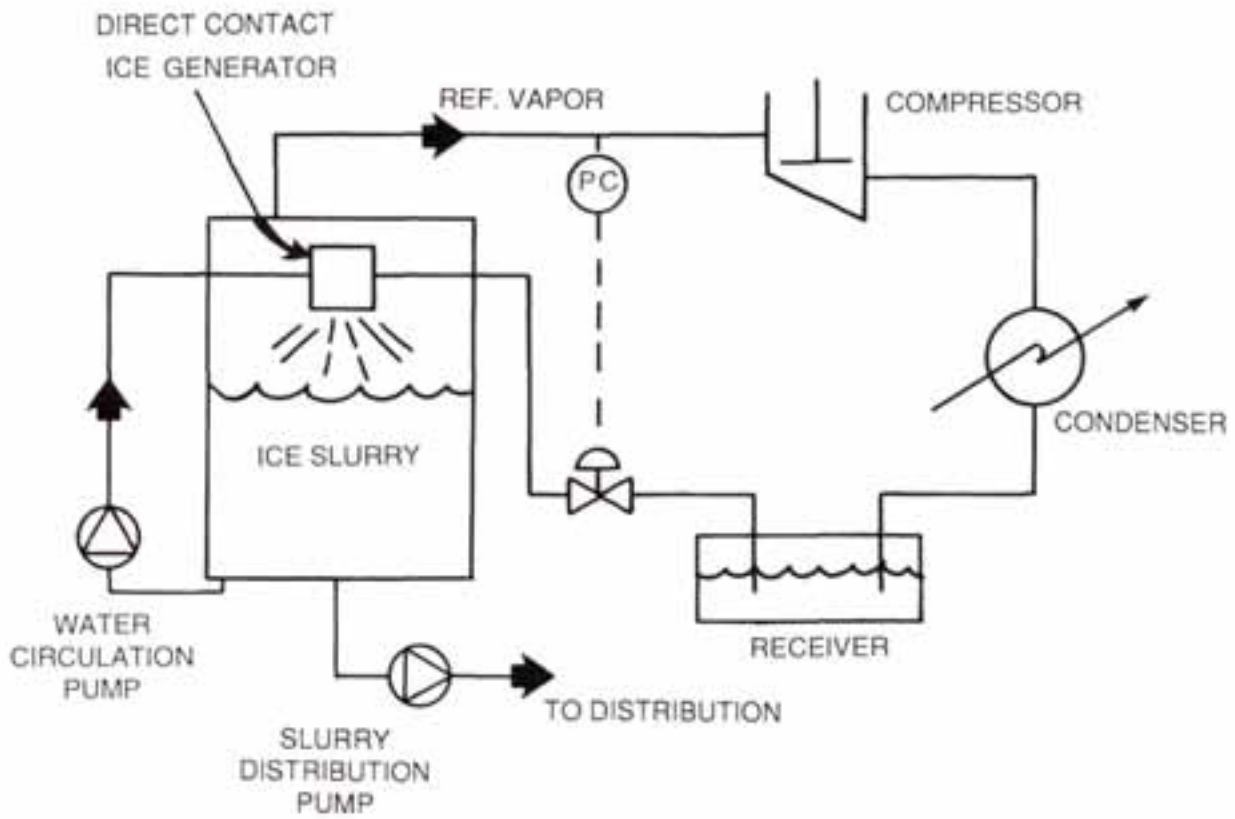
The direct contact evaporator/freezer is a compact, high efficiency, multi-phase heat exchanger. The direct contact design allows the evaporator/freezer to operate with a minimal temperature difference between the refrigerant and water. Also, high refrigerant evaporation temperatures, up to -1°C, provide optimum thermodynamic efficiency. The direct freeze ice generation technology cannot be implemented with "off the shelf" packaged refrigeration equipment. A unique condensing unit has been specifically developed to work in conjunction with the super saturated mixture of refrigerant vapour and water which exits the direct contact evaporator.

Ice Slurry Characteristics

The ice slurry consists of large crystals which are roughly spherical in shape with a jagged surface texture. The crystal size ranges from 3 mm to 6 mm diameter. The relatively large, uniform crystals are the outcome of eliminating freezing point depressants from the fluid and providing adequate residence time in the evaporator/freezer. The flow characteristics have been studied for district cooling applications. The larger ice crystals exhibit a non-Newtonian behaviour which results in lower pressure drop than chilled water at the same velocity. Additional information regarding the specific flow characteristics of this slurry is provided in Section 5.2.3.2.

Figure 5.6

Direct Freeze Ice Slurry Generator



Status

The Direct Freeze process was developed by Chicago Bridge & Iron, Oak Brook, Illinois. The process has been demonstrated on a small scale. Three machines with nominal capacities of 2.5, 5, and 25 tons have been successfully operated. Extensive testing of this technology in conjunction with ice slurry distribution and storage concepts for district cooling applications has been completed. Ice slurry distribution tests simulating cooling requirements of over 1000 tons have been conducted.

5.2.3 Ice Slurry Distribution System

The distribution of ice slurry in a piping network is a challenging fluid dynamics problem. The distribution system will be discussed in four parts. The first section deals with the Ice Slurry Vessel which provides the interface between ice slurry generator and the distribution piping. Next, ice slurry flow characteristics are presented separately for fine and coarse ice slurries. Design options for ice slurry pumping equipment follow. Then, the piping system and controls are reviewed. Finally, the challenges of restarting a charged ice slurry distribution system are examined.

5.2.3.1 Ice Slurry Vessel

The slurry vessel provides the interface between the ice slurry generation system and the ice slurry distribution system. The ice slurry generation circuit receives liquid from the slurry vessel. The liquid is pumped through the ice slurry generator where a portion of it is converted to ice before it returns to the ice slurry vessel.

The ice slurry distribution circuit receives concentrated ice slurry from the slurry vessel. The ice slurry vessel provides a reservoir in which the ice fraction can increase prior to introduction to the network. Maintaining fluidity of the slurry within the vessel is the most significant design obstacle relative to this component. Three fundamental ice slurry vessel design concepts have been used experimentally; a mechanical mixer design, a free surface vortex flow, and a flooded vortex flow design.

The mechanical mixer provides a simple solution to the problem of maintaining fluidization within the ice slurry vessel. The concept simply involves fitting the ice slurry vessel with an electrically powered mixer. As the slurry concentration increases in the vessel, the mixer maintains a homogeneous dispersion of crystals throughout the fluid, providing a consistent source for the distribution network.

To successfully implement this design concept, the designer must consider several factors. A strong relationship exists between the geometry of the vessel and the location and power requirements of the mixer. The design of the vessel, as well as the size and placement of the mixer, must be carefully optimized to insure uniform agitation over the entire volume. Failure to effect uniform agitation will result in local stagnant zones in which ice will gather. As the ice accumulates, it further restrains fluid motion and the problem may grow.

Another important design consideration is the requirement of low or no ice content in the liquid supply stream for most ice slurry generators. To accomplish this, a portion of the ice slurry vessel must be isolated from the mixer turbulence to allow the ice slurry to stratify, producing the desired ice free liquid source. The magnitude of the ice free liquid flow may be higher than that of the ice slurry supply to the network - increasing the difficulty of the problem.

The combination of these two contradictory design objectives requires the designer to achieve some level of compromise for a successful application. The mixer also adds heat to the system in the form of mechanical energy which must be accounted for as a parasitic loss for the system.

Another method used to maintain fluidity within the slurry vessel is a free surface vortex flow pattern. The free surface vortex flow pattern is well suited for use with ice slurries. The ice crystals, which are less dense than water, naturally float on the free liquid surface of the vortex and concentrate in reaction to centrifugal forces toward the apex of the vortex.

Experimentation has shown that a "Rankine" vortex, which is a combination of both a "Free" vortex and "Forced" vortex, provides an optimal flow pattern for slurry handling. The "Free" component of the vortex is generated by the distribution pump suction which is connected to a bottom outlet on the slurry vessel. The "Forced" component of the vortex is produced by a tangential return connection from the distribution network.

The vortex flow pattern generates a natural ice slurry concentration gradient which is highest at the suction of the ice slurry pump and lower below the surface of the water and away from the centre. The vortex design concept works with minimal additional energy input to the system. The position of the apex of the vortex can be controlled by satisfying the ice slurry distribution pump with flow from a second tangential outlet which reduces the "Free" vortex component. Ice slurry flows up to 20% ice with flow rates from 25 to 80 l/s have been handled with this design.

A source of ice free liquid for continued ice production can be obtained from the bottom of the vessel near the perimeter. A false bottom in the vessel composed of a coarse screen material assures an ice free liquid source below. In addition, the large cross-sectional area of the screen minimizes the downward velocity, thereby further reducing the possibility of ice entrainment.

A third ice slurry vessel design concept is based on a flooded vortex flow pattern or cyclone effect. Low concentration slurry is pumped to the vessel from the ice generator and introduced tangentially. A swirling flow within the vessel results. The less dense ice crystals, in response to both the centrifugal and buoyancy forces, concentrate in the centre of the flow and rise to the top. The distribution pump is connected to the top of the vessel drawing a steady flow of concentrated ice slurry. The vessel is typically conical in shape. Ice free liquid is removed from the bottom of the vessel where the large cross sectional area reduces downward velocity and eliminates ice crystal entrainment. The flooded vortex design concept works with minimal additional energy input to the system.

5.2.3.2 Ice Slurry Flow Characteristics

Published results describing the flow characteristics of ice slurries vary dramatically depending upon the physical geometry of the ice crystals. Two basic classifications of ice slurry have been characterized thus far: fine binary ice slurry and course fresh water ice slurry. The flow characteristics of these two slurry types are presented separately below. Due to the differences in flow characteristics for these two slurry types, care should be exercised in generalizing these results for any other slurries.

Fine Binary Ice Slurry

Fine binary ice slurries are dominated by a predominantly homogeneous, Newtonian flow behaviour. The flow characteristics presented below were obtained on an experimental system which used a Sunwell Binary Solution Ice Slurry Generator with a mechanical wiper and ethylene glycol freezing point depressant. The ice particles were roughly spherical in shape with a smooth exterior texture. The crystals had a diameter in the range of 0.1 mm to 0.25 mm. The initial glycol concentration in the system was 6%. For more detailed information relative to this research refer to References 4, 5 and 6.

The flow characteristics are presented in three topics; agglomeration, pressure drop, and flow splitting:

Agglomeration

Agglomeration in this context is defined as an accumulation of ice crystals into a large mass, either on a surface or in the fluid, leading to large solid ice masses which ultimately block the distribution system. Agglomeration of this type has not been observed.

Pressure Drop

The pressure drop characteristics of fine, binary ice slurry have been evaluated relative to chilled water/glycol, of the same concentration, flowing at the same volumetric flow rate. The results show essentially no change in pressure drop for the ice slurry. This similarity has been observed for ice fractions up to a maximum of 16 to 30%, depending upon the flow velocity. The maximum ice fraction, for which this pressure drop similarity exists, increases with higher fluid velocities. In addition to investigating the effect of ice concentration and fluid velocity, the effect of pipe diameter upon the pressure drop was also examined. In general, for the same fluid velocity, the maximum ice fraction up to which the pressure drop results were similar to the all liquid case, increased for larger diameter pipes. In all cases, the pressure drop results for ice fractions above the maximum value rose sharply and diverged rapidly from the equivalent all-liquid case.

Flow Splitting

The distribution system of a district cooling system must deliver the ice slurry to many different buildings with a wide range of flow requirements. Therefore, the ability to

split the ice slurry while sustaining a uniform concentration is important. Detailed flow splitting tests for fine, binary ice slurries have not been performed. However, some limited ice slurry testing has revealed a strong homogeneous behaviour. No problems were encountered when ice slurry was transferred through both parallel sections of an experimental loop. The fine ice crystals have negligible body forces relative to the turbulent diffusion within the flow itself. Therefore, it is reasonable to expect the ice concentration to distribute uniformly as the flow is separated.

Fresh Water Ice Slurry

The flow characteristics of coarse fresh water ice slurries are complex and non-Newtonian. The flow characteristics presented below were obtained on an experimental system which used a Direct Freeze Ice Slurry Generator. The ice crystals were essentially spherical in shape with a rough exterior texture. The crystals had a diameter of approximately 5 mm. For more detailed information relative to this research refer to References 7 - 12.

The flow characteristics are presented in three topics: agglomeration, pressure drop, and flow splitting.

Agglomeration

As previously mentioned, agglomeration in this context can be defined as the accumulation of ice crystal into a large mass, either on a surface or in the fluid, leading to large solid ice masses which ultimately block the distribution system.

Agglomeration of ice slurry in the form of ice adhesions on the walls of the piping, fittings, or valves in the experimental distribution system were not observed. Agglomeration of the ice slurry in the form of ice clusters in the flow have been observed in all cases. Details of the behaviour of these ice clusters have been obtained by visual observation of the ice slurry over a range of ice fractions.

At low ice fractions, below 2%, discrete ice crystals can be seen throughout the cross section of the flow. The ice crystals dance within the bulk fluid, propelled by random fluid motion associated with conventional turbulent single-phase flow. As the ice fraction increases, small clusters of ice crystals begin to form within the flow. These clusters are three to four times the diameter of a single crystal. The motion of the small clusters is more restrained than the random motion of the initial discrete crystals.

Further increases in the ice fraction generate larger clusters and still less random motion. At ice fractions of approximately 8 to 10%, depending upon fluid velocity, the clusters have combined and fill the cross section of the pipe. The ice slurry has achieved a fully developed laminar plug flow pattern. A relatively uniform ice cluster fills the cross section of the pipe with no observable motion within the cluster. The ice crystals move as a single mass through the distribution piping.

A further increase in the ice fraction causes the cluster to appear denser but has little effect on the overall flow pattern. The laminar ice plug just described is not a rigid ice mass. The plug is easily broken up as the flow moves through areas of increased turbulence such as pumps, valves or fittings.

This flow transition from turbulent to laminar plug flow is attributed to the inertial effects of the large ice crystals. The flow pattern identified as turbulent for a typical single-phase fluid, is a combination of random eddy currents and bulk fluid motion. The relatively large ice crystals possess sufficient inertia to dampen the effect of these eddy currents and effectively straighten the flow.

Pressure Drop

The pressure drop characteristics of this coarse particle ice slurry have been evaluated relative to chilled water flowing at the same volumetric flow rate. The results show a reduction in pressure drop in all cases of ice fractions tested. A reduction in pressure drop of over 40% relative to water at the same mass flux has been observed.

The reduction in pressure drop has been attributed to the transition from a classical turbulent flow pattern, typical of chilled water systems, to a laminar plug flow described above. The pressure drop of the ice slurry decreases gradually with increasing ice fraction down to its minimum level as the ice fraction approaches 8 to 10%. This is the same concentration where the laminar plug flow is fully developed. The pressure drop reduction has been shown to remain essentially constant for increased ice fractions up to 16%.

Flow Splitting

The distribution system of a district cooling system must deliver the ice slurry to many different buildings with a wide range of flow requirements. Therefore, the ability to split the ice slurry uniformly is an important design issue. Detailed flow splitting tests for coarse ice slurries have not been performed. However, some observation concerning the potential behaviour of this ice slurry can be made.

The unique ability for the coarse ice slurry to undergo a flow transition from turbulent to laminar plug is a tremendous benefit for the distribution system resulting in a natural friction reduction behaviour. However, the laminar plug must be agitated at flow bifurcations to insure uniform ice concentration in each leg. The turbulence required to break up the laminar plug will increase for higher ice fractions. However, for ice fractions up to 16% a simple change in flow direction is sufficient to disrupt the laminar plug. It is recommended that a static mixer be located upstream of each branch.

5.2.3.3 Pumping Equipment

When considering pumping equipment for ice slurry service, many options are available. Commercial equipment has been developed to pump extremely difficult liquid-solid mixtures including coal-water slurries and even concrete. The question of

interest for the district cooling system designer concerns the extent to which specialized equipment will be required.

Both fine, binary ice slurries and coarse fresh water ice slurries have been successfully handled using conventional centrifugal or positive displacement pumps. Centrifugal designs have been successfully tested with both a "closed" impeller, typically used for water applications, and an "open" impeller, usually specified for slurry applications. Therefore, the designer is free to choose the most cost effective option for the required flow and pressure of the particular application.

Performance curves for these commercial pumps are readily available for water service. Gupta has measured the change in pump characteristic for a range of ice slurry fractions. At constant flow, Gupta found that between 0 and 0.25 ice fraction, the pump head decreased by $\approx 10\%$ (Reference 13). In general, for positive displacement designs, no change in flow rate and minimal changes in power are expected. In the case of centrifugal designs, the designer should expect nominal changes in both flow and power consumption.

5.2.3.4 Piping Network

The actual piping network is the single most expensive element in many district cooling systems. Ice slurry technology represents an exciting method for reducing the mass flow rate of a district cooling system for the same cooling capacity. The lower mass flow translates directly into smaller pipes and lower distribution system costs. Compared to a water supply at 7°C, a 0.20 fraction ice slurry can reduce the pipeline diameter requirement by more than half. Cost saving for the distribution piping network is one of the major motivations supporting this development.

A further concept that may reduce pipeline sizes is the diversity factor. This diversity factor quantifies the decrease possible in the installed chilling capacity of a district energy system because of the small likelihood of all loads having a co-incident peak demand. Depending on the layout of the piping network, the load diversity may permit the use of reduced diameter pipes, especially near the pumps.

The total energy requirement of the system remains unchanged. Therefore, the diversity factor cannot be applied to reduce the chiller capacity in cases where the load is levelled by central or distributed storage. With central storage, pipeline size reductions can still be achieved if the diversity factor is well below 1.0.

Piping Materials

The selection of available piping materials for district cooling systems is on the rise. Numerous plastic and fiberglass piping materials have gained considerable popularity in recent years. In addition, several internal coatings for conventional metallic pipe are also available.

Insulation systems are also enjoying a surge of technical advances. Pre-insulated pipes offer exciting prospects for future systems. In many systems there will be a small temperature difference between the return pipe and surrounding soil. In these

cases, no insulation is required on the return lines. Limitations on piping materials for use with ice slurries have not been observed.

Fittings and Isolation Valves

The design of an actual district cooling piping network must incorporate a variety of fittings and isolation valves to properly distribute the cooling medium throughout the network and facilitate maintenance. The following section will consider these components and elaborate on design considerations unique to ice slurry applications.

Experimental systems constructed thus far have included a wide variety of common commercial pipe fittings such as elbows, tees, couplings, bushings, and reducers. The ice fraction limit, in experimental evaluations published thus far, was achieved due to ice generator limitations or test section maximum pressure drop constraints. Ice fraction limitations due to plugging resulting from the presence of these fittings have not been observed in any ice slurry research including both fine binary and course fresh water slurry systems. Therefore, restrictions on the use of fittings for ice slurry applications are not anticipated.

The experimental systems mentioned above also incorporated many isolation valves. Their purpose was to isolate various system components and test sections to facilitate maintenance and periodic system modifications. Of the valve styles available for this service, ball valves are particularly well suited for ice slurry applications. They offer negligible pressure drop when opened, a positive seal when closed, and are no more likely to experience a blockage than a straight run of pipe.

For large pipe sizes, beyond the range of cost effective ball valves (above 10cm diameter), the best choice for isolation service in ice slurry applications is a butterfly valve. Experimental systems constructed with this valve style have experienced no problems relative to its performance. In general, valve designs with complex internal flow paths such as diaphragm and globe designs should not be used.

Control Valves

The use of conventional control valves for ice slurry service is not considered technically viable. Although a study of specific valve performance has not been performed relative to ice slurry applications, most manufacturers are opposed to installing conventional valve designs including needle, sliding gate, diaphragm and globe into any type of slurry service. Some specialty valves have been developed for use in other slurry applications. These valves represent possibilities which have not been thoroughly evaluated. The most simple solution is to avoid installing control valves in ice slurry lines at all. Sections 5.2.4 and 5.2.5 contain system control strategies which effectively eliminate the need for control valves in ice slurry supply lines by adopting an on/off control methodology or by installing control valves on the warm water return side of the system to provide proportional load following control.

5.2.3.5 Restarting Ice Slurry Flow

Potential problems associated with re-establishing flow in a stagnant ice slurry distribution system, which is fully charged with the design ice fraction, have fostered speculation for many years. These discussions primarily focus upon the pumping power required to overcome the "Break Away" friction of the ice crystals. This problem, which is described in detail below, can be minimized by adopting operating strategies which effectively avoid the situation during normal operation - two such operating strategies are presented later in this section. However, the problem can still arise as the result of unforeseen circumstances such as pump or power failure. For this reason, some design guidelines are presented at the end of this section to make it easier to restart flow in a stagnant, fully charged, ice slurry distribution system.

When an ice slurry is allowed to come to rest, the normally uniform mixture begins to stratify due to density differences between the ice crystals and surrounding fluid. As previously mentioned, the buoyancy or body force associated with an ice crystal is quite small. Therefore, the ice crystals do not "pack" in the pipe.

The degree of stratification is strongly dependent upon ice crystal size. The concentration limit for fine ice crystals in a buoyancy driven stratified layer is approximately 30%. For coarse ice crystals, an upper limit of approximately 15% is more likely. Therefore, for most systems in which the design distribution ice fraction is in the range of 20 to 30% little or no "packing" would be expected with a loss of flow. The negligible magnitude of packing associated in a stagnant slurry is an important consideration which simplifies the restarting problem. However, the presence of a stationary solid at the wall of the pipe, throughout a distribution network, still represents a unique condition which conventional district cooling systems have not faced.

Another key factor which must be understood in order to quantify the impact of restarting flow is the "Shear Force" associated with a stagnant ice slurry. The "Shear Force" is defined as the force required to establish relative motion within the slurry. Clearly, if the "Shear Force" is greater than the "Break Away" force, the ice crystals will initially move as a single mass. If the reverse is true, motion will begin at the centre of the pipe cross section and gradually diffuse toward the wall as the velocity increases. This latter condition is most desirable for minimizing the problem. Gupta (Reference 13) has performed a large number of stop/start tests in the NRC ice slurry loop without encountering any problems.

Two operating strategy options have been devised to avoid having to restart the flow of ice slurry during normal operations.

Option #1: Constant Flow/Variable Ice Fraction

This control option can be used on systems without thermal storage or with central thermal storage. The design premise for this concept is to maintain a constant flow at all times in the distribution network while still optimizing the thermodynamic efficiency of the system by maximizing the evaporator temperature.

The maximum thermodynamic efficiency is obtained when the return leg of the system is maintained at a maximum temperature. Changes in cooling load are satisfied by adjusting the temperature or ice fraction in the supply leg.

By way of illustration, consider a system operating at its design capacity with 20% ice fraction supply and 13°C return. If the cooling load decreases, the temperature of the return stream will drop. In the simplest operating mode, the system responds by lowering the ice fraction in the supply stream while keeping the flow constant. Further reductions in the cooling load will result in lower ice fractions until only chilled water is required to meet the load. With further load reductions, the flow will be decreased. The advantages of this option are constant flow (down to zero % ice) and maximum thermodynamic efficiency.

In reality, the cost of pumping may be significant. Therefore, in a given situation it must be considered whether it may be financially more attractive to lower the flow at a given ice slurry percentage. It must be remembered to maintain the ice slurry velocity above the minimum required for proper ice slurry fluidization.

Option #2: Purge and Stop

This control system can be used on systems with distributed thermal storage. The distributed thermal storage concept, which is presented in detail in Section 5.2.4.2, eliminates the need for part-load operation. The ice generation system is either on or off. When the ice generation is no longer required, water is circulated through the system to purge the ice prior to stopping flow.

As mentioned in the introduction of this section, unforeseen circumstances may still cause a shut down of the distribution system in the fully charged condition. Therefore, the following guidelines should be observed to minimize the problem.

1. Avoid long vertical piping runs. The higher the fluid column the more severe the stratification.
2. Oversize the distribution pumps. Use variable speed drives to maximize performance.
3. Provide redundant pumping equipment designed for rapid deployment.
4. Provide a Uninterrupted Power Supply for critical components.

5.2.4 Ice Slurry Storage and Recovery

The advantages of including ice slurry storage in the design of an ice slurry based district cooling system are to reduce the installed refrigeration capacity and allow the system to take advantage of lower off-peak energy costs. These concepts were introduced earlier in Section 5.2.1.3.

By way of review, ice slurry storage provides a buffer between the refrigeration system and the cooling load. This buffer allows these systems to be decoupled such that the refrigeration system no longer has to respond to fluctuations in the cooling load. Instead, the refrigeration system is either operated at its optimal full rated capacity if the storage system is not fully charged, or shut down. In this manner, the refrigeration system is sized for the average cooling load rather than the peak, which represents a potentially significant reduction in installed capacity for most systems.

With the motivation for ice slurry storage firmly in mind, specific techniques for integrating ice slurry storage can now be presented. The following sections will investigate specifics including the recovery of stored cooling, strategies for incorporating ice slurry storage, storage sizing methodology, and storage tank design.

5.2.4.1 Recovering Stored Cooling

Two basic techniques have been proposed to recover cooling from storage; mechanical and passive. Each of these alternatives is discussed in detail below.

Mechanical Technique

Mechanical techniques for recovering stored cooling from an ice storage tank have been discussed for some time. Research is ongoing to test the viability of different concepts.

Mechanical recovery involves an attempt to harvest and re-slurry the ice stored in the tank for introduction into the distribution network. The basic concept requires a system of mechanical augers which move within the ice storage tank to scrape the ice crystals out of storage and convey them to the suction of the distribution pump. This type of approach has been successfully employed for removing granule solids such as sugar and grains from storage silos.

The storage technique is strongly affected by the method of ice slurry generation. Pure ice slurry has been observed to agglomerate as the crystal to crystal pressure in storage can result in partial melting and re-crystallization. However, slurry generation systems using glycol or similar freeze point depressants appear to store well with little or no agglomeration even though crystal growth is observed over time.

Experiments at the National Research Council showed that the addition of a small amount of glycol (less than 0.5% by volume) stopped agglomeration in pure ice techniques.

Commercially, a rotating scraper at the top of the storage tank has been successfully employed with Sunwell commercial systems to remove ice crystals. This technique has been widely used in generating ice crystals for the fishing industry where salt brine has been the preferred freeze point depressant. The crystals can be back-washed with clean water to minimize the carry-over of freeze point depressant.

Passive Technique

The passive technique for recovering cooling from the ice storage tank eliminates the need to harvest and re-slurry the ice. The cooling capacity stored in the ice slurry is simply recovered by melting the ice. The warm water returning from the cooling load is directed over the ice pack in the storage tank and chilled prior to entering the ice generator. In this manner, the stored cooling is utilized without handling the ice.

It is interesting to note that even though ice slurry from pure ice generation techniques can agglomerate into a semi-solid block, the ice appears to remain porous so that water can still pass through the ice particles to melt the ice and be chilled before being returned to the system.

5.2.4.2 Ice Slurry Storage Strategies

Two strategies have been developed for integrating ice slurry storage in the design of a district cooling system, distributed storage and central storage. The details of these two methods are presented below.

Distributed Storage

In a distributed storage system, ice slurry is distributed to and stored in a number of tanks located at each building (or group of buildings) around the network. The ice slurry enters the tank where the lighter ice crystals are separated, usually by gravity. Ice free water from the storage tank may be used by the building cooling system, as shown in Figure 5.7.

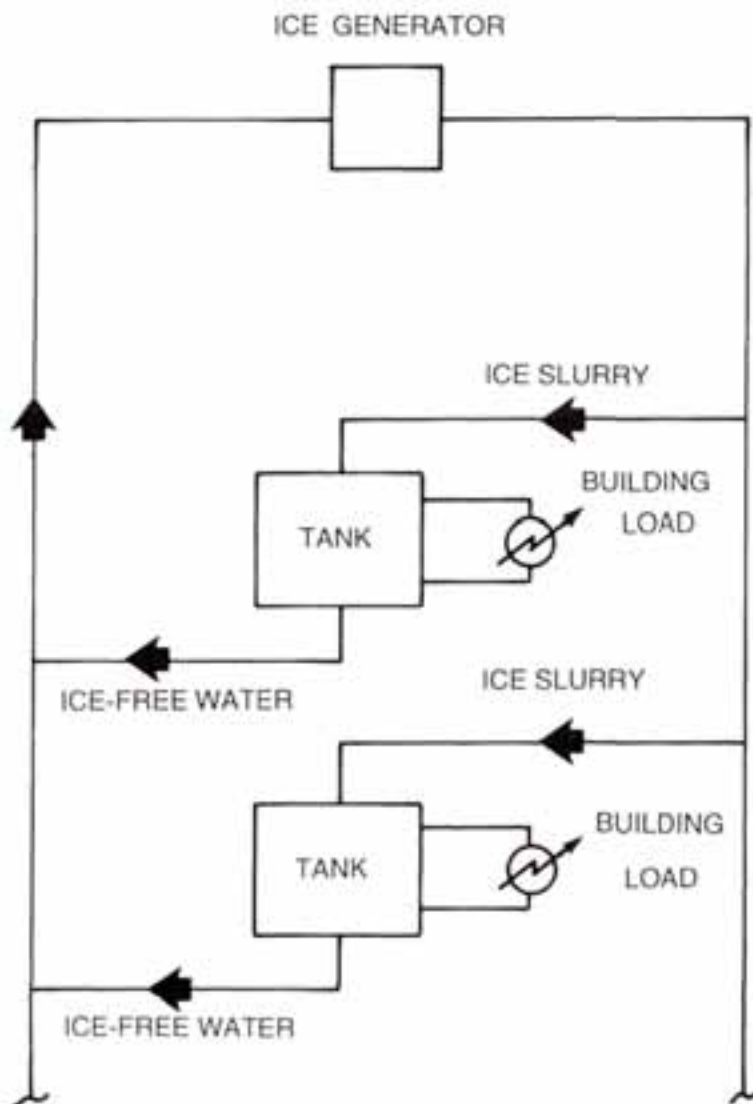
The distributed storage tanks provide a buffer between the distribution system and the individual building cooling load requirements. The decoupling of the refrigeration system allows the distribution system to operate to meet the average cooling load rather than the peak. For many buildings, the average cooling load can be up to 50% lower than the peak cooling load. To meet the maximum design cooling load, the refrigeration system must generate slurry on a continuous basis. This slurry is pumped to the distributed storage tanks. Depending upon the time of day, if the building cooling load is low, the ice slurry will accumulate in the storage tank. Later, as the cooling load increases, the storage tank is simultaneously being charged by the distribution system and discharged to meet to building cooling load.

At times when the building load is small, the return water may be at a lower than optimal temperature with a certain amount of cooling potential still unused. The loss of this sensible cooling during part of the load curve means that the maximum enthalpy difference cannot be delivered to the storage facility continuously. Therefore, distribution pipes for a capacity somewhat greater than average load must be installed.

In general, distributed storage facilities will be most economical if the peak to average load ratio is greater than 2 and the latent to sensible heat ratio is greater than 1. Also, distributed storage becomes more attractive if the base load is a substantial fraction of the average load, i.e., when the peak load is of short duration.

Figure 5.7

Ice Slurry Storage - Distributed Storage



The design process must insure a match between the storage tank capacity, supply rate, and discharge rate. The storage tank design process is covered in detail in Section 5.2.4.3. The role of distributed storage to simplify connection to existing building HVAC systems is presented in Section 5.2.5.

Central Storage

In the central storage approach, the district cooling system is designed with a central storage tank, or tanks, preferably near the central refrigeration plant. The concept is shown in Figure 5.8. Like distributed storage, central storage retains the advantage of providing a buffer between the refrigeration system and the actual cooling demand generated by the buildings on the network. However, in central storage the distribution system is not decoupled. The cooling capacity within the distribution system must follow the actual cooling demand.

Central storage can be used in two operating strategies. Ice slurry can be stored but not circulated and used only to cool return water for re-distribution. Alternatively, ice slurry can be stored and fluidized during peak hours for distribution. With both approaches, the volume of storage is reduced compared to chilled water storage. Distribution of ice slurry will additionally reduce the distribution network pipe diameters.

In making a choice of storage method, a design where ice does not need to be fluidized or harvested may be favoured at this time until problems of distributing ice from storage can be resolved.

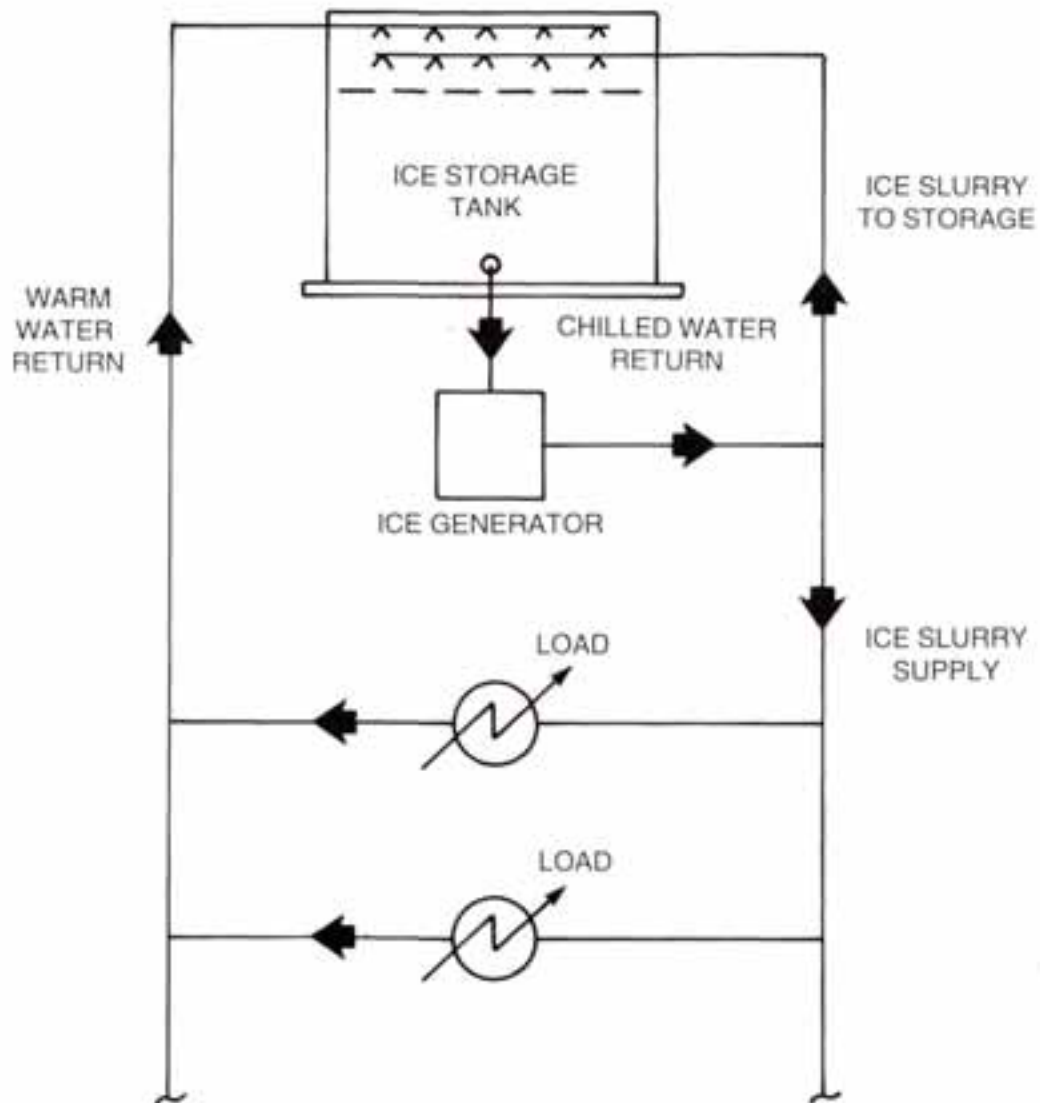
The most cost effective compromise at this time may be to use storage to chill return water to 0°C at the peak loads to mix with ice slurry delivered directly from the chillers. The proportion of the load served by ice slurry chillers will depend on the load curve.

To meet the maximum design cooling load, the refrigeration system operates continuously. During periods of low or no cooling load, the generated ice slurry is delivered to the storage tank. As the cooling load increases, the flow of ice slurry is gradually diverted to meet the cooling demand. The flow of ice slurry to the storage tank eventually comes to a stop.

The ice slurry is delivered to the cooling loads where it is melted and warmed to approximately 13°C before returning to the central plant. The flow of slurry delivered to the cooling loads is controlled to insure that the total available cooling, per unit mass circulated, is removed. The details of this control scheme are presented in Section 5.2.5. At peak loads, to recover the cooling capacity stored in the central storage tank, a portion of the warm 13°C return water is directed through the tank. The ice stored in the tank is melted as the return water is chilled to the freezing point. The pre-chilled water is then removed from the storage tank and returned to the distribution system. The remainder of the return water is directed to the chillers as usual.

Figure 5.8

Ice Slurry Storage - Central Storage



To insure accurate control of the central storage system, the ice fraction in the storage tank must be known. Ice fraction instrumentation based upon a low cost conductivity transmitter have been used to provide a reliable indication of the overall ice fraction within fresh water ice slurry systems. The overall ice fraction within a system of this type is basically a reading of the ice fraction in storage. The entire return piping system is controlled at approximately 13°C so it does not affect the ice fraction. Therefore, differences in the conductivity of the water can be attributed to changes in ice fraction within the central storage tank.

The design of a central storage district cooling system should be engineered to match the actual load profile of the installation and provide the optimum balance of refrigeration capacity and storage capacity. Once the overall system requirements for installed refrigeration and ice storage have been determined, the ice fraction of the slurry can be adjusted to match the system. The sensible and latent cooling of the optimum slurry should be proportional to the installed ice storage and real-time refrigeration respectively. The storage tank design process is covered in detail below.

5.2.4.3 Ice Slurry Storage Sizing

Determining the optimum balance of real-time refrigeration and ice slurry storage is an important aspect of a successful system design. The method of ice slurry recovery has a direct bearing on the ice storage sizing methodology. Due to its obvious simplicity, the passive ice slurry recovery concept will be used as the method of choice for the remainder of the ice slurry storage and recovery section.

A system design procedure for sizing the installed refrigeration capacity and ice slurry storage requirements for both the distributed and central storage concepts will be presented. The system design procedure is relatively insensitive to the particular storage method selected. Therefore, the sizing procedure will be presented for both concepts together, with differences noted where appropriate.

Installed Refrigeration Capacity

The capacity of the installed refrigeration system is sized by summing the hourly cooling loads for each building serviced by the district cooling network for a "design" day. The total cooling load calculated is then divided by the desired number of continuous hours of operation for the refrigeration equipment per day. (Typically, the number of hours per day of continuous operation is set at 20 to 22 hours to allow time for routine maintenance). The result of this calculation is the peak average daily cooling load. The minimum installed capacity should be equal to this number. An example of this calculation is shown in Figure 5.9.

Installed Ice Storage Capacity

The required central storage capacity is calculated from composite hourly cooling load data for all of the buildings serviced by the network. Ice storage is required to store the excess capacity delivered to the storage tank during periods of low or no cooling loads. The ice storage capacity is calculated by summing the hourly difference

Figure 5.9

Refrigeration and Storage Capacity Sizing

Time of Day	Actual Cooling Load	Cooling Supplied	Excess Capacity (Supplied - load)	Ice Storage (Ton-hrs)
1 AM	13.05	69.35	56.30	158.67
2	0	69.35	69.35	228.02
3	13.05	69.35	56.30	284.32
4	25.88	69.35	43.47	327.79
5	38.27	69.35	31.08	358.87
6	50.00	69.35	19.35	378.22
7	60.88	69.35	8.47	386.69
			Max. storage Capacity	
8	70.71	69.35	-1.36	385.33
9	79.34	69.35	-9.99	375.34
10	86.60	69.35	-17.25	358.09
11	92.39	69.35	-23.04	335.05
12 Noon	96.59	69.35	-27.24	307.81
1 PM	99.14	69.35	-29.19	278.02
2	100.00	Maintenance	-100.00	178.02
3	99.14	Time	-99.14	78.88
4	96.59	69.35	-27.24	51.64
5	92.39	69.35	-23.04	28.60
6	86.60	69.35	-17.25	11.35
7	79.34	69.35	-9.99	1.36
8	70.71	69.35	-1.36	0.0
				no ice left
9	60.88	69.35	8.47	8.47
10	50.00	69.35	19.35	27.82
11	38.27	69.35	31.08	58.90
12	25.88	69.35	43.47	102.37

1525.7 Ton-hours (Total Cooling Load)

Installed Capacity : $\frac{1525.7 \text{ Ton.hrs}}{22 \text{ op.hrs}} = 69.35 \text{ Tons}$

Maximum Storage Capacity : 386.67 Ton.hrs

(Note: Maintenance time can be scheduled for any convenient time slot)

between the composite hourly system cooling load and refrigeration system capacity calculated above for the "design day".

For a distributed storage system, the ice storage capacity is determined for each building individually. The ice slurry delivery rate for each building's storage tank is determined first. The method is similar to sizing the installed capacity for the entire system. For each building, the slurry delivery rate is determined by summing the hourly cooling loads and dividing by the desired number of hours of continuous operation. If maximum enthalpy difference cannot be maintained during periods of low load, the slurry delivery rate has to adjusted to compensate.

The storage capacity is estimated by summing the hourly difference between the actual building cooling load and the slurry delivery rate to the storage system for the "design day".

The actual storage volume also depends on the degree of ice packing, room required for diffuser piping, harvesting equipment, room for expansion of the ice, etc.

5.2.4.4 Ice Slurry Storage Tank Design

The design of the ice storage tank will be limited to the passive style of cooling recovery described in Section 5.2.4.1. The ice storage tank can be either a "free liquid" or "flooded" design. These options will be considered in detail below.

"Free Liquid" Storage Tank Design

The "free liquid" storage tank design has been used extensively in single building thermal energy storage applications. It is typically a large, unpressurized tank. The storage tank is filled to approximately 80% with water. As the ice slurry enters the tank, ice crystals stratify and float to the surface of the liquid. The ice gradually accumulates from the surface of the storage tank down to the bottom of the tank.

Top Charging

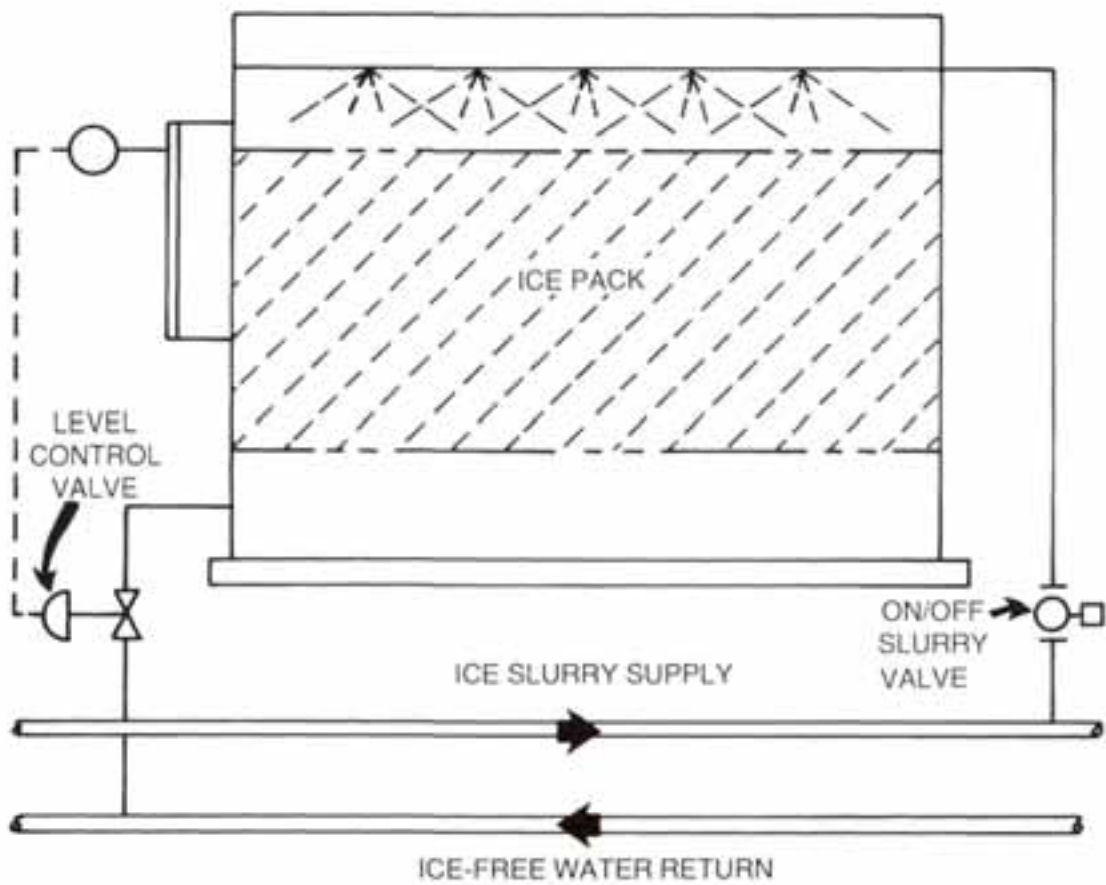
The most common method of charging a "free liquid" ice storage tank is to supply the ice slurry from the top using a simple distribution system above the liquid level. Figure 5.10 shows the concept. The top charging configuration enhances the maximum ice fraction within the storage tank, minimizing the size of this component. The weight of each successive layer of ice creates a compacting force as the ice pack tries to float on the surface. Continued charging forces the ice pack gradually towards the bottom of the tank. Once the bottom is reached, further ice production causes the liquid level to drop. The exposed ice is no longer partially supported by the water and the ice is compressed further.

Bottom Charging

In the bottom charging method, ice slurry is distributed across the bottom of the tank using a simple piping system. A bottom charging configuration relies upon the buoyancy of ice to push the ice pack up. Continued ice storage gradually causes the

Figure 5.10

Ice Slurry Storage - "Free Liquid" Storage Tank



ice to build to the bottom of the storage tank. However, once the ice has reached the bottom, the distribution piping may be blocked preventing further ice storage.

Tank Geometry

Several basic storage tank shapes are particularly attractive from a construction point of view. These include a horizontal cylinder, vertical cylinder and square tank. However, the physical characteristics of ice slurry are more suitable to certain styles. Although the ice slurry is delivered to the storage tank as a pumpable mixture, the fluid characteristic is lost soon after entering the tank. The free liquid used to maintain fluidity during transport is quickly drained away when the ice and water separate by gravity in the storage tank. The ice pack is not a fused mass of ice. However, after the slurry enters the storage tank, an ice pack is formed with very little relative motion within the pack. Continued charging with ice will force the pack to move gradually as a thick mass.

Unless a bottom-charging system is used, the horizontal cylinder is the least desirable geometry from an ice storage perspective. The curved sides of the vessel below the centerline provide a subsurface support for the ice pack to rest upon. Consequently, the ice pack does not move as easily into the bottom portion of the tank causing the ice to accumulate above the liquid. Eventually, the rising ice pack will block the slurry distribution piping, severely limiting the ice fraction achievable.

The vertical cylinder and square tank geometries can be considered together. The vertical sides of either tank style are conducive to bulk ice motion within the tank enhancing the packing performance. The use of internal stiffeners should be avoided to eliminate barriers to ice pack motion within the tank. In general, a taller tank can hold higher ice fractions than a shorter tank. It is expected that ice fractions of up to 60% can be achieved in a properly designed storage tank.

Melting The Stored Ice

Regardless of which configuration, top or bottom, is used to charge the "free liquid" ice storage tank, melting of the stored ice is typically the same. Warm water returning from the cooling load is sprayed over the top of the ice pack. The water is chilled as it filters down through the ice. Cold water is withdrawn from the bottom of the storage tank to return to the process.

Controls

To maintain the correct liquid level in the tank, the flow of ice slurry into the storage tank must be balanced by the flow of ice free water out of the storage tank for return to the distribution network. No proportional flow control on the ice slurry supply is required. The refrigeration system is decoupled from the actual cooling loads imposed by the users. The ice storage tank is charged in an on/off mode of operation. The flow of water pumped out of the storage tank back to the distribution system can be controlled with a level transmitter mounted on an ice free standpipe on the side of the tank and a flow control valve.

"Flooded" Storage Tank Design

The "flooded" ice storage tank design is a relatively new approach to ice slurry storage. The storage tank is filled completely with water. Ice slurry is pumped into the storage tank where the ice is filtered out so that the water leaving the tank is ice free. Since flooded storage tanks are pressurized, this concept is intended for use in a distributed storage system with multiple smaller tanks, as shown in Figure 5.11. The system has several advantages over conventional "free liquid" designs which increase the ice fraction in storage and simplify the controls.

Increased Ice Fractions

The ice fraction in "flooded" storage is improved by utilizing the entire volume for ice storage. Unlike "free liquid" tanks which have a vapour space above the liquid, the entire "flooded" storage tank is available for ice storage. However, with flooded storage tanks in a system, expansion vessels are required as explained below. The unused vapour space of conventional "free liquid" tanks can amount to 20% of the total volume.

The ice fraction is also improved by using hydraulic forces instead of gravitational forces to pack the ice into the tank. The "flooded" ice storage tank is essentially an ice filter. The entering ice slurry is filtered allowing only ice free water to leave. Like most filters, the pressure drop across the tank will rise as the ice fraction increases. The limit of the maximum ice fraction will be essentially dependent upon the maximum pressure drop across the tank.

Expansion Tank

The "flooded" storage tank concept requires an expansion tank to accommodate the increasing volume of fluid within the system as ice is produced. Conventional "free liquid" storage concepts accommodate the expanding volume within the vapour space at the top of the tank.

Controls

The controls of the "flooded" storage tank are simplified by eliminating the second pump and liquid level control loop associated with conventional "free liquid" storage tanks. The flow into the storage tank is equal to the flow out.

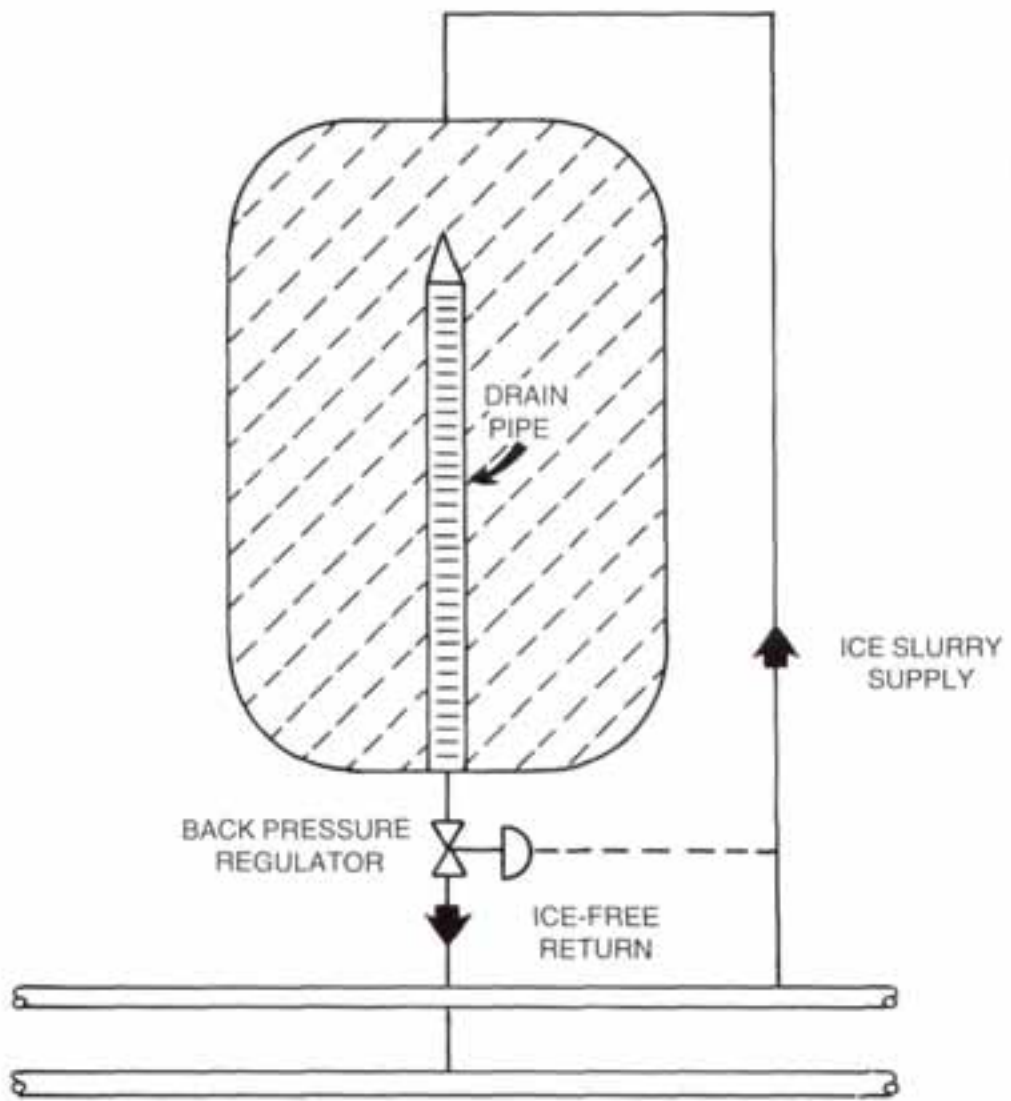
To prevent the storage tank from acting like a short circuit at start-up when the ice fraction is low and the pressure drop across the tank is at a minimum, a simple flow control valve can be used in the ice free water outlet line.

Melting the Stored Ice

The "flooded" storage tank design simplifies the charging aspect of the problem. However, the discharging is complicated by the lack of an obvious method of insuring good contact between the warm water returning to the storage tank and the ice

Figure 5.11

Ice Slurry Storage - "Flooded" Storage Tank



stored inside. The ice crystals within the storage tank will still tend to float to the top of the tank. Therefore, locating the warm return water distribution system in the upper portion of the tank will insure good contact even when the ice content is low.

A bottom, cold water outlet, is also most desirable since the colder water is more dense and should accumulate in the lower portion of the tank. Water has its maximum density at 4°C.

Construction Limitations

The physical geometry of a "flooded" storage tank is less critical than that of the "free liquid" design. The ice is packed using hydraulic rather than gravitational forces. The primary design consideration is the pressure drop across the vessel. The cost impact resulting from a pressurized design can be minimized by operating the tank at less than 15 psig. Even using this modest differential pressure, the compressive force can be 3 to 6 times higher than that of conventional designs. The pressurized design also favours cylindrical storage tanks of smaller diameter to minimize shell thickness. The concept may be particularly well suited for the distributed storage operation with many smaller storage tanks.

5.2.5 Ice Slurry Utilization

The use of ice slurry in district cooling systems can dramatically impact the distribution piping size and pumping power requirements. However, using an ice slurry in existing buildings designed for chilled water requires additional consideration. Three implementation strategies are currently being evaluated: direct ice slurry technique, distributed storage technique, and warm water recycle technique.

5.2.5.1 Direct Ice Slurry Technique

Methodology

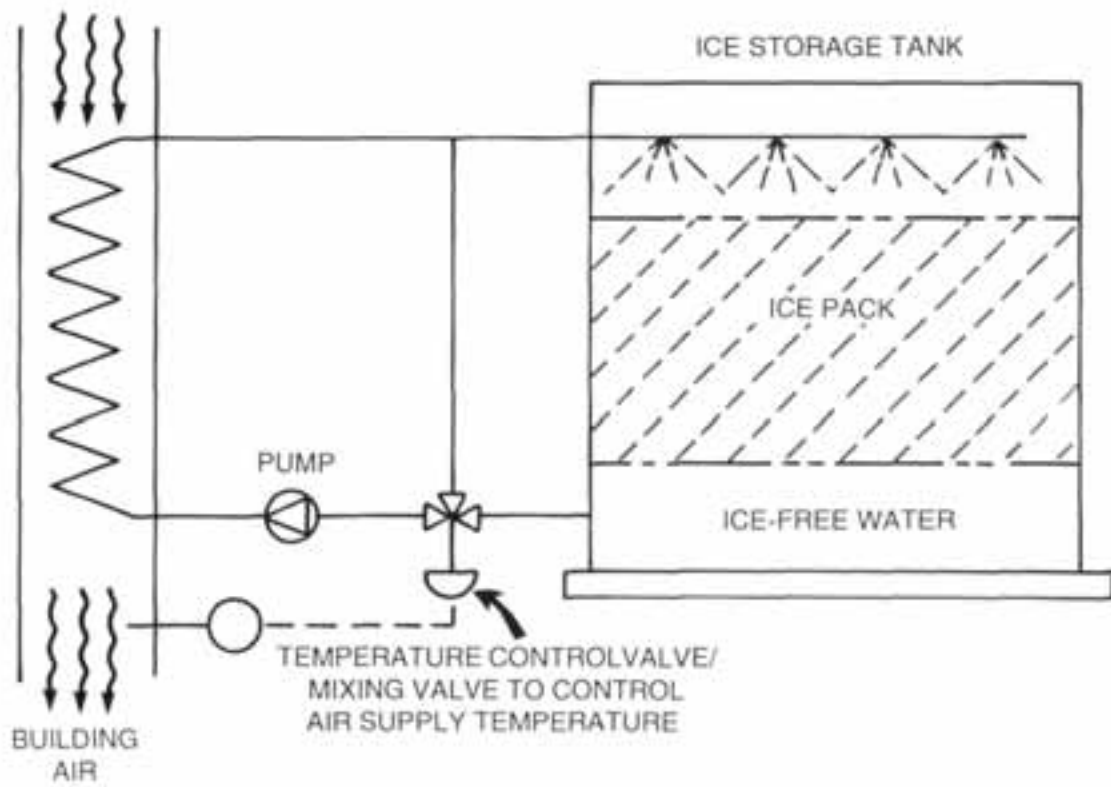
The Direct Ice Slurry method involves sending the ice slurry from the distribution piping directly to the cooling coils as shown in Figure 5.12. Initially, this may appear to be the simplest approach for implementing ice slurry at the end user. However, the technical and economic problems associated with this concept may prove unacceptable. Existing heat transfer equipment installed in large buildings is designed for chilled water, not ice slurry service. A direct conversion of existing chilled water equipment into ice slurry service would result in a lower internal heat transfer coefficient, an increased temperature difference and create a potential for ice blockage within the heat exchanger. Experiments with plate heat exchangers at the NRC indicate that the potential for ice blockages is very limited.

Lower Heat Transfer Coefficient

The increased energy carrying capacity of an ice slurry will result in a substantial decrease in the required flow rate to meet a given cooling load. Even a modest ice fraction of 20% will reduce the flow rate by a factor of 5.2 in chilled water cooling coils originally designed for a temperature differential of 5°C. The reduced flow rate

Figure 5.12

Ice Slurry Utilization - Direct Ice Slurry



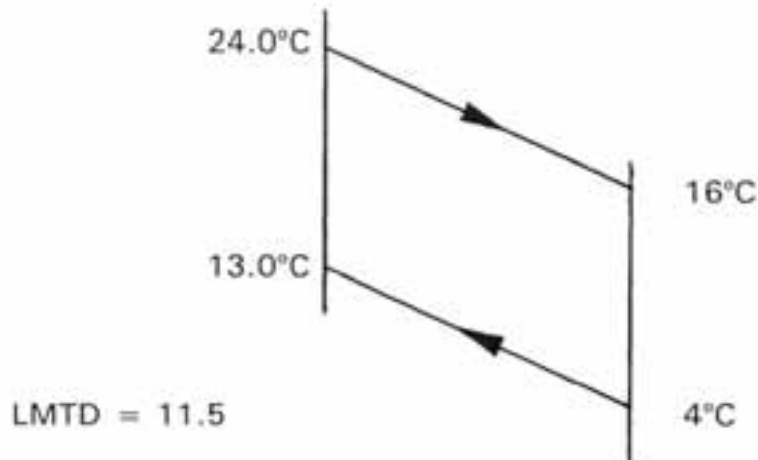
translates directly into a lower fluid velocity inside the exchanger by the same factor.

The heat transfer coefficient within this equipment is proportional to the Reynolds number to the 0.8 power and the Prandtl number to the 0.4 power. Neglecting the slurry's effect on viscosity and molecular momentum, the Prandtl number can be taken as a constant and the change in the Reynolds number will be limited to velocity effects only. Under these assumptions, the internal heat transfer coefficient would be proportional to the reduction in velocity to the 0.8 power. Consequently, the internal heat transfer coefficient will be reduced by a factor of 3.7 for a chilled water coil originally designed for a 5°C temperature difference when operated with a 20% ice slurry.

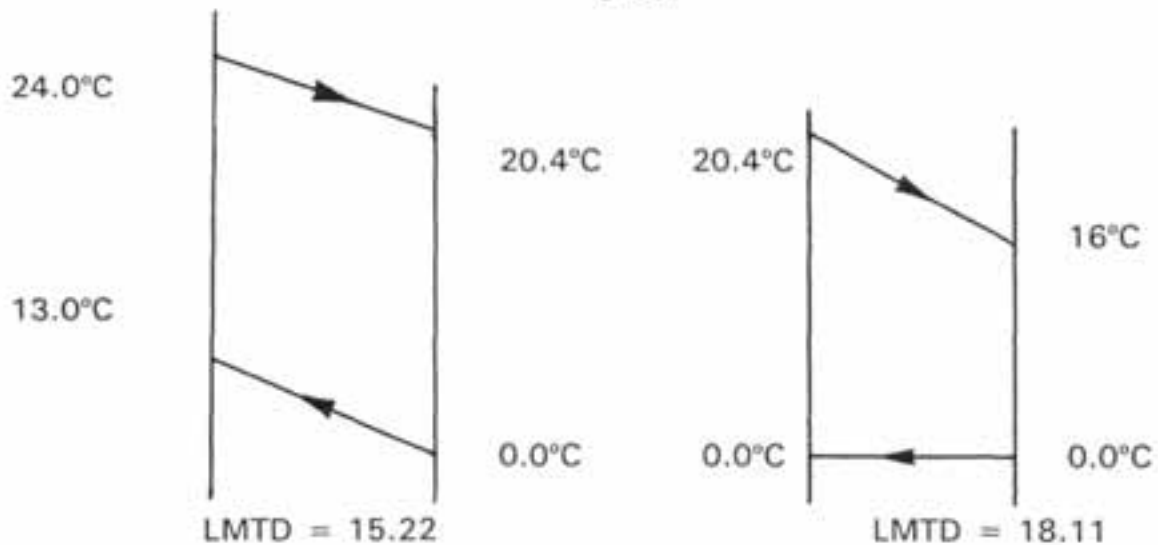
The final impact of a lower internal heat transfer coefficient on the actual cooling capacity of the coil will depend upon the combined effects of internal and external heat transfer coefficients on the overall heat transfer coefficient.

Increased Temperature Difference

The temperature difference between the air and slurry will be greater than the original air to chilled water temperature difference. However, the magnitude of this increase may not be large enough to offset the reduced heat transfer coefficient due to lower velocities described above. The impact of this factor can be shown using the hypothetical conditions below.



Assuming that the high side of the exchanger remains unchanged, the impact of the slurry is limited to an isothermal behaviour for part of the duty and lower temperatures throughout. The isothermal portion is associated with the slurry melting region. To correctly analyze this situation the heat exchanger should be divided into two sections where the latent and sensible heat of the slurry is recovered.



The latent heat of a 20% ice slurry represents approximately 55% of the available cooling. The balance is sensible heat. With this in mind, the weighted average LMTD for ice slurry is 16.81. This is a net increase in LMTD of approximately 46% for the ice slurry. For a 30% ice slurry this increase would be approximately 49%. The larger LMTD is thought to augment the heat transfer to the extent that the negative effects of the reduced internal heat transfer coefficient are negated.

Ice Slurry Blockage

The small flow passages in many high efficiency heat exchangers may be susceptible to blockage from the ice slurry if the flow paths are not uniform and continuous. Stagnant fluid pockets typically found at the end of piping manifolds may be sufficient to allow ice to accumulate and eventually plug the flow. This problem is further aggravated by the low velocities which would exist in this situation.

New Heat Exchanger Design

To alleviate the problems of converting existing chilled water equipment for ice slurry service, new heat transfer equipment specifically designed for use with ice slurry could be installed. However, the cost implications of this approach in retrofit applications should be considered.

Controls

Typically, for building air-conditioning applications the temperature of the air leaving the cooling coil is the critical control point. The flow of chilled water is regulated to maintain the desired air delivery temperature. For a direct ice slurry system, the air delivery temperature is still the critical control point. The desired air delivery temperature must be maintained by regulating the flow of the ice slurry entering the cooling coil. The use of conventional control valves for ice slurry applications is not recommended. Therefore, the control valve must be located on the other side of the air-handler where it can directly control the flow of warm water leaving the unit and indirectly control the flow of ice slurry entering the coil.

Metering

Metering the amount of cooling delivered to the end user is an important aspect of a successful district cooling system. To determine the cooling delivered to the end user, without resorting to measuring the air side of the exchanger, a sensor which can measure the ice fraction within the supply stream will be required. Instrumentation to accomplish this is currently available, e.g., coriolis density/mass flow meters. Instrumentation based on di-electrics are under development (Reference 13).

5.2.5.2 Distributed Ice Storage Technique

Methodology

One of the early solutions proposed to overcome the potential problem associated with sending ice slurry directly into conventional air-handling equipment was the distributed ice storage technique. The ice storage tank is used to separate ice from the carrier water. In the storage tank, ice and water separate by gravity. The lighter ice floats to the upper portion of the tank leaving ice free water in the bottom. The ice free water can then be pumped from the storage tank and delivered to the air-handling equipment.

The flow rate of the cold water can be selected to match the design requirements of the existing chilled water equipment. Similarly, the design inlet temperature requirements can be matched by installing a mixing valve upstream of the circulation pump. One part of the warmed water leaving the heat exchanger is returned to the ice storage tank for re-chilling as the water passes through the ice pack. The other part is re-circulated with the cold water entering from the tank. The concept is shown in Figure 5.13.

The distributed ice storage technique is a relatively simple way to integrate ice slurry without affecting the operation of existing heat transfer equipment. Distributed ice storage also provides a simple means of load levelling. See Section 5.2.4 "Ice Slurry Storage" for a complete description of distributed ice storage for load levelling. Although the concept of distributed storage may be suitable for some applications, the high cost of space for many urban district cooling systems may preclude the use of an ice storage tank at each building.

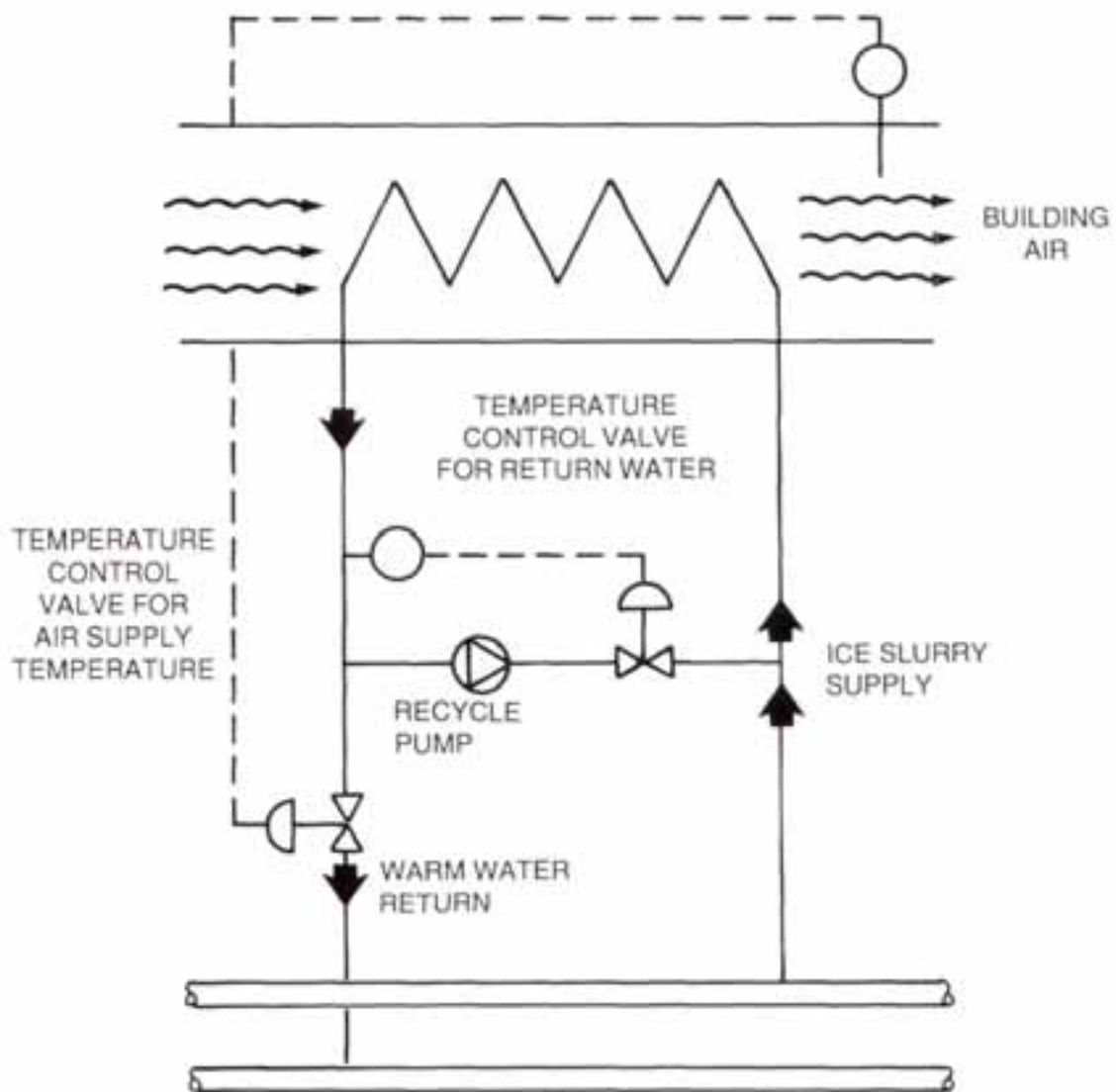
Controls

The distributed ice storage tanks provide a relatively simple means of eliminating ice slurry handling at the end user. The controls for this approach are identical to any conventional chilled water air conditioning application with the addition of a mixing valve up stream of the coil to raise the inlet water temperature to avoid excessive dehumidification.

Depending on the load, a fraction of the return water from the heat exchanger is sent back to the local ice storage tank and some of it is recirculated. The remainder, being equal to the ice slurry supply flow, is returned to the distribution system. There is a requirement for controlling the water outlet temperature to maximize energy delivery.

Figure 5.13

Ice Slurry Utilization - Distributed Ice Storage



It is possible that during periods of very low load, and while the storage tank is being replenished, the maximum enthalpy difference between supply and return lines cannot be maintained. The district cooling pipe diameter must be sized to account for this period of lower enthalpy delivery.

Additional controls at the central cooling system are required to monitor the quantity of ice slurry in the storage tanks at all times. This information is essential to avoid running out of ice during peak cooling periods.

Metering

The distributed ice storage technique can be metered using conventional chilled water equipment on an "as used" basis.

5.2.5.3 Warm Water Recycle Technique

Methodology

The warm water recycle concept was conceived to facilitate the use of ice slurries without effecting the design conditions of existing heat transfer equipment - while eliminating the need for local ice storage. The basis of the idea is to transform a low flow, high cooling capacity, ice slurry into high flow, lower cooling capacity, chilled water.

The method involves the use of a warm water recycle stream from the discharge of the heat exchanger as shown in Figure 5.14. The warm water is mixed with the incoming ice slurry to completely melt the ice and produce the desired flow rate and design inlet temperature. In this manner, the exact design conditions of both flow and temperature can be matched for each specific end user around the entire district cooling network.

Controls

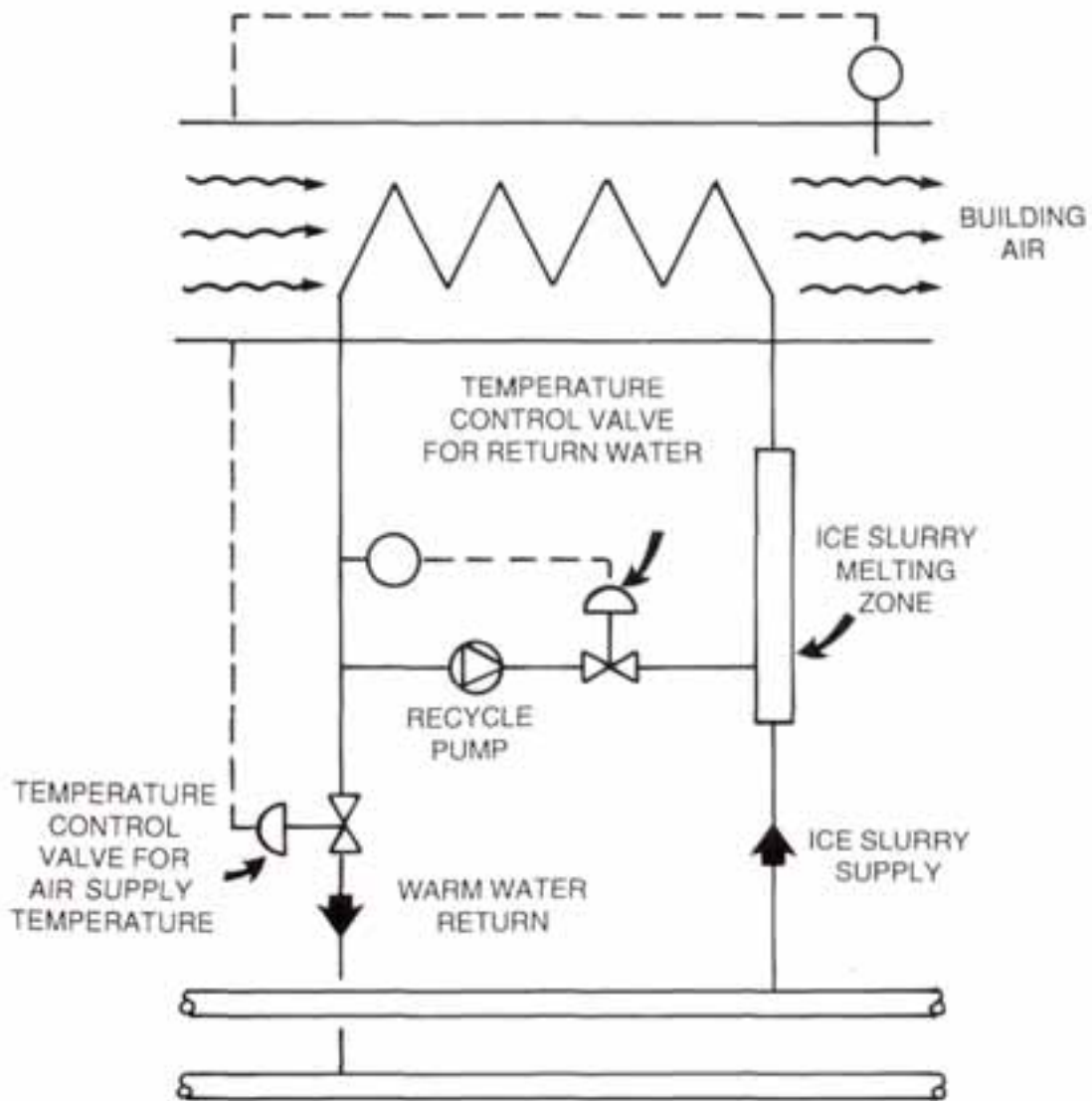
The warm water recycle technique requires two independent control loops. The first control loop regulates the flow of ice slurry into the mixing section just upstream of the cooling coil to control the air temperature delivered to the building. The slurry flow is controlled indirectly by restricting the flow of warm water returning to the distribution system. Installing the control valve in the warm return piping eliminates the complexity of installing a control valve directly in the ice slurry lines.

The second control loop maintains the desired temperature of the warm water exiting the heat exchanger. Sustaining the highest possible return temperature is critical to optimize the performance of the ice slurry distribution system.

The warm water exit temperature is controlled by regulating the flow of warm water in the recycle stream to increase the inlet temperature at the cooling coil. If the exit temperature of the heat exchanger begins to drop, due to a reduction in cooling load, the flow of warm recycle water is increased. The result is an increase in the equilibrium temperature leaving the mixing zone and entering the exchanger. The

Figure 5.14

Ice Slurry Utilization - Warm water Recycle



warmer inlet temperature effectively reduces the cooling capability on the cold side in response to the lower cooling load.

Metering

The cooling load can be measured directly with conventional chilled water equipment at the heat exchanger since the ice slurry has melted prior to entering the heat exchanger. Care must be exercised in the design of the mixing section upstream of the heat exchanger to ensure complete melting and a uniform fluid temperature at the temperature probe used to perform the metering calculations.

5.3 ICE SLURRY DISTRICT COOLING - RESEARCH OPPORTUNITIES

The design alternatives presented in the previous section illustrate the diversity which currently exists in the technologies being developed for ice slurry district cooling systems of the future. A short summary of research opportunities to assist in further developing these options is provided below. The goal of continued research is not simply the analysis of specific system elements, but rather, the systematic development of a prototype district cooling system.

5.3.1 Ice Slurry Generation

The ice generation equipment must be selected as the starting point for continued research. The technology which is used to generate the slurry determines the characteristics of the ice crystals formed. The remainder of the system including ice slurry distribution, ice storage, and ice slurry utilization depend in varying degrees upon the ice crystal characteristics. Technical development needs for each of the ice generation technologies presented earlier in Section 5.2.2 will be discussed separately.

In general, the capital cost of ice slurry chillers is higher than that of common chillers. To bring the cost of ice slurry production down should be the highest research priority.

5.3.1.1 Binary Solution Ice Slurry Generator

The "Sunwell Engineering" binary solution ice slurry generation system is the most commercially developed ice slurry technology currently available. At this time, an ice slurry district cooling system based on this technology is under development at the Energy Research Laboratories of Energy, Mines and Resources Canada. In Japan, several Sunwell systems are operational. These systems make use of time-of-day electricity rates to make ice slurry at night for daytime use.

Sunwell systems have been installed worldwide for other ice slurry generation needs such as the food industry. The primary technical problem limiting the use of this concept is the environmental and/or economic impact of the glycol. The glycol content of the system is normally about 6%.

Ethylene glycol, the most commonly used freezing point depressant for these systems, is environmentally hazardous. In many areas, systems which contain this substance must be constructed with double walled pipe to guarantee leak proof operation. The economic impact of ethylene glycol is also an issue. Double walled pipe is an additional cost penalty.

Propylene glycol, while eliminating the environmental hazard, does not completely resolve the problem. Propylene glycol is even more expensive than ethylene glycol.

Salt solutions also provide the required freezing point depression. However, corrosion problems within the distribution network and end user heat transfer equipment may still result in major economic consequences.

A low cost, environmentally safe, freezing point depressant would eliminate the economic and environmental concerns related to this technology and secure its position as a leading ice slurry generation system for district cooling applications.

It would be a benefit to separate the glycol containing ice slurry production part of the system from the distribution network. Several commercial installations exist that can accomplish the separation of the glycol from the ice by back washing techniques. Refinement of these techniques could potentially reduce the operating cost of district heating systems.

As referred to before, the storage of ice decouples the load from the installed capacity. In the case of central storage, to minimize the pipeline diameter, the distribution of ice slurry is paramount. The harvesting of ice from a storage vessel in slurry form would greatly enhance the capacity of the system. The development of systems to reliably effect this re-slurryfication would therefore minimize the distribution cost of cooling.

5.3.1.2 Scraped Surface Ice Generator

The scraped surface ice generation technology is readily available commercially. Numerous commercial installations are currently operating for bulk ice generation using this concept. However, the capacity of this technology is relatively small for direct application to district cooling applications. The most significant technical barrier for this concept is the inability of the system to produce an ice slurry directly.

The scraped surface system produces bulk ice, not an ice slurry. Demonstrating the missing elements required to convert the bulk ice into an ice slurry is essential for further analysis of this technology. Increased capacity, efficiency and reliability are also important factors.

The scraped surface technology may be suitable for applications with central storage where distribution of ice slurry is not required.

5.3.1.3 Defrost Cycle Ice Generator

The defrost cycle ice generation technology is similar in many ways to the scraped surface design mentioned above. The technology is readily available, boasts many commercial installations for bulk ice generation, but does not produce an ice slurry directly. In addition, the defrost cycle is also a batch process. The ice is built on a refrigerated surface until the desired thickness is achieved. The refrigeration cycle is then reversed causing the ice to melt free of the surface and fall into a storage reservoir.

The implementation of this concept will require demonstration of the missing elements necessary to convert the bulk ice into a pumpable slurry. In addition, a continuous version of the process must be perfected for application in the district cooling system of the future.

As with the scraped surface technology, this technology may be suitable for applications with central storage where distribution of ice slurry is not required.

5.3.1.4 Supercooled "Superpac" Ice Slurry Generator

The supercooled "Superpac" ice slurry generation system is a relatively new technology. Demonstration of the system has thus far been limited to the laboratory. Technical questions for this system are related to scale-up and the ability to achieve high ice fractions in slurry form. However, the technical questions relating to the scale-up of the evaporator appear to have been resolved. A 300 Ton unit has recently been designed for use as a heat pump with low temperature water as the source.

Producing a supercooled liquid without premature crystallization within the evaporator, is critical for system operation. The supercooled state can be overcome by many factors including seed crystals in the feed stream, impurities in the water, flow instability, and heat flux instability. Production of 0°C water with "Superpac" is considered risk-free. A demonstration of supercooled operation under actual district cooling conditions is planned.

Achieving high ice fractions in slurry form is essential. For each degree of subcooling, the ice fraction increases by about 1.25%. Controlling crystallization to prevent ice buildup on surfaces instead of in the bulk fluid has been successfully demonstrated in several laboratory settings. Increasing the ice slurry fraction per pass is a research priority.

5.3.1.5 Direct Freeze Ice Slurry Generator

The direct freeze ice slurry generation system is the most unique technology currently being developed for district cooling applications. The unconventional design is both the greatest strength and most profound weakness of the system.

The concept of direct contact between a refrigerant and fresh water has the potential for producing the highest thermodynamic efficiency of any ice generation concept.

Continuous operation has been demonstrated with a consistent refrigerant evaporation temperature of -1°C . The system produces an ice slurry directly with ice fractions as high as 10% per pass.

The use of a direct contact evaporator/freezer also leads to many new challenges for the associated condensing system. The refrigerant vapours are saturated with water vapour as they enter the compressor. Due to the presence of water vapour, all of the other components must be customized. The compressor is a water lubricated, water cooled design which had previously never been used in refrigeration equipment (Reference 11).

The condenser exploits the water mixed with the incoming vapour to enhance heat transfer. The receiver doubles as a separator to recover the lubrication water and return it to the compressor. The expansion device is designed to handle the water saturated refrigerant without freezing. The unique direct contact evaporator, while providing excellent efficiency, effectively eliminates the use of commercially available packaged refrigeration equipment.

Research must be performed to continue the development and scale-up of refrigeration components. The direct contact evaporator/freezer and water based compressor are the most critical components deserving careful systematic attention to maximize the potential thermodynamic efficiency.

The use of a direct contact evaporator/freezer also results in new challenges for the refrigerant used in the system. The refrigerant must be relatively insoluble and essentially inert in water to prevent chemical reactions such as hydrolysis or the formation of complex crystal inclusions known as hydrates. The vast majority of commercially available refrigerants fail to meet one or both of these requirements.

The refrigerant which was used to develop the initial prototype systems is a CFC. Scientific evidence has shown a relationship between CFC's and a breakdown of the ozone layer. This information has led to an international agreement to restrict the use of CFC's. As a result, the refrigerant used in this process is scheduled for elimination within the decade. Other existing refrigerants have been identified for use in the system including C-318 and butane.

Research should be pursued to demonstrate an environmentally acceptable and commercially available alternate refrigerant for use in the direct freeze system using existing or new refrigerant candidates.

5.3.2 Ice Slurry Distribution

The distribution of ice slurry has demonstrated a wide variety of results depending upon the physical size of the ice crystals produced in the system. The ice slurry distribution studies, therefore, should be conducted for each successful ice generation technology to determine the actual behaviour.

5.3.2.1 Ice Slurry Flow Characteristics

The hydraulic behaviour of ice slurries studied thus far have revealed wide variations in fundamental flow characteristics. Homogeneous, Newtonian ice slurries which have little variation compared with water have been reported. Non-homogeneous, non-Newtonian ice slurries which transform turbulent flow to a laminar plug, resulting in a reduction in pressure drop, have also been observed. Due to this wide variation, the flow characteristics must be studied for each viable ice generation technology. The main characteristics which should be evaluated are the agglomeration, pressure drop and flow splitting behaviour.

Agglomeration of the ice slurry during transport would cause serious operating difficulties in the distribution network. Flow visualization should be incorporated in future research.

Ice slurry pressure drop data is fundamental for the design of any district cooling system. Pressure drop behaviour as a function of ice fraction and slurry velocity is most useful. Additional data documenting the break away friction for ice slurry is also important.

Uniform flow splitting to deliver a consistent ice fraction to multiple locations about the network should be demonstrated.

5.3.2.2 Pump performance

Pump sizing is a relatively small technical detail in the design of most chilled water district cooling systems. Pump performance data is readily available for chilled water. The same data is not always available for ice slurry operation.

Gupta has measured the change in pump characteristics between water and ice slurry at various ice fractions. His results show that for a constant flow, the pump head decreases slightly for an increase in ice slurry fraction. In Gupta's experiments (Reference 13), the pump head decreased by about 10% for an increase in ice fraction between 0 and 0.25. Ice slurry flow studies should always include this data to facilitate the design of new systems.

5.3.2.3 Piping Material Compatibility

The materials of construction for the distribution network can be important for some ice slurry generation systems. Potential material problems can include corrosion, air permeability, and ice agglomeration. The newness of ice slurry technology and the variety of ice generation technologies make it difficult to ask all the right questions when it comes to material compatibility. Only continued research will reveal or dismiss this issue.

5.3.3 Ice Slurry Storage

Two ice storage tank design concepts have been described which provide the required thermal energy storage without the need to re-slurry ice from storage. The

performance of either concept will depend upon the physical characteristics of the ice slurry to be stored. Larger ice crystals provide superior drainage and generally higher ice fractions in storage compared to fine ice crystals. The research needs of the two ice storage tank design concepts, "Free Liquid" and "Flooded", will be presented individually.

Free liquid storage tanks are usually large tanks open to the atmosphere. The top section of this type tank is used as expansion vessel. Flooded storage tanks are commonly pressurized, and therefore smaller.

5.3.3.1 "Free Liquid" Ice Storage Tank

The "Free Liquid" ice storage tank has been used extensively for thermal energy storage on single building installations. However, a detailed parametric study of the performance of this ice storage tank design has not been published. For single building thermal energy storage applications the reported ice fraction limit in storage is approximately 40 to 60% depending upon the storage tank geometry. In general, taller vertical cylinder style tanks perform better than horizontal cylinders.

The operating conditions of an ice storage tank used in a district cooling system will vary dramatically from those of a single building installation. Many of the existing ice storage systems do not form an ice slurry which is pumped to the tank. Instead, ice is formed directly over the tank and falls into the storage tank. Compared to these systems, the pumpable ice slurry of an ice slurry district cooling system will distribute much more evenly in the tank.

Research should be performed to determine the actual ice storage performance under district cooling system conditions. Additionally, work should be done to determine the tank size at which free liquid tanks are more economical than flooded tanks.

5.3.3.2 "Flooded" Ice Storage Tank

The "Flooded" ice storage tank design has had only limited laboratory testing. The basic design eliminates the need for ice slurry distribution during charging. The hydraulic force presses the ice uniformly into the tank. The leading performance parameter is the ice fraction achievable as a function of differential pressure across the storage tank.

Several variables can be used to enhance the performance of the tank including increased drainage, reduced free water in the ice slurry supply and increased differential pressure. The drainage can be improved by operating with larger ice crystals which increase the porosity of the ice pack. Drainage can also be enhanced geometrically by shortening the exit path from the storage tank.

Research should be performed to determine the performance of this ice storage concept under district cooling conditions.

5.3.4 Ice Slurry Utilization

Three ice slurry utilization techniques have been presented to implement ice slurry district cooling at the end user: the direct ice slurry technique, distributed ice storage technique, and warm water recycle technique.

5.3.4.1 Direct Ice Slurry Technique

The direct ice slurry method is the most uncertain ice slurry utilization scheme when the system is being installed using existing chilled water heat transfer equipment at the end user. Ensuring equivalent cooling capacity and reliable operation will require careful analysis for each individual case. The method also requires the installation of new metering equipment capable of measuring the ice fraction of a flowing slurry.

Future new installations may be designed using a new concept for ice slurry heat exchangers and energy metering equipment. However, in the short term, the other methods presented achieve the same end result with far less potential problems.

5.3.4.2 Distributed Ice Storage Technique

The distributed ice storage ice slurry utilization method is limited to district cooling systems which have sufficient space available to install local ice storage tanks at each end user. The storage tank greatly simplifies the problems of handling ice slurry at the end user. Instead, cold water from the storage tank is used to supply the chilling coils. Conventional chilled water metering equipment can be applied directly to this concept.

The performance of the ice storage tank must be carefully tested to determine the effectiveness of the re-chilling process. The warm return water must be cooled by passing through the stored ice pack. The consistency of the outlet temperature over a melting cycle is an important design parameter.

5.3.4.3 Warm Water Recycle Technique

The warm water recycle method is ideal for use in systems with central ice storage or no storage at all. A warm water recycle stream is used to eliminate the ice crystals and achieve the desired chilled water flow and inlet temperature prior to entering the conventional heat exchanger. Conventional chilled water metering equipment is used with this technique.

The performance of the mixing zone should be demonstrated to ensure an ice free water supply and uniform temperature to the heat exchanger. The control valve on the warm water return to the district cooling network which regulates the flow of ice slurry into the mixing zone, and the control valve which regulates the warm water recycle flow into the mixing zone should be tested under fluctuating loads.

5.4 CONCLUSIONS

The field of district cooling systems using ice slurries as the prime mover of energy is a new, exiting branch of technology which holds considerable promise for the future. The economy of installation of ice slurry producing chillers and the distribution of ice slurry will make this a technology of choice for the future.

Because of superior ice storage possibilities, installed capacity does not need to be much more than average design load instead of maximum load. With the increased enthalpy carrying capacity of the ice slurry, the distribution network can consist of smaller diameter pipelines with associated smaller installation and operating costs.

The present high cost of ice slurry production is still hindering the widespread use of district cooling systems based on ice slurry. Work is continuing to bring the price of ice slurry chillers down.

The ongoing research in the field of ice slurry based district cooling promises that the increasing benefits of this technology will shortly be exploited ubiquitously.

5.5 REFERENCES

1. P. Metz and P. Margen. "The Feasibility and Economics of Slush Ice District Cooling Systems." ASHRAE Transactions, vol. 93, Pt. 2, pp 1672-1686, 1987.
2. M.A. Paradis and G. Faucher. "A New Ice Maker Heat Pump." ISES Solar World Congress, Hamburg, FRG, Sept 13-18, 1987.
3. M.A. Paradis, R. Turcot, and G. Faucher. "Development of a Prototype Ice Slurry Generator for D.C.." Proceeding of the 80th Annual Conference of the International District Heating and Cooling Association, Virginia Beach, Virginia, June 1989.
4. B. Larkin and J.C. Young. "Influences of Ice Slurry Characteristics on Hydraulic Behaviour." Proceedings of the 80th Annual Conference of the International District Heating and Cooling Association, Virginia Beach, Virginia, June 1989.
5. Graham, T., Tokunaga, K. and Goldstein, V., (1989), "Application of Crystal Ice Generation in District Heating and Cooling", Proceedings of the Eightieth Annual Conference of the International District Heating and Cooling Association, Virginia Beach, Vol. LXXX, Published by the IDHCA, Washington, D.C.
6. Gupta, R.P. and Fraser, C.A., (1990), "Effect of a New Friction Reducing Additive on Sunwell Ice Slurry Characteristics", National Research Council

of Canada, Institute of Mechanical Engineering, Low Temperature Laboratory, Report No. TR-LT-023, NRC No. 32123.

7. B.D. Knodel and D.M. France. "Pressure Drop in Ice-Water Slurries for Thermal Storage Applications." *Experimental Heat Transfer*, vol. 1, pp. 265-275, 1987-1988.
8. B.D. Knodel and D.M. France. "Ice-Water Slurry Flow in a Circular Pipe." *International Communications in Heat and Mass Transfer*, vol. 15, No. 2, pp. 239-245, March-April 1988.
9. B.D. Knodel. "R&D Pilot Plant Project for Evaluating a Direct Freeze Ice Slurry Based district Cooling System." Final Report to the U.S. Department of Energy, May 1988.
10. B.D. Knodel. "Phase I - Direct Freeze Ice Slurry District Cooling." Proceeding of the 79th Annual Conference of the International District Heating and Cooling Association, Jamestown, New York, June 1988
11. B.D. Knodel. "Phase II - Direct Freeze Ice Slurry District Cooling." Proceedings of the 80th Annual Conference of the International District Heating and Cooling Association, Virginia Beach, Virginia, June 1989.
12. A.Sellgren. "Hydraulic Behaviour of Ice Particles in Water." Proceeding of the 10th International Conference on Hydraulic Transport of Solids in Pipes, pp 213-217, Innsbruck, Austria, October, 1986.
13. Gupta, R. P., Unpublished Results, 1992.

6. THE INFLUENCE OF FRICTION REDUCTION ADDITIVES ON CORROSION RATES OF DISTRICT HEATING SYSTEM MATERIALS

Jacques L. Zakin, Bryan C. Smith and Bin Lu
The Ohio State University
Columbus, Ohio, USA 43210

6.1 INTRODUCTION

The phenomenon of drag reduction in turbulent flow was discovered more than 40 years ago [1,2]. Significant reductions in frictional energy losses or increases in throughput in pipe flow can be achieved by the addition of small amounts of drag reducing additives to the system.

In northern and eastern Europe, the use of district heating systems is widespread. In these systems, cogeneration or waste heat is utilized to supply hot water (ranging from 80 to 130°C) for circulation to homes, businesses and industries within a district. The hot water is pumped through a 10 to 20 km loop, exchanging heat with the various installations along the way. It is then reheated and recirculated.

Major costs of district heating systems are the cost of pumping the recirculating water, and the capital expenses for the pipes, fittings and pumps in the recirculation loop. Friction losses in the turbulent pipe flow in the recirculation loop can be significantly reduced by the use of drag reducing additives, increasing the energy carrying capacity of the system and/or reducing the operating power costs or the capital costs of pipes, fittings and pumps for new systems.

While high polymer drag reducing additives have received a great deal of attention in the literature [3-7], their use in recirculation systems is not feasible due to their irreversible degradation in regions of high shear such as pumps. Low molecular weight surfactants, on the other hand, have been found which demonstrate drag reducing behavior at concentrations as low as several hundred parts per million, and demonstrate reversible shear degradation [8]. Promising surfactant additives which are useful up to 110 to 120°C have been identified in the United States [9,10] and up to 145°C in Germany [11] and they have great potential for use in district heating and district cooling systems.

Accordingly, at their September 1987 meeting at Ohio State, the Advanced Transmission Fluids Experts Group recommended a one-year exploratory study of the effect of friction reducing additive systems on corrosion of metals commonly used in district heating systems. The study was carried out in 1989-90, at Ohio State. It examined the effects of several cationic surfactant drag reducers in unadjusted solutions of tapwater, tap water plus corrosion inhibitor, and deionized water [12].

Uniform attack (general corrosion) is the most common form of corrosion. This type of corrosion is characterized by an attack which proceeds uniformly over the entire exposed surface or over a large area. The metal becomes thinner and eventually fails. Linear polarization accelerated corrosion rate tests can be utilized to estimate

corrosion rates of different metals in various corrosion environments [12].

Pitting corrosion, on the other hand, is a form of localized attack which quickly results in small holes in the metal [13]. The differences between these two types of attack are illustrated in Figure 6.1.

The problem of pitting is an extremely serious one due to the fact that subsurface damage is usually more severe than indicated by the surface appearance. Detection of the phenomenon in service is difficult because of the small size of the pits (on the surface of the metal) and the fact that they are often covered by corrosion products. Premature, undetected failure is not uncommon due to the localized nature of pitting.

Susceptibility to pitting can be determined utilizing the method of anodic polarization [12]. In this method the voltage applied to a metal specimen in a corrosive environment is increased in a step-wise fashion and the current required to maintain the overvoltage is measured. A typical curve for a system undergoing general corrosion is shown in Figure 6.2. The upward deviation from linearity in Figure 6.2 is due to concentration polarization. Concentration polarization occurs when the reaction rate or the applied external current is so large that the species being oxidized or reduced cannot reach the metal surface at a sufficiently rapid rate, i.e. the corrosion rate is mass transfer rate limited.

Figure 6.3 shows a polarization curve for a material where polarization occurs (region 2) followed by either a region of general corrosion or a region in which localized pitting corrosion occurs (curve with arrow indicates the material is undergoing localized pitting). The pitting potential is defined as the absolute potential above which pitting corrosion may occur and is shown in Figure 6.2 as a sharp break in the curve at E_C and a marked increase in the anodic dissolution current. The measured current increases with time during the three minute interval in which the voltage is applied (as emphasized by the arrows), whereas it decays with time to a steady state value during uniform attack. The pitting potential is a characteristic of a metal/environment combination and is a measure of the susceptibility of the metal to the corrosion environment to which it is exposed in the test [12].

Pit initiation can not occur below a specific potential, E_C , the critical pitting potential [14]. Metals with higher values of E_C have proven to be more resistant to pitting corrosion [15]. The requirements for chemical breakdown appear to be potential in excess of E_C , presence of a damaging species (chloride or other halide), an induction time for initiation and highly localized sites [16].

6.2 RESULTS OF EARLIER EXPLORATORY STUDY

The results of the earlier Ohio State study (12) indicated that the presence of chloride ions in the surfactant generally increased the susceptibility to pitting of stainless steel at high temperatures but not of carbon steel in both tap water with corrosion inhibitors and also in deionized water. Surfactants without chloride, such as Habon, had no adverse effect on the iron-based metals in tap water with corrosion inhibitor

and in deionized water. In general all surfactants reduced pitting susceptibility for copper, 90/10 copper/nickel and 60/40 copper/zinc in tap water with a corrosion inhibitor (hydrazine) and in deionized and deoxygenated water.

Corrosion rates at 110°C were low for all surfactants in stainless steel but were relatively high for all surfactants for carbon steel in tap water plus hydrazine. In deionized water, they were also low for all surfactants for stainless steel and were moderate for carbon steel. Corrosion rates for the copper-based samples were relatively low for all surfactants in tap water plus hydrazine. Both Dobon and chloride-containing surfactants gave moderate rates of corrosion in deionized water.

The hydrazine corrosion inhibitor had no serious deleterious effects on drag reduction effectiveness of the chlorine containing surfactants and on Dobon in tap water and only moderate effect on Habon. Thus, this additive is both effective as a corrosion inhibitor and compatible with the surfactant additives typical of those under consideration for use in district heating systems. Unfortunately, it is a suspected carcinogen and its commercial use is banned in several countries and is diminishing in others although its use is still fairly common in Finland, Sweden and the United States.

As a result of this preliminary investigation, a more detailed study of corrosion effects was proposed and the results are reported here. The proposal was to take into account additional variables such as temperature (60 to 110°C for district heating systems and 25°C for district cooling systems), pH (6.0 to about 10), surfactant composition (quaternary ammonium salts with one large (C₁₆ to C₂₂) alkyl group and trimethyl, dimethyl hydroxyethyl, methyl bis hydroxyethyl and tris hydroxyethyl head groups and sodium salicylate and 3 hydroxy-2-naphthoate counter-ions). Also, quaternary ammonium amine acetates were compared with chlorides and with surfactants without inorganic anion (Habon-G, etc).

6.3 CORROSION TEST PROCEDURES

The metals tested in these corrosion experiments were AISI Type 304 stainless steel, SAE 1112 carbon steel (equivalent to API-5 Grade B and DIN 1626), copper, 90/10 copper/nickel and 60/40 copper/zinc. Samples were 6-inch long, 1/8-inch diameter rods. Immediately prior to testing, the samples were sanded with a very fine sand paper and degreased to expose a fresh surface. Heat shrink polyolefin tubing was used to expose a known surface area on the sample (teflon, known to be very inert in testing, could not be used as it could not be sealed against the capillary action of the solution between the metal surface and the inside of the tubing at the 110°C operating temperature).

Experiments on both iron-based metals were carried out in the same solutions as were the experiments with the three copper-based. Fresh solutions were used for each run to eliminate any galvanic effects.

The samples were inserted into the system shown schematically in Figure 6.3,

constructed entirely of stainless steel. The samples were electrically isolated from the system by the use of Conax fittings with teflon seals. The samples were inserted into the flow loop at the positions labelled test coupons in Figure 6.3. Not shown in the figure is the capability to insert three metal samples using the same type of fitting in the autoclave. Anodic polarization (pitting potential) tests were conducted in the autoclave, while linear polarization (corrosion rate) tests were conducted under flow conditions in the 1-inch diameter loop (mean velocity of approximately 3 m/s). Although the static and flow systems are connected, the valves separating the two systems were kept closed and the systems operated independently.

6.3.1 Pitting Corrosion Test

An important method for study of pitting corrosion is potentiostatic anodic polarization testing. This technique can be utilized to evaluate a metal's susceptibility to localized corrosion (pitting) in a certain environment [17].

Anodic polarization testing was conducted by applying a known potential (versus the inconel sheathed thermocouple) to the metal exposed to the desired environment in a step-wise manner (50 mV/3 min) and measuring the current required to maintain this potential difference, i_{app} , under static conditions. A potentiostat was utilized for this purpose (Figure 6.4). The results were then plotted semilogarithmically as potential vs current density (as shown in Figure 6.2). The current density was the current required to maintain the overvoltage per unit sample surface area.

Figure 6.2 illustrates typical anodic polarization results. General corrosion (defined as uniform surface attack) was evidenced by a straight line in these coordinates, often deviating from linearity as a result of concentration polarization.

Figure 6.2 also shows a typical anodic polarization curve for a material which became passive. With increasing potential, the material either remained passive or localized pitting occurred. The critical pitting potential, E_C , is illustrated as a sharp break in the curve and a dramatic increase in the anodic dissolution current.

It should be noted that pitting susceptibility does not necessarily imply pitting in service. The degree of susceptibility of a metal/environment combination, however, or the risk of pitting corrosion, may be ranked utilizing the results of the technique, i.e. the magnitude of the pitting potential. Generally, pitting potentials above 0.5 volt indicate a relatively low risk of pitting corrosion.

Pitting susceptibility was used as a screening technique before performing the longer (up to two weeks) corrosion rate tests. Tests on iron-based metals were more commonly made than experiments on the copper-based samples (which are much more expensive). Iron-based metals, especially carbon steel, are the most widely used metals in district heating systems [18].

The value of the pitting potential, E_C , is estimated to be reliable to within ± 0.10 Volt although a few anomalous results were observed. The reason for this fairly large

range is that the reference electrode was not a standard reference electrode, and its potential could also change with environment (although the potential was assumed to change very little).

In the case of uniform attack (general corrosion designated as GC), the required current decayed with time to a steady state value. During localized attack, however, the applied current increased over time, illustrating the autocatalytic nature of pitting [13].

6.3.2 Corrosion Rate Test

A second important corrosion measurement technique is linear polarization which was used to measure the actual corrosion rate of a metal. Corrosion testing by the weight loss method is generally a long, tedious affair, often giving unsatisfactory results [19]. The weight loss of the metal over an increment of time also does not give a true corrosion rate but rather, an average rate over the time interval [19]. Stern and Geary [20] have demonstrated, however, that an accurate determination of the instantaneous corrosion rate over extended periods of time can be achieved utilizing the method of linear polarization.

Again using a potentiostat, a 10 mV or smaller cathodic or anodic potential difference was applied to the sample and the current required to maintain this difference was measured. The steady state current density, i_{corr} , was then calculated from [13]:

$$i_{corr} = \frac{\beta_a \cdot \beta_c}{2.3(\Delta E/i_{app})(\beta_a + \beta_c)} \quad (1)$$

where i_{corr} is the required current per metal surface area under actual corrosion conditions, β_a and β_c are the anodic and cathodic Tafel slopes, respectively and i_{app} is the applied current required to maintain the voltage difference, ΔE (See Figure 6.5 insert).

Measurement of the anodic and cathodic Tafel slopes is complicated by many factors [19]. Fortunately, the slope of the linear polarization curve, $\Delta E/i_{app}$, is relatively insensitive to changes in β values as demonstrated from Equation (1) by Fontana and Greene [13]. Assuming anodic and cathodic β values of 0.12 Volt, which represents the average for all corrosion systems [13], Equation (1) reduces to:

$$i_{corr} = \frac{0.026 \cdot i_{app}}{\Delta E} \quad (2)$$

The instantaneous corrosion rate, usually expressed in mils (0.001 inch) per year (mpy) can then be calculated from the current density information. The corrosion rate, expressed as a penetration rate (assuming general corrosion, i.e., no localized attack) was calculated from Equation (2) based on Faraday's law [19]:

$$\text{Corrosion Penetration Rate} = K \frac{MW \cdot i_{\text{corr}}}{n \cdot \rho} \quad (3)$$

where K is a constant (0.129 for units of mpy), MW is the atomic weight of the metal, n is the valence of the metal and ρ is the metal density.

Utilizing this procedure, the steady state corrosion rate of a specific metal/environment combination was determined by periodic testing as illustrated in Figure 6.5. Typical tests required 5 to 14 days to come to steady state. The method of linear polarization and the assumptions outlined here gave individual corrosion rates reliable to about a factor of two [19].

6.3.3 Water Treatment

Water quality has a great effect on corrosion. It is therefore desirable to know the quality of the water involved before testing. Average daily properties of Columbus, Ohio tap water were obtained from the City of Columbus Water Division and are listed in Table 6.1. The pH is about 7.6.

Deionization was performed on cold tap water using a Barnstead Bantam system with a two bed anion/cation cartridge. The resultant (unadjusted) pH was 6.5. Deoxygenation was carried out in a Barnstead system with an oxygen removal cartridge. The resultant (unadjusted) pH was 6.0. pH adjustments were made by addition of sodium hydroxide.

Baseline anodic polarization (pitting corrosion susceptibility) tests in tap water and in treated waters were performed. Temperature and pH were varied over a range corresponding to typical district heating and cooling systems. Particular emphasis was placed on the temperatures 60 and 110°C, which are the usual limits encountered in district heating systems.

Measurements were also made at 25°C, the lowest temperature we could achieve, to approach conditions at the Minneapolis District Cooling System where a field test may be carried out. The water in that system has lower concentrations of contaminants than found in the Columbus water so those tests were carried out with a 50% tap water-50% deionized water mixture.

6.3.4 Surfactants

A number of quaternary ammonium salt surfactants were tested. They fell into two

broad groups, the Habon-G and Dobon-G surfactants produced by Hoechst (saturated C₁₆ or C₂₂ dimethyl hydroxyethyl 3-hydroxy-2-naphthoates) and quaternary ammonium chlorides or acetates (saturated and unsaturated) C₁₆ or C₂₂ trimethyl, methyl bis hydroxyethyl or tris hydroxyethyl ammonium chlorides or acetates produced by Akzo or Humko) plus excess sodium salicylate. Earlier results for Habon and Dobon are also reported for comparison. The chemical structures of the surfactants tested are given in Table 6.2.

6.3.5 Corrosion Inhibitors

In many applications in the United States, Canada and Europe, corrosion inhibitors are added to untreated, municipal water instead of treating it. Consequently a number of high temperature corrosion inhibitors were tested with surfactants for pitting potential and corrosion rate. In many cases (for which data are not shown), inhibitors were found to be incompatible with surfactants causing precipitation. Generally inhibitors containing molybdate, molybdate/nitrite or borate/nitrite/nitrate plus organic material were not compatible with these surfactants. A few compatible corrosion inhibitors tested are listed in Table 6.3. Also listed is a biocide (Nalco 2593) recommended by Nalco for use in district cooling systems.

In a few cases where promising surfactant-corrosion inhibitors systems were found, drag reduction measurements were made to determine if the corrosion inhibitor had any effect on drag reducing effectiveness. In some cases drag reducing effectiveness was reduced at the manufacturer's recommended concentration but the reduction was smaller at reduced inhibitor concentration.

A formulation for use in the Minneapolis District Cooling System was developed. This system uses untreated water with Nalco-2819 corrosion inhibitor and Nalco 2593 biocide. This inhibitor was found to cause precipitation of quaternary ammonium amine surfactants. Nalco modified the formulation which is designated Nalco-2819(mod) and is more compatible with the surfactants. They also supplied an experimental corrosion inhibitor Nalco 7375RM which showed excellent compatibility. Tests were run in a 50% tap-50% deionized water solution which simulated the water in the Minneapolis system. Our system did not permit corrosion testing at low (5-15°C) temperatures so all corrosion tests on these systems were carried out at 25°C (Tables 6.5.3 and 6.7.1) which gave results on the safe side (conservative).

6.4 RESULTS AND DISCUSSION

6.4.1 Baseline Tests of Pitting Potential with Various Water Treatments, pH levels and Temperatures

The results of baseline tests of pitting potentials for tap water, deionized water, deoxygenated water and deionized/deoxygenated water are shown in Tables 6.4.1-6.4.4.

Since iron-based metals, especially carbon steel, are the most widely used metals in

district heating systems (18), emphasis in testing was placed on the iron-based metals. The carbon steel-water system showed no susceptibility to pitting under any of the water treatment, pH or temperature conditions tested.

6.4.1.1. Tap Water

Stainless steel showed no susceptibility at 25°C at pH = 7.0 to 10.6 (Table 6.4.1) in tap water or a mixture of tap and deionized water. At 50°C and above, stainless steel showed some susceptibility to pitting corrosion in tap water at higher pH values, for example 10.6 at 50°C, 9.9 at 60°C, 9.0 at 80°C, 7.5 at 85°C and 110°C but no susceptibility at lower pH values at 60°C and 80°C, ie 9.5 at 60°C and 7.5 at 80°C. It should be noted, however, that all the measured pitting potentials were greater than 0.50 volts indicating that susceptibility to pitting is quite low.

The tests with carbon steel in tap water showed general corrosion or no susceptibility to pitting at all temperatures and pH values.

Only a few runs were made with the copper-based metals. The results indicate that these metals are quite susceptible to pitting in tap water as their pitting potentials are low.

6.4.1.2. Deionized Water

The results for the deionized water measurements are given in Table 6.4.2. Only a few runs were made with carbon steel as no pitting problems are expected. For stainless steel, surprisingly, slightly lower pitting potentials were obtained at 60°C for deionized water than for tap water. At 110°C, however, no pitting potential (general corrosion) was observed at both low (6.5) and high pH (10.0 and 10.7). This improvement may be due to the reduction of oxygen content in the water at 110°C.

For copper-based metals, moderately high pitting potentials were obtained at pH = 9.0 at 60°C for copper and copper/nickel but a low value was obtained for copper/zinc. At 110°C and 7.5 pH, pitting potentials were relatively low for the copper-based metals. At 110°C and pH = 9.0, pitting potentials were higher for copper, copper/nickel and copper/zinc. For all three copper-based metals at 110°C and pH = 10.0, general corrosion was observed. Thus, for the copper-based metals temperature, pH and oxygen content all affect pitting susceptibility with higher temperature and accompanying reduced oxygen content and higher pH leading to lower pitting susceptibility.

6.4.1.3. Deoxygenated Water

In the few tests of pitting potential for deoxygenated (but not deionized) water, stainless steel showed general corrosion at pH = 10.4 at 60°C and 6.0 and 10.4 at 110°C (Table 6.4.3). Carbon steel tests were not run as general corrosion is expected in this system based on the results for untreated tap water.

6.4.1.4. Deionized/Deoxygenated Water

All tests run with deionized deoxygenated (DI/DO) water showed general corrosion (Table 6.4.4).

6.4.2 Pitting Potentials with Surfactants with Various Water Treatments

Pitting potentials for surfactant systems in tap water, tap water with corrosion inhibitors, 50% tap and 50% deionized water, deionized water and deionized and deoxygenated water are shown in Tables 6.5.1-5.

6.4.2.1. Surfactants in Tap Water

For carbon steel with tap water, general corrosion was observed in all cases tested (Table 6.4.1). At 60°C pitting potentials for carbon steel were lowered significantly for all quaternary ammonium salts with sodium salicylate, even for Ethoquad T/13-50 which contains no chloride ions, whereas Habon-G gave no deleterious effect at 60°C or 85°C (Table 6.5.1). On the other hand, for stainless steel in tap water at high pH levels, at which high pitting potentials were observed at 60°C, pitting susceptibility was reduced with Ethoquad T/13-50 plus NaSal as general corrosion was observed. That is, this surfactant had a deleterious effect on carbon steel but improved resistance somewhat for stainless steel.

At 110°C, both Ethoquad T/13-50 plus NaSal and Habon-G showed better resistance to pitting with stainless steel than tap water alone but significantly lowered pitting potentials with carbon steel.

6.4.2.2. Surfactants Plus Corrosion Inhibitors in Tap Water (60 and 110°C)

High temperature pitting potential measurements were carried out in tap water with Dearborn 519 and Betz Corrshield K7 with a variety of surfactants (Table 6.5.2). At 110°C, all stainless steel and carbon steel tests with these corrosion inhibitors and quaternary ammonium salts plus NaSal, Habon, Dobon and Dobon plus NaSal (except Kemamine EX-300 with stainless steel) showed general corrosion. This was true even when the Betz Corrshield K7 concentration was reduced to 1400 ppm, only a fourth of the manufacturer's recommendation. The chloride containing Arquad T-50 plus NaSal with 2800 ppm Betz Corrshield K7 showed the same susceptibility to pitting at 60°C and pH = 9.2 for both metals as without inhibitor (Table 6.5.1) but more susceptibility than with tap water alone especially for carbon steel. Pitting potentials with the copper-based metals consistently showed general corrosion or very high pitting potentials with Betz Corrshield K7 even at low concentrations of inhibitor, but lower values were obtained with Dearborn 519.

6.4.2.3. Surfactants and Corrosion Inhibitors in 50% Tap Water-50% Deionized Water at 25°C.

The experimental study for this system was not part of the current project. The results, however, may be of interest to potential users of surfactants in district cooling systems and so are included in this report (Table 6.5.3).

In preparation for a field test in a district cooling system, pitting potential measurements were carried out in a 50% tap water-50% deionized water system whose cation and anion contents were similar to those of the water in the district cooling system. The system uses 2000 ppm of a nitrite type corrosion inhibitor (Nalco N-2819) which also contains other proprietary additives. Ethoquad T/13-50 (which has an acetate anion) plus NaSal surfactant is effective as a drag reducer in the 5 to 15°C temperature range of interest [21]. Corrosion properties equivalent to those of the commercial working fluid were desired, but Nalco N-2819 was not compatible with the surfactant.

Nalco provided a modified form of this corrosion inhibitor, labelled Nalco-2819 (mod) which was more compatible. Nalco also provided a second experimental inhibitor, Nalco 7375 RM (nitrite/molybdate/phosphonate) which was even more compatible with the surfactant. It was tested for its effect on friction reduction and found to be satisfactory. In some tests Nalco 2593, a substituted isothiazolinone biocide, was also added. Since our corrosion testing loop had no chilling capabilities, it was fitted with tap water cooling coils and measurements were made at 25°C, which provided conservative results.

It should be noted that in a series of tests with commercial corrosion inhibitors containing molybdate, molybdate, molybdate/nitrate and borate/nitrite/nitrate plus organic components, quaternary ammonium salt surfactants were incompatible with these types of additives.

While the tap-deionized water mixture displayed general corrosion properties on carbon steel and stainless steel at 25°C (Table 6.4.1), the addition of Nalco N-2819 lowered the pitting potential for carbon steel to 0.25 volts (Table 5C). Nalco N-2819 (mod.) lowered the carbon steel value to 0 volts. The carbon steel value for the other experimental inhibitor, Nalco 7375RM, was 0.30 volts at 1200 ppm, the manufacturer's recommended concentration. All three raised the pitting potential values for the copper-based metals, with the Nalco N-2819 (mod.) giving the highest values. The addition of 40 ppm of the biocide (Nalco 2593) had no effect on the iron-based metals but in some cases lowered the copper and copper/zinc values for Nalco 7375RM slightly.

In general, pitting potentials with Ethoquad T/13-50 plus NaSal and Nalco N-2819 (mod.) were at least as high as with Nalco N-2819 and the water mixture (without surfactant) for all five metals. The same is true for Nalco 7375RM even at concentrations down to 600 ppm, which is half of Nalco's recommendation and which reduces the risk of compatibility problems. Results with Ethoquad O/12 which is also a good low temperature friction reducing additive were poor, probably because of the presence of chloride ion and this surfactant was not considered further.

Ethoquad T/13-50 plus NaSal with Nalco 7375RM was judged to be an appropriate

surfactant-corrosion inhibitor system for a district cooling system. Unfortunately because of environmental concerns, the field test has not yet been carried out.

6.4.2.4. Surfactants in Deionized Water

In deionized water at 60°C, Ethoquad T/13-50 plus NaSal and Habon-G showed improved resistance to pitting by stainless steel with no pitting potential observed (Table 6.5.4). For carbon steel at 60°C, general corrosion was observed with addition of these two surfactants (Table 6.5.4) as in deionized water alone (Table 6.4.2).

No pitting susceptibility for both iron-based metals was also observed at 110°C for Ethoquad T/13-50 plus NaSal and for Habon-G. At 110°C in stainless steel both Arquad R-50 (which contains chloride) at pH = 10 and Ethoquad R/12-75 (which also contains chloride) at pH = 9 showed pitting susceptibility. With carbon steel at 110°C, the latter showed high susceptibility while the former gave general corrosion.

In tests on copper-based metals at 60°C, Habon-G showed improved pitting susceptibility results (Table 6.5.4) compared with deionized water alone (Table 6.4.2).

At 110°C, Ethoquad T/13-50 plus NaSal and Habon-G in deionized water showed slightly improved or the same (general corrosion) pitting results for the copper-based metals as for deionized water alone. Arquad R-50 plus NaSal showed greater pitting susceptibility with copper/zinc at this temperature while Ethoquad R/12-75 plus NaSal showed greater pitting susceptibility with copper/nickel and copper/zinc.

6.4.2.5. Deionized and Deoxygenated Water

Ethoquad 18/13-50 plus NaSal, Ethoquad R-13 plus NaSal, Habon G, Dobon-G plus NaSal and Dobon (all of which have no chloride ion) all gave general corrosion on both carbon steel and stainless steel (Table 6.5.5). Arquad 18-50 plus NaSal and Ethoquad 18/12 plus NaSal at 80°C and Kemamine EX-300 plus NaSal and Kemamine Q2983C plus NaSal, at 110°C, all of which contain chloride ion, gave pitting potential values of 0.4 to 0.5 volts for stainless steel.

Copper, copper/nickel and copper/zinc all gave general corrosion with all the surfactants tested at 80°C and 110°C .

6.4.3. Baseline Tests of Corrosion Rates with Various Water Treatments, pH Levels and Temperatures

The results of baseline tests of corrosion rates for tap water, deionized water, deoxygenated water and deionized/deoxygenated water are shown in Tables 6.6.1-4.

Again, the emphasis was on measurements on the iron-based metals. Corrosion rates below 0.5 mpy are generally considered moderate, below 0.1 mpy are good and below 0.01 mpy are excellent. Since corrosion rate tests are lengthy (5 to 14 days),

in some cases tests were terminated when rates fell to low values even when still lower equilibrium corrosion rates could be attained. The measurements are inherently accurate only within a factor of about two because of uncertainties in the Tafel constants. Thus, only implications from broad trends in the data should be considered valid.

6.4.3.1. Tap Water

Corrosion rates for stainless steel are low at all temperatures (Table 6.6.1). The rates at 110°C were as expected, higher than at 60°C. No pH effects can be seen within the uncertainty of the measurements. Those in carbon steel are moderately high at 60°C and high at 110°C. Moderate rates were observed with copper and copper/zinc at 110°C while copper/nickel gave a high reading. At 25°C, the copper-based metals all had low corrosion rates.

6.4.3.2. Deionized Water

Again corrosion rates for stainless steel are low at 60°C and 110°C (Table 6.6.2). For carbon steel at 60°C, they are also low but they are significantly higher at 110°C.

6.4.3.3. Deoxygenated Water

Stainless steel showed low corrosion rates while carbon steel had fairly high rates (Table 6.6.3).

6.4.3.4. Deionized and Deoxygenated Water

Stainless steel corrosion rates were low while carbon steel rates at low pH are relatively high (Table 6.6.4). At pH near 10, corrosion rates for carbon steel are satisfactory.

At 110°C and pH = 6.0, corrosion rates for copper-based metals are moderate.

6.4.4. Corrosion Rates with Surfactants (and Corrosion Inhibitors) with Various Water Treatments

6.4.4.1. Corrosion Rates with 50% Tap and 50% Deionized Water at 25°C.

All corrosion rate measurements at 25°C with Ethoquad T/13-50 plus NaSal and Nalco 7375RM, Nalco N-2819 and Betz 66P (Table 6.7.1) were very low even at concentrations half of the manufacturer's recommendation (600 ppm 7375RM). The presence of the biocide (Nalco 2593) had no measurable effect. Corrosion rates of the copper based metals were also low with the exception of copper/nickel with the Ethoquad T/13-50 plus NaSal and Nalco-2819 where a moderate but acceptable rate was observed.

6.4.4.2. High Temperature Corrosion Rates in Tap Water with Surfactants and Corrosion Inhibitors

Corrosion rate tests at 60°C for stainless steel in tap water plus surfactants showed low corrosion rates (Table 6.7.7). The addition of Betz Corrshield K7 to Ethoquad T/13-50 plus NaSal did not reduce the already low corrosion rate of stainless steel and may, in fact, have increased it. For carbon steel at 60°C, the addition of Ethoquad T/13-50, with or without Betz Corrshield K7 reduced the corrosion rate at 60°C compared with tap water alone. For Arquad T-50 plus NaSal and for Habon-G at 60°C, the corrosion rates for carbon steel were not changed by the presence of the surfactant.

Only two tests were made at 60°C with copper-based metals. For Ethoquad T/13-50 plus NaSal corrosion rates were high for all copper-based metals. With the addition of 1400 ppm Betz Corrshield K7 to this system, corrosion rates were high for copper/zinc and moderate for copper/nickel and copper.

The corrosion rates for surfactants with and without corrosion inhibitor for stainless steel at 110°C are generally higher than at 60°C but are all quite low. The Dearborn 519 corrosion inhibitor at 110°C does not affect corrosion rates for carbon steel in tap water either alone or in the presence of Kemamine EX-300 plus NaSal, Kemamine Q2983C plus NaSal, or Dobon. Ethoquad T/13-50 plus NaSal with Betz Corrshield K7 gives reduced corrosion rates for carbon steel even at one fourth of the recommended concentration of the inhibitor (1400 ppm). Habon-G at 110°C provides some improvement in the carbon steel corrosion rate.

The Dearborn 519 inhibitor, on the other hand, gives considerably reduced corrosion rates for copper and copper/zinc and some reduction for copper/zinc.

6.4.4.3. High Temperature Corrosion Rates in Deionized Water with Surfactants.

Corrosion rates for stainless steel at 60°C in deionized water are very low and are not greatly changed by the presence of Ethoquad T/13-50 plus NaSal or of Arquad R-50 (Table 6.7.3). For carbon steel at 60°C, corrosion rates for deionized water are also low and not greatly changed by Ethoquad T/13-50 plus NaSal. For Arquad R-50 plus NaSal, however, corrosion rates of carbon steel at 60°C are adversely affected and they are high.

Corrosion rates for stainless steel in deionized water at 110°C are also low. The addition of Ethoquad T/13-50 plus NaSal at 110°C causes an increase in corrosion rates but they are at an acceptable level. This is also true of Ethoquad R/12-75 plus NaSal and of Ethoquad R/13 plus NaSal and of Arquad R-50 plus NaSal. The results for Habon-G on stainless steel are also quite low.

Thus, it appears that all of these surfactants at all pH levels tested will give acceptable to very low corrosion rates on stainless steel in deionized water.

For carbon steel at 60°C, no increase and possibly reduced rates are observed with

the tris hydroxyethyl head group and acetate anion (Ethoquad T/13-50). On the other hand Arquad R-50 with a head group containing trimethyl and a chloride anion gives greatly increased, unacceptably high corrosion rates.

At 110°C, the carbon steel results are even more revealing. The addition of Ethoquad T/13-50, or Ethoquad R/13 which have tris hydroxyethyl head groups and acetate anion gave moderate corrosion rates as did Habon-G. The addition of a bis hydroxyethyl methyl head group with chloride ion (Arquad R/12-75) increased the corrosion rate by about an order of magnitude. Arquad R-50 which has a trimethyl head group and chloride anion caused still another increase of an order of magnitude in the corrosion rate.

6.4.4.4. High Temperature Corrosion Rates in Deionized/Deoxygenated Water with Surfactants.

At 60°C the corrosion rates of stainless steel and carbon steel are unaffected by the addition of Ethoquad T/13-50 plus NaSal. The carbon steel rates with or without surfactant are higher than expected, however (Table 6.7.4).

At 110°C corrosion rates for stainless steel are somewhat higher than for water alone when Kemamine EX-300 plus NaSal, Kemamine Q2983C plus NaSal or Arquad R-50 plus NaSal are added. For Dobon and Dobon-G plus NaSal they are also higher while for Habon-G they are very low.

Carbon steel corrosion rates at 110°C appear to be unchanged by addition of Kemamine EX-300 plus NaSal, Dobon and Dobon-G plus NaSal. For Habon-G corrosion rates are lower than for the deionized/deoxygenated water alone. Kemamine Q2983C (trimethyl head group and chloride anion) gave high corrosion rates with carbon steel. Arquad R-50 plus NaSal which has a similar chemical structure to Q2983C and generally gave high corrosion rates in other water environments gave a very high rate with this water treatment.

Corrosion rates for the copper-based metals were generally moderate. The two exceptions were for copper/zinc at 110°C with Kemamine EX-300 plus NaSal and Kemamine Q2983C plus NaSal.

6.5 CONCLUSIONS

6.5.1. Pitting Susceptibility

6.5.1.1. Pitting Potentials in Tap Water

- a) In tap water carbon steel shows no pitting susceptibility at temperatures ranging from 25 to 110°C and pH levels ranging from 7.0 to 10.8.
- b) In tap water stainless steel shows a slight susceptibility to pitting at high pH

values, the pH value at which susceptibility begins decreases somewhat with increase in temperature.

- c) Copper-based metals show high pitting susceptibility in tap water.
- d) In tap water, the pitting susceptibility of stainless steel is improved by the addition of Ethoquad T/13-50 (which contains an acetate anion) and NaSal and of Habon-G. It is adversely affected by the addition of Arquad T-50 (which contains a chloride anion) plus NaSal.
- e) In tap water, pitting susceptibility of carbon steel is greatly increased by the addition of Ethoquad T/13-50 plus NaSal and of Arquad T-50 plus NaSal. At 60°C and 85°C, Habon-G has no deleterious effect but at 110°C it too causes increased pitting susceptibility of carbon steel. Since its recommended temperature range is up to 100°C, pitting potential measurements at this temperature should be made.
- f) Several corrosion inhibitors were found to be compatible with cationic surfactants and the combinations generally had no adverse effect on high temperature pitting susceptibility of stainless steel in tap water and improved the susceptibility of carbon steel if no chloride ions were present. Results at 110°C with Habon or Dobon plus Dearborn 519 on carbon steel were improved over Habon-G results with no corrosion inhibitor at that temperature.
- g) High temperature pitting susceptibility of copper-based metals in tap water was reduced when corrosion inhibitors were added to the surfactant in tap water compared with tap water with no additives present.

6.5.1.2. Pitting Potentials in Deionized Water

- a) In deionized water at 60°C, stainless steel shows some pitting susceptibility at pH above 9.0 but none at 110°C where the oxygen content of the water is lower.
- b) In deionized water, carbon steel shows no pitting susceptibility at 60 and 110°C.
- c) Copper-based metals generally have reduced susceptibility to pitting in deionized water compared to tap water. Susceptibility appears to be reduced at high pH.
- d) At 60°C the presence of Ethoquad T/13-50 plus NaSal and Habon-G in deionized water improved the pitting susceptibility of stainless steel. They had no deleterious effect on carbon steel (general corrosion) at 60°C or at 110°C. Ethoquad T/13-50 plus NaSal and Habon-G reduced the susceptibility of copper-based metals at 60°C and 110°C compared with deionized water alone. In fact, no pitting susceptibility in deionized water was observed for any metal at either temperature with either surfactant present.

6.5.1.3. Pitting Potentials in Deoxygenated Water

- a) In deoxygenated (not deionized) water stainless steel showed no pitting susceptibility. Carbon steel was not tested but is expected to give the same result.

6.5.1.4. Pitting Potentials in Deionized/Deoxygenated Water

- a) In deionized/deoxygenated water, stainless steel, carbon steel and copper-based metals show no pitting susceptibility.
- b) In deionized/deoxygenated water, surfactants with no chloride ion caused no pitting susceptibility for stainless or carbon steel. All surfactants caused no pitting susceptibility of copper-based metals in this water environment.

6.5.1.5. Pitting Potentials in 50% Tap-50% Deionized Water at 25°C

- a) In a mixture of 50% tap water and 50% deionized water at 25°C, a low temperature drag reducing surfactant (Ethoquad T/13-50 plus NaSal) compatible with a nitrite/molybdate/phosphonate corrosion inhibitor (Nalco 7375 RM) showed good drag reducing capabilities and equivalent or reduced pitting susceptibility compared with the commercial nitrite inhibitor Nalco N-2819 now in use in the Minneapolis District Cooling System. This surfactant-corrosion inhibitor combination is recommended for field testing in a district cooling system.

6.5.2. Corrosion Rates

6.5.2.1. Corrosion Rates in Tap Water

- a) In corrosion rate tests in tap water, rates were very low for stainless steel at 60 and 110°C. For carbon steel, rates were moderate at 60°C but high at 110°C and also for copper/nickel at 110°. No strong trends with pH were observed. At 25°C corrosion rates in 50% tap-50% deionized water were low for stainless steel and moderate for carbon steel.
- b) In corrosion rate tests in tap water at 60°C, Ethoquad T/13-50 plus NaSal caused rates to decrease from moderate to low for carbon steel. Arquad T-50 plus NaSal and Habon-G at 60°C had no effect on the moderate corrosion rates observed in tap water for carbon steel. At 110°C, Ethoquad T/13-50 plus NaSal and Habon-G lowered the high corrosion rates for carbon steel to moderate.
- c) The Dearborn 519 corrosion inhibitor caused no reduction in carbon steel's corrosion rates at 110°C either alone or in combination with surfactants but it is effective in reducing corrosion rates in combination with Dobon, Kemamine EX-300 plus NaSal and Kemamine Q2983C plus NaSal for copper and copper/nickel. Betz Corrrshield K7 reduced corrosion rates of carbon steel at

60°C and 110°C for all surfactants tested.

6.5.2.2. Corrosion Rates in Deionized Water

- a) In deionized water, corrosion rates for stainless steel were also very low. Carbon steel rates ranged from very low to moderate. At 60°C there is a trend to lower rates with increase in pH. Rates at 110°C are higher for carbon steel than at 60°C.
- b) In corrosion rate tests in deionized water at 60°C, stainless steel rates remained very low when Ethoquad T/13-50 plus NaSal or Arquad R-50 plus NaSal were added. Rates with the former for carbon steel remained moderate. The latter, however, caused corrosion rates of carbon steel to increase to an unacceptably high level. Corrosion rates at 110°C for stainless steel increased somewhat on the addition of Ethoquad T/13-50 plus NaSal but are still low. They are also low in the presence of Habon-G. For carbon steel at 110°C, Ethoquad T/13-50 plus NaSal and Habon-G gave moderate corrosion rates as did Ethoquad R/13 plus NaSal. Ethoquad R/12-75 plus NaSal gave high corrosion rates at 110°C and Arquad R-50 plus NaSal gave extremely high rates. There is some evidence that the presence of three or even two hydroxyethyl groups on the surfactant head group lowers corrosion rates for carbon steel compared with alkyl trimethyl ammonium surfactants.

6.5.2.3. Corrosion Rates in Deoxygenated Water

- a) In deoxygenated water, corrosion rates for stainless steel were low while for carbon steel they were relatively high.

6.5.2.4. Corrosion Rates in Deionized/Deoxygenated Water

- a) In deionized/deoxygenated water, corrosion rates for stainless steel were very low while for carbon steel and copper-based metals they were moderate.
- b) In deionized/deoxygenated water with a variety of surfactants, very low to moderate corrosion rates were observed for stainless steel. For carbon steel, moderate rates were generally observed with or without surfactant except in two cases. Kemamine Q2983C plus NaSal at 110°C caused the carbon steel corrosion rate to become excessive and Arquad R-50 plus NaSal was worse. For copper and copper/nickel at 110°C, corrosion rates were moderate for Ethoquad T/13-50 plus NaSal, Kemamine Q2983 plus NaSal, Kemamine EX-300 plus NaSal and Dobon. For copper/zinc, however, Kemamine Q2983 plus NaSal and Kemamine EX-300 plus NaSal, the chloride-containing surfactants, caused excessive corrosion.

6.5.2.5. Corrosion Rates in 50% Tap-50% Deionized Water

- a) In a 50% tap-50% deionized water mixture similar to that used in the Minneapolis District Cooling System, a compatible mixture of Ethoquad T/13-50

plus NaSal and Nalco 7375 RM corrosion inhibitor gave very low corrosion rates at 25°C for stainless steel, carbon steel and in all copper-based metal tests.

Table 6.1

Average Columbus Tap Water Analysis

Source	Value
Alkalinity, Phenol	0.0 mg/l
Alkalinity, Total	36 mg/l
Anion, Total	2.88 meq/l
Calcium	27 mg/l
Cation, Total	3.13 meq/l
Chloride	23 mg/l
Chlorine, Free	1.7 mg/l
Conductivity	280 μ mho/cm
Fluoride	0.9 mg/l
Hardness, Noncarbonate	73 mg/l
Hardness, Total	108 mg/l
Magnesium	10 mg/l
Nitrate	1.5 mg/l
Phosphate, Total	0.34 mg/l
pH	7.6
Silica	2 mg/l
Sodium	9 mg/l
Solids, Total	133 mg/l
Sulfate	58 mg/l
Trihalomethane	55 μ g/l
Turbidity	0.21 mg/l
Zinc Orthophosphate	490 μ g/l

Table 6.2

Sources and Formulae of Surfactants

<u>Surfactant Name</u>	<u>Supplier</u>	<u>Chemical Formula</u>
Kemamine EX-300	Witco	$C_{22}H_{43}-N-(C_2H_4OH)_2CH_3Cl$
Kemamine Q2983C	Witco	$C_{22}H_{43}-N-(CH_3)_3Cl$
Kemamine Q2803C	Witco	$C_{22}H_{45}-N-(CH_3)_3Cl$
Arquad R-50	Akzo	Rapeseed- $N-(CH_3)_3Cl$
Ethoquad R-13	Akzo	Rapeseed- $N-(C_2H_4OH)_3Ac$
Ethoquad R/12-75	Akzo	Rapeseed- $N-(C_2H_4OH)_2(CH_3)Cl$
Ethoquad T/13-50	Akzo	Tallow- $N-(C_2H_4OH)_3Ac$
Ethoquad 18/13-50	Akzo	$C_{18}H_{37}-N-(C_2H_4OH)_3Ac$
Ethoquad 18/12	Akzo	$C_{18}H_{37}-N-(C_2H_4OH)_2(CH_3)Cl$
Ethoquad 0/12	Akzo	$C_{18}H_{35}-N-(C_2H_4OH)_2(CH_3)Cl$
Arquad T-50	Akzo	Tallow- $N-(CH_3)_3Cl$
Arquad 18-50	Akzo	$C_{18}H_{37}-N-(CH_3)_3Cl$
Habon	Hoechst	$C_{16}H_{33}-N-(CH_3)_3-(3-OH-2-naphthoate)$
Habon-G	Hoechst	$C_{16}H_{33}-N-(C_2H_4OH)(CH_3)_2-(3-OH-2-naphthoate)$
Dobon	Hoechst	$C_{22}H_{45}-N(CH_3)_3-(3-OH-2-naphthoate)$
Dobon-G	Hoechst	$C_{22}H_{45}-N-(C_2H_4OH)(CH_3)_2-(3-OH-2-naphthoate)$

Table 6.3

Sources and Types of Corrosion Inhibitors

NAME	Chemical Type	Manufacturers Recommended Concentration, ppm*
Dearborn 545	Molybdate/Amine (sodium molybdate/morpholine)	3500
Dearborn BW1500	Organic/passivator/amine (morpholine)	400
Dearborn 547	Nitrate/Nitrite (sodium nitrate/sodium nitrite)	12370 (1% by volume)
Dearborn 519	Hydrazine/amine (hydrazine/morpholine)	400
Betz Corrshield K7	Nitrite/Borate/Silicate	5600
Betz 66P	Nitrite	1500
Nalco N-2819	Nitrite	2000
Nalco N-2819 (mod)	Nitrite	2000
Nalco 7375RM	Nitrite/Molybdate/Phosphonate	1200
Nalco 2593 (Biocide)	Substituted Isothiazolinone	40

*Concentration of inhibitor as received, not of active ingredients.

Table 6.4.1

Pitting Potential Tests in Tap Water

	Temp, °C	pH	Pitting Potential in Volts*				
			Stainless Steel	Carbon Steel	Copper	Copper/ Nickel	Cu/ Zn
**TAP/DI	25	7.0	GC	GC	0.05	0.10	-0.10
	25	7.5	GC	GC	0.10	-0.05	-.10
	25	10.6	GC	GC	0.15	0.05	.05
**TAP/DI	25	10.6	GC	GC			
	50	10.6	0.65	GC			
	60	7.5	GC	GC			
	60	9.2	GC	--			
	60	9.5	GC	--			
	60	9.9	0.60	GC			
	60	10.6	0.65	GC			
	80	7.5	GC	GC			
	80	9.0	0.60	--			
	80	10.6	0.65	GC	.15	.15	.30
	85	7.5	0.70	--			
	85	7.5	0.60	GC			
	110	7.5	0.55	GC			
	110	7.5	0.60	GC			
	110	10.6	0.70	GC			
	110	10.8	0.75	GC			

* GC is general corrosion with no pitting potential observed.

** TAP/DI is 50% tap and 50% deionized water. All other runs are tap water.

Table 6.4.2

Pitting Potential Tests in Deionized Water

Temp, °C	pH	Pitting Potential in Volts*				
		Stainless Steel	Carbon Steel	Copper	Copper/Nickel	Copper/Zinc
60	6.5	GC	--			
60	9.0	GC	GC	0.45	0.45	0.15
60	9.6	0.50	--			
60	10.4	0.55	--			
110	6.5	GC	--			
110	7.5	--	--	0.25	0.30	0.15
110	9.0	GC	GC	0.45	0.55	0.50
110	10.0	GC	GC	GC	GC	GC
110	10.7	GC	GC			

* GC is general corrosion with no pitting potential observed.

Table 6.4.3

Pitting Potential Tests in Deoxygenated Water

Temp, °C	pH	Pitting Potential in Volts*				
		Stainless Steel	Carbon Steel	Copper	Copper/Nickel	Copper/Zinc
60	10.4	GC	--			
110	6.0	GC	--			
110	10.4	GC	--			

* GC is general corrosion with no pitting potential observed.

Table 6.4.4

Pitting Potential Tests in Deionized/Deoxygenated Water

Temp, °C	pH	Pitting Potential in Volts*				
		Stainless Steel	Carbon Steel	Copper	Copper/Nickel	Copper/Zinc
60	10.7	GC	--	--	--	--
80	10.4	GC	GC	GC	GC	GC
110	6.0	GC	GC	GC	GC	GC
110	10.7	GC	GC			

* GC is general corrosion with no pitting potential observed.

Table 6.5.1

Pitting Potential Tests in Tap Water with Surfactants

Surfactant	Conc. ppm	Temp. °C	pH	Pitting Potentials in Volts*	
				Stainless Steel	Carbon Steel Copper/Nickel Zinc
Ethoquad T/13-50 NaSal	1702 1500	60	7.5	--	0.20
Ethoquad T/13-50 NaSal	1702 1500	60	8.5	--	0.20
Ethoquad T/13-50 NaSal	1702 1500	60	9.2	GC	0.20
Ethoquad T/13-50 NaSal	1702 1500	60	10.6	GC	0.15
Ethoquad T/13-50 NaSal	1702 1500	60	10.6	GC	0.10
Arquad T-50 NaSal	1275 1500	60	9.2	0.55	0.05
Habon-G	500	60	7.5	GC	GC
Habon-G	500	60	9.0	GC	GC
Habon-G	500	85	7.5	GC	GC
Habon-G	500	85	9.0	GC	GC
Ethoquad T/13-50 NaSal	1702 1500	110	9.0	GC	0.30
Ethoquad T/13-50 NaSal	1702 1500	110	9.2	GC	0.30

*GC = general corrosion

Table 6.5.1 (cont.)

Pitting Potential Tests in Tap Water with Surfactants

Surfactant	Conc. ppm	Temp. °C	pH	Pitting Potentials in Volts*	
				Stainless Steel	Carbon Steel Copper Copper/ Nickel Zinc
EthoquadT/13-50 NaSal	1702 1500	110	10.0	GC	0.40
EthoquadT/13-50 NaSal	1702 1500	110	10.6	--	0.40
EthoquadT/13-50 NaSal	1702 1500	110	10.6	GC	0.50
Habon-G	500	110	9.0	GC	0.45
Habon-G	500	110	10.0	GC	0.50

* GC = general corrosion

Table 6.5.2

High Temperature Pitting Potentials in Tap Water
with Surfactants and Corrosion Inhibitors

Surfactant/ Corrosion Inhibitor	Conc. ppm	Temp. °C	pH	Pitting Potentials in Volts*				
				Stainless Steel	Carbon Steel	Copper Copper	Copper/ Nickel	Copper/ Zinc
EthoquadT/13-50 NaSal Betz Corrrshield K7	1702 1500 5600	60	10.7	GC	GC	----	----	----
EthoquadT/13-50 NaSal Betz Corrrshield K7	1702 1500 1400	60	9.7	----	--	0.60	0.80	0.75
Arquad T-50 NaSal Betz Corrrshield K7	1275 2000 2800	60	9.2	0.55	0.05			
Dearborn 519	400	110	9.3	GC	GC	0.35	0.60	0.50
Kemanine EX-300 NaSal Dearborn 519	2306 2000 400	110	8.9	0.55	GC	0.40	0.35	0.30
Kemanine Q2983 C NaSal Dearborn 519	2000 2000 400	110	8.9	GC	GC	0.25	0.35	0.10
Kemanine Q2803 C NaSal Dearborn 519	2000 2000 400	110	8.7	GC	GC	----	----	----
Dobon Dearborn 519	1500 400	110	8.2	GC	GC	0.45	0.45	0.45

*GC = general corrosion

Table 6.5.2 (cont)

High Temperature Pitting Potentials in Tap Water
with Surfactants and Corrosion Inhibitors

Surfactant/ Corrosion Inhibitor	Conc. ppm	Temp. °C	pH	Pitting Potentials in Volts*				
				Stainless Steel	Carbon Steel	Copper Copper	Copper/ Nickel	Copper/ Zinc
Dobon NaSal Dearborn 519	1500 1500 400	110	8.1	GC	GC	----	----	----
Habon Dearborn 519	500 400	110	8.4	GC	GC	----	----	----
EthoquadT/13-50 NaSal Betz Corrshield K7	1702 1500 5600	110	10.7	GC	GC	GC	GC	GC
EthoquadT/13-50 NaSal Betz Corrshield K7	1702 1500 2800	110	10.3	GC	GC	GC	GC	GC
EthoquadT/13-50 NaSal Betz Corrshield K7	1702 1500 1400	110	9.7	GC	GC	0.50	GC	GC

* GC = general corrosion

Table 6.5.3

Low Temperature Pitting Potentials in a Mixture of 50% Tap and 50%
Deionized Water with Surfactants and Corrosion Inhibitors

Surfactant/ Corrosion Inhibitor	Conc. ppm	Temp. °C	pH	Pitting Potentials in Volts*				
				Stainless Steel	Carbon Steel	Copper/ Copper	Copper/ Nickel	Copper/ Zinc
Nalco N-2819	2000	25	10.5	GC	0.25	0.25	0.45	0.25
Nalco N-2819(mod)	2000	25	10.5	GC	0.0	0.40	0.45	0.40
Nalco 7375RM	1200	25	9.7	GC	0.30	0.30	0.25	0.10
Nalco 7375RM	900	25	9.5	GC	0.25	----	----	----
Nalco 7375RM	600	25	9.3	GC	0.25	----	----	----
Nalco 7375RM	300	25	8.9	GC	0.20	----	----	----
Nalco 7375RM Nalco 2593	1200 40	25	9.3	GC	0.30	0.15	0.30	0.05
Nalco 7375RM Nalco 2593	600 40	25	8.6	GC	0.30	----	----	----
Ethoquad 0/12 NaSal Nalco N-2819(mod)	1500 900 2000	25	10.2	0.35	0.05	0.30	0.40	0.35
EthoquadT/13-50 NaSal Nalco N-2819(mod)	1702 900 2000	25	10.0	GC	0.50	0.35	0.40	0.35
Ethoquad 0/12 NaSal Nalco 7375RM	1500 900 1200	25	9.9	0.45	0.15	0.30	0.25	0.20

*GC = general corrosion

Table 6.5.3 (cont)

Low Temperature Pitting Potentials in a Mixture of 50% Tap and 50%
Deionized Water with Surfactants and Corrosion Inhibitors

Surfactant/ Corrosion Inhibitor	Conc. ppm	Temp. °C	pH	Pitting Potentials in Volts*				
				Stainless Steel	Carbon Steel	Copper Copper	Copper/ Nickel	Copper/ Zinc
EthoquadT/13-50 NaSal Nalco N-7375RM	1702 900 1200	25	9.0	GC	0.45	0.30	0.45	0.25
EthoquadT/13-50 NaSal Nalco N-7375RM	1702 900 900	25	8.7	GC	0.25	----	----	----
EthoquadT/13-50 NaSal Nalco N-7375RM	1702 900 600	25	8.3	GC	0.25	----	----	----
EthoquadT/13-50 NaSal Nalco N-7375RM	1702 900 300	25	8.0	GC	0.20	----	----	----
EthoquadT/13-50 NaSal Nalco N-7375RM Nalco 2593	1702 900 1200 40	25	8.7	GC	0.30	0.30	0.50	0.20
EthoquadT/13-50 NaSal Nalco N-7375RM Nalco 2593	1702 900 600 40	25	8.4	GC	0.30	----	----	----
EthoquadT/13-50 NaSal Betz 66P	1702 900 600	25	9.2	GC	0.30	0.15	0.65	0.10

* GC = general corrosion

Table 6.5.4

Pitting Potential in Deionized Water with Surfactants

Surfactant	Conc. ppm	Temp. °C	pH	Pitting Potentials in Volts*				
				Stainless Steel	Carbon Steel	Copper/ Copper	Copper/ Nickel	Zinc
EthoquadT/13-50 NaSal	1702 1500	60	7.0	GC	GC			
EthoquadT/13-50 NaSal	1702 1500	60	8.5	GC	GC			
EthoquadT/13-50 NaSal	1702 1500	60	9.0	GC	GC	GC	GC	GC
EthoquadT/13-50 NaSal	1702 1500	60	9.6	GC	GC			
EthoquadT/13-50 NaSal	1702 1500	60	10.4	GC	GC			
Habon-G	500	60	9.0	GC	GC	GC	GC	GC
EthoquadT/13-50 NaSal	1702 1500	110	9.0	GC	GC	GC	GC	GC
EthoquadT/13-50 NaSal	1702 1500	110	10.0	--	--	GC	GC	GC
EthoquadT/13-50 NaSal	1702 1500	110	10.4	GC	GC			
Arquad R-50 NaSal	1844 2000	110	10.0	0.35	GC	GC	0.70	0.10
EthoquadR/12-75 NaSal	2139 2000	110	9.0	0.30	0.05	0.45	0.35	0.10

Table 6.5.4 (cont)

Pitting Potential in Deionized Water with Surfactants

Surfactant	Conc. ppm	Temp. °C	pH	Pitting Potentials in Volts*				
				Stainless Steel	Carbon Steel	Copper Copper	Copper/ Nickel	Copper/ Zinc
Habon-G	500	110	9.0	GC	GC	GC	GC	GC
Habon-G	500	110	10.0	--	--	GC	GC	GC

* GC = general corrosion

Table 6.5.5

Pitting Potentials in Deionized and Deoxygenated Water with Surfactants

Surfactant	Conc. ppm	Temp. °C	pH	Pitting Potentials in Volts*				
				Stainless Steel	Carbon Steel	Copper Copper	Copper/ Nickel	Copper/ Zinc
Arquad 18-50 NaSal	1738 2000	80	10.4	0.50	----	GC	GC	GC
Ethoquad 18/12 NaSal	2038 2000	80	10.4	0.40	----	GC	GC	GC
Ethoquad 18/13-50 NaSal	2305 2000	80	10.4	GC	GC	GC	GC	GC
Kemamine EX-300 NaSal	2306 2000	110	6.2	0.45	GC	GC	GC	GC
Kemamine Q2983 C NaSal	2000 2000	110	6.9	0.40	GC	GC	GC	GC
Ethoquad R-13 NaSal	2395 2000	110	10.7	GC	GC			
Habon-G	500	110	10.7	GC	GC			
Dobon-G NaSal	1500 700	110	10.7	GC	GC			
Dobon	1500	110	6.8	GC	GC	GC	GC	GC

* GC = general corrosion

Table 6.6.1

Corrosion Rate Tests in Tap Water

	Temp, °C	pH	Corrosion Rate in mpy				
			Stainless Steel	Carbon Steel	Copper	Copper/Nickel	Copper/Zinc
*TAP/DI	25		0.003	0.4	0.009	0.02	0.007
	60	7.5	0.002	0.6			
	60	9.2	0.007	0.7			
	60	10.6	0.003	0.2			
	110	7.5	0.02	2.5	0.4	1.1	0.3
	110	10.6	0.01	2.0			
	110	10.8	0.02	1.5			

* TAP/DI is 50% tap and 50% deionized water. All other runs are tap water.

Table 6.6.2

Corrosion Rate Tests in Deionized Water

Temp, °C	pH	Corrosion Rate in mpy			
		Stainless Steel	Carbon Steel	Copper/ Copper	Copper/ Nickel Zinc
60	6.5	0.01	0.09		
60	10.7	0.004	0.01		
110	6.5	0.01	0.3		
110	10.0	0.009	0.3		
110	10.7	0.002	0.2		

Table 6.6.3

Corrosion Rate Tests in Deoxygenated Water

Temp, °C	pH	Corrosion Rate in mpy			
		Stainless Steel	Carbon Steel	Copper/ Nickel	Copper/ Zinc
60	6.0	0.01	1.3		
110	10.4	0.06	0.7		

Table 6.6.4

Corrosion Rate Tests on Deionized and Deoxygenated Water

Temp, °C	pH	Corrosion Rate in mpy				
		Stainless Steel	Carbon Steel	Copper	Copper/Nickel	Copper/Zinc
60	6.0	0.004	0.7			
110	6.0	0.01	0.3	0.06	0.1	0.1
110	10.4	0.02	0.1			
110	10.7	<0.02	0.1			

Table 6.7.1

Low Temperature Corrosion Rate Tests in 50% Tap and 50% Deionized Water
with Surfactants and Corrosion Inhibitors Added

Surfactant/ Corrosion Inhibitor	Conc. ppm	Temp. °C	pH	Corrosion Rate in mpy				
				Stainless Steel	Carbon Steel	Copper/ Copper	Copper/ Nickel	Copper/ Zinc
100% Tap Water	----	25	7.5	0.003	0.4	0.009	0.02	0.007
Nalco N-2819	2000	25	10.4	0.002	0.002	0.007	0.02	0.009
Nalco 7375RM	1200	25	9.7	0.002	0.003	0.01	0.02	0.02
Nalco 7375RM	900	25	9.5	<0.002	<0.003			
Nalco 7375RM	600	25	9.3	<0.002	<0.004			
Nalco 7375RM	300	25	8.9	<0.002	<0.005			
Nalco 7375RM Nalco 2593	1200 40	25	9.3	<0.002	<0.006			
Nalco 7375RM Nalco 2593	600 40	25	8.6	<0.003	<0.005			
Ethoquad T/13-50 NaSal Nalco N-2819	1702 900 2000	25	10.1	0.002	0.004	0.01	0.2	0.04
Ethoquad T/13-50 NaSal Nalco 7375RM	1702 900 1200	25	9.0	<0.002	<0.004	<0.02	<0.07	<0.02
Ethoquad T/13-50 NaSal Nalco 7375RM Nalco 2593	1702 900 1200 40	25	8.7	<0.002	<0.005			

Table 6.7.1 (cont)

Low Temperature Corrosion Rate Tests in 50% Tap and 50% Deionized Water
with Surfactants and Corrosion Inhibitors Added

Surfactant/ Corrosion Inhibitor	Conc. ppm	Temp. °C	pH	Corrosion Rate in mpy				
				Stainless Steel	Carbon Steel	Copper/ Copper	Copper/ Nickel	Copper/ Zinc
Ethoquad T/13-50	1702	25	8.6	<0.002	<0.005	<0.01	<0.03	<0.02
NaSal	900							
Nalco 7375RM	900							
Nalco 2593	40							
Ethoquad T/13-50	1702	25	9.2	0.009	0.003			
NaSal	900							
Betz 66P	1500							

Table 6.7.2

High Temperature Corrosion Rate Tests in Tap Water
with Surfactants and Corrosion Inhibitors

Surfactant/ Corrosion Inhibitor	Conc. ppm	Temp. °C	pH	Corrosion Rate in mpy				
				Stainless Steel	Carbon Steel	Copper/ Copper	Copper/ Nickel	Copper/ Zinc
Tap Water		60	7.5	0.002	0.6			
Tap Water		60	9.2	0.007	0.7			
Tap Water		60	10.6	0.003	0.2			
Ethoquad T/13-50 NaSal	1702 900	60	8.8	<0.005	<0.06			
Ethoquad T/13-50 NaSal	1702 1500	60	8.3	0.004	0.01			
Ethoquad T/13-50 NaSal	1702 1500	60	9.0	---	----	0.9	1.8	2.0
Arquad T-50 NaSal	1275 1500	60	7.5	0.008	0.6			
Habon G	500	60	9.0	0.01	0.6			
Ethoquad T/13-50 NaSal Betz Corrrshield K7	1702 1500 5600	60	10.7	<0.02	<0.004			
Ethoquad T/13-50 NaSal Betz Corrrshield K7	1702 1500 1400	60	9.7	0.02	0.02	0.5	0.2	1.1
Tap Water		110	7.5	0.002	2.5			
Tap Water		110	10.6	0.01	2.0			

Table 6.7.2 (cont)

High Temperature Corrosion Rate Tests in Tap Water
with Surfactants and Corrosion Inhibitors

Surfactant/ Corrosion Inhibitor	Conc. ppm	Temp. °C	pH	Corrosion Rate in mpy				
				Stainless Steel	Carbon Steel	Copper/ Copper	Copper/ Nickel	Copper/ Zinc
Tap Water		110	10.8	0.02	1.5			
Ethoquad T/13-50 NaSal	1702 1500	110	9.3	<0.2	<0.2			
Dearborn 519	400	110	9.3	0.02	1.4	0.05	0.05	0.1
Kemamine EX-300	2306	110	8.9	0.04	1.0	0.07	0.09	0.1
NaSal Dearborn 519	2000 400							
Kemamine Q2983C	2000	110	8.9	0.05	0.7	0.09	0.10	0.07
NaSal Dearborn 519	2000 400							
Dobon	1500	110	8.2	0.034	2.0	0.06	0.09	0.3
Dearborn 519	400							
Ethoquad T/13-50 NaSal Betz Corrshield K7	1702 1500 5600	110	10.7	<0.002	<0.004			
Ethoquad T/13-50 NaSal Betz Corrshield K7	1702 1500 2800	110	10.3	0.005	0.03			
Ethoquad T/13-50 NaSal Betz Corrshield K7	1702 1500 1400	110	9.7	0.08	0.2			

Table 6.7.2 (cont)

High Temperature Corrosion Rate Tests in Tap Water
with Surfactants and Corrosion Inhibitors

Surfactant/ Corrosion Inhibitor	Conc. ppm	Temp. °C	pH	Corrosion Rate in mpy			
				Stainless Steel	Carbon Steel	Copper/ Copper/ Nickel	Copper/ Zinc
Habon-G	500	110	9.0	0.05	0.5		
Arquad T-50	1275	110	10.2	0.003	0.02		
NaSal	1500						
Betz Corrshield K7	2800						

Table 6.7.3

High Temperature Corrosion Rate Tests in Deionized Water with Surfactants

Surfactant	Conc. ppm	Temp. °C	pH	Corrosion Rate in mpy		
				Stainless Steel	Carbon Steel	Copper/ Copper/ Nickel Zinc
Deionized Water		60	6.5	0.01	0.09	
Deionized Water		60	10.7	<0.004	<0.01	
EthoquadT/13-50 NaSal	1702 1500	60	8.5	0.003	0.02	
EthoquadT/13-50 NaSal	1702 1500	60	8.5	0.003	0.007	
Arquad R-50 NaSal	1844 2000	60	9.0	0.007	1.2	
Arquad R-50 NaSal	1844 2000	60	10.0	0.007	1.2	
Deionized Water		110	6.5	0.01	0.3	
Deionized Water		110	10.0	0.009	0.3	
Deionized Water		110	10.7	0.002	0.2	
EthoquadT/13-50 NaSal	1702 1500	110	6.0	0.08	0.1	
EthoquadT/13-50 NaSal	1702 1500	110	8.5	0.08	0.1	
EthoquadT/13-50 NaSal	1702 1500	110	9.0	0.1	0.3	

Table 6.7.3 (cont)

High Temperature Corrosion Rate Tests in Deionized Water with Surfactants

Surfactant	Conc. ppm	Temp. °C	pH	Corrosion Rate in mpy		
				Stainless Steel	Carbon Steel	Copper/ Copper/ Nickel Zinc
Ethoquad T/13-50	1702	110	10.0	0.2	0.3	
NaSal	1500	110	10.0	0.1	0.3	
Ethoquad R/13	2395	110	9.0	0.09	0.2	
NaSal	2000					
Ethoquad R/12-75	2139	110	9.0	0.05	1.3	
NaSal	2000	110	9.0	0.05	1.5	
Arquad R-50	1844	110	6.5	0.3	19.0	
NaSal	2000					
Arquad R-50	1844	110	9.0	0.2	13.2	
NaSal	2000	110	9.0	0.2	16.4	
Habon-G	500	110	9.0	0.06	0.08	
Habon-G	500	110	9.5	0.01	0.2	
Habon-G	500	110	9.5	0.04	0.09	

Table 6.7.4

High Temperature Corrosion Rate Tests
in Deionized/Deoxygenated Water with Surfactants

Surfactant	Conc. ppm	Temp. °C	pH	Corrosion Rate in mpy				
				Stainless Steel	Carbon Steel	Copper/ Copper	Copper/ Nickel	Copper/ Zinc
		60	6.0	0.004	0.7			
Ethoquad T/13-50 NaSal	1702 1500	60	7.7	0.005	0.3			
		110	6.0	0.01	0.3	0.06	0.1	0.1
		110	10.4	0.02	0.1			
		110	10.7	<0.02	0.1			
Kemamine EX-300 NaSal	2306 2000	110	8.5	0.04	0.3	0.3	0.3	1.1
Kemamine Q2983 C NaSal	2000 2000	110	8.6	0.08	1.4	0.1	0.2	1.2
Arquad R-50 NaSal	1844 2000	110	10.0	0.1	11.9			
Dobon	1500	110	7.7	0.12	0.2	0.1	0.2	0.3
Habon-G	500	110	10.7	<0.007	<0.08			
Dobon-G NaSal	1500 700	110	9.0	0.09	0.3			

6-47

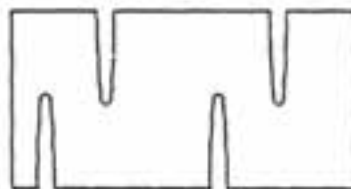
Figure 6.1



No corrosion

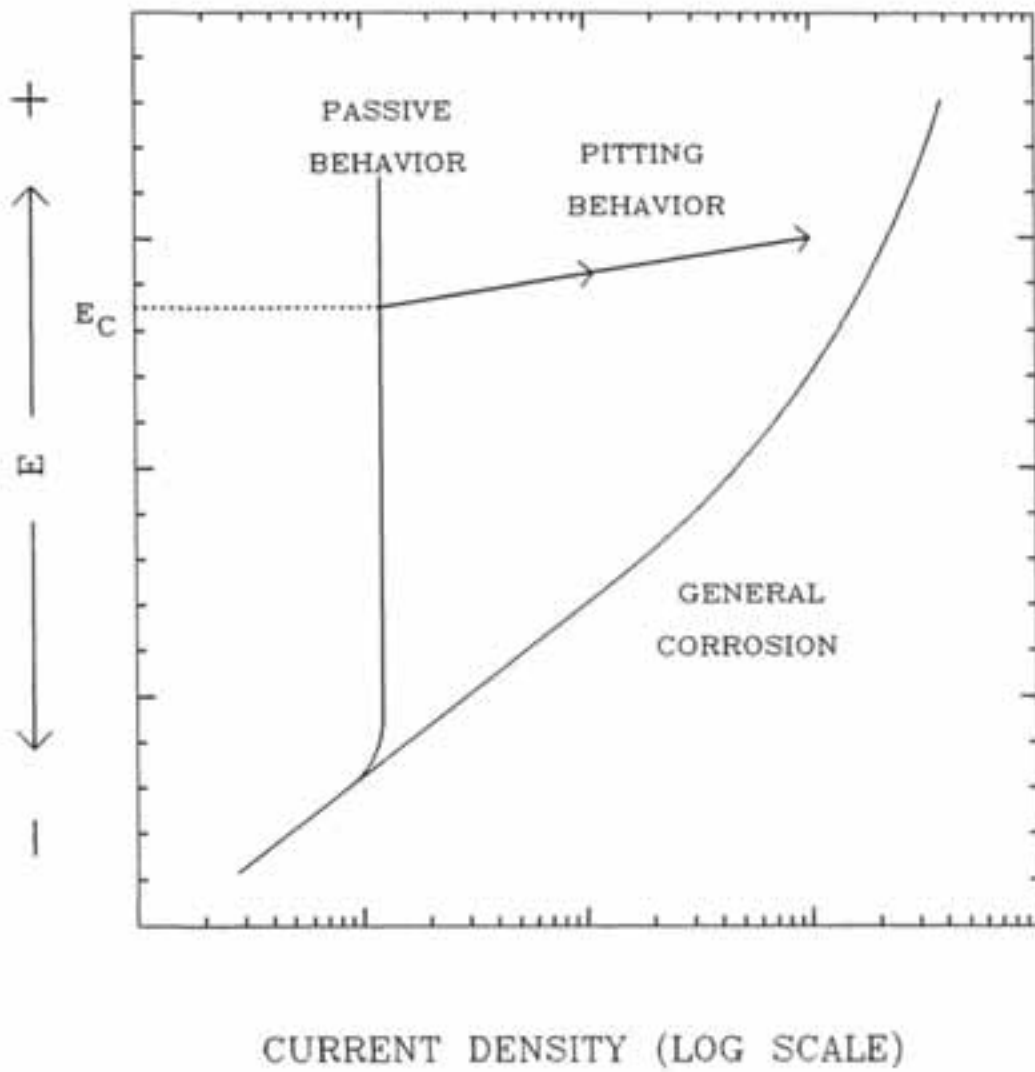


General corrosion



Pitting

Figure 6.2



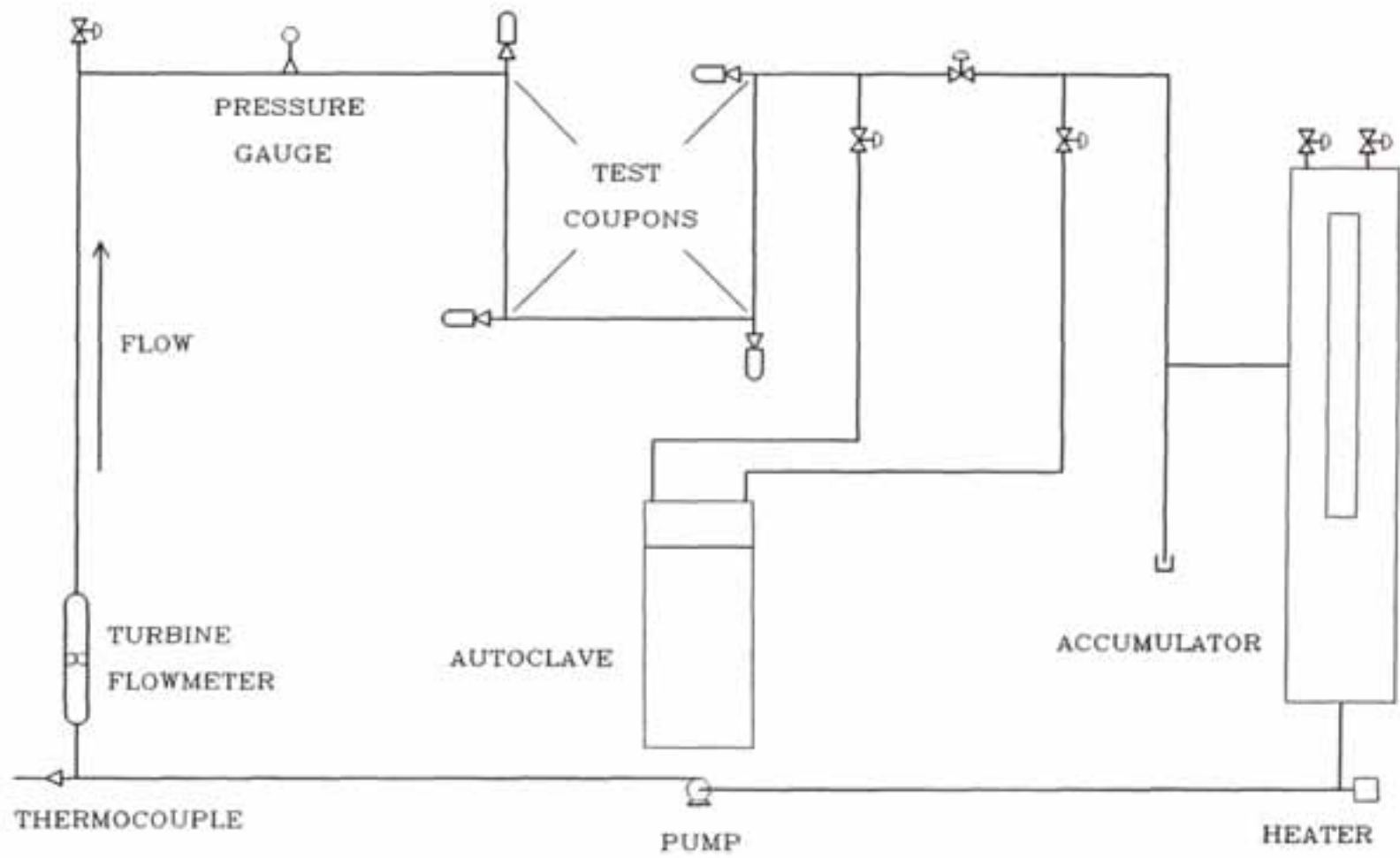


Figure 6.3

Figure 6.4

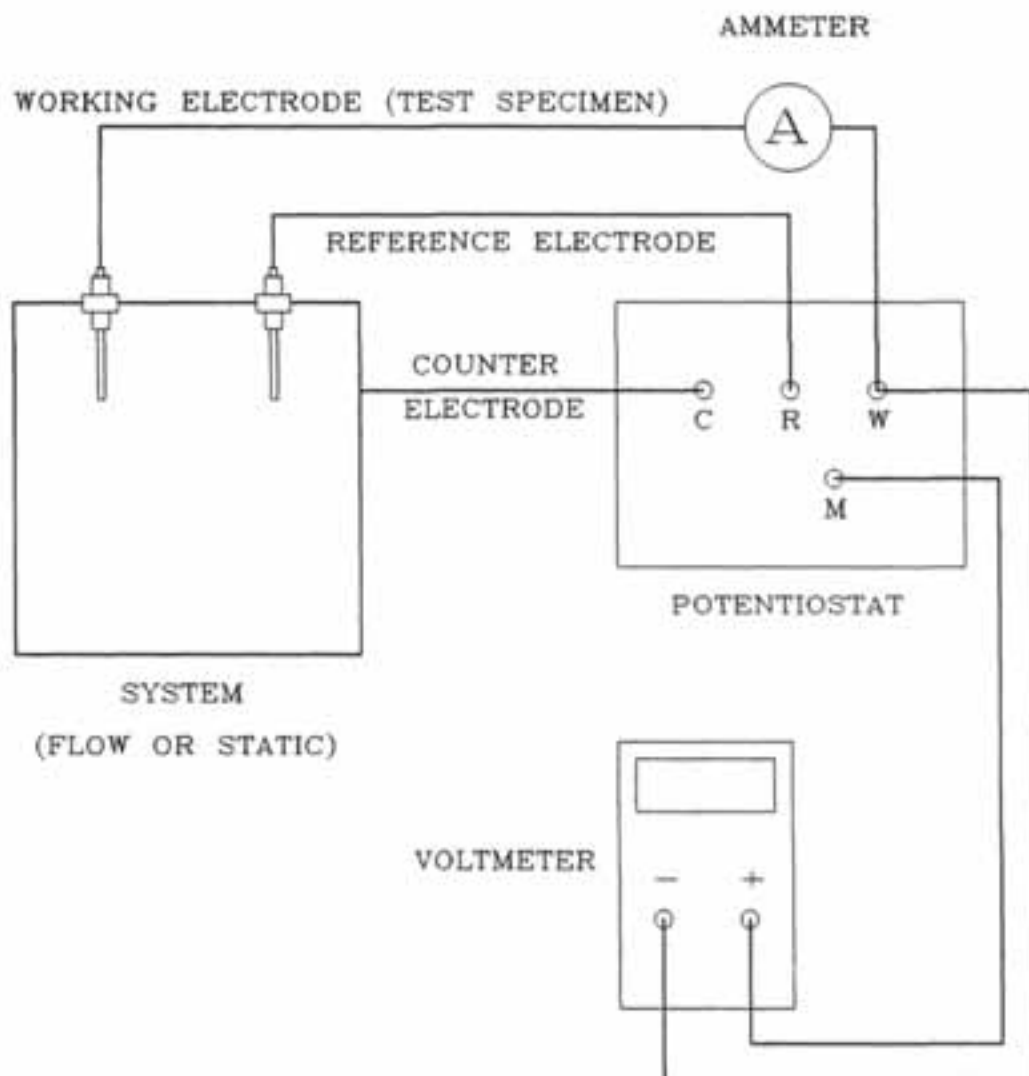
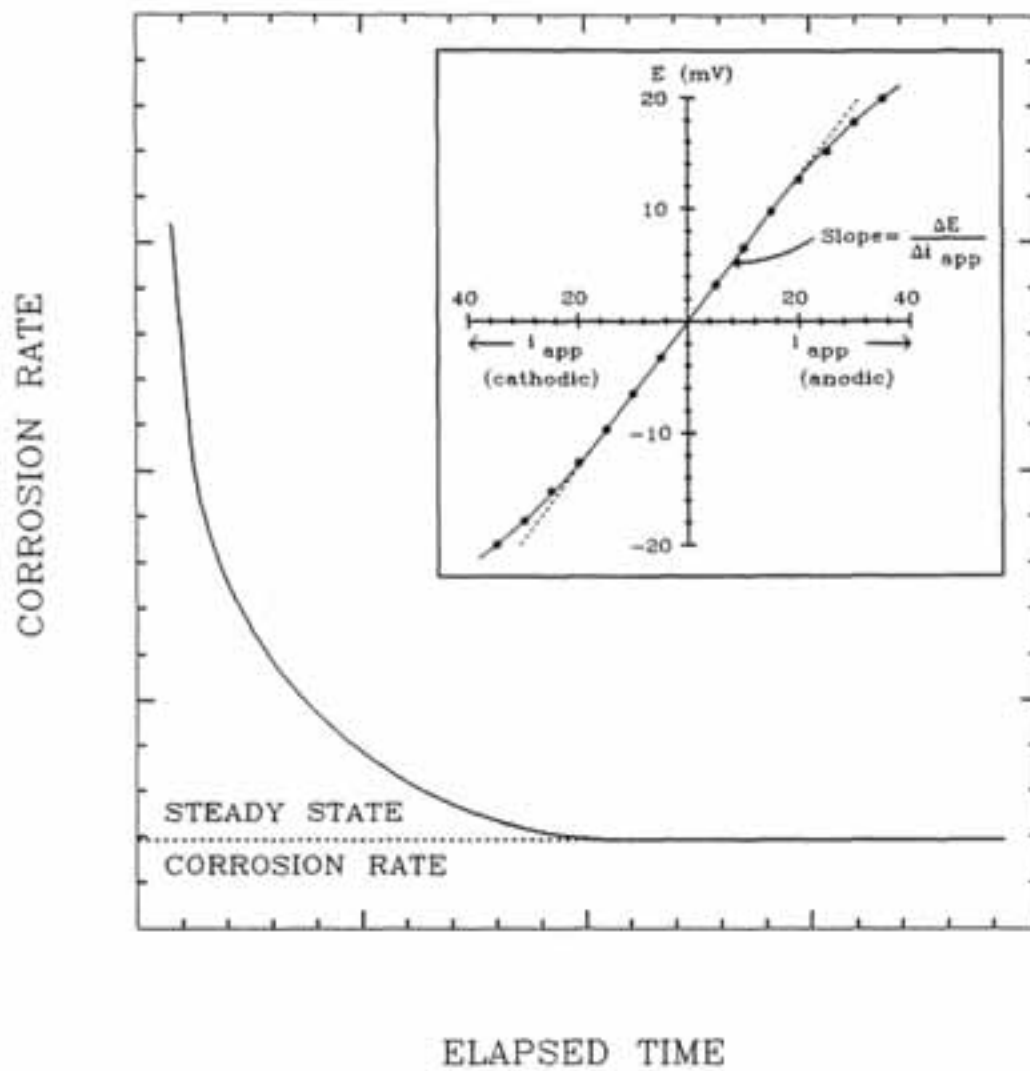


Figure 6.5



6.6 BIBLIOGRAPHY

1. Agoston, G.A., W.H. Hart, H.C. Hottel, W.A. Klemm, K.J. Mysels, H.H. Pomery and J.M. Thompson, *Ind. Eng. Chem.*, **46**, 1017-1019 (1954).
2. Toms, B.A., *Proceed. 1st Intern. Rheological Congress* (Netherlands, 1948), North-Holland Publish Co., Amsterdam, **II, Part 2**, 135-142 (1949).
3. Patterson, G.K., J.L. Zakin and J.M. Rodriguez, *Ind. Eng. Chem.*, **61**, 22-30 (1969).
4. Hoyt, J.W., *J. Basic Eng. Trans. ASME, Series D*, **94**, 248-285 (1972).
5. Virk, P.S., *Am. Inst. Chem. Eng. J.*, **21**, 625-656 (1975).
6. Sellin, R.H.J., J.W. Hoyt and O. Scrivener, *J. Hydr. Research*, **20**, 29-68 (1982).
7. Sellin, R.H.J., J.W. Hoyt and J. Pollert, *J. Hydr. Research*, **20**, 235-292 (1982).
8. Shenoy, A.V., *Colloid and Polymer Sci.*, **262**, 319-337 (1984).
9. Chou, L.C., R.N. Christensen and J.L. Zakin, "Effectiveness of Drag Reducing Surfactant Additives in District Heating Systems," pp 530-548 in *Proceedings 79th International District Heating and Cooling Association*, Chautauqua, N.Y., June, 1988.
10. Chou, L.C., "Drag Reducing Cationic Surfactant Solutions for District Heating and Cooling Systems," Ph.D. Dissertation, The Ohio State University, Columbus, 1991.
11. Personal Communication from Hoechst Aktiengesellschaft, Frankfurt, West Germany, October 27, 1987.
12. Smith, B.C., B.E. Wilde and J.L. Zakin, "Impact of Friction Reduction Additives on Corrosion, Contamination and Interaction with Other Additives in District Heating Systems," pp 4-1-56, in *IEA District Heating Advanced Transmission Fluids Final Report*, Novem, Sittard Netherlands, 1990.
13. Fontana, M.G. and N.D. Greene, *Corrosion Engineering*, McGraw-Hill, New York, 1978.
14. Wilde, B.E. and E. Williams, *Electrochimica Acta*, **16**, 1971-1985 (1971).
15. Wilde, B.E. and E. Williams, *J. Electrochemical Soc.*, **118**, 1057-1062 (1971).
16. Kruger, J., "On Passivity of Iron and Its Alloys," pp. 91-98 in *Passivity and Its Breakdown on Iron and Iron Base Alloys*, R.W. Staehl and H. Okada, eds., National Association of Corrosion Engineers, Houston, TX, 1976.

17. Wilde, B.E., *Corrosion*, 28, 283-291 (1972).
18. Hammer, F., in *Minutes of International Energy Agency Annex III, District Heating and Cooling Advanced Transmission Fluids Experts Group Meeting*, Copenhagen Denmark, April 9, 1991.
19. Stern, M. and E.D. Weisert, *Proc. ASTM*, 59, 1280-1290 (1959).
20. Stern, M. and A.L. Geary, *J. Electrochemical Soc.*, 104, 56-63 (1957).
21. Chou, L.C., R.N. Christensen and J.L. Zakin, "Drag Reducing Additives for District Cooling Systems," pp. 352-367, in *Proceedings 80th International District Heating and Cooling Association*, Virginia Beach June 1989.

IEA District Heating

**ADVANCED ENERGY
TRANSMISSION FLUIDS
FOR DISTRICT HEATING
AND COOLING**

Published by

Netherlands Agency for Energy and the Environment

Mailing Address: P.O. Box 17, 6130 AA Sittard, The Netherlands

Street Address: Swentiboldstraat 21, Sittard

Telephone: +31 46 595295

Telefax: +31 46 528260

1993: P 7

ISBN 90-72130-34-0